SPATIAL EXPLICIT ASSESSMENT OF WATER FOOTPRINT FOR RICE PRODUCTION IN BANGLADESH

M. M. Rahman, A. A. Saeem & M. R. A. Mullick*

Department of Civil Engineering, Chittagong University of Engineering and Technology, Chittagong, Bangladesh
**Corresponding Author: reazmullick@gmail.com*

ABSTRACT
This study is a quantitative assessment of the green, blue and grey water footprint of rice in Bangladesh. It concentrates on three fiscal years ranging from 2011 to 2014 and covers all the three types of rice produced in Bangladesh, namely Aus, Aman and Boro. This is a pioneering study in this kind in Bangladesh and has the novelty in using localized data. Rainfall data is taken from 35 rainfall measuring stations of Bangladesh Meteorological Department whereas yield data is taken from Bangladesh Bureau of Statistics. CLIMWAT 2.0 and Harmonized World Soil Database 1.21 are used to extract climate and soil information respectively. Lastly, CROPWAT 8.0 is used for estimating the actual crop evapotranspiration. The grey water footprint is calculated based on the application rate of Nitrogen based fertilizers. The three distinct water footprints are analyzed for each district of Bangladesh. This very first study, using local data finds the green and blue water footprint of Boro rice in Bangladesh to be 147 cubic meter/M. ton and 1162 cubic meter/M. ton respectively. Maximum total water footprint is found for Aus rice. Results from such analyses will help in regional water resource management in a more efficient way.

Keywords: Bangladesh; blue water; green water; grey water; water footprint.

INTRODUCTION
Terrific economic development results loss of natural resources on the earth and amid those loss gradual depletion of available freshwater throughout the world has become one of the major concerns in the recent years. An efficient and effective distribution of water with other economic resources has become instrumental to ameliorate the crisis. Along this line, the concept of "water footprint" was coined by Hoekstra in 2002 (Hoekstra, 2003). The water footprint of an individual or community is defined as the total volume of freshwater that is used directly and indirectly to produce any goods and services consumed by the individual or community. The water footprint is therefore a consumption based indicator of freshwater use (Hoekstra et al., 2008). The assessment of the water footprint, from a hydrological, ecological, and economic perspective, is very significant to facilitate an efficient allocation of water resources as it can provide a transparent and realistic guidance for optimizing the water policy decisions. In the recent years of water scarcity in many parts of the world, water footprint and virtual water trade have received much attention as both policy instrument and practical means to balance the local, regional, national and global water budget.

Water footprint assessment includes both direct and indirect water footprint as suggested by Hoekstra et al. (2011). In case of assessment of water footprint of a crop there exists two stages, namely- crop processing and crop to product processing. In crop processing, direct water footprint includes direct blue, green and grey water footprint, on the other hand, indirect water footprint comprises of water use associated with fertilizers, pesticides, machineries etc. The green water is defined as that part of the precipitation on land that does not run off or recharge the groundwater but is stored in the soil or momentarily stays on top of the soil or vegetation and ultimately, evaporates or transpires through plants. In monetary perspective, the blue water is of foremost importance because it costs higher than the other types and it is a major concern to limit the use of blue water i.e. the surface water and the ground water. In crop processing, the blue water refers to the amount of water supplied to the crop by

irrigation. The last type is the grey water footprint, which is an indicator of water pollution, associated in the crop processing and is defined as the volume of freshwater that is required to assimilate the load of pollutants based on natural background concentrations and existing ambient water quality standards.

A number of studies were carried out so far in some developed and developing countries e.g. USA, China, Indonesia, India etc. to explore the facts regarding water resource management that were not in concern before the introduction of water footprint concept. A study on consumption perspective (Chapagain et al., 2010) reveals that the green water footprint is noticeably larger than blue water footprint in India, Indonesia, Vietnam, Thailand, Myanmar and the Philippines for rice whereas USA and Pakistan showed larger blue water footprint compared to green water footprint. In recent past, a study on the past and future trends of grey water footprint of anthropogenic nitrogen (N) and Phosphorus (P) exhibits terrible condition of river due to increasing grey water footprint. The study was conducted over 1000 rivers within a time period of 1970 to 2000 and found that the pollution assimilation capacity of these rivers have been fully disbursed (Liu et al., 2011). Majority of these well-recognized studies on water footprint are conducted on large area basis where corresponding data are extracted predominantly from international database. However, analyses based on such dataset may not be reliable enough because of difference between local and international data set. The novelty of the current study lies here. Perception of the significance of water footprint of one of the most water intensive crops, rice in Bangladesh and the absence of assessment with local data leads to this study. This paper estimates the direct water footprint of main three types of rice (Boro, Aus, Aman) crop processing stage which is candid as per the guideline in "The water footprint assessment manual (Hoekstra et al., 2011)" to simplify the study and prevent it from being intricate.

METHODOLOGY AND DATA

This assessment is a level B spatial explication, which estimates the direct water footprint of rice processing (planting to harvesting) in Bangladesh conforming "The Water footprint Assessment manual" by Hoekstra et al. (2011). There are two popular systems of rice cultivation in Bangladesh, namely up land system and wet land system; however, wet land system is the practice in Bangladesh. The wetland system follows preparation of field by tillage & puddling. A standing water layer is also maintained throughout the cultivation period to saturate the soil. The study covered altogether the districts in Bangladesh. It also used data predominantly from local sources and checked with global database to reassure right assessment. The assessment of water footprint of rice processing (planting to harvesting) could be depicted in Eq. 1.

$$WF_{proc.\ rice} = WF_{blue} + WF_{green} + WF_{grey} \qquad (1)$$

Assessment of the blue and green water footprint

Both green and blue water is consumed by rice in the form of evaporation, incorporation in crop and change of catchment area. Quantitative assessment of loss of water due to change of location of water between different catchment areas is not feasible and a cumbersome task therefore it is neglected along with the incorporated water which is found usually as maximum as 1% of evapotranspiration. The study computed only the water that evaporates. Table 1 shows planting and harvesting dates of three major types of rice namely Aus, Aman and Boro.

Table 1: Major types of rice and their planting and harvesting date for Bangladesh

Rice Type	Planting Date	Harvesting Date
Boro	15-Dec	13-Apr
Aus	1-May	28-Aug
Aman	15-Aug	12-Dec

The green and blue water footprint (m^3/ton) of rice is obtained by dividing the corresponding evapotranspiration (m^3/ha) by yield (M.ton/ha). Yield data is obtained from Bangladesh Bureau of Statistics (BBS, 2013). Evapotranspiration was estimated using CROPWAT 8.0 model developed by the Food and Agriculture Organization of the United Nations (FAO, 2010b). CROPWAT 8.0 offers two different options to compute evapotranspiration, namely crop water requirement option and irrigation requirement option. Crop water requirement option is based on optimal condition and gives

comparatively unrealistic results compared to irrigation requirement option. This study obtained actual evapotranspiration (ET_c) using irrigation requirement option. The monthly rainfall data for the 35 stations over Bangladesh is collected from Bangladesh Meteorological Department and the effective rainfall is computed using USDA SCS (United States Department of Agriculture, Soil Conservation Service) method which calculates effective rainfall according to the Eq. (2) and (3).

$$P_{eff} = P_{month} * (125 - 0.2 * P_{month}) / 125 \text{ for } P_{month} <= 250 \text{ mm} \quad (2)$$

$$P_{eff} = 125 + 0.1 * P_{month} \text{ for } P_{month} > 250 \text{ mm} \quad (3)$$

where, P_{eff} = effective rainfall and P_{total} = total rainfall in the concerned period. In Bangladesh wet land method is utilized in which the standing water layer comes with a constant percolation and seepage loss varies from 2 mm/day (heavy clay) to 6 mm/day (sandy soil) (Chapagain et al., 2010). An average of 3 mm/day is used in this study as percolation loss. In last 15 days of rice cultivation the field is left to dry for harvesting. Factors like soil moisture prior to land preparation, contribution from shallow ground water through capillary rise and outflow of the overland runoff from adjacent rice fields are neglected in this study. The value of k_c is taken from Allen et al, (1998). Soil data for 64 districts is formatted with the help of FAO's Harmonized World Soil Database Viewer 1.2 and Soil Water Characteristics 6.02.74.

The crop water requirement is obtained by multiplying reference evapotranspiration (ET_o) with crop coefficient (K_c). It is assumed that the water stress co-efficient K_s=1, which means water requirements (CWR) are fully met. Therefore, CWR= ET_c where, ET_c= Actual crop evapotranspiration. Reference crop evapotranspiration (ET_o, mm/day) is taken from CLIMWAT 2.0 model output in monthly basis. Actual crop evapotranspiration and effective rainfall calculated with the help of climate file, rainfall file, crop file and soil file are used to determine green and blue water footprint. Green water footprint is the minimum of actual crop evapotranspiration (ET_c) and effective rainfall (P_{eff}) while blue water footprint is either zero or the difference between actual crop evapotranspiration and effective rainfall.

$$ET_{green} = \text{Min. } (ET_c, P_{eff}) \quad (4)$$

$$ET_{blue} = \text{Max. } (0, ET_c - P_{eff}) \quad (5)$$

Assessment of grey water footprint

Numerous formulations are found in literature to calculate of grey water requirement for point sources of water pollution but in case of crop processing the source of pollution is diffuse. To overcome the unfeasibility of apportioning the measured concentrations to different sources, "The Water Footprint Assessment Manual" (Hoekstra et al., 2011) recommends to estimate the fraction of applied chemicals that enters the water system by using simple or more advanced models. The simplest model assuming that a certain fixed fraction (Leaching Run-off Fraction, α) of the applied chemicals (AR kg/ha) finally reach the ground- or surface water gives a simple and workable formula shown in Eq. (6).

$$WFproc, grey = \frac{\alpha * AR}{(C\max - Cnat)} * \frac{1}{Y}\left(\frac{Volume}{Mass}\right) \quad (6)$$

where, C_{max}=Maximum acceptable concentration for the pollutant considered (kg/m^3), C_{nat}=Natural concentration for the pollutant considered (kg/m^3), Y=Crop yield (kg/ha). Since a number of chemical components are present in fertilizers and pesticides, selection of a certain or all the chemicals for the grey water footprint calculation becomes a question. The answer comes from another assumption: grey water footprint will be calculated only for the "Critical Pollutant", which creates most severe effect on environment. This work assumes Leaching-run-off fraction, α to be 10% and Nitrogen-based fertilizers to be the Critical Pollutant (Chapagain et al. 2006b).

RESULTS AND DISCUSSIONS

Water footprint of 64 districts in Bangladesh of three different type of crops is shown in Table 2. A number of districts located in the south east, south west, north and north east part of the country is greatly facilitated by the moon soon rain during the rainy season. As a result Aus and Aman growing in this season show a large amount of green water footprint and small or no blue water footprint.

Table 2: Green, blue and grey water footprint of Boro, Aman and Aus rice of 64 districts in Bangladesh

Water footprint (m^3/M.ton)

District	Boro			Aus			Aman		
	Green	Blue	Grey	Green	Blue	Grey	Green	Blue	Grey
Bagerhat	32.0	1414.8	8.8	2817.8	0.0	15.2	2694.8	0.0	16.5
Bandarban	547.6	814.8	9.5	2760.4	0.0	15.7	1768.0	0.0	12.4
Barguna	4.8	2126.4	13.2	2734.7	0.0	15.4	2702.0	0.0	17.0
Barisal	178.3	1137.7	8.2	3160.9	0.0	17.8	2453.2	0.0	15.4
Bhola	33.1	1403.0	8.9	3340.8	0.0	18.8	2536.5	0.0	15.9
Bogra	49.0	1318.5	8.0	2815.2	297.4	14.6	1953.0	210.8	13.1
Brahmanbaria	153.9	1110.2	7.8	2910.1	133.2	17.1	2150.5	153.6	14.8
Chandpur	136.6	1106.7	7.7	2462.9	0.0	13.8	2706.1	0.0	17.3
Chittagong	47.0	1235.1	9.0	2237.4	0.0	12.7	1679.3	0.0	11.8
Chuadanga	55.6	1257.7	7.8	2336.2	812.0	13.0	1690.5	343.9	11.8
Comilla	154.4	1113.8	7.9	2278.4	104.3	13.4	1858.2	132.7	12.8
Cox's Bazar	179.3	1408.5	9.3	2337.7	0.0	11.5	1797.0	0.0	10.5
Dhaka	103.3	1276.5	7.2	4344.7	28.8	20.8	3047.8	549.1	20.7
Dinajpur	104.5	1190.2	8.0	2706.6	0.0	13.3	1854.7	0.0	11.9
Faridpur	81.5	1076.2	7.2	5865.6	0.0	33.7	2260.3	34.5	15.4
Feni	88.4	1347.1	8.9	2518.6	0.0	14.1	1675.0	0.0	10.6
Gaibandha	48.3	1299.6	7.8	3054.3	322.7	15.9	1908.6	162.9	12.4
Gazipur	106.6	1317.5	7.4	3559.6	23.6	17.1	1630.0	293.6	11.1
Gopalgonj	53.3	1022.6	6.7	5882.4	0.0	33.1	3962.8	0.0	24.9
Hobigonj	419.9	928.7	8.6	2415.0	0.0	12.9	1986.4	0.0	12.7
Jamalpur	46.7	1167.0	7.6	3895.0	204.4	20.2	2046.8	197.4	13.7
Jessore	111.2	1154.9	7.4	2603.1	0.0	12.9	2000.9	0.0	12.4
Jhalakathi	197.6	1260.8	9.0	2924.7	0.0	16.4	2721.2	0.0	17.1
Jhenaidah	54.8	1260.8	7.7	2344.9	292.8	13.0	1651.9	208.9	11.5
Joypurhat	44.4	1195.1	7.2	2969.5	313.8	15.4	1771.8	191.2	11.9
Khagrachari	524.9	781.1	9.1	2654.0	0.0	15.1	1488.0	0.0	10.4
Khulna	73.2	1284.7	8.3	3867.5	0.0	20.8	1981.1	256.1	13.7
Kishoregonj	74.8	1114.0	7.4	2973.0	0.0	14.7	1527.5	272.9	11.0
Kurigram	93.8	1078.8	7.6	4178.7	0.0	21.0	1867.6	244.7	13.2
Kushtia	53.2	1089.1	7.4	2489.3	728.3	13.8	1883.1	315.4	13.1
Lakshmipur	103.7	1192.2	8.4	3494.6	0.0	17.6	2110.4	276.5	14.9
Lalmonirhat	56.7	1122.4	7.3	3851.8	0.0	21.5	1865.8	0.0	11.8
Madaripur	59.2	1138.8	7.4	5780.0	0.0	33.2	3597.3	0.0	24.2
Magura	119.2	1163.3	7.9	2157.9	0.0	12.4	1838.9	0.0	12.3
Manikgonj	104.3	1288.3	7.3	6342.3	42.0	30.4	4178.8	752.8	28.4
Maulavibazar	69.7	1427.7	9.8	2344.2	685.8	13.0	1622.3	271.7	11.3
Meherpur	377.8	835.6	7.8	2286.5	0.0	12.2	1862.5	0.0	11.9
Munsigonj	109.6	1353.6	7.6	4362.6	28.9	20.9	3791.8	683.1	25.8
Mymenshing	85.0	1265.5	8.4	3200.7	0.0	15.8	1970.9	352.1	14.2
Narail	103.9	1255.2	7.2	5375.1	899.7	25.7	2125.6	746.7	16.2
Narayangonj	114.0	1184.8	7.6	3223.8	0.0	15.9	3476.5	0.0	21.5
Narsingdi	107.9	1065.7	7.5	3648.5	0.0	18.3	1889.2	287.0	12.9
Natore	94.4	932.1	6.6	3365.5	0.0	16.9	2071.0	314.6	14.1
Nawabgonj	198.5	1276.9	8.3	2386.3	987.4	15.1	1774.3	263.2	11.8
Netrokona	612.7	625.5	7.7	3299.6	0.0	16.3	2150.6	0.0	13.1
Nilphamari	81.9	1016.8	7.7	3009.0	0.0	14.4	1867.4	0.0	11.5
Noagaon	104.6	1263.0	7.3	2660.9	445.4	12.7	1489.5	523.2	11.4
Noakhali	61.0	1208.6	7.9	3380.3	0.0	18.9	2606.2	0.0	16.5
Pabna	178.0	1145.0	7.4	3704.6	1532.9	23.5	2203.5	326.8	14.7
Panchagar	82.9	1028.3	7.7	8074.2	0.0	38.6	2007.6	0.0	12.3
Patuakhali	4.5	1989.2	12.4	2910.6	0.0	16.4	2834.6	0.0	17.8
Perojpur	197.7	1261.5	9.0	2752.8	0.0	15.5	2671.6	0.0	16.8
Rajbari	84.5	1115.4	7.4	6030.8	0.0	34.7	2081.8	31.8	14.2
Rajshahi	110.1	1063.8	7.6	2681.5	300.3	12.8	1481.4	416.8	11.3

Rangamati	483.7	719.8	8.4	3412.3	0.0	19.4	1688.2	0.0	11.8
Rangpur	97.3	1175.0	7.9	8418.8	0.0	41.4	1630.0	152.3	11.5
Satkhira	162.4	1223.0	8.5	2264.5	0.0	12.2	1843.6	0.0	11.3
Shariatpur	59.9	1374.9	7.5	7126.3	0.0	33.9	4059.9	0.0	23.4
Sherpur	74.1	1103.7	7.4	3119.6	0.0	15.4	1846.5	329.9	13.3
Sirajgonj	80.6	1226.4	7.3	3260.2	604.3	17.3	1898.4	614.5	14.6
Sunamgonj	721.3	602.6	9.1	1588.4	1327.1	20.0	2031.0	0.0	12.5
Sylhet	831.3	694.6	10.5	2703.8	0.0	14.2	2121.2	0.0	13.1
Tangail	84.7	1290.0	7.7	5014.3	929.5	26.7	2050.2	663.7	15.8
Thakurgaon	94.7	1078.5	7.3	2638.3	0.0	13.0	1743.4	0.0	11.2
Bangladesh	**146.7**	**1162.2**	**8.0**	**3146.9**	**168.5**	**16.8**	**2060.0**	**156.6**	**13.7**

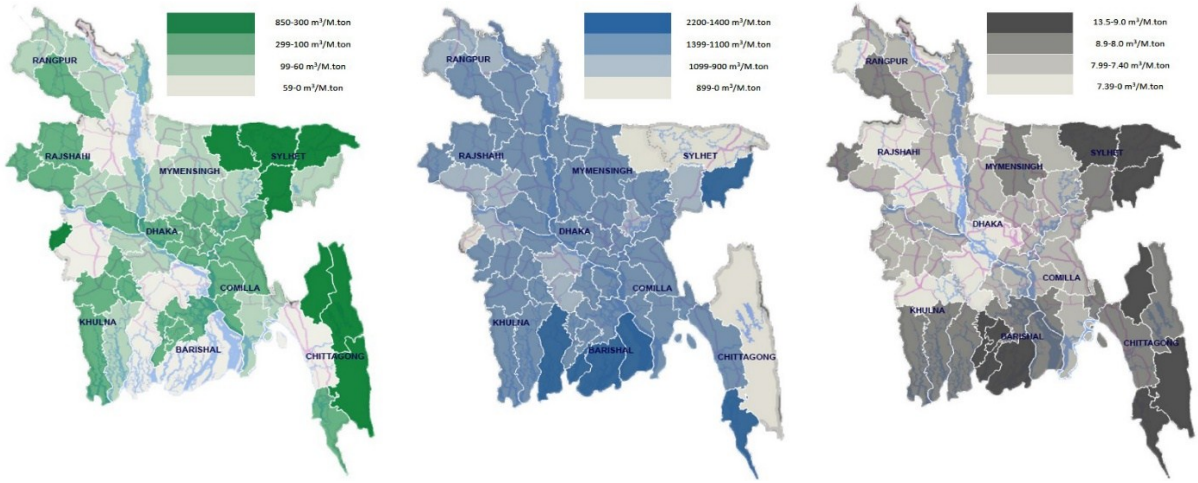

Green Water Footprint Blue Water Footprint Grey Water Footprint

Fig. 1: Graphical representation of water footprint of Boro rice

Absence of rainwater in most part of the country during Boro cultivation is making the average blue water footprint of Boro rice of Bangladesh (1162.2 m^3/M.ton) larger than that of Aman rice (156.6 m^3/M.ton) and Aus rice (168.5 m^3/M.ton). In some districts, the green water footprint of Aus and Aman show larger values compared to corresponding average green water footprint of the country, the reason behind this is the small yield values in these districts compared to others. At the same time, some districts show zero blue water footprint indicating sufficient rainfall and zero irrigation. Fig. 1 shows graphical representation of water footprint of Boro rice.

The primary aim of water footprint assessment is to plan to reduce the green, blue and grey water footprints. The green water footprint is to be kept as low as possible because an efficient use of green water confirms greater chance of storage of blue water. Again, if the blue water footprint can be lessened, there exists a greater chance of surplus storage of blue water, which will certainly give a greater freedom of reallocation to policy makers. A lower grey water footprint represents a lower degree of pollution and vice versa. Forthrightly, steps should be taken before disposal of effluent to lower the grey water footprint and mitigate the severity of the situation. Recycling and Reuse of effluent could be a good instrument to reduce the grey water footprint. Desalination of seawater or brackish water may seem to be an alternative solution for water scarcity; but desalination and transportation of the desalinated water to the lands far from the coastal belts consume huge energy; and the earth cannot fight one scarce resource with another scarce resource, energy. Although water is a renewable resource, there lefts no better solution than sustainable water budgeting. Furthermore, being renewable resource does not mean that it is always available anywhere. The water footprint assessment helps the allocation of proper amount of proper type (green, blue and grey) water at proper place at proper time.

CONCLUSIONS

With the limited resources, this study finds the green, blue and grey water footprint for Boro rice in Bangladesh to be 146.7, 1162.2 and 8.0 m^3/M.Ton respectively. The footprints are found to be 3147, 168.5 and 16.8 m^3/M.Ton respectively for Aus rice. And the Aman rice gives the footprints as 2060, 156.6 and 13.7 m^3/M.Ton respectively. In the modern era when rivers are running dry, lake and ground water levels are dropping, species are endangered by contaminated water, source of safe drinking water is shrinking, Bangladesh is not an exception. In this circumstances, water footprint concept can be utilized to discover the links between the problems and probable solutions to achieve a more sustainable and equitable use of the limited fresh water resource. To achieve additional perspective from the water footprint of rice, concentration should go to the assessment of water footprint of other main crops like wheat, potato etc. as well. Such assessment over main crops will help to understand the efficiency of different crops over each other based on nutritional values and water consumption. With the help of comparative assessment, decision on sustainable water allocation could be taken. Further study considering water availability in the catchment area could help identify environmentally endangered areas and make meticulous policy for achieving water-based environmental sustainability. In the present days, water may be available in Bangladesh to grow water extensive crops like rice, but a benchmark should be introduced to achieve a sustainable water allocation. Additional study over future and past trends could help to setup such benchmark for rice production.

REFERENCES

Allen, R G; Pereira, L S; Raes, D and Smith, M .1998. *Crop evapotranspiration: Guidelines for computing crop water requirements*. *FAO* Irrigation and Drainage Paper 56. Food and Agriculture Organization, Rome.

Bangladesh Bureau of Statistics .2013. [Online]. Available at: http://www.bbs.gov.bd/PageWebMenuContent.aspx?MenuKey=24 [Accessed 15th January 2016]

Chapagain, AK and Hoekstra, A Y. 2010. *The green, blue and grey water footprint of rice from both a production and consumption perspective.* Value of Water Research Report Series No.40. UNESCO-IHE, Delft, Netherlands.

Chapagain, AK; Hoekstra, AY; Savenije, HHG and Gautam, R. .2006b. The water footprint of cotton consumption: An assessment of the impact of worldwide consumption of cotton products on the water resources in the cotton producing countries. *Ecological Economics,* 60(1):186–203.

FAO 2010b. CROPWAT 8.0 model. FAO. Rome. [Online]. Available at: www.fao.org/nr/water/infores_ databases_cropwat.html. [Accessed 30th January 2016]

FAO 2010a. CLIMWAT 2.0 database. FAO. Rome. [Online]. Available at: www.fao.org/nr/water/infores_ databases_climwat.html [Accessed 30th January 2016]

Hoekstra, AY. 2003. *Virtual water trade: Proceedings of the International Expert Meeting on Virtual Water Trade.* Value of Water Research Report Series No 12. UNESCO-IHE, Delft, Netherlands.

Hoekstra, AY and Chapagain, AK. 2008. *Globalization of Water: Sharing the Planet's Freshwater Resources.* Blackwell Publishing, Oxford.

Hoekstra, AY; Chapagain, AK; Aldaya, MM and Mekonnen, MM .2011. *The water footprint assessment manual: setting the global standard.* Erthscan London, London, UK. ISBN 978 84971 279 8.

Liu, C; Kroeze, C; Hoekstra, AY and Gerbens-Leenes, W. 2012. Past and future trends in grey water footprints of anthropogenic nitrogen and phosphorus inputs to major world rivers. *Ecological Indicators,* 18, 42–49.

Mekonnen, MM and Hoekstra, AY. 2011. *National water footprint accounts: the green, blue and grey water footprint of production and consumption.* Value of Water Research Report Series No. 50, UNESCO-IHE, Delft, the Netherlands.

CLIMATE CHANGE IMPACTS ON CROP YIELD, ARABLE LAND AND CHANGES IN WETLAND AREA IN RAJSHAHI DISTRICT, BANGLADESH

M. S. Islam*, S. Khatun & M. S. U. Miah

Department of Civil Engineering, Rajshahi University of Engineering and Technology, Rajshahi, Bangladesh.
**Corresponding Author: shumonengcivil01@gmail.com*

ABSTRACT
Today climate change is an issue of great concern for the world. This paper explores the effect of climate change on water resources and agriculture in greater Rajshahi district of Bangladesh and deals with the effect of climate change on crop yield, long-term effect of drought over cropland and changes of wetland. For these purposes, rice, Wheat, and Potato crop has been selected. The effect of climate change on crop yield is shown by developing a relationship among maximum temperature, minimum temperature and rainfall. The change in the wetland area is shown by analysing Landsat satellite images using GIS and Remote Sensing technology. Results revealed that maximum temperature positively influenced Aus, Aman, potato yield and negatively affected yield of Boro and wheat. Minimum temperature adversely affected all crops except Aman and Boro. Rainfall showed less prominent influence for increase in yield. Rice, sugarcane, maize had decreasing trend in cropland area whereas increasing trend of cropland area was noticeable for potato, wheat, pulse etc. From 2006-2011, Rajshahi lost about 17% of its wetland and about 7% wetland lost from 2011-2016. All these information prove that Rajshahi district is very vulnerable in face of food security and existing water resources in this region.

Keywords: Climate change; agriculture; wetland; remote sensing; GIS; Bangladesh

INTRODUCTION
The problem of climate change is extensive, broad, and a threat to human civilization. The factors, which influence climate change, also affect the agricultural production. So it is natural that climate change will affect the agriculture. Agriculture in Bangladesh is mostly influenced by temperature and rainfall. Due to impact of climate change there may result a change in property and yield of crop. So food security will face a great risk. A study found that 1°C increase in maximum temperature at vegetative, reproductive and ripening stages there was decrease in *Amman* (Nvember and December harvest) rice production by 2.94, 53.06, and 17.28 tons respectively and with the change in temperature (by 2°C and 4°C), the prospect of growing Wheat and Potato would be severely impaired (Baten et al., 2008). It is predicted that yield of rice and Wheat will decrease 8% and 32% respectively in Bangladesh within 2050 and by the end of 21st century overall crop production will decrease 30% *(IPCC*, 2007). Rajshahi, a district of northwestern part of Bangladesh is mostly affected by climate change where two seasons are seen to be appeared among six seasons in a year, summer, and rainy season. Other seasons can be realized very little. In this district, there is almost no rainfall in rainy season (Ashar and Sravon month). In the month of October (Ashwin), there occurs so intense rainfall that creates waterlogging. So rain fed crops face a great problem and their growing season also hampers. Due to this, agricultural lands are used for another crop production, which can withstand this weather. Rice, Wheat and Potato are the crops, which are very sensitive to temperature and rainfall. They need different temperature and rainfall for their different growth stages. Due to increased temperature, ponds, canals are drying out. Also for earning more benefit, farmers are more interested to make cropland into water-body to cultivate fish. So the area of wetlands is not constant but changing day by day. Several papers have shown temperature and rainfall change effect on crop yield and their risk assessment in northwestern part of Bangladesh but no paper, to my best of my knowledge, have shown temperature and rainfall effect on cropland and crop yield simultaneously in

Rajshahi district. Shopan and Islam (2013) have shown changes in wetland area in northwestern area of Bangladesh but this paper focuses only changes in wetland area in most climate change prone district Rajshahi. The objectives of this study are i) to investigate the effect on crop yield due to change in temperature and rainfall in the area for three main cereal species i.e. rice, Wheat, Potato ii) to evaluate changing pattern of cropland for these crops due to cultivation of alternative crops which are more sustainable in changed weather iii) to estimate the changes of wetland.

METHODOLOGY

In order to investigate the effect of climate change on crop yield, data of last 12 years (2004-2015) of rice, Wheat, Potato of different upozilla in Rajshahi district are collected from Department of Agricultural Extension, Rajshahi. Data includes yield of the crops mentioned above, amount of cropland and average crop yield and last 12 years temperature and rainfall data. Here, ArcGis 10.1® has been used for analyzing satellite image to estimate wetland area.

Satellite Image

To estimate the wetland area, GIS and remote sensing technology is applied. Shopon and Islam (ICWFM 2013) have shown this method before. The difference is that here Landsat scenes of 2006, 2011 and 2016 are used. Images represent dry season of Bangladesh as they have been captured in Late January to Late February on different images. It is assumed that temporal changes of water bodies remain insignificant over this period. Properties of the images are presented in Table 1.

Table 1: Properties of downloaded satellite images

Image No.	Acquisition Date	Satellite Sensor
1	February 27, 2006	Landsat 4-5 TM
2	February 17, 2011	Landsat7ETM+SLC-off
3	January 06, 2016	Landsat8 OLI/TIRS

Image Processing

ArcGIS® 10.1 has been used to process Landsat images Satellite data as mentioned earlier are geocoded with topographical maps using ground control points. Conversion of image from digital number to At-sensor and radiance to top-of-atmosphere (TOA) reflectance is done according to the equation given in Landsat handbook of NASA. In order to determine wetland area, in Rajshahi district of Bangladesh, the Normalized different water index (NDWI) (described in details in section 2.3) maps are prepared from satellite images. Then the map is reclassified into different NDWI values using "Reclassify" in spatial analyst toolbox of ArcGis. NDWI with positive values are taken into consideration as water features have positive values while soil and terrestrial vegetation features have zero for negative values (McFeeters, S.K, 1996). Then this raster map is converted to vector map (the summation of many polygons). Area of polygon, corresponding to water-body is calculated in square-metre. Then this area is converted to hectare. Wetland area obtained from three different satellite images for different time interval is used to find out the changes.

Using NDWI to delineate water body feature

Normalized different water index (NDWI) is a method developed primarily to delineate open water features and to enhance their presence in remotely sensed digital imagery while simultaneously eliminating soil and terrestrial vegetation features (McFeeters, S.K, 1996). The NDWI is calculated as follows:

$$\text{NDWI} = \frac{GREEN - NIR}{GREEN + NIR} \quad \ldots\ldots (1)$$

Where, green is band that encompasses reflected green light and NIR represents reflected near infrared radiation.

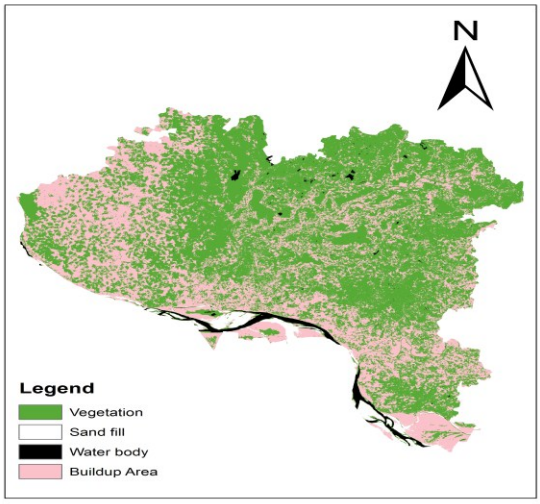

Fig. 1: Supervised classified image of Rajshahi district showing different land use.

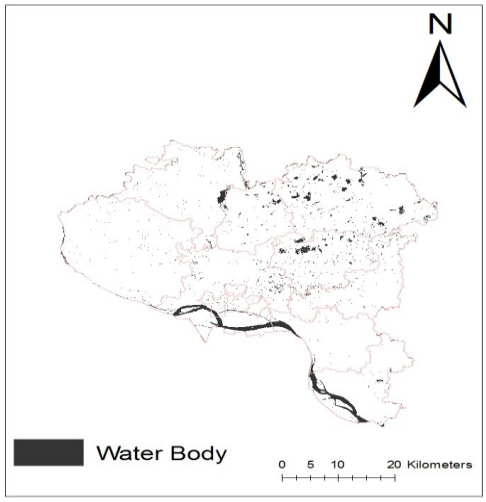

Fig. 2: Map of wetland area in Rajshai district on 06 January 2016.

NIR is observed strong by water and is reflected strongly by vegetation and dry soil. NIR data shows vegetated surfaces as being white, white water surfaces appear dark. The selection of green and NIR band was done to 1) maximize the typical reflectance of water features by using green light wavelength 2) minimize the low reflectance of NIR by water features and 3) take advantage of the high reflectance of NIR by terrestrial vegetation and soil features. Image processing software can easily be configured to delete negative values. This effectively eliminates the terrestrial vegetation and soil information and retains the open water information for analysis. The range of NDWI is then from zero to one. Multiplying equation (1) by a scale factor (e.g., 255) enhances the resultant image for visual interpretation.

Estimation of wetland area

NDWI values which have positive value indicate water feature if the digital number of NIR band of a pixel is less than digital number of red band and the green band the NDWI is ≥ 0.44, then it is classified as water, otherwise not. So wetland=NDWI$\geq$0.44 (Goel et al., 2009). Figure 2 shows a NDWI map of water body of Rajshahi district on o6 january 2016.

DESCRIPTION OF THE STUDY AREA

Location and topography

Rajshahi district is a district in north western Bangladesh and bounded by Naogaon district to the north, Natore district to the east and Chapai Nababganj district and the river Padma to the south. There are different types of land found in Rajshahi district. Among these lands, high lands 37.97%, medium high land 23.38%, medium low land 23.36%, low land 8.43% and very low land 6.86% covers the total land area.

Rainfall

Rajshahi has a tropical wet and dry climate. The climate of Rajshahi district is marked with moderate rainfall. Between driest and wettest months, the difference in precipitation is 299 mm. The annual rainfall in the district is about 1448 mm (57 in).

Temperature

The climate of Rajsahi district is marked with high temperature. The hot season commences early in March and continues till the middle of July. The maximum mean temperature observed is about 32 to

36°C. During the month of April, May, June and July and the minimum temperature recorded in January is about 7 to 16°C.

Major crops

There are three cropping seasons Rabi, Kharif-I and Kharif-II in Rajshahi district. Important crops in Kharif season are Aman, Sugarcane, Jute, Maize, Cotton etc. In the Rabi season, crops need cool climate during growth period but warm climate during the germination period of seed and maturation. The major crops are Wheat, linseed, mustard, Potato etc.

RESULTS AND DISCUSSIONS

Temperature and rainfall variation

Maximum temperature is statistically significant for all rice yields with positive effects on Aus and Aman rice. The influence of maximum temperature and minimum temperature compared with that rainfall (Sarker et al., 2012). Optimum Temperature for maximum photosynthesis ranges from 25°C to 30°C for rice under the climatic condition of Bangladesh (Basak, 2010).

In figure 3, the trend of change in temperature shows that highest maximum temperature was in 2014 and deviates 1.62°C from mean temperature 40.83°C. Lowest minimum temperature was found in 2013 and deviates 1.03°C from mean 6.42°C. In figure 4, the trend of change in rainfall shows a decreasing trend over the period 2004-2015. Lowest rainfall was in 2010 and deviates 237mm from mean 1263mm.

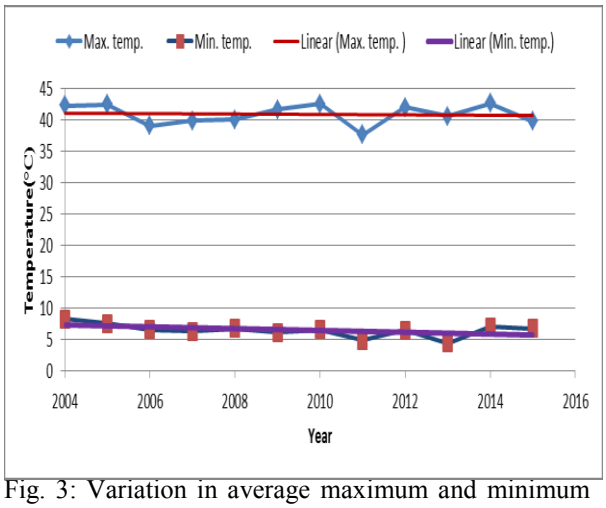

Fig. 3: Variation in average maximum and minimum temperature, 2004-2015.

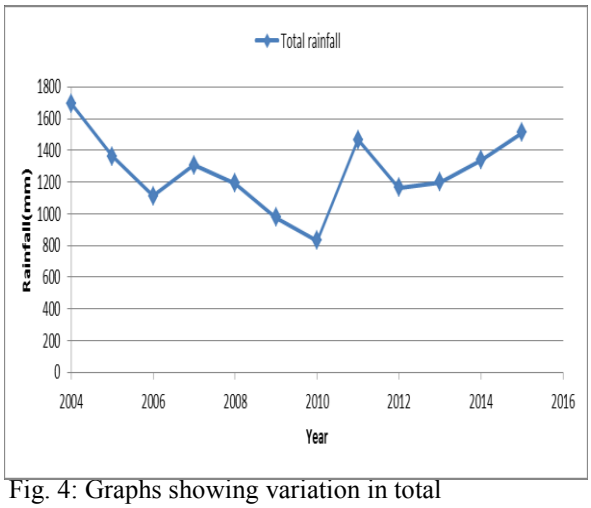

Fig. 4: Graphs showing variation in total rainfall, 2004-2015.

Effect on Crop Production

From figure 5, it is found that, maximum temperature shows a positive trend on yield of Aus rice. From 2010 to 2011, increase in maximum temperature of 1.69°C increased yield from 2.3 to 2.76 metric ton/ha. On the other hand, decrease in minimum temperature increases the yield. From figure 6, it can be shown that, rainfall trend doesn't play any dominant role on yield of Aus rice.

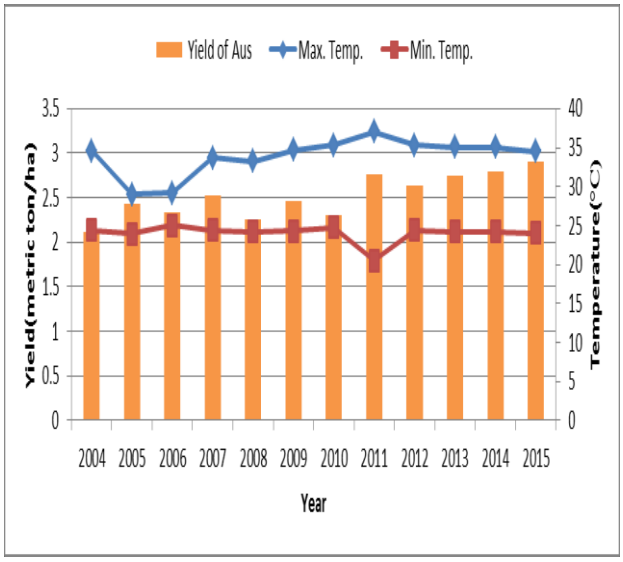

Fig. 5: Combined graph for Aus rice yield and temperature, 2004-2015

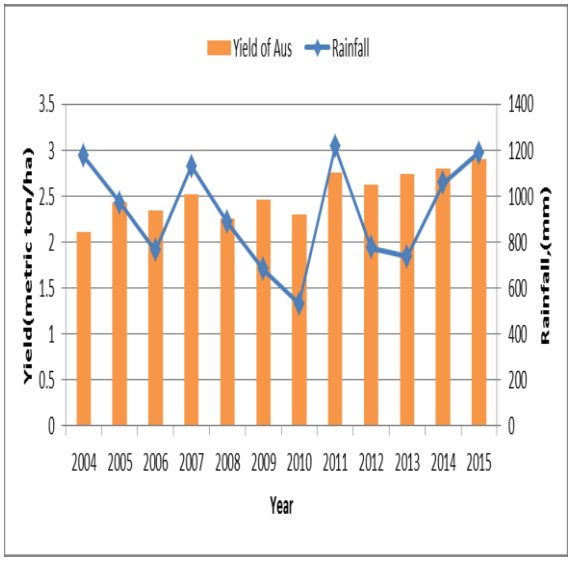

Fig. 6: Combined graph for Aus rice yield and rainfall, 2004-2015

In case of Aman rice, both maximum and minimum temperature shows positive influence on yield of Aman rice (Figure 7). Effect of rainfall is not much prominent for yield of Aman rice (Figure 8).

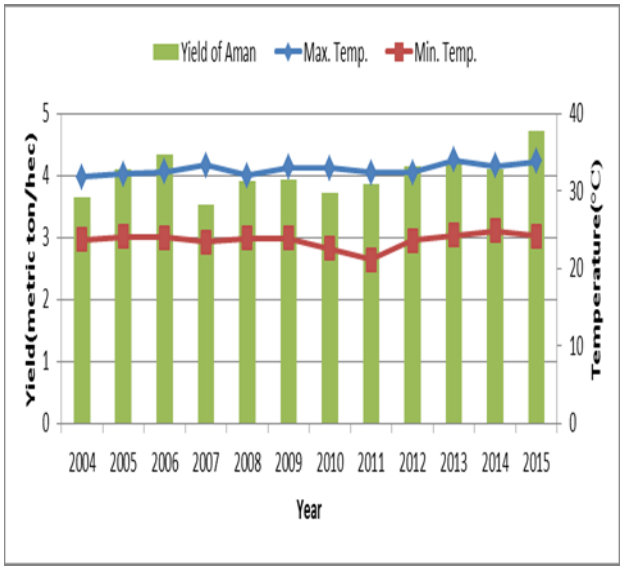

Fig. 7: Combined graph for Aman rice yield and temperature, 2004-2015

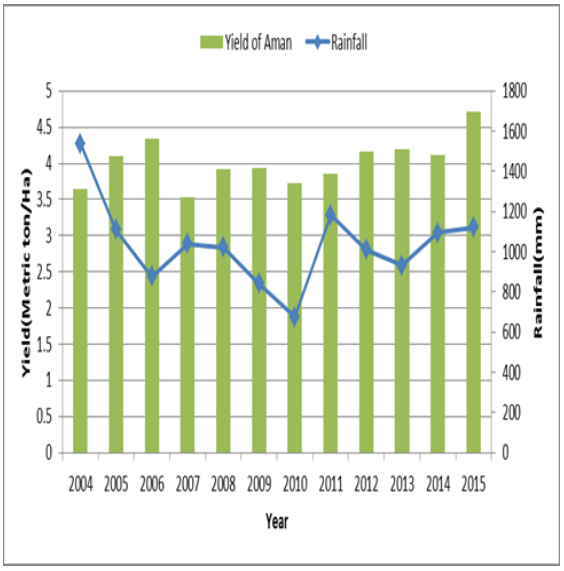

Fig. 8: Combined graph for Aman rice yield and rainfall, 2004-2015

In case of Boro rice, maximum temperature shows adverse effect on yield of Boro rice while minimum temperature benefited the yield (figure 9). Rainfall shows positive influence on yield of Boro rice with some exception (figure 10).
In case of wheat, both maximum temperature and minimum temperature adversely affected yield of wheat (figure 11). Rainfall shows positive influence with some exception (figure 12).
In case of potato, maximum temperature shows a positive effect on yield of potato and minimum temperature shows opposite relation with yield (figure 13). Here, influence of rainfall adversely affected yield of potato (figure 14).

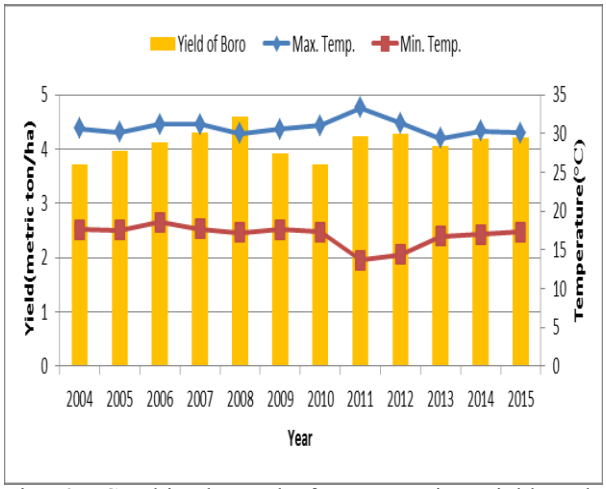

Fig. 9: Combined graph for Boro rice yield and temperature, 2004-2015.

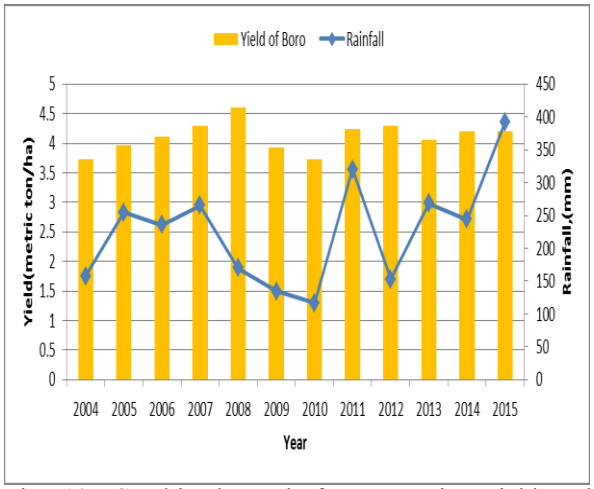

Fig. 10: Combined graph for Boro rice yield and rainfall, 2004-2015.

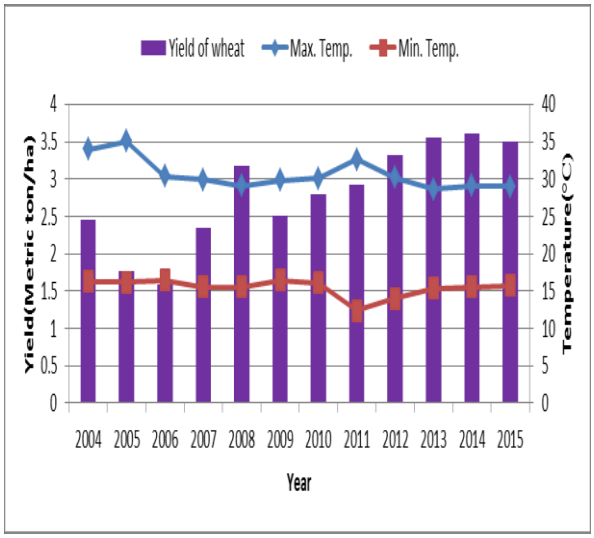

Fig. 11: Combined graph for wheat yield and temperature, 2004-2015.

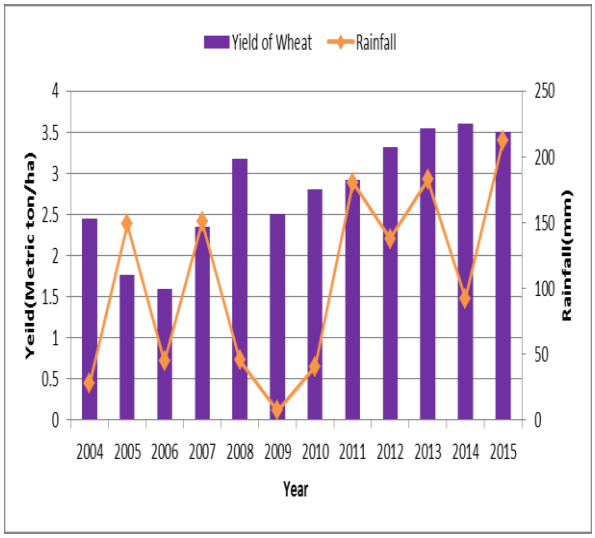

Fig. 12: Combined graph for wheat yield and rainfall, 2004-2015

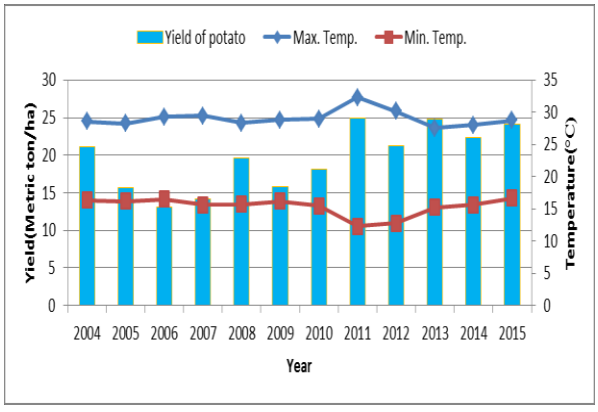

Fig. 13: Combined graph for potato yield and temperature, 2004-2015.

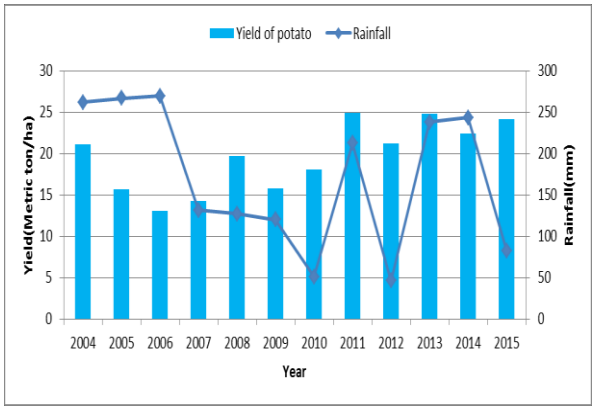

Fig. 14: Combined graph for potato yield and rainfall, 2004-2015.

Effect on Cropland

From the graph, it is clear that there is decreasing trend of cropland area for rice, sugarcane, maize, jute. On the other hand, it shows an increasing trend of cropping area for vegetable, Pulse, mustard, onion, Potato and Wheat.

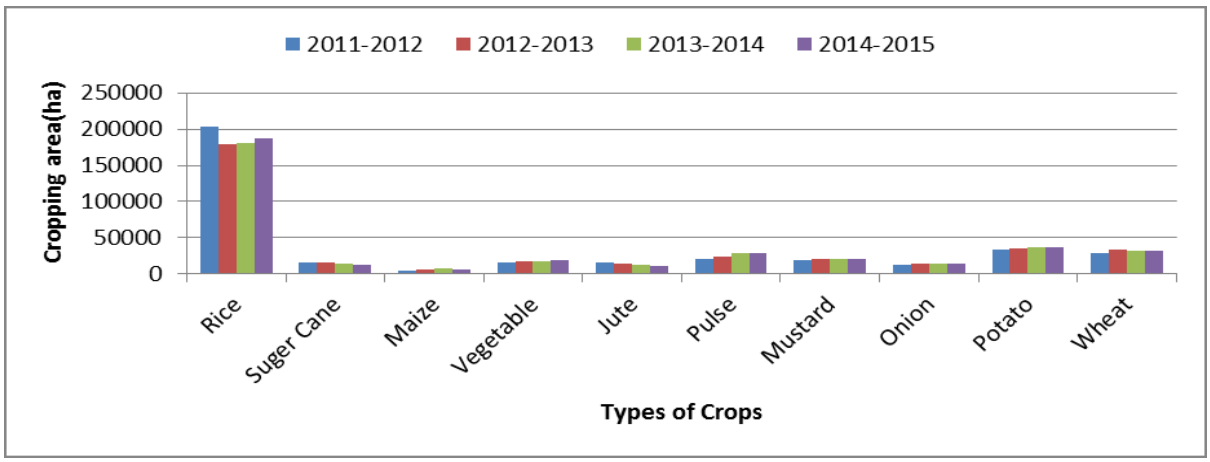

Fig. 15: Graph showing variation in changing pattern of cropping area for different crops

Effect on Wetland Area

Table 2: Changes in wetland areas in Rajshahi district during the dry period

Time Period			Change in wetland area(Ha)	Percentage Change (%)	Change in Wetland area per year(Ha)	Percentage Change per year (%)
From	To	Year Interval				
2006	2011	5	-1114.58	-17.82	-222.92	-3.56
2011	2016	5	-390.87	-7.6	-78.17	-1.52

From the above table, it is found that, there is a decreasing trend in wetland since 2006. During 2006-2011 and 2011-2016, Rajshahi district has lost more than 17% and 7% of its wetland.

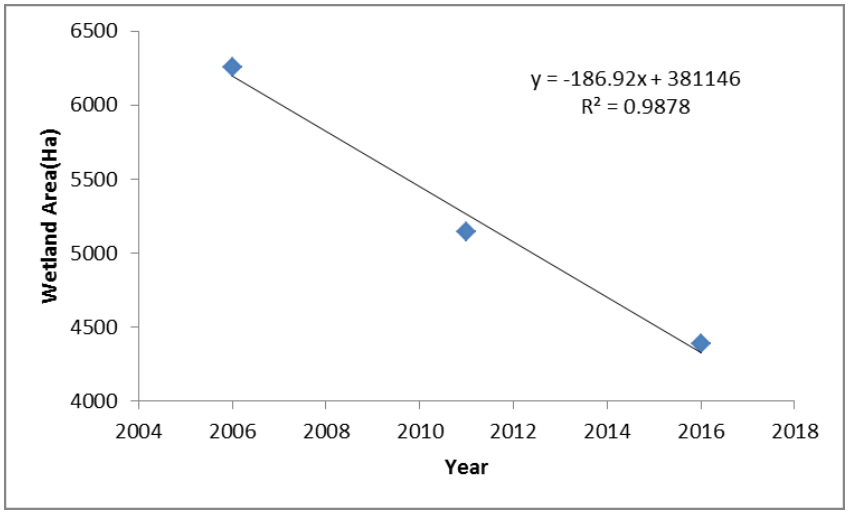

Fig. 16: Change in wetland area in Rajshahi district during the dry period

CONCLUSIONS AND RECOMMENDATION

To investigate the impact of climate change in Rajshahi district, change in crop yield due to temperature and rainfall variation, changing pattern of cropland area and changes in wetland area are the prime concern of this study. In case of Aus and Aman rice, maximum temperature shows positive influence on yield. Boro, wheat and potato are negatively affected by maximum temperature. According to (Sarker et al., 2012), maximum temperature is statistically significant for all rice yields with positive effects on Aus and Aman rice and negative effects on Boro rice. Minimum temperature inversely related to Aus, wheat, and potato yield and positively related with Aman and Boro. According to (Kabir, 2015), an increase in minimum temperature is likely to decrease the yield variability for Aus and Aman rice production while the yield variability for Boro rice is increased. On the other hand, rainfall shows very little on yield of major crops in this region. According to (Sarker et al., 2012), the influence of maximum and minimum temperature is more pronounced with that of rainfall. In case of cropland area, rice, sugarcane, maize have decreasing trend whereas pulse, wheat, potato are becoming more popular as they are more sustainable in changed weather. Sharp decreasing trend in wetland area are observed in Rajshahi district. During 2006 to 2011, about 17% of wetlands have been lost and 2011 to 2016, about 7% wetlands are converted into other types of land. Shopan and Islam (2013) have shown about 15% and 22% of wetland had been lost from 1989 to 2000 and 2000 to 2010 respectively in Rajshahi district. This indicates future desertification in this region. For future study, there also needs consideration for technology development, groundwater, humidity, sunshine, soil property in this region.

ACKNOLEDGEMENTS

The authors would like to acknowledge the contribution of all team members of this project. The first author wishes to acknowledge Dev Dulal Dhali, deputy director, DAE, Rajshahi and Md. Aminul Islam, sub-assistant agriculture officer, DAE office, Rajshahi.

REFERENCES

Basak, J K. 2010. *Climate Change Impacts on Rice Production in Bangladesh: Results from a Model.* Unnayan Onneshan-The Innovators, Dhanmondi, Dhaka-1209, Bangladesh.

Goel, MK; Jain. SK; Agarwal, PK; Assessment of sediment deposition rate in Bargi Reservoir using digital image processing. *Hydrological Sciences Journal*, 47:S1:81-92, DOI: 10.1080/02626660209493024

IPCC 2007. Climate change 2007:impacts, adaptation, and vulnerability, Working Group II, *Inter-governmental Panel on Climate Change (IPCC)*, Geneva.

Islam, MN; Baten, MA; Hossain, MS and Islam, MT. 2008. Impact of few important Climatic Parameters on Aman Rice Production in Mymensingh District. *J. Environ. Sci. & Natural Resources*. 1(2): 49-54.

Kabir, H. 2015. Impacts of Climate Change on Rice Yield and Variability; an Analysis of Disaggregate Level in the Southwestern Part of Bangladesh Especially Jessore and Sathkhira Districts. *Journal of Geography & Natural Disasters*, *2015*

McFeeters, SK. 1996. The use of the Normalized Difference Water Index (NDWI) in the delineation of open water features. *International journal of remote sensing*, *17*(7):1425-1432.

Sarker, MAR, Alam, K, & Gow, J. 2012. Exploring the relationship between climate change and rice yield in Bangladesh: An analysis of time series data. Agricultural System, Elsevier Ltd. 11-16.

Shopan, AA; Islam, AS; Dey, NC and Bala, SK. 2013. Estimation of the changes of wetlands in the northwest region of Bangladesh using Landsat images. *International Conference on Water & Flood Management*, 4-5 October, 2013, BUET, Dhaka-1000, Bangladesh.

DOWNSCALING OF A SELECTED GCM RESULTS FOR GBM BASIN USING SDSM

M. M. Ali*, A. T. M. H. Zobeyer, M. M. Rahaman & G. C. Paul

Department of Water Resources Engineering, Bangladesh University of Engineering and Technology, Dhaka, Bangladesh
**Corresponding Author: wremostafa@gmail.com*

ABSTRACT
The aim of this research is to perform downscaling using statistical downscaling tools, namely the SDSM (Statistical DownScaling Model), to downscale canESM2 GCM output to examine future change of temperature and rainfall for three time periodsis 2030s, 2050s and 2080s.The R^2, NSE and PBIAS statistical parameters shows good agreement with observed and model simulated data. In case of temperature projection, it is found that the range of monthly temperature change of twenty twostations is -1.1^{o}C to 8.3 ^{o}C but 17 stations have their temperature change range between 0.5^{o}C to 3^{o}C. Almost all stations, all season temperature will ascend. Yearly mean temperature will be raised 0.3 to 1.8^{o}C for 2030s, 0.4 to 3.2^{o}C for 2050s and 0.6 to 4.2^{o}C 2080s with respect to base period. The range of sum of monthly rainfall change is -180mm to 240 mm but for 16 stations it is about -50 to +50 mm. The seasonal rainfall % change varies between -48% to +80%. Yearly mean rainfall varies in different stations from -5% to 10% for 2030s, -10% to 30% for 2050s, and -12% to 42% for 2080s. Changes in temperature and rainfall will affect water availability in major rivers. Statistical downscaling scenarios can be applied to the climate change impact assessment to inform strategic decision making and policy.

Keywords: Climate changes; statistical downscaling; temperature and rainfall; canESM2; SDSM

INTRODUCTION
Changes in climate system in recent decades are very much clear because of the observational evidence which confirm the increase in global average air and ocean temperatures (Fischer et al., 2005). These in turn influences the way of living and economy. Specially, the changes in different components (rainfall, temperature, soil moisture, evaporation etc) of hydrological cycle have direct impact on agriculture, productivity of industry, flood, fisheries and many others. Several studies have previously been conducted to assess the impact of climate change on water availability, agriculture, sea level rise etc at different regions (Fischer et al., 2005; Middelkoop et al., 2001). It is evident that Ganges-Brahmaputra-Meghna basin falls under one of the most vulnerable regions with respect to climate changes (Pervez et al., 2015; Masood et al., 2014).So a better understanding of the effects of climate changes on several sectors (e.g., water availability, flood peak etc.) has become necessary to develop resilience to future disasters. Researchers all over the world have already developed some methods to predict different climate change scenarios. General Circulation Model (GCM) is one of the most eminent climate change research advancements and most advanced tool to simulate the climate change response due to change in atmospheric composition. However, GCMs available all over the world have coarse resolution which is not suitable for climate change impact study at a local scale. So these GCM outputs are further downscaled using statistical or dynamic downscaling methods. Dynamic downscaling method is robust, but it requires high computational facilities. Statistical downscaling method uses different statistical methods to obtain higher resolution climate data. Different statistical downscaling methods include Delta change method, Regression methods, Weather generator, Weather typing, etc. In this research statistical downscaling method will be used to downscale different GCMs to study the spatial and temporal change in climatic parameters rainfall and maximum temperature of selected stations in the GBM basins. These downscaled climatic parameters will be helpful for further modeling applications, e.g., hydrologic modeling, flood modeling, morphological modeling etc., to simulate future scenarios.

METHODOLOGY

Study area

The study area consists of three river basins: the Ganges, the Brahmaputra and the Meghna (GBM) basins which are located in south Asia. The drainage area are 96, 2480 km^2 for the Ganges basin, 570,195 km^2 for the Brahmaputra basin and 64871 km^2 for the Meghna basin (Masood et al., 2015). Total areas of 1.6 million km^2 are distributed among India (64 percent), China (18 percent), Nepal (9 percent), Bangladesh (7 percent) and Bhutan (3 percent) (Nepal and Shrestha, 2015). Twenty two weather stationsof GBM basins are chosen to implement the statistical downscaling approach to generate sets of temperature and rainfall projections to assist regional to local scale climate change impact studies. The map of the study area and selected stations for downscaling is shown in Fig1.

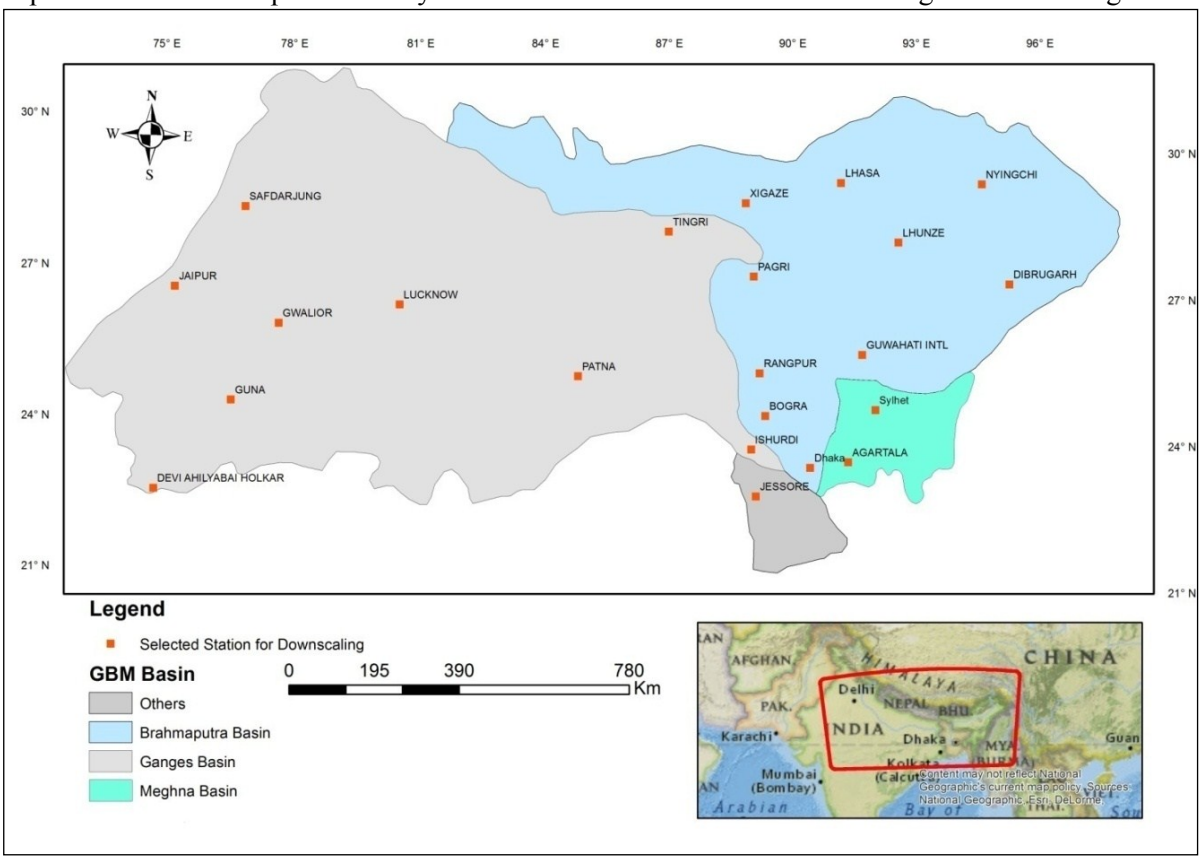

Fig 1: The map of study area and selected stations for downscaling

Data collection

Two distinct sets of data, observed data and synthetic data which include climate model data and reanalysis data are collected for this study. Observed data were collected from Bangladesh Water Development Board (BWDB) and National Climate Data Center (NCDC). Synthetic data were collected from the US National Centers for Environmental Prediction (NCEP)and Canadian Centre for Climate Modelling and Analysis (CCCMA).

Statistical Downscaling (SDSM)

CanESM2 (Canadian Earth System Model) GCM model resultswereselected for downscaling rainfall and temperature future scenarios of GBM basins. The Statistical Downscaling Model (SDSM), developed by Wilby et al. (2002), is used in this study.It is aopen source software. The SDSM is developed on usinga combination of Multiple Linear Regression (MLR) and the Stochastic Weather Generator (SWG) model. The MLR method generates statistical/empirical relationships between NCEP predictors and predictands during the screening process of predictors, and the calibration process of SDSM results in some regression parameters. These parameters, along with NCEP and GCM predictors, are used to generate a maximum of 100 daily time series to fit closely with the observed data during validation, and twenty time series are considered as the standard, a precedent set

by other studies as well (Wilby et al., 2002, Gagnon et al., 2005 and Chu et. al., 2010).First step of statistical downscaling is data processing that is done to make the data useable for SDSM input.To develop SDSM, two kinds of daily time series are needed: NCEP predictor daily time series and observed daily time series (Huang et al., 2011). Second and the most important process of statistical downscaling is screening of predictor variables for the predictand to calibrate and validate the model. Predictor variables are selected on basis of a combination of the correlation matrix, partial correlation, and P-value. In this study most used predictor for temperature and rainfall projection are s500, temp and p8_v, p8_z respectively.

RESULTS AND DISCUSSIONS

Calibration and validation of SDSM model for maximum temperature

Table 1 shows all the statistical parameters of all stations for calibration and validation of maximum temperature. The values of R^2range between 0.95 to 0.99 for calibration and 0.91 to 0.99 for validation of all 22 stations. The NSE range is between 0.90 to 0.99 for calibration and 0.76 to 0.99 for validation of all 22 stations. The percentage (%) BIAS range is between -0.07 to 4.25 for calibration and 0.05 to 7.83 for validation of all 22 stations.Based on table 1 it can be concluded that for all 22 stations, the agreement between the modeled and observed maximum temperature is good.

Table 1: Summary statistics for the calibration and validation of maximum temperature for different stations

Stations Name	Calibration			Validation		
	NSE	R^2	PBIAS	NSE	R^2	PBIAS
Bogra	0.96	0.96	0.22	0.92	0.93	-0.94
Jessore	0.94	0.95	-0.25	0.91	0.94	0.44
Rangpur	0.92	0.95	-0.07	0.88	0.96	-0.58
Dhaka	0.97	0.97	-0.10	0.95	0.96	0.85
Sylhet	0.91	0.96	-0.96	0.76	0.91	0.57
Tingri	0.97	0.99	4.25	0.95	0.99	7.83
Pagri	0.97	0.98	3.34	0.95	0.98	6.78
Lhunze	0.98	0.99	-2.38	0.98	0.98	0.91
Xigaze	0.96	0.97	1.71	0.96	0.96	1.53
Guna	0.90	0.95	3.41	0.90	0.92	1.55
Devi	0.97	0.99	1.74	0.93	0.97	2.57
Dibrugarh	0.96	0.97	-0.62	0.95	0.98	0.05
Gwalior	0.98	0.98	0.49	0.98	0.98	0.17
Ishurdi	0.98	0.99	0.14	0.77	0.93	-2.41
Jaipur	0.99	0.99	-0.61	0.99	0.99	-0.55
Lhasa	0.99	0.99	0.68	0.99	0.99	0.75
Lucknow	0.99	0.99	0.35	0.98	0.98	-0.43
Nyingchi	0.99	0.99	-1.92	0.99	0.99	0.52
Patna	0.98	0.98	0.50	0.98	0.98	0.17
Arartala	0.97	0.97	0.16	0.89	0.94	1.94
Gowhati	0.98	0.98	-0.18	0.92	0.93	1.06
Safdarjun	0.98	0.99	1.50	0.97	0.98	2.45

Calibration and validation of SDSM model for rainfall

Table 2 shows all the statistical parameters for calibration and validation of rainfall. The R^2range is between 0.95 to 0.99 for calibration and 0.75 to 0.99 for validation of all 22 stations. The NSE range is between 0.88 to 0.99 for calibration and 0.69 to 0.99 for validation of all 22 stations. The percentage (%) BIAS range is between -0.33 to -16.99 for calibration and -0.65 to -13.25 for validation of all 22 stations. Based on table 2 it can be concluded that for all 22 stations, the agreement between the modeled and observed rainfall is good.

Table 2:Summary statistics for the calibration and validation of rainfall for different stations

Stations Name	Calibration			Validation		
	NSE	R^2	PBIAS	NSE	R^2	PBIAS
Bogra	0.97	0.99	8.85	0.95	0.96	5.11

Jessore	0.89	0.95	-6.86	0.88	0.92	-4.55
Rangpur	0.98	0.97	-2.89	0.97	0.98	6.07
Dhaka	0.98	0.98	1.99	0.97	0.97	-0.76
Sylhet	0.98	0.99	7.12	0.99	0.99	-2.61
Tingri	0.99	0.99	0.99	0.99	0.99	-0.65
Pagri	0.93	0.93	-0.33	0.92	0.95	-5.26
Lhunze	0.98	0.98	4.30	0.98	0.99	7.86
Xigaze	0.98	0.98	-4.31	0.87	0.88	7.95
Guna	0.95	0.96	-5.64	0.94	0.98	12.95
Devi	0.98	0.98	-0.62	0.98	0.98	4.26
Dibrugarh	0.88	0.96	-16.99	0.69	0.75	-13.25
Gwalior	0.94	0.95	-3.88	0.92	0.92	-5.02
Ishurdi	0.95	0.95	-4.25	0.87	0.90	1.11
Jaipur	0.95	0.97	-11.75	0.96	0.98	-9.97
Lhasa	0.94	0.95	10.22	0.95	0.96	11.79
Lucknow	0.96	0.96	-5.25	0.84	0.89	16.36
Nyingchi	0.96	0.96	1.13	0.98	0.98	1.46
Patna	0.97	0.98	1.99	0.94	0.96	9.85
Agartala	0.99	0.99	1.6	0.96	0.96	-2.79
Gowhati	0.97	0.97	4.13	0.95	0.96	2.76
Safdarjun	0.97	0.98	0.53	0.97	0.98	4.26

TEMPERATURE PROJECTIONS

The monthly maximum temperature, percentage changes of seasonal maximum temperature and changes in annual mean maximum temperaturewere projected for the future time periods of 2030s (2021 to 2040), 2050s (2041 to 2060) and 2080s (2071 to 2090) with respect to baseline (1986 to 2005) for RCP4.5 and RCP8.5 scenarios of 22 stations.

Changes in monthly maximum temperature

The range of maximum temperature change is -1.1^{o}C to 8.3 ^{o}C but for 17 stations maximum temperature changes are in the range between 0.5^{o}C to 3^{o}C. Table 3 shows the monthly maximum temperature ranges of 2030s; 2050s and 2080s for scenarios RCP4.5 and RCP8.5.

Table 3: Ranges of monthly maximum temperature changes in ^{o}C of 30s; 50s and 80s for RCP 4.5 and RCP 8.5

Time period	RCP4.5	RCP8.5
2030s	-0.75 to 5.1	-0.7 to 5.2
2050s	-0.8 to 6.0	-0.93 to 6.8
2080s	-1.1 to 7.5	-0.4 to 8.3

Changes in seasonal maximum temperature

Four seasons, e.g., winter, spring, summer and autumn consist of December to February, March to May, June to August, and September to November respectively. The range of maximum temperature changes in winter, spring, summer, autumn are -0.54^{o}C to 6.39^{o}C, 0.39^{o}C to 5.04^{o}C, 0.02^{o}C to 7.79^{o}C and -0.65^{o}C to 4.83^{o}C respectively.Table 4 shows the seasonal maximum temperature ranges of 2030s; 2050s and 2080s for different scenarios RCP4.5 and RCP8.5.

Table 4:Ranges of seasonal maximum temperature changes in ^{o}C of 30s; 50s and 80s for RCP 4.5 and 8.5

Years	2030s		2050s		2080s	
Season	RCP4.5	RCP8.5	RCP4.5	RCP8.5	RCP4.5	RCP8.5
Winter	-0.54 to 2.73	-0.52 to 3.13	-0.39 to 3.95	-0.46 to 4.27	-0.33 to 3.79	-0.43 to 6.39
Spring	0.12 to 2.23	-0.28 to 2.92	0.06 to 3.71	-0.39 to 3.41	-0.09 to 3.21	-0.39 to 5.04
Summer	0.02 to 3.21	0.05 to 3.27	0.11 to 2.78	0.06 to 4.97	0.09 to 4.75	0.13 to 7.79
Autumn	-0.25 to 2.58	-0.34 to 3.1	0.04 to 2.57	-0.65 to 3.03	-0.64 to 3.25	-0.06 to 4.83

Changes in annual mean maximum temperature

Yearly maximum temperature will be raised in the range of 0.1^{o}C to 2.3^{o}C for 2030s, 0.3^{o}C to 3.2^{o}C for 2050s and 0.2^{o}C to 5.2^{o}C2080s respectively with respect to the base period.

RAINFALL PROJECTIONS

As like temperature projection, the change of monthly rainfall, percentage changes of seasonal rainfall and yearly mean rainfall were projectedfor the future time periods of the 2030s (2021 to 2040), 2050s (2041 to 2060) and 2080s (2071 to 2090) with respect to baseline (1986 to 2005) for RCP4.5 and RCP8.5 scenarios of 22 stations.

Changes in monthly rainfall

The rainfall prediction is very much difficult because no similarities is followed by the projection and for different station the changing pattern are different but in case of different scenarios (RCP4.5 &RCP8.5) changing pattern are similar for a selected station. Between 22 selected stations the range of sum of rainfall change is -180 mm to 250mm. Table 5 shows the monthly rainfall ranges of 2030s; 2050s and 2080s for different scenarios RCP4.5 and RCP8.5.

Table 4: Ranges of monthly rainfall changes in mm of 30s; 50s and 80s for RCP 4.5 and 8.5

Time period	RCP4.5	RCP8.5
2030s	-74 to 98	-70 to 92
2050s	-110 to 140	-100 to 130
2080s	-180 to 250	-100 to 220

Percentage Changes of seasonal rainfall

Analysing the results, it is found that the percent changes of sum of seasonal rainfall vary between -48 to +98%. The variation of rainfall changes is higher in summer and autumn compared to winter and spring. Table 6 shows the seasonal rainfall ranges of 2030s; 2050s and 2080s for different scenarios RCP4.5 and 8.5.

Table 5 Ranges of seasonal rainfall changes (in %) of 30s; 50s and 80s for RCP 4.5 and RCP8.5

Season	Winter		Spring		Summer		Autumn	
Time Period	RCP4.5	RCP8.5	RCP4.5	RCP8.5	RCP4.5	RCP8.5	RCP4.5	RCP8.5
2030s	-5 to 18	-2 to 25	-2 to 12	-5 to 16	-20 to 38	-30 to 62	-6 to 40	-4 to 42
2050s	-3 to 20	-3 to 26	-1 to 14	-10 to 20	-30 to 42	-40 to 78	-5 to 62	-5 to 62
2080s	-4 to 22	-5 to 29	-2 to 16	-12 to 42	-40 to 50	-48 to 98	-4 to 80	-6 to 82

Changes in (%) mean annual Rainfall

Yearly mean rainfall varies in different stations from -7.6% to 15% for 2030s -13.1% to 31.8% for 2050s and -17.1% to 42.6% for 2080s respectively. In the projections, the rainfall will be increased for most of the stations except Bogra, Tingri and Agartala.

CONCLUSIONS

The main purpose of this study was to estimate the future scenarios of maximum temperature and rainfall for the GBM basins. At first, we have selected a representative GCM for the GBM basins and downscaled that GCM to study the spatial and temporal change of climate parameter (rainfall and maximum temperature) in local scale.Calibration and validation of 22 gauge stations are made and are evaluated by statistical parameters R^2,NSE and PBIAS.The statistical parameters indicate good agreement between observed and model simulated data.In case of maximum temperature projection, it is found that the range of monthly maximum temperature change is -1.1^{o}C to 8.3^{o}Cbut for 17 stations maximum temperature changes are in the range of 0.5^{o}C to 3^{o}C.The range of maximum temperature change in winter, spring, summer, autumn are -0.54^{o}C to 6.39^{o}C; 0.39^{o}C to 5.04^{o}C; 0.02^{o}C to 7.79^{o}C and -0.65^{o}C to 4.83^{o}C respectively. The changes in yearly mean maximum temperatureare0.1^{o}C to 2.3^{o}C for 2030s, 0.3^{o}C to 3.2^{o}C for 2050s and 0.2^{o}C to 5.2^{o}C 2080s with respect to base period. Here it is observed that yearly mean maximum temperature will be increased gradually with time period.Among 22 selected stations the range of sum of monthly rainfall change is -180mm to 250 mm but 16 stations it is about -50 to +50 mm. The seasonal rainfall % change varies between -48% to +98%. The variation of rainfall changes is higher in summer and autumn compared to winter and spring. Yearly mean rainfall varies in different station from -7.6% to 15% for 2030s -13.1% to 31.8% for 2050s and -17.1% to 42.6% for2080s. Statistical downscaling scenarios can be applied to the climate change impact assessment to inform strategic decision- making and policy.

ACKNOWLEDGMENTS
The authors gratefully acknowledge the grant from the Dutch government for the project 'Scenario Development in IWRM in Bangladesh', provided under the Netherlands Initiative for Capacity Development in Higher Education, NICHE/BGD/155 through NUFFIC.

REFERENCES
Chu,J;Xia,J;Xu,CYandSingh,V.2010.Statisticaldownscalingofdailymeantemperature,panevaporationa ndprecipitationforclimatechangescenariosinHaihe River.*China.Theor.Appl.Climatol*.99(1):149–161.
Fischer, G; Shah, M; Tubiello, FN, and Van Velhuizen, H. 2005. Socio-economic and climate change impacts on agriculture: an integrated assessment, 1990–2080. Philosophical Transactions of the Royal Society of London B: Biological Sciences, 360(1463):2067-2083.
Gagnon,S;Singh,B;Rousselle,JandRoy,L.2005.AnapplicationoftheStatisticalDownScalingModel(SDS M)tosimulateclimaticdataforstreamflow modelling in Québec.Can.WaterResour.J.30(4):297–314.
Huang,J;Zhang,J;Zhang,Z;Xu,C;Wang,BandYao,J.2011.EstimationoffutureprecipitationchangeintheY angtzeRiverbasinbyusingstatisticaldownscalingmethod. *Stoch.Environ.Res.RiskA*25(6),781–792.
Karl, TR. 2003. Modern Global Climate Change. Science, 1090228(1719), 302.
Masood, M; Yeh, PJ F; Hanasaki, N and Takeuchi, K. 2014. Model study of the impacts of future climate change on the hydrology of Ganges–Brahmaputra–Meghna (GBM) basin. *Hydrology and Earth System Sciences Discussion.* 11(6): 5747-5791.
Nepal, S and Shrestha, AB. 2015. Impact of climate change on the hydrological regime of the Indus, Ganges and Brahmaputra river basins: a review of the literature. *International Journal of Water Resources Development.* 31(2):201-218.
Middelkoop, H; Daamen, K; Gellens, D; Grabs, W;Kwadijk, JC; Lang, H and Wilke, K. 2001. *Impact of climate change on hydrological regimes and water resources management in the Rhine basin. Climatic change.* 49(1-2): 105-128.
Pervez, M. S., and Henebry, G. M. (2014). Projections of the Ganges–Brahmaputra precipitation—Downscaled from GCM predictors. *Journal of Hydrology*.517: 120-134.
Wilby, RL; Dawson, CW; Barrow,EM.2002.SDSM—a decision support tool for the assessmentofregionalclimatechangeimpacts.*Environ.ModelSoftw*.17(2):145–157.

AN EXPERIMENTAL STUDY ON DUMPING OF BANK PROTECTION MATERIALS UNDER FLOWING WATER

M. Jahan[1*], R. Sharmin[1], M. A. Rahman[2] & M. M. A. Chowdhury[3]

[1]*Department of Water Resources Engineering, Bangladesh University of Engineering and Technology, Dhaka, Bangladesh*
[2]*Department of Civil Engineering, Ahsanullah University of Science and Technology, Dhaka, Bangladesh*
[3]*Institute of Water and Flood Management, Bangladesh University of Engineering and Technology, Dhaka, Bangladesh*
[*]*Corresponding Author: momtaz.rumi@gmail.com*

ABSTRACT
In Bangladesh, erosion-deposition, channel shifting and bar development are common phenomenon in large rivers. Bank materials of these rivers are mainly unconsolidated, fine non cohesive and uniformly graded that possesses little resistance against erosive forces generated by the flow of river. This study provides an insight into the behaviour and movement of bank protection materials (CC blocks and Geobags) under flowing water.A physical model was built and tested in the flume. The experiment was carried out for two sets of discharge of 760 m^3/h and 623 m^3/h. Materials were dumped from three different dumping conditions. For most of the materials the lateral displacement was found in the range of 0 to 2 m. Greater the velocity higher is the average lateral displacement of Geobags and more numbers of Geobags are lost. The percentage of loss is more in case of Geobags and is negligible in case of CC blocks.

Keywords: River erosion; dumping characteristics; bank protection; CC block; geobag

INTRODUCTION
Bangladesh is located at the lower part of the three mighty rivers, the Ganges, the Brahmaputra and the Meghna. The basin of these three rivers is called GBM basin. The total catchment of this basin is 1.72 million sq.km covering areas of China, India, Nepal, Bhutan and Bangladesh of which only about 8% lie within Bangladesh. The country is criss-crossed by more than 230 rivers, most of which are either tributary or distributary to the three major rivers. There are 57 trans-boundary rivers which originate outside the boundary of Bangladesh. The total length of the river course is approximately 24000 km and cover 9770 km^2 or 7% of the country. Studies by ISPAN (1995) indicate that the Brahmaputra-Jamuna River widened in the 1834-1992 period from 6.2 to 10.6 km representing a widening of some 27 m/year on average. In 19 years period from 1973-1992 the rate of erosion accelerated to some 140 m/year on average.Ahmed (1989) reached the same conclusion of secular widening of the river. They found the widening at a rate of 172 m/year between 1972 and 1986.Recent analysis of the satellite image by CEGIS (April, 2000) for the last few decades shows that the river is widening along both banks. During the last three decades (1973-2007) the net erosion along the 240 km reach of the Jamuna River were about 77840 ha. The rate of widening of Jamuna River declined from 150 m/year in 1970s and 1980s to 48 m/year in last 14 years.There is active bank erosion almost in all major rivers in the country causing damage to valuable lands, settlements and infrastructures from year to year. Because of high density of population along the river bank a great number of people are also displaced due to this continuous bank erosion process.
In Bangladesh, Standard practices of river bank protection are Groynes and Revetments.Groynes are stone, gravel, rock, earth or pile structures built at an angle to the river bank to deflect flowing water away from the bank. A typical groyne has mainly two parts: head, and shank. The part joining the head and the bank/embankment is the shank. Maximum flow convergence and divergence occur around the groyne head and deep scour holes are formed. So additional protection measures around the head of the groyne are required. The upstream and downstream sides of the shank also need protection but with less amount of erosion resisting materials than the groyne head.Revetment is

artificial roughening of the bank slope with erosion-resistant materials. A revetment mainly consists of a cover layer, and a filter layer. Toe protection is provided as an integral part at the foot of the bank to prevent undercutting caused by scour. The protection can be divided as falling apron or launching apron, which can be constructed with different materials, e.g., CC blocks, rip-rap, and geobags.

Launching apron consists of interconnected elements that are placed horizontally on the floodplain and normally anchored at the toe of the embankment. The interconnected elements are not allowed to rearrange their positions freely during scouring but launch down the slope as a flexible unit. The falling apron, on the other hand, consists of loose elements (e.g., CC blocks, geobags, stones) placed at the outer end of the structure. When scour hole approaches the apron, the elements can adjust their position freely and fall down the scouring slope to protect it. The scouring and undermining process of the developed scour hole in front of the revetment initiates the deformation process at the toe of the revetment.Falling apron is a multi layer system of protection element placed on a sloping or horizontal surface as protection against scour. The individual units are rearranged freely with the morphodynamic forces of the river and stabilize the eroding bank. The single weight of each unit and the volume of protective material within a defined area are the decisive factors for designing an efficient falling apron. Apron is intended to launch when the underlying sand/sandy soil is scoured by the river current so as to form a continuous protection below the water level. A revetment may fail due to instability of the cover layer caused by external loads (current, waves etc.) or internal loads (e.g., due to pore water pressure), insufficient toe protection and instability or improper launching or falling behaviour of the apron materials, sliding of cover layer over intermediate layer, different micro and macro-instability arising from geotechnical characteristics of soil and changed boundary conditions e.g., due to rapid scour development or water level changes.In Bangladesh, different bank protection materials like flexible launching apron of C.C blocks or boulders, rocks, geobags, gabions of galvanized wire mesh filled with bricks or boulders are used. Proper size and amount of falling apron is required for safety of structure. As it is difficult and costly to investigate the launching characteristics of bank protection materials under water, laboratory experiment was done for better understanding of the characteristics. From the experiment, movement and position of materials can be determined.

The main purposes of this study are to investigate the launching characteristics of C.C blocks and geobags with different launching configurations for different weight and width-length.

METHODOLOGY

Fall velocity is the velocity at which a sediment particle falls through a column of still water. In moderately deep streams the velocity is observed at two points; (i) at 0.2 times the depth of flow below the free surface ($V_{0.2}$) and (ii) at 0.8 times the depth of flow below the free surface ($V_{0.8}$). The average velocity in the vertical V is calculated using Eq. (1)

$$V = (V_{0.2} + V_{0.8}) / 2 \qquad (1)$$

$V_{0.2}$ and $V_{0.8}$ are usually measured by current meter. A current meter is so designed that its rotation speed varies linearly with the stream velocity V at the location of the instrument. A typical relationship is defined by Eq. (2)

$$V = aN_s + b \qquad (2)$$

Where,

V = stream velocity at the instrument location in m/s

N_s = revolutions per second of the meter

a, b = constants of the meter

Nominal diameter is the equivalent spherical diameter of a hypothetical sphere of the same volume as a given sediment particle.Neil established a formula for calculating the nominal diameter for stones Eq. (3).

$$D_n = 0.034V^2 \text{ [m]} \qquad (3)$$

Where,

V = mean flow velocity (average over a vertical) in m/s

D_n = nominal stone diameter in m

The angle of slope formed by particulate material under the critical equilibrium condition of incipient sliding or the maximum angle (as measured from the horizontal) at which gravel or sand or granular particles can stand.
Whilst dumping blocks under flowing water, they may be displaced downstream by the distance L as mentioned in Eq. (4).

$$L = 0.25hVD_n^{-0.5} \text{ [m]} \qquad (4)$$

Where,

h = water depth in m
V = mean flow velocity (average over a vertical) in m/s
D_n = nominal stone diameter in m

EXPERIMENTAL SETUP

The experimental model was constructed in a laboratory flume shown in [Fig. 1] following guidelines from literature (BRTC; RRI 2010). It is possible to change its configuration as and when needed for carrying out further studies, using the experimental facilities without any drastic constructive changes. The experimental set-up is shown in [Fig. 2].

Fig. 1: Laboratory Flume

Fig. 2: Experimental set-up (Top View)

A small current meter is used for measurement of flow velocity at low water level, e.g. in laboratories, river models, small canals etc. The meter with the extension rods is usually applied for measurements in shallow creeks or rivers with low current velocities. The highly precise, reinforced spindle bearing and a non-conduct signaling system give the possibilities for measuring flow velocities as of 0.025 m/s. Minimum depth of water required for this device is approximately 4 cm. The digital counter, fitted with a carrier belt, registers up to 10 pulses per seconds.A flow meter is used to measure the amount of water passing through the flow meter during a time period. The total discharge was taken as the sum of the two flow meter used during the experiment. The discharge data was checked frequently as the discharge rate fluctuates frequently. An angle measuring device is used to measure the angle of repose. A sloping platform was prepared to measure the angle of repose. The angle scale is adjusted with a large thumb screw on the handle. When the bubble vial reads level, the angle was set. The angle scale ranges from 0 to 130° in 2° increments. The rise scale ranges from 0 to 0.8 in 0.05 increments, and above 0.8 it reads in fixed increments up to 2.0.The lateral displacement was determined with the help of a linear scale. After dumping of CC blocks and geobags, lateral displacement of each cc block and geobag was measured. The materials were considered as lost when the lateral displacement was more than 3 m.Different stages of the experiments are shown from [Fig. 3] to [Fig. 8].

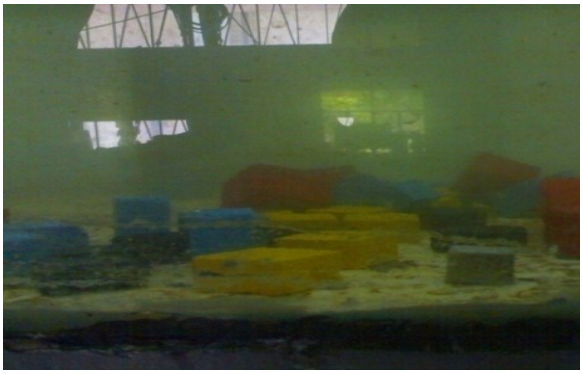

Fig. 3: Dumping of CC blocks

Fig. 4: Dumping of geobags

Fig. 5: Discharge measurement

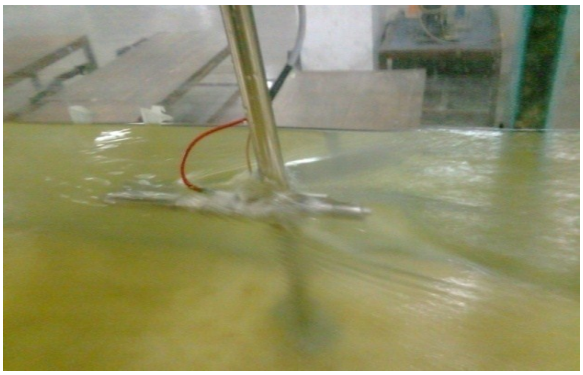

Fig. 6: Velocity measurement

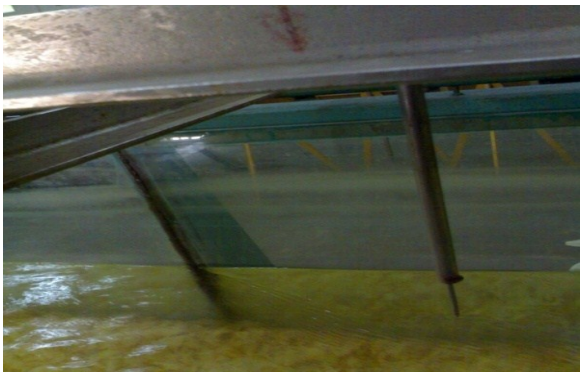

Fig. 7: Depth measurement

Fig. 8: Lateral displacement measurement

RESULTS AND DISCUSSIONS

The experiment was conducted with two set-ups of velocity 0.582m/s and 0.577 m/s. Average lateral displacement of CC blocks was found 0.61 m when dumped from the experimental horizontal platform at a water depth of 0.40 m for five different block configurations. Average lateral displacement of CC blocks was found 0.66 m when dumped from the sloping platform at a water depth of 0.40 m and at an angle of 38o for five different block configurations. Average lateral displacement of CC blocks was found 0.57 m when dumped from the water surface and at an angle of 0o for five different block configurations. Average lateral displacement is greater when CC blocks are dumped at the angle of repose of 38o. Average lateral displacement of CC blocks was found 0.58 m when dumped one at a time for different block and launching configurations. Average lateral displacement of CC blocks was found 0.65 m when dumped five at a time for different block and launching configurations. Average lateral displacement of CC blocks was found 0.61 m when dumped ten at a time for different block and launching configurations. Average lateral displacement is greater when CC blocks are dumped ten at a time. Average lateral displacement of CC blocks was found 0.66

m from the experiment and theoretically the displacement was 0.583 m. Average lateral displacement of Geobags was found 3.73 m when dumped from the experimental platform at a water depth 0.40 m, at the velocity 0.582 m/s and 70% bags were lost. Average lateral displacement of Geobags was found 3.65 m when dumped from the water surface at the velocity 0.582 m/s and 70% bags were lost. Average lateral displacement of Geobags was found 3.7 m when dumped from the experimental platform at a water depth 0.40 m, at the velocity 0.577 m/s and 55% bags were lost. Average lateral displacement of Geobags was found 4.38 m when dumped from the water surface at a water depth 0.40 m, at the velocity 0.577 m/s and 60% bags were lost. Greater the velocity higher is the average lateral displacement of Geobags and more numbers of Geobags are lost. The percentage of loss is more in case of Geobags and is negligible in case of CC blocks.

CONCLUSIONS

For smaller velocity or still water, percentage loss of materials is less than higher velocity. Average lateral displacement is greater when CC blocks are dumped at the angle of repose of 38^{o}. Average lateral displacement is greater when CC blocks are dumped ten at a time. The percentage of loss is more in case of Geobags and is negligible in case of CC blocks. Greater the velocity higher is the average lateral displacement of Geobags and more numbers of Geobags are lost.

The experiment was carried out for fixed bed condition and doesn't represent any particular river problem, only deals with laboratory cases. The experiment was conducted with two set-ups of velocities with five different sizes of CC blocks. Further study can be carried out for other sizes and velocities. This study may be applied for a particular alluvial river to assess the applicability for field condition.

REFERENCES

Bhuiyan, AMTH. 2009. *A Study on the Performance of Geo Bags as an Alternative Approach to River Bank and Bed Protection*. M. Engg. Thesis, Department of Water Resources Engineering, Bangladesh University of Engineering and Technology, Bangladesh

ISPAN.1995. *The Dynamic Physical and Human Environment of the Riverine Charlands and Charland*, Socio-economic RRA reports for the Brahmaputra –Jamuna, Meghna, Ganges and Padma rivers, and the charland flood proofing study, prepared for Flood Plan Coordination Organization (FPCO), Dhaka, Bangladesh

CEGIS.2000.*Morphological dynamics of the Brahmaputra –Jamuna River*, Research Report, Environmentand GIS Support project for water sector planning (CEGIS and Delft Hydraulics), Ministry of WaterResources, Government of Bangladesh, Dhaka

Ahmed, N. 1989. *Study of Some Bank Protection Works in Bangladesh*. MSc. Engg. Thesis, Department of Water Resources Engineering, Bangladesh University of Engineering and Technology, Bangladesh

BRTC, BUET.2008. *Design Guidelines and Manual for Riverbank Protection works*, Report prepared for BWDB

River Research Institute (RRI). 2010. *Additional Tests to Carryout Investigation Regarding Performance of Falling Aprons, Drop Tests for Dumping of Geo Bags and Outflanking Problems by Physical Modeling to Address the Bank Erosion Problems of Bangladesh*, Draft final report prepared for BWDB.

SPATIO-TEMPORAL CHARACTERISTICS OF RAINFALL AND TEMPERATURE IN BANGLADESH

K. Roy*, M. Kumruzzaman & A. Hossain

Department of Civil Engineering, Rajshahi University of Engineering and Technology, Rajshahi, Bangladesh
**Corresponding Author: roykeya0944@gmail.com*

ABSTRACT
This study deals with some available rainfall and temperature data for 31 stations of Bangladesh. Data for rainfall and temperature are collected during 1971 to 2012 time periods. Data of number of plantation and industries are also collected from the respective organizations. Annual rainfall, highest maximum and minimum annual temperatures have been analyzed by least square method. From the analysis it is found that, during study period the maximum rainfall occurred at Teknaf. On the other hand, minimum rainfall is found at Rajshahi. In most of the cases, the temperature of northern part is generally higher than the southern part of the country. From present study it has observed that the number of tree plantation was insufficient to reduce climatic degradation in Rajshahi region. Because of increasing the number of industries in Rajshahi, Dhaka, Khulna and Chittagong divisions, climatic parameters changed intensely in the following regions in last 14 years rather than the first and second 14 years which consequences the vulnerable threat to our modern civilization.

Keywords: climatic change; climatic data; least square method; regression equation; contour map

INTRODUCTION
Climate in a narrow sense is usually as the 'average weather', or more rigorously, as the statistical description in terms of the mean and variability of relevant quantities over a period of time.Climatic variability refers to variations in the mean state and other climate statistics (standard deviations, the occurrences of extremes, etc.) on all temporal and spatial scales beyond those of individual weather events (Ahmed, A.U. 2006). Climate change in Bangladesh is an extremely crucial issue and according to National Geographic, Bangladesh ranks first as the nation most vulnerable to the impacts of climate change in the coming decades. The main objectives of this study are as follows:

i) To study the spatio-temporal characteristics of annual rainfall in Bangladesh.
ii) To study the spatio-temporal characteristics of highest maximum and lowest minimum annual temperature.
iii) To find the effect of plantation and industrialization on different climatic parameters.

METHODOLOGY
Rainfall, temperature (1971-2012) data were divided into three periods, used for different analysis to perform this study at different stations. Less industrialization period is taken as first period (1971-1984), moderate industrialization period is taken as second period (1985-1998) and modern industrialization period is taken as third period (1999-2012). The daily rainfall, temperature (maximum, minimum), data were collected from the Bangladesh Meteorological Department (BMD) at 31 stations of Bangladesh for 42 years (1971-2012).

Plantation data of different years is collected from Barind Multipurpose Development Authority (BMDA) for Rajshahi division. Number of industries of different years is collected from Bangladesh Small & Cottage Industries Corporation (BSCIC) for Rajshahi, Dhaka, Khulna and Chittagong division.

To analysis the data of climatic parameters the least square method has been used where the regression equations show the variations of annual rainfall and temperature with time (Garg, S. K., 1976). This resulting curve is called a regression line of Y on X, since Y is estimated from X.

Mathematically, Y = mX + C (Shamsuddin S. 2009)
where, C = constant, m = slope of regression line of Y on the X to the X axis and is called coefficient of regression of Y on X

ANALYSIS OF DATA

Annual rainfall at different stations has been analyzed from 1971-2012, 1971-1984, 1985-1998 and 1999-2012. There are about 186 graphs of 31 stations. Fig.1, Fig.2, Fig.3, Fig.4, Fig.5, Fig.6 shows the analysis of rainfall and temperature data of Rajshahi station.

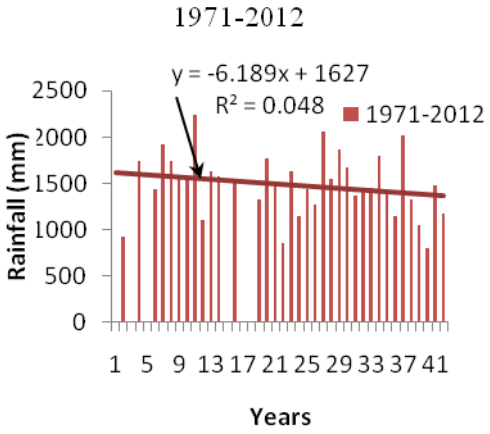

Fig.1: Variation of annual rainfall from 1971-2012 period at Rajshahi

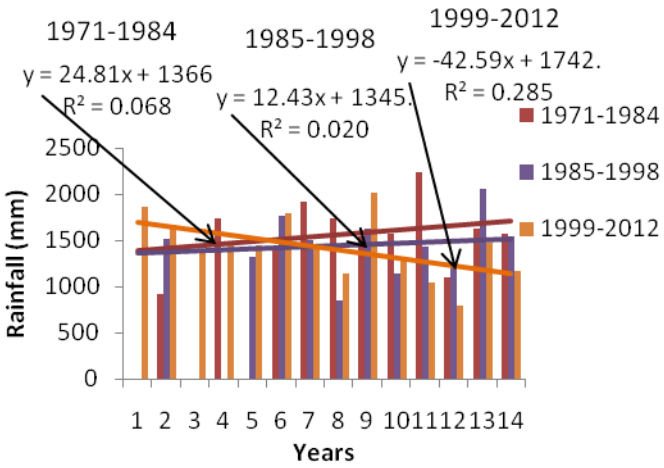

Fig. 2: Variation of annual rainfall from 1971-1984, 1985-1998, 1999-2012 period at Rajshahi

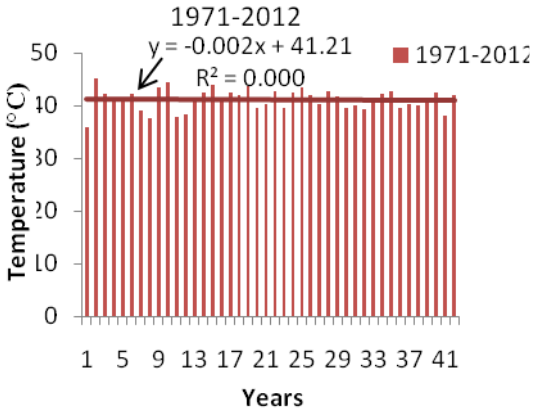

Fig.3: Variation of highest maximum annual temperature from 1971-2012 period at Rajshahi

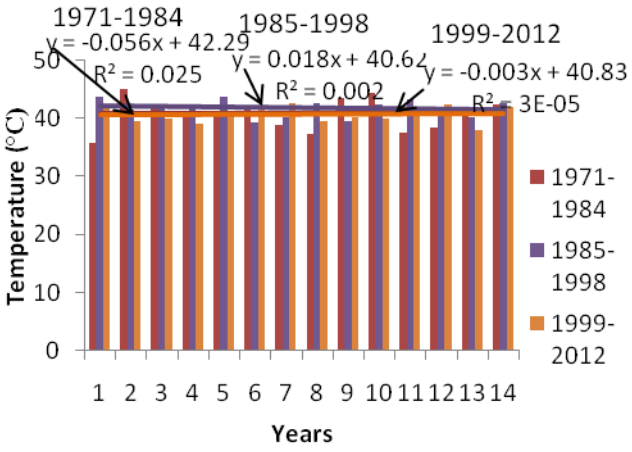

Fig.4: Variation of highest maximum annual temperature from 1971-1984, 1985-1998, 1999-2012 period at Rajshahi

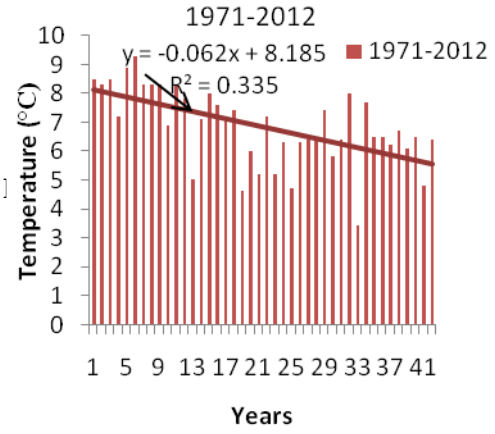

Fig.5: Variation of lowest minimum annual temperature from 1971-2012 period at Rajshahi

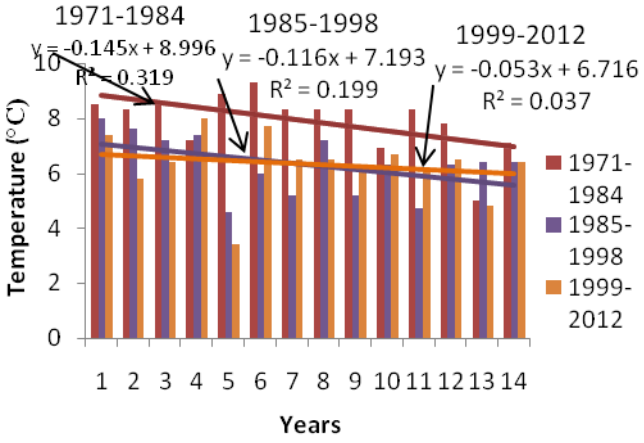

Fig.6: Variation of lowest minimum annual temperature from 1971-1984, 1985-1998, 1999-2012 period at Rajshahi

Fig.7, Fig.8, Fig.9, Fig.10, represents the number of industries of different years of Dhaka, Chittagong, Khulna and Rajshahi divisions.

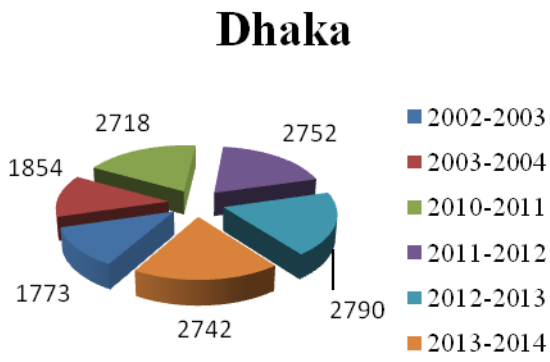

Fig.7 : No. of industries of Dhaka division for different years

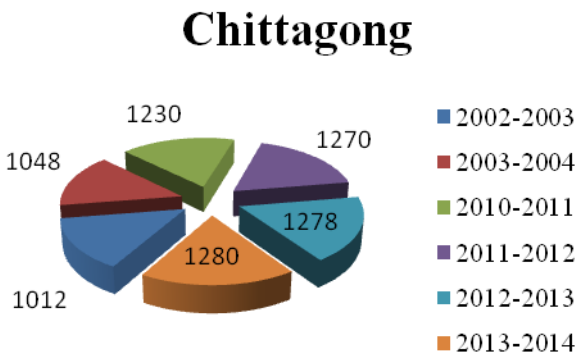

Fig.8 : No. of industries of Chittagong division for different years

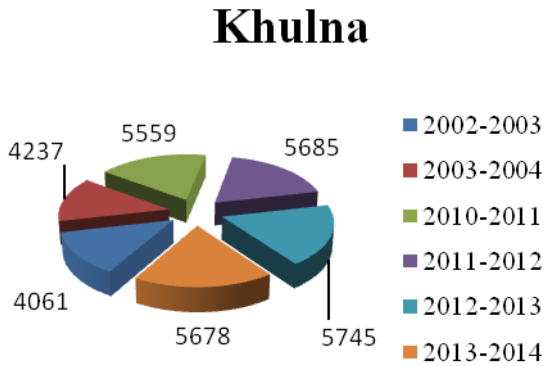

Fig.9 : No. of industries of Khulna division for different years

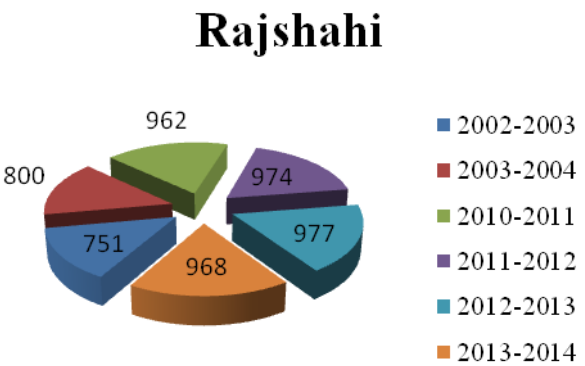

Fig.10 : No. of industries of Rajshahi division for different years

Fig.11, Fig.12, Fig.13 represents the number of existing trees of Rajshahi, Nawabganj and Naogaon regions.

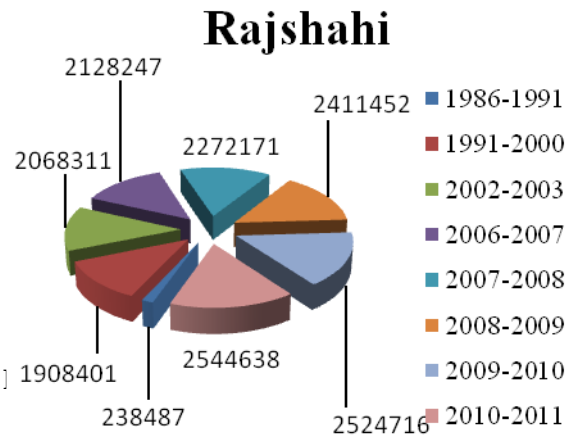

Fig.11: No. of existing trees of Rajshahi region for different years

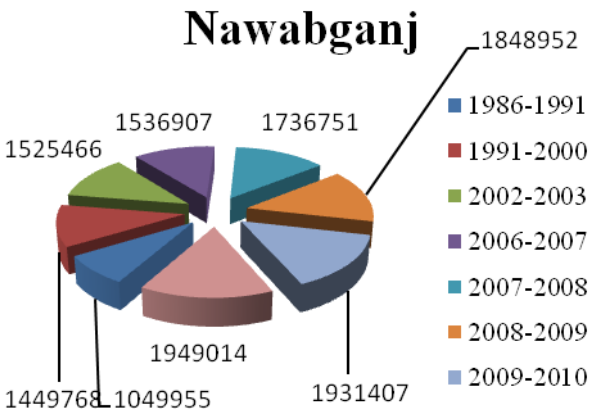

Fig.12 : No. of existing trees of Nawabganj for different years

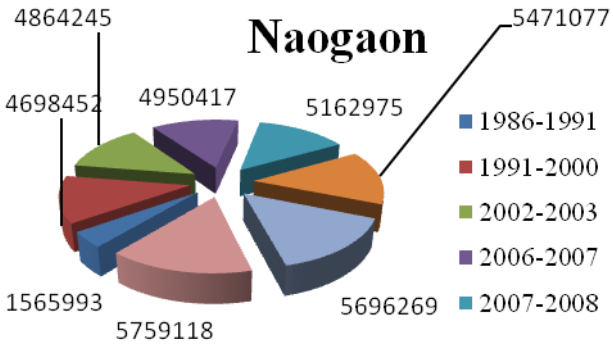

Fig.13 No. of existing trees of Naogaon region for different years

RESULTS & DISCUSSIONS

From the analysis it has been found that among 31 stations for annual rainfall, downward trend at 18 stations, rising trend at 10 stations and nearly constant trend at 3stations. For highest maximum annual temperature downward trend at 12 stations, rising trend at 8 stations and nearly constant trend at 11 stations and for lowest minimum annual temperature downward trend at 16 stations, rising trend at 6 stations and nearly constant trend at 9 stations. From the study it is found that among 31 stations rainfall rate is decreasing in most of the stations. Normally northern part is warmer than the southern part and from the contour map it has found that temperature is increasing from south to north. In the last 14 years number of industries has greatly increased in Bangladesh for this reason it has found from this study that climatic parameters have greatly changed in the last 14 years rather than the first and second 14 years. Table.1, 2, 3, shows the nature of trend of annual rainfall, highest maximum annual temperature and lowest minimum annual temperature of 6 stations among 31 stations for 42 years. It is also found that the trend of annual rainfall is decreasing for 42 years at Rajshahi. Trend of rainfall for first and second 14 years is increasing but for the last 14 years the trend is decreasing. Despite of large plantation the rainfall trend is decreasing. So may be plantation rate is not enough for this region as well as no. of industries has also increased in different divisions. From the total result different maps has drawn to show the overall climatic condition of Bangladesh in terms of rainfall and temperature. Contour maps of these parameters have also drawn (Ahmed, A.U. 2006). Fig, 14, Fig.15, Fig.16, Fig.17, Fig.18 and Fig.19 have represented them.

Table.1 Nature of trend of annual rainfall for 42 years at different stations

Name of stations	Rising Trend			Downward Trend			Nearly constant Trend	Average rate of decrease in Rainfall mm/year	Average rate of increase in Rainfall mm/year
	Start year	Finish year	Diff	Start year	Finish year	Diff			
Rajshahi	-	-	-	1621	1367	254	-	6	-
Bogra	-	-	-	1980	1622	358	-	8.5	-
Dinajpur	-	-	-	2116	1892	224	-	5	-
Rangpur	-	-	-	2801	1889	912	-	22	-
Ishurdi	-	-	-	1755	1346	409	-	10	-
Syedpur	-	-	-	-	-	-	Nearly constant	-	-

Table.2 Nature of trend of highest maximum annual temperature for 42 years at different stations

Name of stations	Rising Trend			Downward Trend			Nearly constant Trend	Mean highest maximum annual temperature
	Start year	Finish year	Diff	Start year	Finish year	Diff		
Rajshahi	-	-	-	-	-	-	Nearly constant	41
Bogra	-	-	-	-	-	-	Nearly constant	39
Dinajpur	-	-	-	-	-	-	Nearly constant	38.9
Rangpur	-	-	-	38.7	36.9	1.8	-	-
Ishurdi	-	-	-	-	-	-	Nearly constant	40.7
Syedpur	-	-	-	-	-	-	Nearly constant	38.3

Table.3 Nature of trend of lowest minimum annual temperature for 42 years at different stations

Name of stations	Rising Trend			Downward Trend			Nearly constant Trend	Mean lowest minimum annual temperature
	Start year	Finish year	Diff	Start year	Finish year	Diff		
Rajshahi	-	-	-	8.1	5.6	2.5	-	-
Bogra	-	-	-	-	-	-	Nearly constant	7.8
Dinajpur	-	-	-	-	-	-	Nearly constant	
Rangpur	-	-	-	-	-	-	Nearly constant	7.5
Ishurdi	-	-	-	7.8	5.5	2.3	-	-
Syedpur	-	-	-	-	-	-	Nearly constant	7.1

Fig. 14 Map of annual rainfall trend at different stations

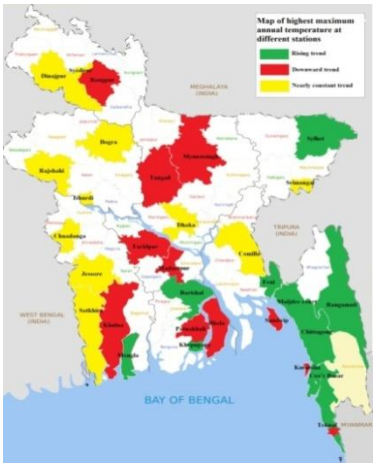

Fig. 15 Map of highest maximum annual temperature at different stations

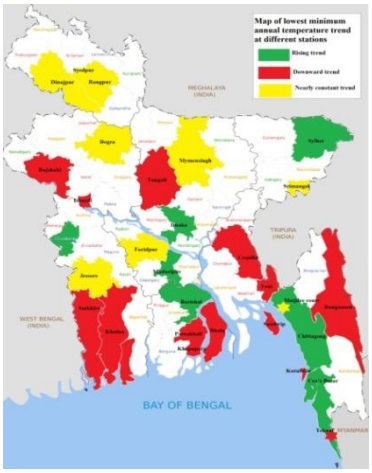

Fig 16 Map of lowest minimum annual temperature at different stations

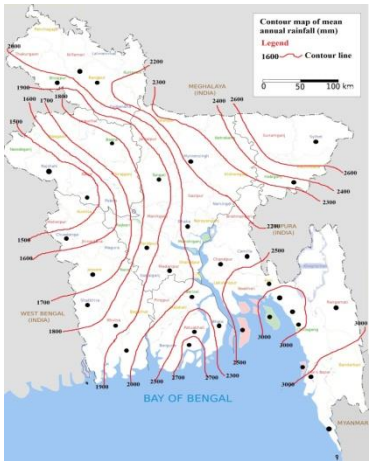

Fig.17. Contour map of mean annual rainfall

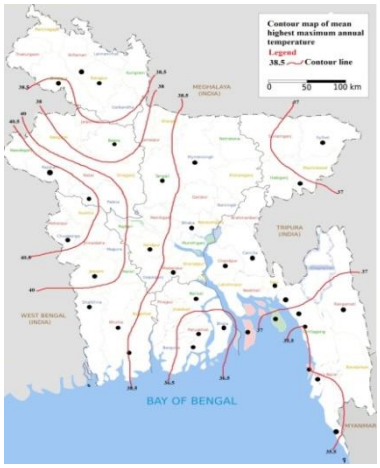

Fig.18. Contour map of mean highest maximum annual temperature

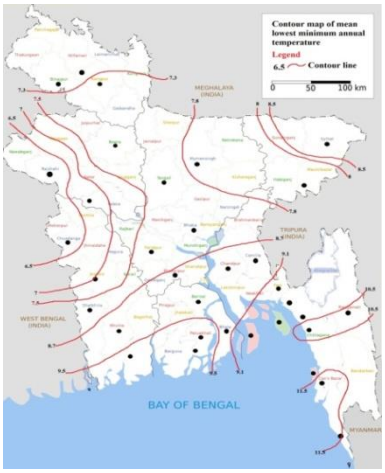

Fig19. Contour map of mean lowest minimum annual temperature

CONCLUSION

Trend of different climatic parameters mainly changed during last 14 years. Average annual rainfall (a.a.r.) varies from 1482 mm at Rajshahi to 4127 mm at Teknaf. The a.a.r. is large in the hilly area i.e. Teknaf, Chittagong, Sylhet, Srimongal and small in the north-western part of the country Highest mean minimum annual temperature varies from 5.9°C at Srimangal to 12°C at Cox's Bazar. Though Rajshahi is not an industrial area, number of industries is increasing day by day. Afforestation of this region seems not to be sufficient. This is one of the reasons of decreasing tendency of rainfall. Decreasing tendency of lowest temperature, increasing tendency of highest temperature have been found in this area. In general, characteristics of different climatic parameters which have impact on climatic degradation have been found in last 14 years period rather than the first and second 14 years periods which may be a vulnerable threat to our modern civilization.

ACKNOWLEDGMENTS

The project was completed under the proper guidance of Dr. Md. Kumruzzaman, Professor, Department of Civil Engineering, RUET, Rajshahi. The author takes this opportunity to thank research guide, Professor Dr. Md. Kumruzzaman for the unstinting efforts and guidance, which made working for this thesis enjoyable. The author is extremely grateful and happy to have him as supervisor.

REFERENCES

Ahmed, A.U. 2006. *Bangladesh Climate Change Impacts and Vulnerability,* A Synthesis. Climate Change Cell, Bangladesh Department of Environment. Dhaka.

Bangladesh Meteorological Department Dhaka, *Different Climatological Data for the period 1971 to 2012 at 31 stations of Bangladesh,*

Briffa, K.R. Van der Schrier, G. and Jones P.D. (2009). *Wet and dry summers in Europe since 1750, Evidence of increasing drought.* International Journal of Climatology, Vol. 29(13), pp. 1894-1905.

Chow, V .T, 1964. *Hand Book of Applied Hydrology*, McGraw-Hill Book Co. New York.

Garg, S. K., 1976. *Irrigation Engineering & Hydraulic Structure*, Khanna Publishers, Delhi.

Raghunath, H. M. 1985. *Hydrology*, New Age International (PVT) Limited, Delhi.

Shamsuddin S. (2009). *Rainfall variability and the trends of wet and dry periods in Bangladesh"*: International Journal of Climatology.

SirajulI., Hasan G M J, Chowdhury, M.A.I., 2005, *International Journal of Environmental Science and Technology*, Vol. 2, No. 4, Winter 2006, pp. 301-308

A STATISTICAL ASSESSMENT OF GROUNDWATER QUALITY IN NILPHAMARI POURASHAVA, NILPHAMARI DISTRICT, BANGLADESH

M. M. A. Chowdhury[1*], M. Jahan[1,] M. N. Sakib[1] & M. A. Rahman[2]

[1]*Institute of Water and Flood Management, Bangladesh University of Engineering and Technology, Dhaka, Bangladesh*
[2]*Department of Civil Engineering, Ahsanullah University of Science and Technology, Dhaka, Bangladesh*
[*]*Corresponding Author: mahabub.iwfm@gmail.com*

ABSTRACT
Groundwater quality is the vital issue in Bangladesh due to extreme value of some parameters. Though the abundance of groundwater is not the problem but concern is in the quality. The present research work deals with the assessment of quality of 15 groundwater samples from Nilphamari Pourashava. In situ measured physical parameters include temperature, pH, Electrical Conductivity (EC), Total Dissolved Solids (TDS). Quality assessment was made through the estimation of major cations(Ca^{2+}, Mg^{2+}, Na^{+}, K^{+} Fe^{total}), and the major anions (HCO_3^-, CO_3^-, SO_4^{2-}, NO_3^-, Cl^-). According to the overall assessment of the basin, all the parameters analysed are below the desirable limits of WHO Facies mapping approach of the groundwater indicate Sodium-Calcium cation facies and Bicarbonate-Chloride-Sulphate anion facies. According to the drinking water quality standards the groundwater of the study area is suitable for public health. The groundwater of the study area is of good quality for irrigation.

Keywords: Groundwater chemistry; inverse distance weight; bar diagram; box and whisker plots, facies mapping.

INTRODUCTION
Water is one of the earth's most important resources for human life. Groundwater has been used to supply living, agricultural and industrial water for a long time in many countries. The water quality depends upon the geological environment, natural movement, recovery and utilization (Senthikumer et al., 2008). Groundwater is a important water supply source in Bangladesh. It is a major source of drinking water in urban Nilphamari area. In this paper an attempt has been made to evaluate the chemistry of groundwater in the Nilphamari pourashava of Nilphamari District. Nilphamari Pourashava is located in the south-western part of Nilphamari District in north-western Bangladesh [Fig. 1]. It is located within the geographical co-ordinates between 25°54′ to 25°58′N latitudes and 88°49′ to 88°53′E longitudes. Physio graphically the study area falls within the Tista river flood plain in the overall physiographic units of Bangladesh. The study area lies on the Northern flood plain of the Tista River. The southern part of this flood plain is a levee. The northern part of the area is influenced by the flow of the Jamuneshwari River. The study area is characterized by moderate rainfall with regional and seasonal variations. The average annual rainfall of the study area of period 1993 to 2008 is about 2095.14 mm. There is excess of rainfall during the rainy season (June to October), which is due to the occasional incursion of cyclonic storms, when heavy rain may fall for several days. The temperature data of the study area of 15 years shows that the temperature varies distinctly both diurnally and seasonally. Maximum temperature recorded in the study area is about 22.4°C to 33.2°C and average minimum temperature varies from 9.8°C to 25°C. In the study area, the highest monthly average humidity was 86.46% in the month of July and the lowest was 71.13 in the month of April during the period of 1993 to 2008.Objectives of the Research Work is to

- To carry out necessary field visits to collect groundwater samples from the study area.
- To carry out detail hydro chemical analysis of groundwater samples.

- Classification on the basis of water chemistry.
- To compare the analytical results with national and international standards for water use in domestic, irrigation and industrial purposes.

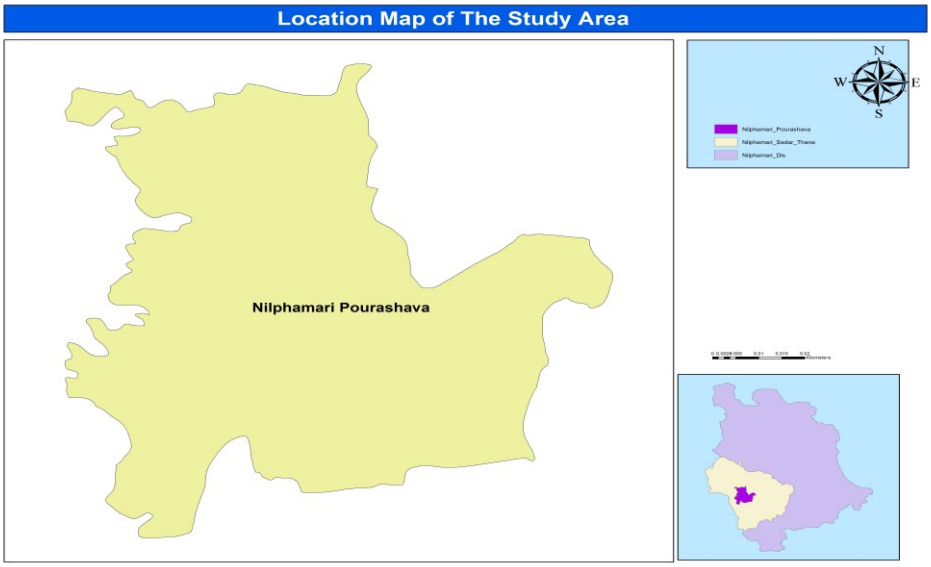

Fig 1: Location Map of the Study Area.

Methodology

Available geologic, climatic, topographic and hydrologic data provided by different organizations related to surface and subsurface water works are used to ascertain the groundwater condition of the studied area. Among the organizations Bangladesh Agricultural Development Corporation (BADC) is one of the most important sources for obtaining this information. Besides, Department of Meteorology, Department of Public Health Engineering (DPHE), Bangladesh water Development Board (BWDB) of Nilphamari district and various published reference reports also served as sources of information and data. In the dry season (2010) the studied area was investigated for several times to know the geological, hydrological and environmental condition prevailing at the surface.Data processing and chemical analysis include data verification and quality control, data entry, data processing and finally the analysis to facilitate the required output generation. The field and laboratory measured parameters has been used to delineate spatial trend. Hydrogeological and hydro-chemical interpretation has been made using necessary hydrogeological and hydro-chemical diagram to decipher the hydro-chemical process taking place in the aquifer. Findings of the total analysis output has compared with national and international water standards for drinking and irrigation purposes to determine their sustainability to use in particular purposes. For the field measurement of pH a portable pH meter (Hanna, HI 7039P) was used and pH of each sample was recorded. The conductivity of a body or mass of fluid of unit length and cross-section at a specific temperature is defined as EC. Measurement of EC was carried out by immersing a conductance cell in water samples and then the EC was recorded from the digital display of the EC meter (Whatman micrometer). Temperature of groundwater samples of the study area was measured by the help of laboratory thermometer. A rapid determination of Total Dissolved Solids (TDS) is made simply by multiplying the measured EC values (in µs/cm) by the constant 0.64 (Todd, 1980). The concentration of some cations (Ca^{2+}, Mg^{2+}, Na^{+}, K^{+}, Fe^{total}) and anions (HCO_3^-, CO_3^-, SO_4^{2-}, NO_3^-, Cl^-,) were determined in the Soil Resources Development Institute (SRDI) of Rajshahi and the Hydrogeology Laboratory of the Department of Geology and Mining, Rajshahi University.

RESULTS AND DISCUSSIONS

The guideline of quality standard values recommended by World Health Organization (WHO, 1984) and Bangladesh Water Pollution control Board (BWPCB, 1976) for drinking water are given in the [Table 1]. From this chart it can be concluded that the parameters as determined show suitability for

drinking and health purposes. Hence the groundwater of the study area is suitable for use as drinking water. From the analysis of the calculated values of EC and SAR of the studied groundwater samples it may be concluded that the groundwater of the study area is of good to medium quality for uses in irrigation purposes.

Table 1: Correlation of groundwater quality in the study area with WHO (1984) and Bangladesh (BWPCB, 1976) standards for drinking purpose

Water quality parameters	WHO standard (1983)		Bangladesh standard (BWPCB, 1976)		Concentration in the study area	
	Max. accept. limit	Max. allow. limit	Max. recom. limit	Max. allow. limit	Min.	Max.
pH	6.5	8.5	6.5	8.5	6.1	7.2
TDS	500	1500	-	1500	32.0	268.8
Total Hardness	100	500	200	500	61.28	197.06
Calcium	75	200	-	-	2.00	44.00
Magnesium	50	150	-	-	10.12	26.08
Sodium	-	200	200	-	0.11	0.56
Potassium	-	-	12	-	0.002	0.022
Bicarbonate	-	-	-	-	3.05	61.00
Chloride	200	600	600	1000	27.28	197.78
Sulfate	200	400	-	400	1.20	2.55

From the analysis of the calculated values of EC and SAR [Table 2] of the studied samples, it may be concluded that the groundwater is good to medium quality for uses in irrigation purposes.

Table 2*:* Values of various hydro-chemical parameters calculated from sample.

Sample No.	PI (meq/l)	SAR (meq/l)	Na%	TH (mg/l)	RSC (meq/l)
HTW-1	1.19	0.05	0.205	161.22	5.80
HTW-2	1.33	**0.14**	1.098	**61.28**	4.26
HTW-3	1.21	**0.03**	**0.194**	125.18	6.98
HTW-4	1.17	0.06	0.483	119.40	**7.25**
HTW-5	1.35	0.04	0.281	195.25	4.97
HTW-6	**0.89**	0.08	0.498	109.15	6.16
HTW-7	1.09	0.11	0.716	103.23	5.32
HTW-8	0.96	0.12	**1.154**	77.72	**4.13**
HTW-9	1.22	0.09	0.700	106.86	4.56
HTW-10	1.02	0.06	0.463	132.55	5.15
HTW-11	1.32	0.06	0.412	184.66	9.56
HTW-12	0.98	0.12	0.873	138.66	6.25
HTW-13	**1.34**	0.05	0.311	**197.06**	5.42
HTW-14	1.06	0.13	0.921	110.58	5.01
HTW-15	0.99	0.06	0.404	166.94	4.98

The Piper Trilinear Diagram (Piper, 1953) is an effective tool in separating hydro chemical analysis data for critical studies with respect to the sources of the dissolved constituents in water (major cations; Ca^{2+}, Mg^{2+}, Na^{+}, K^{+}, Fe^{total} and major anions; HCO_3^{-}, CO_3^{2-}, Cl^{-}, NO_3^{-}, SO_4^{2-}) in waters, modifications in the character of water as it passes through an area, and geochemical problems. The Pipers diagram provides rapid classification of water in to fields according to the combination of dominant cations and anions. The central plotting field (diamond shape) of the trilinear diagram is

divided in lo nine areas and water is classified into nine types depending upon the area in which analysis results fall and the alkali cations (Na^+ and K^+) are called primary constituents and the alkaline earth cations (Ca^{2+} and Mg^{2+}) are called secondary constituents. The strong acid cations ($S0_4^{2-}$, Cl^-) are treated as saline constituents and CO_3^{2-} and HCO_3^- are treated as weak acid. Approximate balancing of these cations and anions determine the chemical character of water [Fig. 5.1].

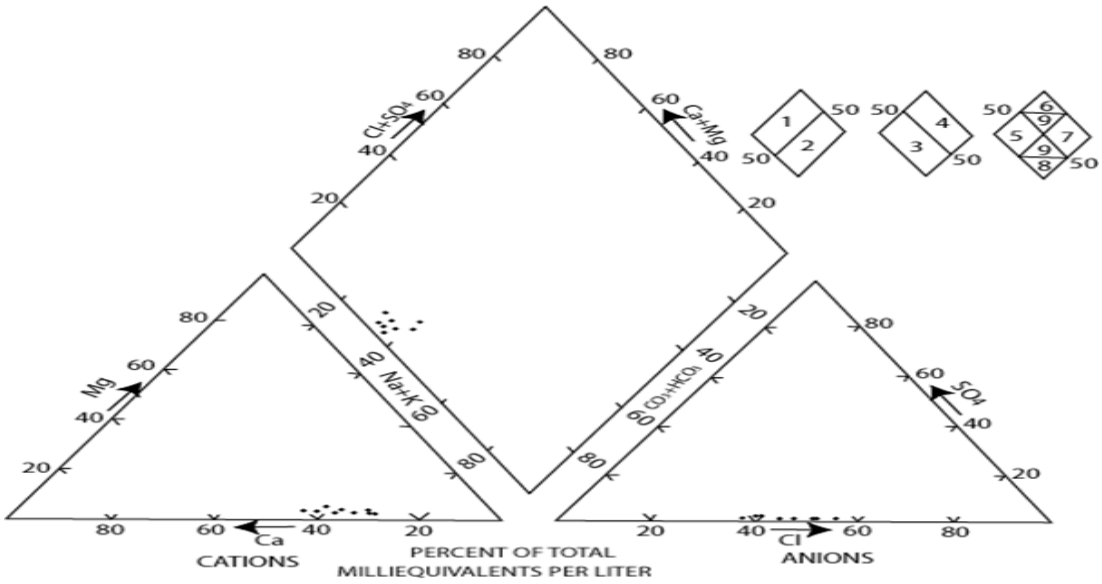

Figure 5.1. Trilinear diagram for groundwater samples from the study area

It is observed that all the groundwater samples collected from the study area show Sodium-Calcium cation facies and Bicarbonate-Chloride-Sulphate anion facies. PH value of the groundwater samples from the study area ranges from 6.1 to 7.2 indicating almost neutral water and suitable for drinking and irrigation purposes. The temperature of groundwater determined in the dry season ranges from 25°C to 27°C. The total dissolved solids (TDS) content of wells ranges from 32.0 mg/l to 268.8 mg/l. The relationship between conductance and TDS depends on the particular ions in solution. Groundwater is classified according to its TDS content (Hem, 1970) [Table. 3]

Table 3: Groundwater classification according to TDS (WHO, 1984)

Water type	**TDS (mg/l)**
Fresh	<1000
Moderately saline	3000-10000
Very saline	10000-35000
Briny	>35000

Concentration of TDS in groundwater of the study area ranges within 1000 mg/l. According to the classification of Hem, WHO standards for TDS (WHO, 1984) (Maximum allowable 500 mg/l and maximum acceptable 1500 mg/l) it could be said that the groundwater of the study area is safe for drinking and irrigation purposes. Water samples have been taken from different shallow and deep tube-wells of the study area are analysed for detailed description of the hydro-chemical changes in groundwater chemistry. Subsurface waters in contacts with sedimentary rocks of marine origin derive most of their calcium from the solution of calcite, aragonite, dolomite, anhydrite, and gypsum. Concentration of calcium in normal portable groundwater generally ranges between 10 mg/l to 100 mg/l. Calcium in health of humans or other animals are needed as much as 1000 mg/l. The calcium concentration in groundwater of the study area ranges from 2.00 mg/l to 44.00 mg/l. Common concentration of magnesium ranges from 1.0 to 40.0 mg/l in drinking water. The Magnesium concentration in groundwater of the study area ranges from 10.12 to 26.08 mg/l, suggesting that the water of the study area is suitable for drinking and irrigation purposes. Sodium unlike the Calcium, Magnesium and Silica is not found as essential constituents of many of common rock-forming

minerals. The primary source of most Sodium in natural water is form the release of soluble product during the weathering of plagioclase feldspars Sodium concentration in fresh water is 10 mg/l. More than 50 mg/l Sodium and Potassium in the presence of suspended matter causes framing. More concentration makes the water brine. Concentration of sodium in groundwater of the study area ranges from 0.11 to 0.56 mg/l. Hence the groundwater of the study area is suitable for drinking and irrigation purposes. Water percolating through evaporate deposits may contain very large quantities derived from the dissolution of sylvite and niter. Its concentration in most drinking water is less than 10 mg/l. In the study area, concentration of potassium ranges from 0.002 to 0.022 mg/l, suggesting that the groundwater of the study area is suitable for drinking and irrigation purposes. Abundant sources of iron exist in the earth's crust. Some of the important minerals and mineral group, which may contain large amounts of iron are pyroxenes, amphiboles, magnetite, pyrite, biotite and garnets. The weathering of these minerals release large quantities of iron in groundwater. The iron (Fe^{total}) concentration in groundwater of the study area ranges from 0.15 to 0.65 mg/l. From the above stated it may be concluded that the groundwater of the study area is suitable for drinking and irrigation purposes.

The properties of alkalinity and acidity are important characteristics of groundwater. The measurement of pH provides values of concentration of H^+ and OH^- in solution. These species contribute to acidity or alkalinity. In almost all natural waters the alkalinity is produced by the dissolved carbon-dioxide (CO_2) species, bicarbonate (HCO_3) and carbonate (CO_3). The principal source of carbon-dioxide species that produce alkalinity in groundwater is the CO_2 gas fraction present in the soil or in the unsaturated zone lying between the surface of the land and the water table. The soil minerals may absorb H^+, which could be released from time to time by addition of soil amendment or by other changes in chemical environment to reinforce the hydrogen ion content of groundwater recharge. It is assumed the pH of the water is controlled by CO_2 equilibria. The bicarbonate concentration of natural water generally held within a moderate range by the effects of carbonate equilibria. Concentrations of bicarbonate more than 200 mg/l are not uncommon in groundwater and higher concentrations can result where carbon dioxide is produced within the aquifer mixed with organic matters (Matthess, 1982). In the present study acidity and alkalinity in groundwater from water sample was measured as bicarbonate (HCO_3). The concentration of HCO_3 in the study area ranges from 3.05 mg/l to 61.00 mg/l, suggesting that the water of the study area is suitable for drinking or irrigation purposes. Most Chloride in groundwater comes from ancient sea water entrapped in sediments; second, solution of halite and related minerals in evaporate deposits; third concentration by evaporation of chloride contributed by rain or snow; fourth, solution of dry fallout from the atmosphere, particularly in arid regions. Chloride is one of the major constituents found in all natural waters in different concentrations, commonly less than10 mg/l in humid region but up to 10000 mg/l in more arid regions. Concentrations greatly in excess of 100 mg/l may cause psychological damage. For public health chloride up to 250 mg/l are not harmful but values greater than this are indication of organic pollution. Chloride concentration in groundwater in the study area ranges from 27.28 mg/l to 197.78 mg/l. Hence the water of the study area is suitable for drinking and irrigation purposes. The occurrence of sulphate (SO_4^{2-}) in groundwater results from the oxidation of sulfur in igneous rocks, the solution of other sulfur bearing minerals and the oxidation of mercasite and pyrite (Matthess, 1982). According to the United States Public Health drinking water standard, the potable water should not contain more than 250 mg/l of sulfate ion. Concentration of sulfate in groundwater of the study area ranges from 1.20 to 2.55 mg/l. The concentrations of sulfate ions obtained in the waters are by all standards, very much within the range recommended for drinking and household purposes. Nitrogen occurs in water as nitrate or nitrite anions (NO_2 and NO_3) in cationic form as ammonium (NH_4^+) at intermediate oxidation states as a part of organic solute. The nitrate and organic species are unstable in aerated water and are generally considered to be indicators of pollution through disposal of sewage organic waste. The presence of nitrate or ammonium might be indicative of such pollution also. Concentration in excess of 10 mg/l as N, equivalent to 44 mg/l of NO_3^- evidently present this hazard (NAS-NAF, 1972). The concentration of nitrate in groundwater from the study area ranges from <0.1 to 0.66 mg/l. The facies mapping approach (Back, l96l) is one of the most significant ways to determine the hydro chemical facies from chemical data. In this case samples are classified according to facies with two templates for the Piper's Trilinear diagram. In the present study

the chemical data were plotted on the facies mapping approach (Back, 1961) and the variations and distributions of hydro chemical facies of groundwater throughout the study area are interpreted. It is observed that all the groundwater samples collected from the study area show Sodium-Calcium cation facies. All the groundwater samples of the study area indicate Bicarbonate-Chloride-Sulfate anion facies.

CONCLUSIONS

Correlation with different guideline values for drinking water and public health it is be concluded that the groundwater of the study area is suitable for drinking purposes. The pH value of groundwater ranges from 6.1 to 7.2 indicating almost neutral groundwater. Average temperature ranges from 25.0°C to 27.0°C. The electrical conductance (EC) of groundwater ranges from 50.0 to 420.0 µs/cm, which is of good to medium quality for irrigation purposes. The TDS value ranges from 32.0 to 268.8 mg/l, which is within allowable limit. The hardness of groundwater ranges from 61.28 to 197.06 mg/l, which is implies very hard, so it requires little softening. Concentration of cations (Ca^{2+}, Mg^{2+}, Na^{+}, K^{+} Fe^{total}) ranges from 2.0 to 44.0 mg/l, 10.12 to 26.08 mg/l, 0.11 to 0.56 mg/l, 0.002 to 0.022 mg/l and 0.15 to 0.65 mg/l respectively. The concentration of calcium is the highest among all of the cations but within the permissible limit. Concentration of Sodium, Potassium, Magnesium and $Iron^{total}$ in all of the studied samples are also within the permissible limit. Concentration of anions (HCO_3^-, CO_3^-, SO_4^{2-}, NO_3^-, and Cl^-) range from 3.05 to 61.00 mg/l, 5.2 to 17.0 mg/l, 1.20 to 2.55 mg/l, <0.1 to 0.66 mg/l and 27.28 to 197.78 mg/l respectively. All of the anions in the groundwater are within allowable limit. Distribution of water samples in the Piper Trillinear Diagram shows that all the samples fall in the field-1, which indicates that the alkaline earth exceeds alkalies. Six samples fall in field-3, indicating week acids exceed strong acids, finally all the samples fall in field-5, indicating that the groundwater has an excess of 50% carbonate hardness (secondary alkalinity). This confirms that alkaline earths and weak acids dominate the chemical properties of groundwater of the study area. From the facies mapping approach of water quality data it is revealed that the groundwater of the region could be classified as Sodium-Calcium cation facies and as Bicarbonate-Chloride-Sulfate anion facies. Correlation with different guideline values for drinking water and public health it is be concluded that the groundwater of the study area is suitable for drinking purposes. Genetically the groundwater of the study area belongs to "Strong Chloride", "Normal Sulfate", and "Normal Carbonate" group. Based on EC, PI and SAR groundwater of the study area is of good to permissible quality for irrigation purposes. As far as the quality for irrigation is concerned the groundwater falls under quality category of low alkali hazard and low to medium salinity hazard.

REFERENCES

Alam, D; Huq, SMI; Rahman, S and Anam, K. 1991. *A Handbook on Chemical Analysis of Soil, Plant and Water.* 1st ed., Ahmed Perveg Shamsuddin Publication, Dhaka.

American Public Health Association (APHA). 1995. *Standard Methods for the Examination of Water and Wastewater,* 16th ed. American Public Health Association, Washington.

American Water Works Association (AWWA). 1981. *1981-82 Officers and Committee Directory Including Policy Statements and Official Documents*: Denver, Colorado, 114p.

Back, W.1961. *Technique for Mapping of Hydrochemical Facies*. U.S. Geol. Survey Prof. Paper 424 D, p.380-382.

Bangladesh Bureau of Statistics 1991. *Population Census.* Nilphamari District. Ministry of Planning, Government of the People's Republic of Bangladesh.

Bangladesh Water Pollution Control Board (BWPCB). 1976. *Bangladesh Drinking Water Quality Standard,* BWPCB, 156p.

Brammer, H. 1996. *The Geography of The Soils of Bangladesh*, 1st Ed. The University Press Limited.

DOE, Bangladesh, 1991. *Environmental Quality Standard for Bangladesh*.

Doneen, LD. 1962. The influence of crop and soil on percolating waters. *Proc. 1961 Biennial Conference on Groundwater Recharge*, p.56-163.

Hem, JD. 1989. *Study and Interpretation of the Chemical Characteristics of Natural Water* 3rd Ed. U.S. Geological Survey Water Supply Paper, 2254.

Khan, AA and Rahman, T. 1992. An analysis of the gravity field and tectonic evolution of the northwestern part of Bangladesh, *Tectonophysics*, v.206, p.351-364.

Lloyd, JW and Heathcote, JA.1985. *Natural Inorganic Hydrochemistry in Relation to Groundwater: An Introduction*, Claredon Press, Oxford, 291p.
Matthess, G.1982. *The Properties of Groundwater*, John Wiley and Sons, New York, 397p.
Maucha R. 1949. The graphical symbolization of the chemical composition of natural waters: *Hidrologie Kozolay*, v.13, p.117-118.
Morgan, JP and McIntire, WG. 1959. Quaternary geology of Bengal Basin, East Pakistan and India. *Geo. Soc. America Bull*. 70:319-342.
Piper, AM. 1944. A graphic procedure in the geochemical interpretation of water analysis, *American Geophysical Union Transaction*.25:914-923.
Piper, AM; Garrett, AA. 1953. *Native and contaminated groundwater in the Long Beach-Santa Ana Area, California*: U.S. Geological Survey Water-Supply Paper 1136: 320.
Raghunath, HM. 1987. *Groundwater*. Wiley Eastern Ltd., Delhi, India, 563.
Rashid, H. 1991. *Geography of Bangladesh*, University Press Ltd., Dhaka, Bangladesh, 529.
Reimann, K.U. 1993. *Geology of Bangladesh*. Gerbruder Bornt Ramerg, Berlin, Stuttgart, Germany, 160.
Schoeller, H. 1962. *Lex eaux souterraines*. Masson and Cie, Paris, 624..
Schoeller, H. 1967. Qualitative Evaluation of Groundwater Resources. In: *Methods and Techniques of Groundwater Investigation and Development*. Water Res. Series, UNESCO.44-52.
Todd, D.K. 1980. *Ground Water Hydrology* (2nd ed.). John Wiley and Sons, New York. 535p.
World Health Organization (WHO). 1983. *Guidelines to Drinking Water Quality*, 1st ed, World Health Organization, Geneva, 186.
World Health Organization (WHO). 1993. *Guidelines to Drinking Water Quality*, 2nd ed, World Health Organization, Geneva, 186.
Zaher, MA and Rahman, A. 1980. Prospects and Investigation for Minerals in the Northern part of Bangladesh*, Petroleum and Mineral Resources of Bangladesh, Seminar*.1-19.

ASSESSMENT OF EROSION VULNERABILITY NEAR THE HYDRAULIC STRUCTURES BY COMPARING THE EROSIVE RESISTNCE OF NON-COHESIVE SOIL WITH FLOW VELOCITY

M. Musfequzzaman[1*], F. Noor [1] & M. A. Matin[2]

[1]*River Engineering Division, Institute of Water Modelling, Dhaka, Bangladesh*
[2]*Department of Water Resources Engineering, Bangladesh University of Engineering and Technology, Dhaka, Bangladesh*
[*]*Corresponding Author: mzn@iwmbd.org*

ABSTRACT
Major rivers of Bangladesh are very dynamic in nature, among which the Jamuna is the extreme example. About twenty thousands of people along the Jamuna River become landless and homeless every year due to erosion. In this regard, BWDB has implemented many structures along the Jamuna River. In this study, vulnerability of erosion is assessed for various important hydraulic structures along the Jamuna River near Bangabandhu Bridge area. This is the largest bridge in Bangladesh that have mainly four important hydraulic structures at the upstream of bridge to guide the flow under the bridge including two guide bunds and two Hard Points. These structures are always under threat due to the dynamic behavior of the Jamuna River. So erosion assessment and monitoring is the primary concern of these structures. Erosion starts when a particle overcomes its incipient motion. The erosion resistance of river bank and river bed can be estimated on the assumption that the load can be characterized by the maximum occurring shear stress or velocity, while the resistance is given in terms of the critical shear stress or velocity. This critical velocity is estimated by using the method of shear stress. Then the actual velocity of the flow near a structure is compared whether it has crossed the critical velocity to initiate the motion of the sediment particle. Results from the study show that the ratios between actual flow velocity to critical velocity near the structures are much higher from unity. So all the structures can be considered as vulnerable according to the study and these need continuous monitoring and erosion preparedness.

Keywords: Erosion; hydraulic structures; incipient motion; critical velocity

INTRODUCTION
Bangladesh is formed by the alluvial deposition of soil in the major river systems and their numerous tributaries and distributaries. So bank erosion is a very common phenomenon for the rivers. Many people living along the river lost their land due to erosion. Among all the rivers, the Jamuna is the most dynamic and complex one. Different types of structures based on the requirements were implemented in this river by Bangladesh Water Development Board. Some of the structures were successful and some of those failed due to lack of understanding about the vulnerability. The Bangabandhu Bridge is one of the most important structures on the Jamuna River. In addition, there are other four major structures in the vicinity of the Bridge. Those are: East Guide Bund, West Guide Bund, Sirajganj Hard point, Bhuapur Hard point. The purpose of these structures is to guide the flow of the river under the bridge. However, these structures are getting vulnerable during the monsoon period. Thus assessment of erosion vulnerability of those structures is necessary. In this study, erosion vulnerability near the hydraulic structures has been assessed by comparing the flow velocity with the critical velocity.

STUDY AREA
The study area covers the Bangabandhu Bridge and its adjacent structures, i.e. East Guide Bund, West Guide Bund, Sirajganj Hardpoint and Bhuapur Hardpoint, Figure 1 shows the study area near Bangabandhu Bridge in the Jamuna River.

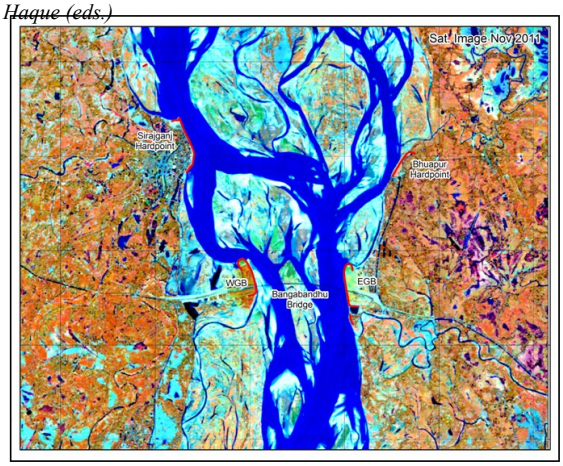

Fig 1: Location of the study area near Bangabandhu Bridge

METHODOLOGY

Description of the Model Setup

To setup a two dimensional morphological model for calculating velocity along various structures of the Jamuna River, MIKE21C (an advanced two-dimensional mathematical modelling software developed by DHI Water & Environment, Denmark) has been used. A number of simulations have been conducted for different hydrological year to get a range of velocity passing along the structures. Setting up of a 2D morphological model comprises firstly, computational grid generation and secondly, preparation of the bathymetry on these grid cells. Figure 2 shows the grid and the bathymetry, respectively. The Curvilinear grid has been generated using the surveyed bankline of 2010 and the initial bathymetry has been prepared by interpolating the surveyed cross-sectional data of December 2010. The upstream boundary and downstream boundary have been set up according to the model area and finally simulations have been carried out for different flood events, e.g. 1 in 10, 1 in 100 and 1 in 2.33 years corresponding to the hydrological years of 1995, 1998 and 2005, respectively. The model was calibrated for the 2010 hydrological year.

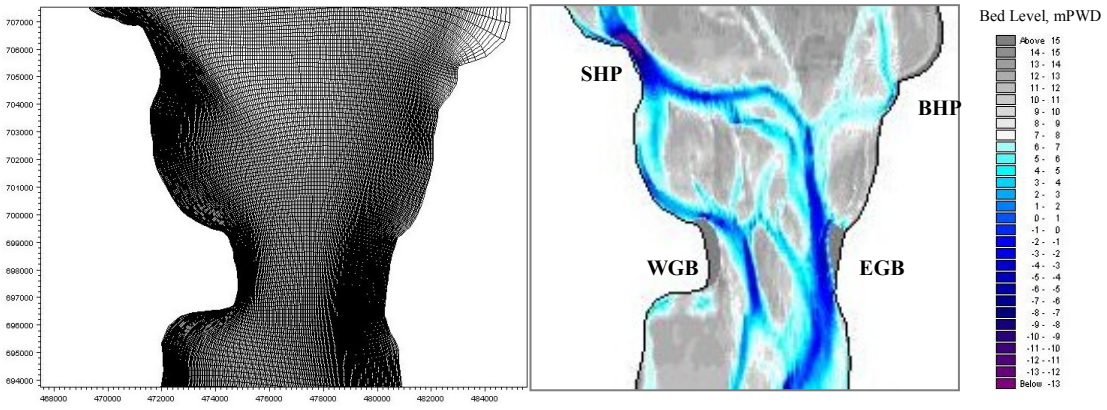

Fig 2: Computational curvilinear grid and Bathymetry corresponding to the year of 2010.

Determination of Critical Velocity

Critical velocity is the velocity needed to transport sediment load (Bull, 2012). For non cohesive soil, assuming a steady uniform flow, the basic stability criterion can be expressed as-

$$\tau_{cr} = \Psi_{cr}(\rho_s - \rho_w).g.D > \tau_o \quad (1)$$

Where,

τ_{cr}= critical shear stress (N/m^2), τ_o= shear stress exerted along the bank/bed boundaries(N/m^2), ψ_{cr}= dimensionless critical Shields shear stress parameter for specific material, D= mean grain size (m), ρ_s= density of soil (kg/m^2) and ρ_w= density of water (kg/m^2)

The value of Ψ_{cr} depends on particle shape, velocity profile, etc. For fine sediments with D< 4 mm, the Shields parameter can be written as:

$$\psi_{cr} = \frac{\tau_c}{(\gamma_s - \gamma_w)D} = \frac{U_*^2}{\Delta_m g.D} \quad (2)$$

where,

$$U_* = \sqrt{g \cdot R \cdot S} = \frac{u \cdot \sqrt{g}}{C} \quad (3)$$

where,

Δ_m (-) $= (\rho_s - \rho_w)/\rho_w$, i.e.,relative density of submerged material, U_*= shear velocity (m/s), R= hydraulic radius or water depth (m), S = slope of energy line, u= mean velocity (m/s), C= Chezy coefficient ($m^{0.5}/s$) and h= depth of flow (m).

For practical cases the following formulas can be used to estimate the critical velocity (U_c) causing subsoil erosion:

$$U_c = (\sqrt{g \cdot \Delta \cdot D_{50}}\sqrt{\psi_{cr}}) * 5.75 * \log \frac{6h}{D_{50}} \quad \text{(For finer sediment)} \quad (4)$$

$$U_c = (\sqrt{g \cdot \Delta \cdot D_{50}}\sqrt{\psi_{cr}}) * 5.75 * \log \frac{2h}{D_{50}} \quad \text{(For coarser sediment)} \quad (5)$$

Determination of Dimensionless Instantaneous Velocity

Incipient motion is important in the study of sediment transport, as this motion of sediment particles in alluvial rivers is a key process for mobility. It represents the difference between bed stability and bed mobility (Matin, 1994). Due to the stochastic nature of sediment movement along an alluvial bed, it is difficult to define precisely at what flow condition a sediment particle will begin to move (Yang, 2012). Consequently, it depends more or less on an investigator's definition of incipient motion.

The initiation of motion of a particle could be identified by comparing the instantaneous velocity with the critical velocity. Therefore if the ratio between instantaneous velocity and the critical velocity is higher than unity, the particle would initiate its motion. In this study, the instantaneous velocity along the structures has been extracted from the model simulation for different flood events and finally dimensionless velocity has been calculated at the expected location.

RESULTS AND DISCUSSION

As mentioned earlier, the vulnerability of erosion has been predicted for the East Guide Bund, West Guide Bund, Sirajganj Hardpoint and Bhuapur Hardpoint. However, it is seen that for 1in100 year flood event the critical velocity ratio exceeds the value 1 for all the four structures. Therefore, average (1in2.33) flood event has been considered here to evaluate the structures vulnerability. The critical velocity for those structures is shown in Table 1.

Table 1: Calculation of Critical Velocity along the structures

Name of the structures	Average water depth, h (m)	Average velocity, u (m/s)	Critical velocity, u_c (m/s)
East Guide Bund	7.13	0.531	0.5
West Guide Bund	3.55	0.722	0.677
Sirajganj	3.67	0.841	0.788
Bhuapur	4.28	0.661	0.62

Summary of Results

East Guide Bund (EGB)

From calculation, the critical velocity is found about 0.5m/s in this location (Table 1). This critical value has been compared with the model simulated maximum velocity along the East Guide Bund at different

location shown in Figure 2, to check the risk of bed scour. Table 2 shows that the probable velocity for different hydrological year along the East Guide Bund varies from 0.21 to 1.43m/sec. It has been observed that the ratio between model estimated velocity and calculated critical velocity is higher along the straight portion of EGB. So straight part of guide bund is vulnerable to bed scour for present bathymetry.

Table 2: Dimensionless Velocity at different point of East Guide Bund for different hydrological year

	1 in 100		1 in 10		1 in 2.33	
Position	**Velocity, u**	**u/ u_c**	**Velocity, u in**	**u/ u_c**	**Velocity, u**	**u/ u_c**
1	0.26	0.52	0.32	0.64	0.21	0.41
2	1.66	3.32	1.60	3.21	1.75	3.50
3	1.18	2.35	1.14	2.28	1.22	2.43
4	1.34	2.69	1.30	2.60	1.34	2.68
5	1.40	2.81	1.34	2.68	1.33	2.65
6	1.43	2.86	1.35	2.71	1.28	2.56
7	1.33	2.65	1.25	2.49	1.19	2.38
8	1.34	2.69	1.27	2.53	1.23	2.45
9	1.37	2.74	1.29	2.57	1.27	2.53
10	1.17	2.33	1.18	2.37	1.16	2.33

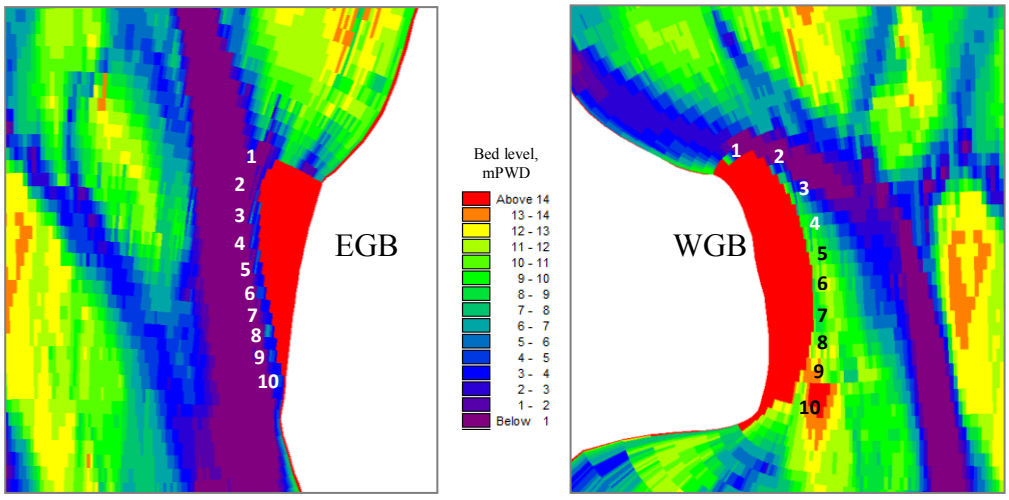

Fig 3: Different location of velocity along the East Guide Bund and West Guide Bund

West Guide Bund (WGB)

From Table 1, the critical velocity is found about 0.677m/s in this location. To check the risk of bed scour, this critical value has been compared with the model simulated velocity along the West Guide Bund. Table 3 shows that the probable velocities along the West Guide Bund vary between 0.24m/sec to 2.05m/sec for different hydrological year. The ratio between model estimated velocity and calculated critical velocity along the upstream termination of West Guide Bund exceeds the value 1.0, which indicates that the upstream location is vulnerable for bed scour for present bathymetry.

Sirajganj Hard Point (SHP)

From Table 1, the critical velocity is found about 0.788m/s for Sirajganj Hard Point. This critical value has been compared with the model simulated velocity along the Sirajganj Hard Point to check the risk of bed scour. Table 4 shows that the probable velocities along the Sirajganj Hard Point vary from 1.00 to 2.77m/sec for different hydrological year. The ratio between model estimated velocity and calculated critical velocity exceeds the value 1 at every point along the Sirajganj Hard Point that indicates that this structure is highly vulnerable for present bathymetry.

Table 3: Critical Velocity Ratio at different point of West Guide Bund for different hydrological year

	1 in 100		1 in 10		1 in 2.33	
Position	**Velocity, u**	**u/ u_c**	**Velocity, u in**	**u/ u_c**	**Velocity, u**	**u/ u_c**
1	0.79	1.16	0.70	1.03	0.61	0.91
2	1.26	1.87	1.18	1.74	1.06	1.57
3	1.35	2.00	1.22	1.80	1.11	1.64
4	1.44	2.12	1.27	1.87	1.14	1.69
5	1.37	2.02	1.20	1.77	1.04	1.53
6	1.32	1.95	1.13	1.67	0.93	1.37
7	2.05	3.02	1.73	2.55	1.32	1.95
8	1.77	2.62	1.43	2.11	1.10	1.63
9	0.24	0.35	0.28	0.42	0.06	0.09
10	0.08	0.12	0.00	0.001	0.02	0.02

Table 4: Dimensionless Velocity at different point of Sirajganj Hardpoint for different hydrological year

	1 in 100		1 in 10		1 in 2.33	
Position	**Velocity, u**	**u/ u_c**	**Velocity, u in**	**u/ u_c**	**Velocity, u**	**u/ u_c**
1	1.17	1.49	1.62	2.06	1.09	1.38
2	2.12	2.69	2.77	3.51	1.91	2.42
3	1.75	2.22	2.06	2.62	1.50	1.90
4	1.49	1.90	1.71	2.17	1.27	1.61
5	1.34	1.70	1.54	1.95	1.15	1.46
6	1.22	1.55	1.44	1.83	1.07	1.36
7	1.13	1.43	1.37	1.74	1.01	1.28
8	1.13	1.44	1.34	1.70	1.00	1.26
9	1.16	1.47	1.35	1.72	1.02	1.30
10	1.18	1.50	1.39	1.76	1.05	1.33

Bhuapur Hard Point (BHP)

The critical velocity is found 0.62m/s along the Bhuapur Hard Point (Table 1). This value has been compared with the model simulated maximum velocity adjacent to the Bhuapur Hard Point as shown in Table 5. It is seen that the estimated velocity along the hard point exceeds the critical value (0.62m/s). The ratio between model simulated maximum velocity and calculated critical velocity at 10 different points along the Bhuapur Hard Point exceeds 1.0, which indicates that this location is in risk for bed scour for present bathymetry.

Table 5: Dimensionless Velocity at different point of Bhuapur Hardpoint for different hydrological year

	1 in 100		1 in 10		1 in 2.33	
Position	**Velocity, u**	**u/ u_c**	**Velocity, u in**	**u/ u_c**	**Velocity, u**	**u/ u_c**
1	1.33	2.15	1.19	1.91	1.36	2.19
2	1.21	1.95	1.14	1.84	1.30	2.09
3	1.18	1.91	1.11	1.79	1.34	2.16
4	1.32	2.14	1.26	2.03	1.47	2.37
5	1.51	2.43	1.46	2.36	1.63	2.63
6	1.61	2.60	1.57	2.54	1.72	2.78
7	1.71	2.76	1.68	2.71	1.81	2.92
8	1.78	2.87	1.76	2.84	1.85	2.99
9	1.73	2.79	1.76	2.84	1.78	2.87
10	1.68	2.71	1.73	2.79	1.70	2.74

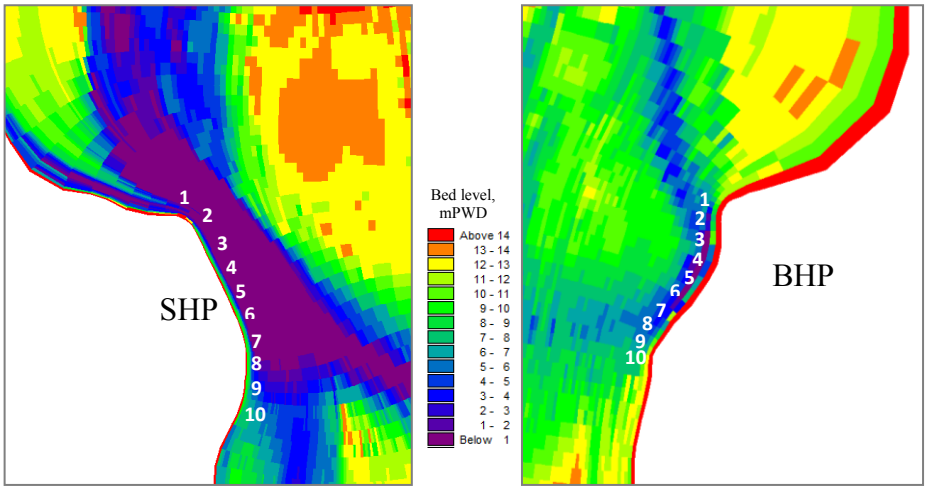

Fig 4: Different location of velocity along the Sirajganj Hard Point and Bhuapur Hard Point

Identification of Vulnerable Locations

The risk areas were categorized according to the Guidelines and Design Manual for Standardized Bank Protection Structures, published in December 2001 in connection with Bank Protection Pilot Project FAP 21. Table 6 shows the vulnerable reaches of the Jamuna River, in the vicinity of the Bangabandhu Bridge.

Table 6: Identified Vulnerable Reaches of the Jamuna

Locations	**Remarks**
Upstream termination of	Vulnerable
Straight part of SHP	Vulnerable
Upstream termination of	Vulnerable
Straight part of WGB	Not Vulnerable
Upstream termination of	Not Vulnerable
Straight part of EGB	Vulnerable
Upstream part of BHP	Vulnerable
Straight part of BHP	Vulnerable

CONCLUSIONS

It has been observed that all the structures near Bangabandhu Bridge area are vulnerable to bed scour for the bathymetry of 2010. The vulnerability of structures depends on the water depth near the structure. Therefore, the vulnerability will be varying for the next year bathymetry.

Due to the stochastic nature of sediment movement along an alluvial bed, it is difficult to predict at what flow condition bed would start eroding. Comparing the erosive resistance of non-cohesive soil with flow velocity allows for a quick assessment of vulnerability of a hydraulic structure. Moreover, this technique will also be helpful for monitoring and disaster preparedness. The assessment of vulnerability would be more accurate if velocity at the toe level of the structure could be calculated through 3D model or field measurement.

ACKNOWLEDGMENTS

The authors express their deepest gratitude to the Institute of Water Modelling (IWM) for the support to use their study findings in the paper.

REFERENCES

Bull, WB. 2012. Threshold of Critical Power in Streams, Geological Society of American Bulletin.

IWM. 2011. Monitoring of Hydraulic and Morphological conditions of Jamuna River for the safety of Bangabandhu Bridge during the year 2010-11, Prepared for Bangladesh Bridge Authority, Dhaka, Bangladesh.

Matin, H. 1994. Incipient Motion and Particle Transport in Gravel Streams, Dissertation abstracts International, Volume: 56-03, Section: B, pp1590.

Yang, CT. 2006. Erosion and Sedimentation Manual, U.S. Department of the Interior Bureau of Reclamation.

IMPACT OF HIGH END EMISSION ON THE PRODUCTION OF BORO RICE IN BANGLADESH USING DSSAT 4.5

A. S. Hasan*, A. S. Islam, S. K. Bala & M. J. U. Khan

Institute of Water and Flood Management, Bangladesh University of Engineering and Technology, Dhaka, Bangladesh
**Corresponding Author: sajidce08@gmail.com*

ABSTRACT
Impact of high end emission on production of BORO rice in Bangladesh has been evaluated using the DSSAT 4.5 crop modeling system. It was calibrated using BR3 variety for the years 2001-2005 and validated for 2006-2010 incorporating BBS data with statistical parameters RMSE and NSE. Impact of future climate is analyzed for the years 2020's (2016-2035), 2050's (2036-2055) and 2090's (2081-2099) with baseline years 1991-2010 using 7 bias corrected ensembles regional climate models (RCM's) for 64 districts divided in 23 regions. The soil profile data was extracted from WISE 1.1 soil database. The results show that, the yield is negative everywhere, reaching over 20% decrease in some regions. The maximum temperature rise exceeds 1.5°C in 2020's and 4°C in 2090's whereas the minimum temperature rises up to 5°C in 2090's. This rise in daily temperature over the growing period of BORO rice indicates the adverse impact of temperature on crops.

Keywords: BORO Rice; RCM; Climate change; DSSAT 4.5

INTRODUCTION
Agriculture contributes to 35% of the GDP and 70% of the labor force in Bangladesh. The problem of huge and increasing demands for food and of agricultural land and water resources depletion make it worse (Ahmed et al., 2000). Bangladesh has to emphasize more on the staple food rice and will require more than 55.0 million tons of rice to feed its people by the year 2050(Basak, 2010). The impacts of climate change on food production very important for Bangladesh. BORO rice is the leading rice producer variety of Bangladesh (BRRI, 2006). However, climate change is the major threat towards rice production. It is very important to evaluate the effect of climate change on BORO production. A number of simulation studies have been carried out to assess impacts of climate change and variability on rice productivity in Bangladesh using the CERES-Rice model of DSSAT. (Mahmood et al., 2003; Mahmood, 1998; Karim et al., 1996). For instance, Basak(2010) has carried out simulations of 12 representative regions from various zones of the country using the regional climate model PRECIS. However, this study covers simulation over all the 23 zones of the country that contains all 64 districts using seven numbers of bias corrected ensembles of regional climate models which has taken high end emission into account while projecting the future climate data.

METHODOLOGY

Study area
This study was done on Bangladesh (20°34″ North Latitude to 26°38″ North Latitude and from 88°01″ East Longitude to 92°41″ East Longitude) which that encompass almost 0.15 million Km^2 territory. Bangladesh is the largest delta of the world as 80% of the land is formed by the floodplains of the GBM

basin (Ganges, Brahmaputra & Meghna) making it a fertile land for rice production. The country experiences huge rainfall during Monsoon. However, some flash floods prior to the monsoon season also occur. This tropical country has annual average rainfall of 1600 mm and a temperature ranging from 8° to 38°during the growth season of Boro rice (Nov-April) over the last 30 years (1981-2010).

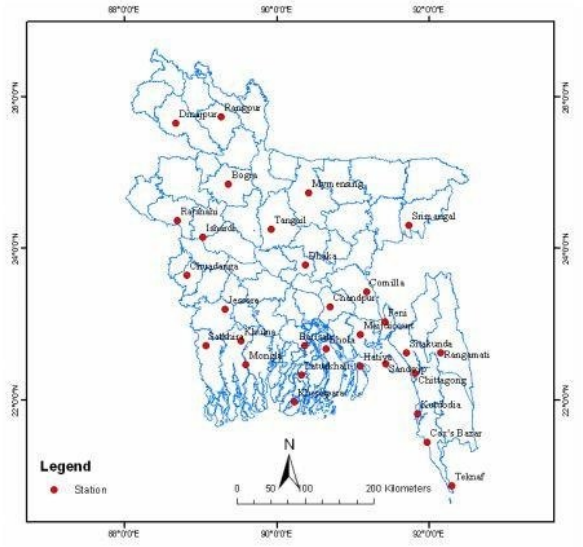

Fig. 1: Thirty five ground base measuring stations of Bangladesh Meteorological Department. Source (Islam 2008)

Selection of Crop Model

Among the various crop modeling software like Crop-wat, DSSAT, PCSE etc. we have chosen DSSAT 4.5 to calibrate and project the crop yields. The CERES-Rice model of the DSSAT modeling system is an advanced physiologically based rice crop growth simulation model and has been widely applied to understanding the relationship between rice and its environment. The model estimates yield of irrigated and non-irrigated rice, determine duration of growth stages, dry matter production and portioning, root system dynamics, effect of soil water and soil nitrogen contents on photosynthesis, carbon balance and water balance. Ritchie et al. (1987) and Hoogenboom et al. (2003) have provided a detailed description of the model.

Selection of Rice Variety

The CERES-Rice model is variety-specific and is able to predict rice yield and rice plant response to various environmental conditions. The model takes into effect of weather, crop management, genetics, and soil water, C and N. The model uses a detailed set of crop specific genetic coefficients, which allows the model to respond to diverse weather and management conditions. The BORO rice variety BR3 has been selected as the genetic coefficients of BR3 is available in the model.

Table 1: Some important information about BR3 variety of Boro rice

Real Name	Biplob Height
95 cm Duration of growth	170 days Grain quality
CoarseYield (Kg/hectares)	6500
Developed on	1975
Developed by	Bangladesh Rice Research Institute (BRRI)

Integrating field data in DSSAT

The DSSAT software team has recently done experiments on 17 soil stations across Bangladesh. The soil station data has been stored in WISE 1.1 database. Once a region is selected from the global map, it enables the user to access the soil station data. This set of data is simply copied and pasted on the soil.sol file. Thus the soil stations can easily be integrated in DSSAT.

Weather data

In this study, the historic weather data was taken from 35 stations of Bangladesh Meteorological Department (BMD). The weather data contains daily rainfall (mm), maximum and minimum temperature (°C) and daily solar hours. Rainfall and temperatures are used directly in DSSAT. However, the weather manager of DSSAT itself converts solar hours into solar radiation. As simulations were carried out over 23 zones, the data of the nearest station of the corresponding district was taken. Figure 1 indicates the location of the meteorological stations of BMD. For calibrating the model, data of the years from 2001-2005 was taken and 2006-2010 was taken for validation.

Climatic Data

The future data was collected from 7 bias corrected ensembles with RCP 8.5 scenario of regional climate models RCM's under 4 GCM's. The baseline period was 30 years (1991-2010) and the projection was made for 2020's (2016-2035), 2050's (2046-2065) and 2090's (2080-2099). Table 2 describes the details of the ensembles.

Table 2: Details of the bias corrected ensembles of regional climate models

Institute	GCM	RCM	Driving Ensemble Member	Res.	RCP
SMHI	CNRM-CERFACS-CNRM-CM5	RCA4	r 1i1p1	0.5°	8.5
SMHI	ICHEC-EC-EARTH	RCA4	r 1i1p1	0.5°	8.5
MPI- CSC	MPI-M-MPI-ESM-LR	REMO2009	r 1i1p1	0.5°	8.5
SMHI	MPI-M-MPI-ESM-LR	RCA4	r 1i1p1	0.5°	8.5
SMHI	NOAA-GFDL-GFDL-ESM2M	RCA4	r 1i1p1	0.5°	8.5
SMHI	IPSL-CM5A-MR	RCA4	r 1i1p1	0.5°	8.5
SMHI	MIROC-MIROC5	RCA4	r 1i1p1	0.5°	8.5

Crop Management

The crop management includes planting details, transplanted date, irrigation and fertilizer management, tillage, harvest and chemical applications. The date of transplant, the date of harvest, the amount ofirrigation and fertilizer applications has been kept the same to a default set value according to the guidelines of BRRI.

Calibration and Validation:

The model was calibrated to find the genetic coefficients for BR3 variety of Boro rice. Statistical parameters root mean square error (RMSE) was used for the calibration. Value of RMSE was ranging from 100- 300 depending on the soil profile and climatic scenario of the region. Table 3 shows the default

values of the genetic coefficients and the calibrated value of these parameters in some important locations (divisions).

Table 3: Values of the genetic coefficients in some important locations (divisions)

Region	P1	P2R	P5	P20	G1	G2	G3	G4	RMSE (Calibration)	RMSE (Validation)
Default value	650	90	400	13	0.65	0.25	1	1	-	-
Dhaka	647	93	415	12.9	67	0.26	1	1	260	125
Chittagong	645	87	395	12.9	62	0.25	1	1	312	213
Rajshahi	647	93	415	12.9	67	0.26	1	1	317	106
Barisal	648	90	400	13	67	0.25	1	1	192	141
Khulna	648	90	400	13	67	0.25	1	1	211	139
Sylhet	650	90	400	13	67	0.25	1	1	169	140
Rangpur	650	90	400	13	65	0.25	1	1	315	154

RESULTS AND DISCUSSIONS

It is observed that, most of the regions experience negative yield of BORO rice, reaching over 20% decrease in some regions (Figure. 2). The maximum temperature rise exceeds 1.5°C in 2030's and 4°C in 2090's whereas the minimum temperature rises up to 5°C in 2090's. (Figure. 3) This rise in daily temperature over the growing period of BORO rice indicates the adverse impact of temperature on crops. The results show a spatial distribution of the change of rice yield. As we see figure 4, for mid future (2050's), the North East zone encounters the minimum reduction in yield (2-6%). On the contrary, the southern zone is the most danger prone region experiencing a 14% to above 20% decrease in yields. Over the near and far future, the western zone of Bangladesh remains moderately affected by reduction of rice yield from 8% to 12%. However, the condition of the central zone is also affected in the far future which indicates how severe the impact of climate change is going to endanger the whole country in future.

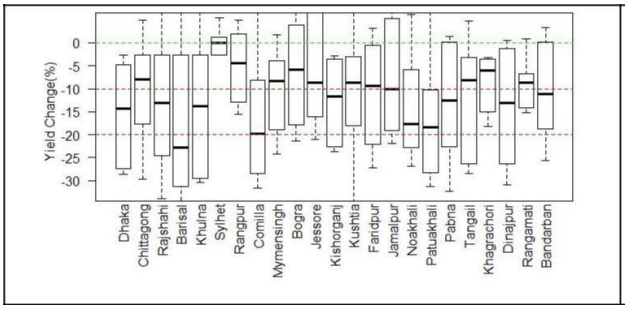

Fig.2: Change of BORO yield in 2090's

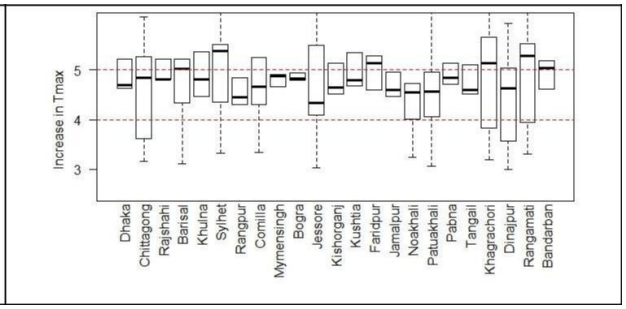

Fig.3: Increase of maximum temperature in 2090's

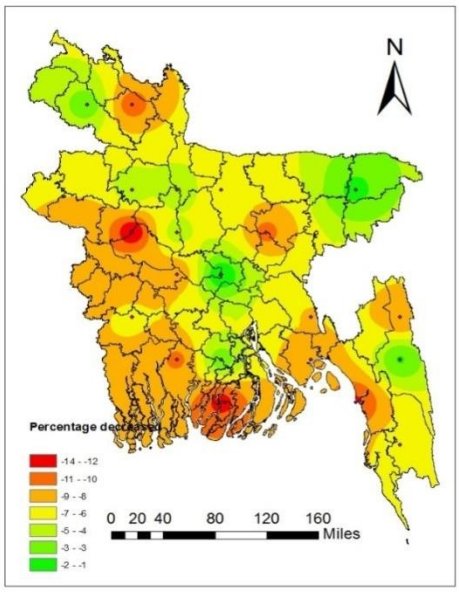

Fig. 4: Change of the yield of Boro rice in mid future (2050's)

CONCLUSION

Most of the regions encountered extreme change in maximum and minimum temperature over the emergence to end period of BORO crop. The yield trend is gradually decreasing at an alarming rate; crossing 10% decrease in 2020's to 20% decrease in 2090's. The growth and yield of crops are directly related to the rate of photosynthesis and their response to temperature, solar radiation and rainfall. Optimum temperatures for maximum photosynthesis range from 25ºC to 30ºC for rice under the climatic conditions of Bangladesh. Increased temperatures during the growing season cause grain sterility. (Basak et al., 2010). Maximum temperatures cause the reduction in rice yield mainly. However CO_2 is also increasing which pose a positive impact on crop production. But, it is not dominant over the impact of temperature. The core finding in our predicted results suggest that, keeping the harvesting date same or shortening the emergence to harvest duration, we can actually get an increased yield in most of the regions. However, due to shortening the growth period, we are also shortening the irrigation water to a significant amount. This amount might be sufficient for many regions, but possibly not for the drought prone regions. Moreover, the growing period of BORO rice experiences no Monsoon at all. For this reason, the probable cause behind the reduction in yield of any zone is supposed to be drought. This finding calls for a more detailed works on SPI (standardized precipitation index) in future. DSSAT crop modeling could prove very effective for this potential study. Moreover, the high end emission as the IPCC could be simulated to assess how intense is the impact of increased emission on Boro rice.

ACKNOWLEDGMENTS

The authors are grateful to HELIX (High End cLimate Impact and eXtremes) project for providing the financial support to carry out the research.

REFERENCES

Ahmed, A. and Ryosuke, S. 2000. Climate change and agricultural food production of Bangladesh: an impact assessment using GIS-based biophysical crop simulation model. *Center for Spatial Information Science*, University of Tokyo, 4-6-1 Komaba, Japan.

Basak, J.K. 2010. Effects of Increasing Temperature and Population Growth on Rice Production in Bangladesh: Implications for Food Security.

BRRI. 2006. Improvement of standard Boro rice. BRRI (Bangladesh Rice Research Institute) Annual Report for July 2005-June 2006. Plant Breeding Division, *BRRI*, Gazipur,Bangladesh.

Islam AKMS (2008) Analyzing Changes of temperature over Bangladesh due to global warming using historic data. Institute of water and flood management, Bangladesh University of Engineering and Technology, Dhaka-1000

Karim, Z., Hussain, S.G. and Ahmed, M. 1996. Assessing Impact of Climate Variations on Foodgrain Production in Bangladesh, *Water Air and Soil Pollution,* pp.92, 53-62.

Mahmood, R.; Meo, M.; Legates, D. R. and Morrissey, M. L. 2003. The Professional Geographer.

Mahmood, R. 1998. Air temperature variations and rice productivity in Bangladesh: A comparative study of the performance of the YIELD and CERES-Rice models. *Ecological Modelling*, pp.106, 201-212.

PREDICTION OF FUTURE DROUGHT IN THE NORTHWEST AND CENTRAL REGION OF BANGLADESH BASED ON PRECIS CLIMATE MODEL PROJECTIONS

U. Khaira* & N. Jahan

Department of Water Resources Engineering, Bangladesh University of Engineering and Technology, Dhaka, Bangladesh
**Corresponding Author: ahmed_choya@yahoo.com*

ABSTRACT
This research examines past drought and predicts future drought in selected locations of the northwest and central region of Bangladesh using two powerful and widely used drought indices namely the Standardized Precipitation Index (SPI) based on precipitation and the Standardized Precipitation and Evaporation Index (SPEI) based on both precipitation and evaporation. The analysis has been done for the observed period (1971-2014) using meteorological data and for future period (2015-2100) using data derived from PRECIS (Providing Regional Climates for Impacts Studies) climate model under emission scenario Representative Concentration Pathway 8.5 (RCP 8.5). These indices have been found to be capable of capturing historical drought events in Bangladesh and the future values indicate very frequent and severe drought events in the 21st century.

Keywords: Drought; precipitation & temperature, climate, SPI & SPEI

INTRODUCTION
Drought is one of the most damaging natural disasters. During the last 50 years, Bangladesh suffered about 20 droughts. Depending on the intensity of drought, the estimated yield reduction of different crops varies from 10% to 70% (Rahman and Biswas 1995). Apart from loss in agriculture drought has significant effect on land degradation, livestock population, fisheries, food quality and price, employment, health and society. Accurate prediction of the onset and durations of future droughts are necessary for better drought management. Previous studies indicate that both SPI and SPEI are very powerful index to detect different features of drought. But very few studies have so far been undertaken to forecast drought features in near future for Bangladesh. In this research projected climate data from PRECIS climate model will be used to forecast drought events in north-western (NW) and central region (CR) of Bangladesh.

METHODOLOGY
In the present study drought analysis were carried out in the NW (Rajshahi, Rangpur, Bogra, Dinajpur, Ishwardi)and CR**(**Dhaka, Mymensingh, Tangail**)** region using the SPI and SPEI indices computed from meteorological data. Monthly total rainfall and maximum and minimum temperature data were collected from Bangladesh Meteorological Department for the year 1971 to 2014. For forecasting future drought rainfall and temperature data were obtained from PRECIS climate model under RCP 8.5 emission scenario for the year 1971 to 2100**.**

Calculation of SPI and SPEI indices
In order to calculate SPI and SPEI, time series of precipitation and moisture deficit (P minus PET) were used, respectively. PET values were obtained from monthly maximum and minimum

temperature using Hargreaves method. These data are fitted to an appropriate probability distribution function. Two parameter gamma distribution function is used for SPI calculation and general logistic distribution function is used for calculating SPEI index in this analysis. These fitted distributions are used to calculate the cumulative probability density function for any given precipitation amount. This cumulative distribution is transformed to a standard normal distribution with a zero mean and standard deviation of unity which is the value of SPI or SPEI. Negative values of SPI or SPEI indicate dry periods while positive values indicate wet periods where a value of zero corresponds to the median precipitation. SPI values between ±0.99 are generally considered normal.

Table 1: SPI values indicate different drought conditions

2.0 or above	Extreme wet
1.5 to 1.99	Severe wet
1.49 to 1.0	Moderate wet
0.99 to -0.99	Near normal
-1.0 to -1.49	Moderate drought
-1.5 to -1.99	Severe drought
-2 or less	Extreme drought

For SPEI calculation, generalized logistic method for probability distribution and Hargreaves method for calculation of potential evapotranspiration found to be more appropriate. At first, SPI and SPEI were calculated for the year of 1971-2014 using observed data. Then SPI and SPEI were calculated for the same period using PRECIS model dataset. The distribution parameters found from this dataset were used to calculate SPI and SPEI of future period. All the drought indices are calculated for 3, 6, 9 and 12-month drought conditions.

RStudio, a programming language for statistical computing and graphics is used to compute SPEI, SPI both for controlled and future periods. In SPEI calculation, different distributions methods and different PET calculation method were applied and best fitted distribution method with PET method was chosen by trial and error that gave reasonably accurate result for observed period (1971-2014) By trial and error generalized logistic method for distribution and Hargreaves method for calculation of potential evapotranspiration were selected. Later SPI and SPEI values for future period of 2015 to 2100 were computed using those distribution parameters obtained for the observed data set.

RESULTS AND DISCUSSIONS

Future drought indices indicate very dry future and more frequent drought. It was observed that for 1971-2014 period most of the drought indices were in the range of ±1. But for future period (2015-2100) those indices are in the range of ±2 which indicates more extreme moisture deficit or surplus for future periods. Plots of 6 and 12 month SPI and SPEI computed from observed data of 1971-2014 are shown in Figure 1 and 2, respectively. SPI and SPEI of the same period (1971-2014) computed from PRECIS data are shown in Figure 3 and 4, respectively.

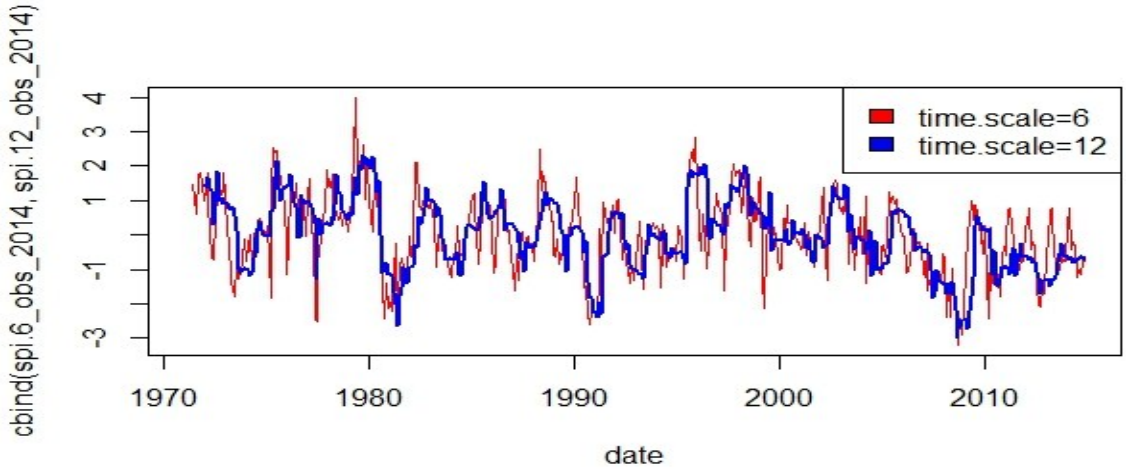

Fig. 1: Rajshahi's SPI series for observed period (1971-2014)

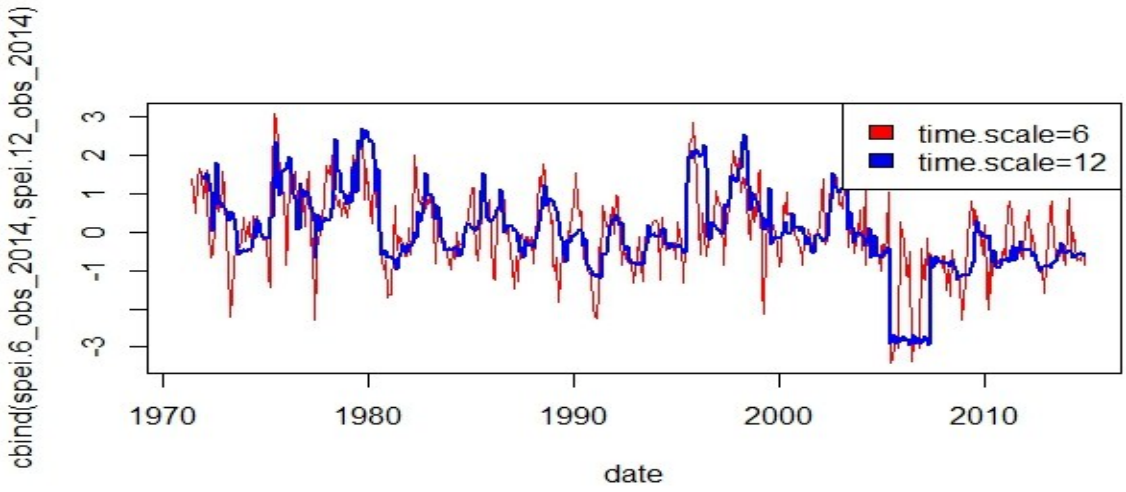

Fig. 2: Rajshahi's SPEI series for observed period (1971-2014)

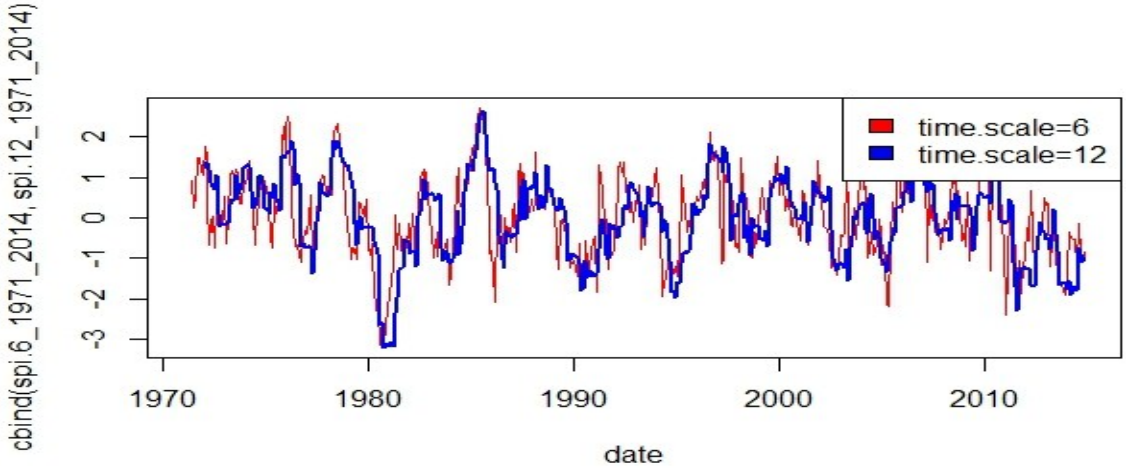

Fig. 3: Rajshahi's SPI series for 1971-2014 using PRECIS dataset

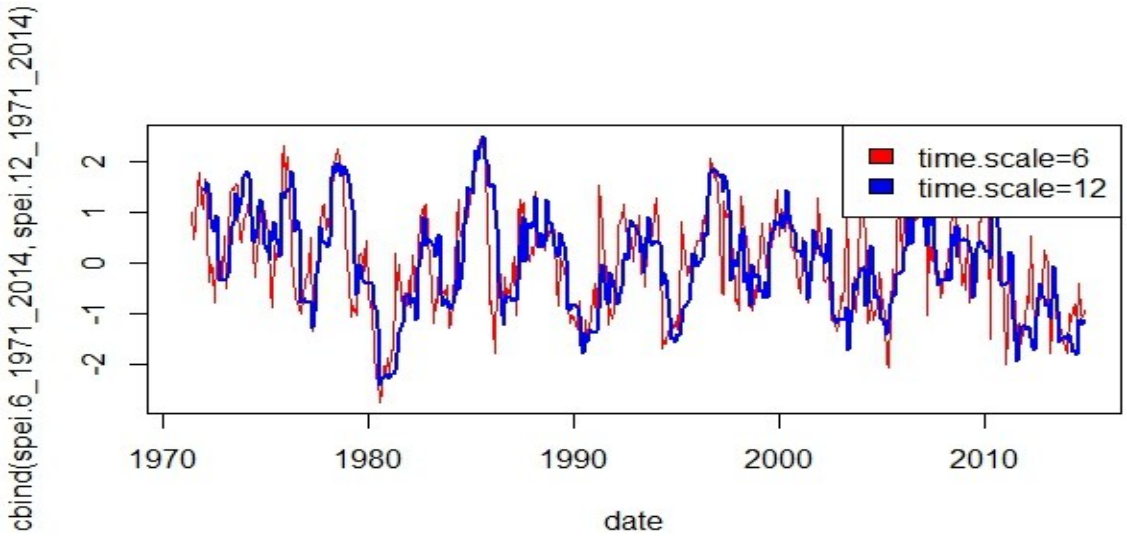

Fig. 4: Rajshahi's SPEI series for 1971-2014 using PRECIS dataset

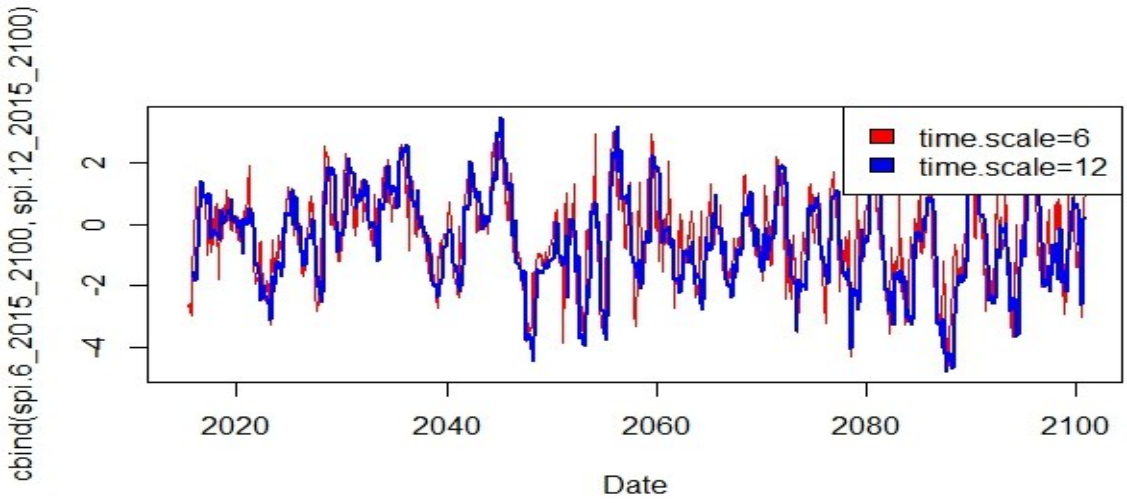

Fig. 5: Rajshahi's SPI time series for future 2015-2100

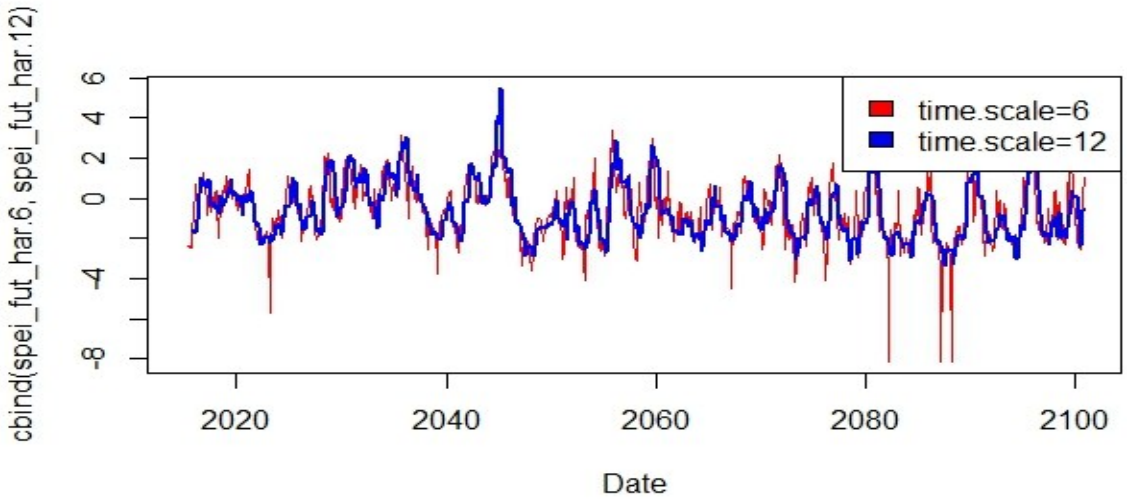

Fig. 6: Rajshahi's SPEI time series for future 2015-2100

It is observed that in future intensity of drought will increase (Figure 5 and Figure 6). The SPI series of future indicate a dry future but SPEI values indicate even more dry future. As world's temperature is increasing day by day due to the emission of greenhouse gases and SPEI depends on both temperature and precipitation, SPEI predicts drier future than SPI which depends only on precipitation. Again as the PRECIS data is for the extreme climatic scenario (RCP 805), therefore both SPI and SPEI indicate high probability of drought in future. However the drought and wet events identified from both SPI and SPEI indexes for 1971-2014 periods indicated almost similar moisture condition. Therefore the correlation between SPI and SPEI values are very high for both observed and PRECIS data for observed period.

Table 2: Correlation of SPI and SPEI for observed data and PRECIS

R^2 Values between SPI and SPEI		
DISTRICT	R^2 (observed)	R^2 (PRECIS)
Rajshahi	0.703265	0.925339
Rangpur	0.751834	0.949239
Dinajpur	0.913151	0.936289
Bogra	0.929033	0.946643
Ishwardi	0.923459	0.946503
Dhaka	0.93378	0.956655
Mymensingh	0.899391	0.948599
Tangail	0.944090	0.953664

The analysis of PRECIS model projection for 1971 to 2100 shows an increasing trend line for monthly average temperature and decreasing line for monthly total rainfall. However results also indicate few extreme rainfall events in 21st century.

Validation of result

Historical drought events record says that Bangladesh has faced some severe and moderate droughts in recent years. SPI and SPEI value from both observed and model dataset detected those drought years reasonably accurately. So this indicates that both SPI and SPEI are good indicator of drought. PRECIS monthly values and the distribution of temperature over the year are also compared with the observed temperature for year 1971-2014 and these values are matched properly.

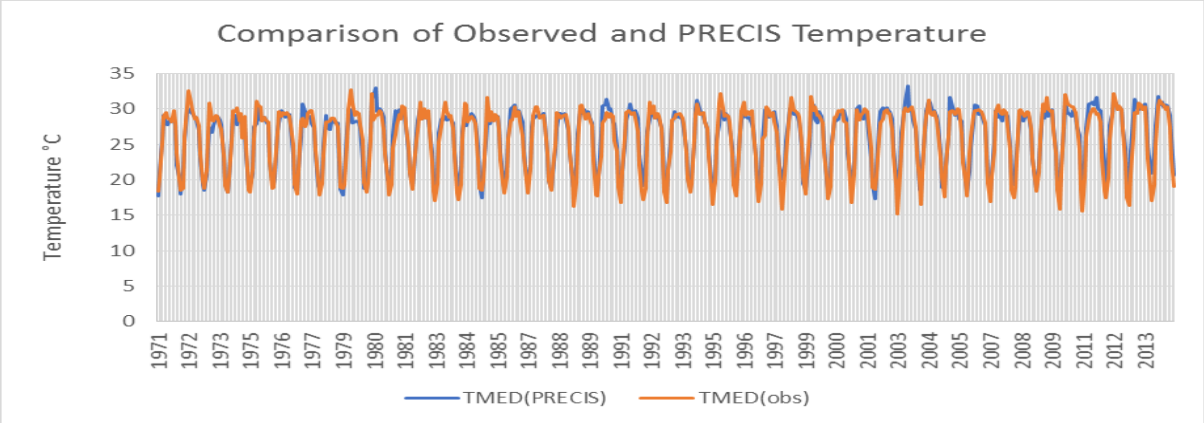

Fig. 7: Comparison of observed and PRECIS temperature for Ishwardi

Table 3: Comparison of the drought severity of Historical drought events with the drought severity obtained from the SPI and SPEI value

Historical Drought Year	SPI (Observed)	SPEI (Observed)	SPI (PRECIS)	SPEI (PRECIS)
1973	Extreme	extreme	moderate	moderate
1974	extreme	severe	moderate	moderate
1975	severe	severe	extreme	Extreme
1976	severe	severe	extreme	moderate
1979	moderate	moderate	moderate	moderate
1980	moderate	severe	extreme	extreme
1981	severe	extreme	moderate	severe
1982	severe	severe	Severe	moderate
1989	severe	severe	Severe	moderate
1992	severe	severe	Severe	severe
1994	severe	severe	Severe	extreme
1995	extreme	severe	extreme	extreme
1996	moderate	extreme	extreme	moderate
2000	extreme	severe	Severe	moderate
2009	severe	severe	moderate	moderate
2011	extreme	extreme	Severe	severe

CONCLUSIONS

The SPI and SPEI results obtained from this study indicate a very dry future with more frequent and severe drought events for PRECIS RCP 8.5 scenario. These results can provide valuable information for long-term regional and national drought risk management

ACKNOWLEDGMENTS

We would like to acknowledge Dr. A. K. M Saiful Islam, Professor, IWFM, BUET for providing PRECIS data and BWDB for providing observed precipitation and temperature data.

REFERENCES

Moukos. 2015. Drought in Greece under future climates. Master's thesis, Department of Geosciences, University of Oslo, Greece.

Shah, Bharadiya, Manekar 2015. Drought Index Computation Using Standardized Precipitation Index (SPI) Method for Surat District, Gujarat. Paper presented at *the International Conference on Water Resources, Coastal and Ocean Engineering.* Volume 4, 1243-1249. Available via: Science Direct. doi: 10.1016/j.aqpro.2015.02.162

Vicente-Serrano, Beguerý´a, Lorenzo-Lacruz, Camarer, pez-Moreno, Azorin-Molina, Revuelto, Mora´n-Tejeda, and Sanchez-Lorenz. 2012. Performance of Drought Indices for Ecological, Agricultural, and Hydrological Applications. *Earth Interactions*.16.

STUDY ON HYDRODYNAMIC RESPONSE OF GORAI RIVER TO DREDGING USING DELFT 3D

A. Rahman* & A. Yunus

Department of Water Resources Engineering, Bangladesh University of Engineering and Technology, Dhaka, Bangladesh
**Corresponding Author: afeefa@wre.buet.ac.bd*

ABSTRACT
Owing to the reduction of upstream water flow after construction of Farakka Barrage on the Ganges River, huge amount of sediment loads are settling down on Gorai river bed, hindering the safe passage of flow. For such sediment dominated rivers, dredging operations can be undertaken with a view to increase the river conveyance. The objective of this study is to investigate the hydrodynamic response of Gorai river to dredging using Delft 3D. A 25 km reach of the Gorai River, subdivided into 5 monitoring points for the year 2010 was selected for the model simulation. Simulated hydrodynamic parameters were compared before and after dredging to assess the functionality of dredged bathymetry. Results reveal that hydrodynamic performance, specifically, flow augmentation for the dredged condition is 9.632% with velocity increase of 9.82% and water level decrease of 14.98%. Thus the dredging strategy can be defined as an efficient one in facilitating the hydrodynamic response of the river. These results suggest that the dredging strategy can be defined as an efficient one in understanding the hydrodynamic response of the river and will help the river regulation authority to undertake appropriate future developments projects for the river restoration.

Keywords: Gorai; hydrodynamic; Delft3D; flow augmentation

INTRODUCTION
The pride of Bangladesh is its rivers, one of the largest networks in the world with a total number of about 700 rivers including tributaries, which have a total length of about 24,140 km. The country is a part of three major river systems of South Asia, namely, the Ganges-Padma, the Brahmaputra-Jamuna and the Meghna. From the time immemorial, rivers have played a significant role in forming the life line for our country, which recently is facing problems due to natural and anthropogenic reasons. In general, diversion of river flow in the upstream, salinity intrusion, excessive sedimentation causing navigability disturbance and flooding are the major problems relating to rivers in our country (FAP-24).Due to increasing withdrawal of the Ganges River in its upstream inside India, its distributaries inside Bangladesh are slowly facing death for not receiving their winter flow. The Ichhamoti is dead, the Baral and the Chandana are dying, the Mathabhanga rarely gets flow during flood months, and the Gorai also gets dried up at its off-take during winter (M. Inamul Haque, 2015).Gorai River is the major distributary of the Ganges River in the right bank and a main source of freshwater within the Bengal Delta area (Addams, 1919). With a total length of about 200 km Gorai has a catchment area of 15160 km² and is located between 21° 30’ N to 24° 0’ N latitude and 89° 0’ E to 90° 0’ E longitude (Bangladesh er Nod Nodi,2010) covering south western region of Bangladesh. The river takes off from the Ganges at Talbaria, north of Kushtia town and 19 km downstream from the Hardinge bridge and discharges into the Bay of Bengal through the Madhumati and Baleswar Rivers (Islam and Gnauck, 2011). Due to implementation of the Farakka Barrage in 1975, the dry season flows in Ganges River started to decline subsequently which results in reduction of flow through the Gorai River and deposition started ensuing in the off-take. As a result, two types of environmental impacts have been created in the Gorai catchment area (BWDB, 2010). The sediment particles are settling down on the river bed rapidly, which is one of the major problems of Gorai River morphology. On the other hand the saline sea water is pushed up in the upstream area due to capillary upward movement. As the Gorai is the main lifeline of South-western part of Bangladesh dredging efforts can be taken to de-silt its off-take to keep the flow coming from the Ganges River(M.Inamul Haque, 2015). In this

study, realizing the importance of rivers in Bangladesh in general and understanding the predicament of river Gorai in particular, efforts have been ensued to address the hydrodynamic analysis of the river Gorai with respect to dredging as a part of solution of sediment problems and flow augmentation. Hydrodynamic parameters including discharge, velocity and water level were compared before and after dredging and portrayed in the graphs and charts.

Effects of Dredging on river hydrodynamics

Dredging operations involve the removal of bed material and associated vegetation from a river channel with an objective of increasing the river channel capacity and its ability to convey water (Andries J. et.al, 2015).The exact ramifications of river dredging upon river hydrology and geomorphology will be a function of the river topology, sediment characteristics, the dredging technique employed, existing floodplain connectivity and antecedent environmental conditions. Channels which have been deepened by dredging silt-up more frequently as they return to their pre-dredged state(Judy England and Lydia Burgess-Gamble, 2013). Dredging can reduce water levels at some locations but this depends on local conditions and is therefore case specific. Local reductions in water levels automatically mean a reduction in flood risk. Dredging would automatically prevent out of bank flow from occurring(Judy England and Lydia Burgess-Gamble, Environment Agency, 2013). Dredging activity is combined with a greater fine sediment load to cause bed armoring and dredging causes increase in the discharge and velocity decreasing in the water level (Trevor Bond, 2013). If a dredged channel is also straightened, the water velocity is increased significantly, due to increased slope and the loss of energy dissipation at bends. Faster water causes much more damage during floods.(Southern Tier Central Regional Planning & Development Board,2013).

Study Area

The study area covers about 25 km reach of the Gorai River flowing from 10km downstream from the Ganges-Gorai off-take within the kushtia district to the 5 km upstream of the Kamarkhali transit within the Kamarkhali upazilla. Figure 1 shows the Google map of the study area.

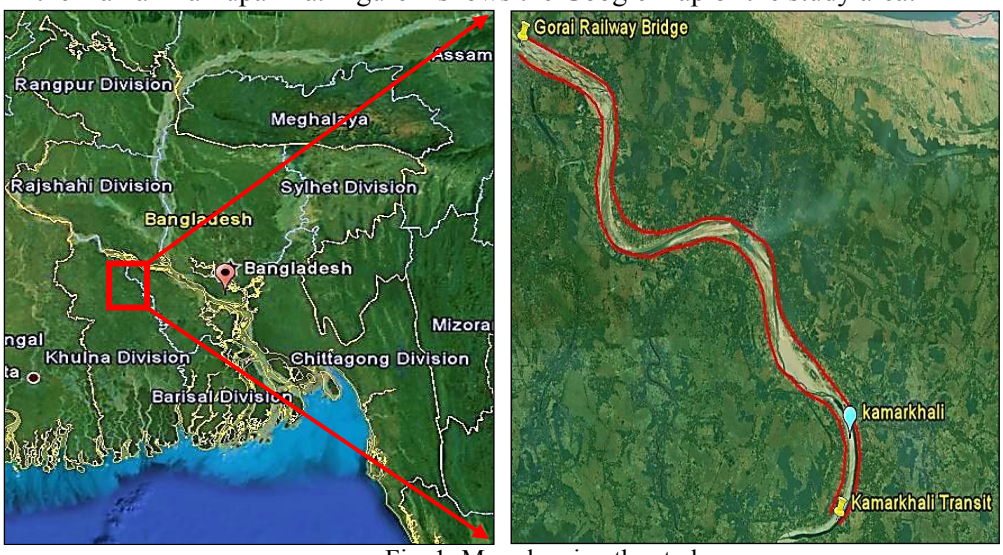

Fig. 1: Map showing the study area

METHODOLOGY

Methodology of the study covers data collection, setting up of a model of 25 km river reach of the upper Gorai and performing analysis for two simulation period; dry and flood period and two settings; pre and post dredging conditions. Cross section data for the year 2009-2010, time series discharge data at the Gorai Railway Bridge (SW-99), Water level data at Kamarkhali (SW-101) and Kamarkhali transit (SW-101.5) have been collected from Bangladesh Water Development Board (BWDB) and Water Resources planning organizations for the model setup. Physics-based nonlinear morpho-dynamic model Delft3D of version 3.28.50.01 was used as a modeling tool. Hydrodynamic parameters such as discharge, velocity and water level were compared before and after dredging and

portrayed in graphs and charts. A25 km long river reach with an average width of 800 m; started from 6 km downstream from the Ganges-Gorai off-take was discretized by 720*36(m*n) cells. The average dimension of each grid cell was approximately 40m*40m.After developing the study area with good quality grids, processed cross section data were imported and has been interpolated and diffused to obtain a spatially varying depth file. Figure 2 shows the grid and depth of the study reach. Bathymetry data was collected during the monsoon period of the year 2010 measured with respect to the PWD datum.120 cross sections at approximately 200 m interval have been used for the setup of the initial bathymetry of the model. Figure 3shows the initial defines the monitoring points which have been used for observing simulated velocities, discharge and water level.

Calibration and Verification of the Model

Calibration and verification of a numerical model requires two independent data sets, one of which is used to calibrate the model and the other to validate the results. Calibration of the model has been done simulating the model from 1st of June, 2010 to 31st of August, 2010 and verified for the time ranging from 1st of September to 30th of November. Computed water surface elevations have been compared with the observed water surface elevations at Kamarkhali station (SW-101). Roughness and eddy viscosity are the parameters that have been used to play to obtain an adequate match with the observed field conditions. Manning's roughness coefficient has been adjusted after several trial of the model during calibration to an average value of n = 0.025, The value of eddy viscosity has been considered as 10.0 m2/s. The model was validated at the Kamarkhali for the period 1st of September to 30th of November that shows a good agreement with the observed data.

Selection of Dredge Section

Proposed dredged section is a trapezoidal one (GRRP, 2000). In this study a dredging section of 200 m base width having side slopes of 1:20 and 13 m deep from the side banks has been used to understand the dredging response on the river hydrodynamics. Figure 2 shows the comparative plot of the river bed.

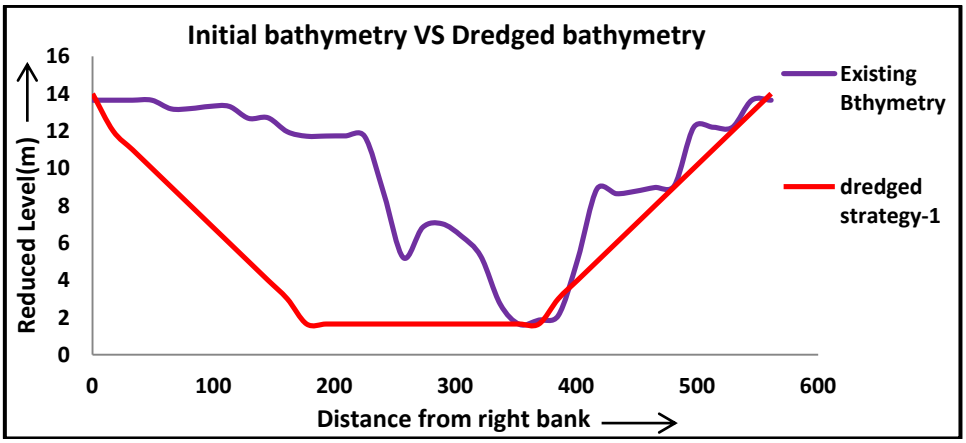

Fig. 2: Initial bathymetry Vs dredged Bathymetry

RESULTS AND DISCUSSIONS

Analysis on Dredging Response:

Simulated depth averaged velocities at 5 different monitoring points are plotted to visualize the changing pattern and the length wise difference in magnitude. The peak velocity ranges from 0.7 m/s-0.9 m/s during the flood period and the value ranges from 0.1m/s-0.25 m/s during the period of lean flow. Trough and peak magnitudes of the velocities show that change in velocity along the reach varies from 4%-7%. Flow velocity along the study reach decreases due to the changing fluvial processes but the percentage change is not so significant due to small length of the study area. A dredging strategy remarkably alters the bathymetry. It induces a change in flow velocity. As the river bed deepens by dredging, it provides a more smooth passage for the flow. Seasonal variation in the flow volume also causes a change in the velocity time to time.

Figure 2(a), (b) show the comparison of depth average velocity of the study reach of the river for the two conditions of pre and post dredging strategy during the wet seasons. It can be visualized that during both the wet and dry season for the year 2010 there is a higher velocity of flow in the main channels and flood plains in case of dredged bathymetry. The velocity in the main channel is obviously greater than the velocity in the side channels. During the wet season flow velocity throughout the study reach varies from 0.3 m/s-0.9 m/s in case of original depth profile whereas the range of velocity increases to 0.4 m/s-1.1 m/s in dredged bathymetry. During the lean period flow velocity falls within the range of 0.06 m/s-0.16 m/s that increases to 0.30 m/s to 0.65m/s in dredged bathymetry.

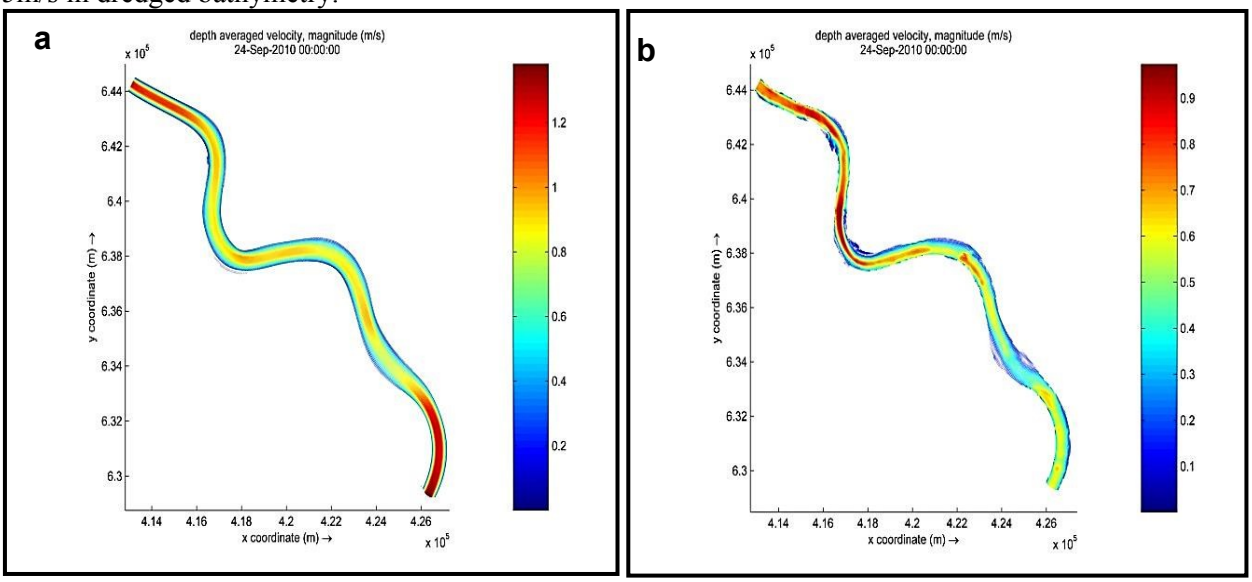

Fig. 2: Simulated depth average velocity during wet season (a) Pre-dredging; (b)Post dredging

Simulated discharges at 5 different monitoring points named are plotted to visualize the changing pattern and the length wise difference in magnitude of discharge. Simulated discharge during the flood period ranges from 2800 m3/s to 4200 m3/s. Trough and peak magnitudes of the discharge show that change in discharge along the reach varies from 12%-17% with maximum discharge at the 1st monitoring point and minimum at 5th monitoring point. To compare the pre and post dredging work, average of the discharges of 5 monitoring points is taken as the mean discharge in case of pre-dredging work. As the flow velocity increases due to dredging, it induces an increase in discharge along the study reach that augments both the dry and wet season flow. Simulated water levels at 5 different monitoring points were plotted to visualize the changing pattern and the length wise difference in magnitude. Water depth increases along the reach as the flow velocity and discharge decreases along the reach. But the simulated water levels showed a decreasing pattern along the reach as the bed level lowers along the bathymetry at an average slope due to land topography. During dry period simulated water level varies from 2 m to 3.5 m and the level rises to 8m to 9.5 m during flood period. As dredging result in narrowing and deepening of the channel, the still water level drops. The series of figures below show the effect of dredging on the water surface elevation of the study reach of the river Gorai in both dry and wet seasons. It can be visualized that during both the wet and dry season for the year 2010 there is a lower water depth in the main channel in case of dredged bathymetry comparing with the original depth

profile. Due to dredging, channel navigability increases contributing more water flow through the main channel, thus the water level drops in both the main channel and flood plains.

Discussion and Results:

The percentage variation of average monthly velocity, discharge and water level for the dredging scenario comparing with the original bathymetry can be tabulated as follows (Table 1) for better visualization. Positive percentage indicates percentage increase in corresponding parameter and negative percentage depicts the percentage decrease of the corresponding parameter.

Table 1 Response of Gorai river to dredging

Months	Velocity (%)	Discharge (%)	Water level (%)
Jan	8.67	6.24	-11.37
Feb	11.03	6.04	-11.77
Mar	10.19	6.44	-13.30
Apr	9.17	6.89	-13.23
May	9.84	8.38	-14.98
Jun	9.59	8.61	-14.17
Jul	9.37	9.81	-14.76
Aug	9.17	10.73	-15.21
Sep	13.39	10.63	-15.78
Oct	7.56	6.55	-14.08
Nov	4.25	6.40	-13.68
Dec	6.56	6.25	-13.38

From the analysis it has been found that for dry period velocity increase was obtained as 8.312%, corresponding percentage increase during wet season are 9.816%.For dry period discharge increase was obtained as 6.403%, corresponding percentage increase during wet season are 9.632%.For dry period water level decrease were obtained as 11.57%, corresponding percentage during wet season are 14.93%.

CONCLUSION, RECOMMENDATIONS AND STUDY LIMITATIONS

The models presented in the study are by far believed to be the most realistic simulation in terms of hydrodynamics. In the present study a deep insight on the effect of backfilling rate has not been considered. The percentage increase in flow discharge is not satisfactory enough to revive the Gorai River, thus dredging cannot be adopted as a permanent solution for the restoration. Moreover dredging has some negative Impacts. The process of dredging can damage ecology by directly affecting its physical habitat, disrupting riverine processes and reduced connectivity with the floodplain. Furthermore as in most of the real cases the spoil dumping areas are within the catchment area, a portion of the deposited sediment from the disposal sites returns to the dredged channel which may affect the sediment transport rate, cumulative erosion and cumulative deposition of the dredged channel. To avoid the difficulties in estimating the exact volume of the spoil deposition in the dredged channel, it is not incorporated in this study. Future study can be performed by counting the fact. For further extension, dredging section with any other dimensions and alignments can be considered to produce variable results.

REFERENCES

Abdullahel Baki, ATM. 2014, Socio-economic impacts of gorai riverbank erosion on people: a case study of kumarkhali, kushtia.

Andries J. et.al, 2015. Optimizing Dredge-and-Dump Activities for River Navigability Using a Hydro-Morphodynamic Model. *Water* 2015(*7)*:3943-3962; doi:10.3390/w7073943,*water*ISSN 2073-444.

BWDB 2012. *Bathymetry survey for pre-work and post-work measurement of dredging for Gorai river restoration project(phase-II),* Progress report-23, 7-10

BWDB, 2011. Bangladesh er Nod-Nodi, Bangladesh Water Development Board (BWDB), Dhaka, Bangladesh

Biswas NK, Ahammad M. Jan-Jun 2014. Application of CCHE2D Mathematical Model in the GoraiOfftake for two-dimensional simulation, International Journal of Surface and Groundwater Management,01(01).

Bond, T. 2013, The geomorphic Effects of river dredging. The river management Blog.
http://en.banglapedia.org/index.php?title=River
Clijncke A. 2001. Morphological response to dredging of the upper Gorai river, thesis main report, TU Delft.
Giardino A and Winterwerp. 2012. Assessment of increasing freshwater input on salinity and sedimentation in the Gorai river system", project report, Deltares.
FAP24, 1994. Study report No. 3: Morphological studies phase 1, Available data and characteristics. FAP24, Dhaka, Bangladesh.
Haque, MI. The Daily Star: http://www.thedailystar.net/gorai-river-can-it-flow-round-the-year-46910 (01:53 AM, March 08, 2015)
Islam; Tarekul, GM and Karim, MR. 2005. Predicting downstream hydraulic geometry of the Gorai river, *Journal of Civil* Engineering (IEB), 33(2): 55-63.
Information and Advisory Note Number 23, http://www.snh.org.uk/publications/on-line/advisorynotes/23/23.htm
Judy England and Lydia Burgess-Gamble, August, 2013. A report on-Evidence: Impacts of dredging, Environment Agency.

FLOOD INUNDATION MAPPING ON JAMUNA BASIN FLOODPLAIN USING HEC-RAS 1D/2D COUPLED MODEL

M. M. Ali*, M. S. B. M. Anik & A. H. N. Khan

Department of Water Resources Engineering, Bangladesh University of Engineering and Technology, Dhaka, Bangladesh
**Corresponding Author: wremostafa@gmail.com*

ABSTRACT
Bangladesh lies at the confluence of worlds three major rivers, namely the Ganges, the Jamuna and the Meghna. Bangladesh is very much prone to flooding owing to its lower elevation. Flood causes tremendous losses in terms of property and life, particularly in the low land areas. At least 20 % areas are flooded every year and in case of severe flood, about three fourth part of the country is inundated. Therefore, the study is carried out to develop inundation maps of the Jamuna River. Therefore, an associative study was made upon the impact of breached levee on particular districts. The study made here is based upon a combined one and two dimensional model which needs cooperation of GIS and HEC-GeoRAS. The later twos help to form appropriate topographic data and channel cross sections. In HEC-RAS, boundary conditions for upstream and downstream are defined by discharge and water level for running the 1D river, while for 2D floodplain discharge data was used in upstream side and rating curve was used in downstream portion. After boundary condition setup, the channel calibration and validation are performed using known hydrological data collected from BWDB. For floodplain calibration we used about 1% discharge flowing through the channel and only when the channel discharge is more than bank full discharge. However calibration and validation showed result much closer to the actual scenario. After calibration and validation flood inundation map are generated using RAS Mapper and calculated in GIS by exporting data from HECRAS to GIS. The average levee height was about 2m which showed significant amount of resistance against flood. Later, the analysis of flood pattern helped to understand the seasonal growth of flood. Thus, ending of the study may help in planning and management of flood plain area of the Jamuna River to mitigate future probable disaster through technical approach. Findings of the study may also help to determine suitability of building flood control structure like embankment, detention ponds for prevention purposes.

Keywords: *HECRAS; GIS; Bathymetry*

INTRODUCTION
Bangladesh is a riverine country which lies at the confluence of world's three major rivers, namely the Ganges, the Meghna and the Jamuna. Owing to its lower elevation, Bangladesh is very much prone to flooding. Flood causes tremendous losses in terms of property and life, particularly in the low land areas. Every year at least 20% areas are flooded in case of severe flood which is about three fourth part of the country. Moreover, Bangladesh is prone to flooding due to being situated on Ganges delta and the many distributaries flowing into the Bay of Bengal. Including three of the world's largest rivers, the Ganges, the Brahmaputra (Jamuna) and the Meghna about 90% of total stream flows through Bangladesh originate from upstream catchment in India, Nepal, Bhutan and China.

For being a braided river, the characteristics of Jamuna is not fixed, rather changes with time. So it is essential to understand the characteristics of flood inundation for the Jamuna River. With this study, we can know how much area will be flooded due to a given discharge. In addition to that, we need to know how fast or at what rate the flood plain areas are flooded due to given discharge, to answer these key

questions, this study has been taken. Flood inundation modeling requires a two dimensional model, however, study of flood inundation can be done using a combined one dimensional (1D) and two dimensional (2D) hydro dynamic model which includes flood plains as 2D part and river as 1D part .In that sense this is a very new study in the subcontinent and also new to the other part of world as coupled 1D and 2D modeling is new in HEC-RAS. In case of this 1D/2D coupled model HEC-RAS has given some special features. The 2D unsteady equations solver uses an implicit finite volume algorithm which allows larger time step in calculation and improved stability and robustness over traditional finite difference and finite element techniques. Moreover it provides detailed hydraulic property table for computational cells and cell faces. Finally in this study we could utilize the detailed flood mapping capability of HEC-RAS 5.0.0 which was not possible in the older versions.

Fig. 1: Study Area

The main objective is to study the capabilities of a 1D/2D coupled hydro dynamic model in simulating flood inundation of the Jamuna River, generate and compare flood inundation map and estimate the effect of construction embankment for particular location. The Jamuna's middle portion and its floodplain, about 25 km in the left bank and 35 km in the right bank of the river, are the study areas in this study (Figure 1). The river reach length is about 90 km and the total area is 6870 square km excluding the river. Only the Jamuna River's floodplains has been considered for this study which includes Gaibandha, Bogra, Sirajganj, Sherpur, Jamalpur and Tangail districts only.

METHODOLOGY

For the study we used different sets of data named bathymetric data, hydrologic data (discharge and water level) and topographic data as Digital Elevation Model (DEM) data. To set up the model preprocessing was necessary in GIS. The river bathymetric data collected from Institute of Water Modeling (IWM) has been used for the generation of the shape file. Data Management tool of ArcGIS has been used to process the data. To create a surface grid in ArcGIS, the 'Spatial Analyst' extension employs one of several interpolation tools. In this study, Kriging interpolation method has been used to create the surface grid of the river bathymetry. The size of the grids has been chosen as 10 meter. The created topographic grid contains some default topographic data that are not appropriate. Only river bathymetric grid is needed. Extraction of grid needs the 'Grid Analyst' extension. A polygon has been drawn in accordance with the river bathymetric size. Using this polygon the bathymetric grid file has been extracted from the topographic grid file. The bed level for bathymetry was referenced with respect to the Public Works

Datum (PWD) of Bangladesh, which is established by the Department of Public Works, Bangladesh. The complete bathymetric grid has been shown in figure 2.

Fig. 2: The River Bathymetric Grid

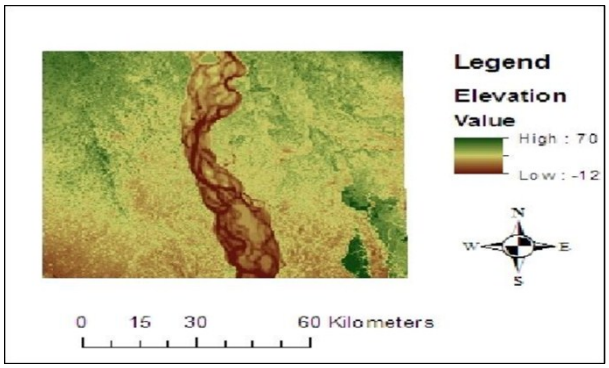

Fig. 3: Merged Bathymetry with DEM Data

After downloading the DEM, the study area DEM has been clipped from the entire DEM by using the data management tool. Finally, DEM has been resampled into 10*10m resolution. The elevation of the DEM has been measured relative to the mean sea level (MSL). DEM's value has been transferred to PWD datum by adding 0.46 m. All the data in the DEM have been projected on to the Bangladesh Transverse Mercator (BTM). Then the bathymetric grid has been merged with the topographic DEM to produce the complete DEM of the river bathymetry along with the topographic DEM (Figure 3). Hence, for the preparation of channel geometry, preprocessing was done in HEC-GeoRAS. To create 1D geometry we used the bathymetric grid only and excluded the nearby floodplain. The goal of this section was to develop the spatial data required to generate a HEC-RAS import file with a 3-D river network and defined 3-D cross sections. This extraction comprises several steps. These are development of a river centerline, cross-sections, river banks, and flow path lines as shape files.

1D geometric data was imported to HEC-RAS. After that we divided the floodplain into two parts of the river and created 2D mesh at both left and right side of the river. In case of creating 2D mesh, we took 300m*300m as cell size. Then the cells have been created after mesh analysis. We did coupling of 1D and 2D model by using lateral structure on the upstream of both sides of the river. In our model, bank elevation and levee height were kept approximately at the same elevation. Then we breached the levee for creating actual condition and ran the geometric preprocessor from RAS Mapper. Finally, boundary condition lines were drawn at the both upstream and downstream side of the floodplain.
We have applied different boundary condition for different time series data for calibration and validation respectively for unsteady flow simulations. For 2D connection, additional boundary condition is necessary to be applied. So we provided discharge data at the upstream boundary condition line in order to allow the entry of the inherent flow from the outside of the area into the floodplain. Rating curves were used at the downstream floodplain so that the flood water can pass away.
The data regarding to the flood year 2004 has been used for calibration and the parameter was Manning's roughness co-efficient 'n'. The model has been simulated using the daily hydrograph for four months from June to September. The 'n' value as 0.032 for main channel and `n' value as 0.035 for flood plain has been fixed as Manning's 'n'. The comparison of observed and simulated stage hydrograph at Kazipur and Mathurapara gauging station was noticed for different Manning's 'n'. After that the flood peak and time to peak for the flood year 2004 is computed and it is observed that there is a close agreement between the observed and computed values (Figure 4). In unsteady calibration, the co-efficient of regression R^2 has been found 0.9295, which indicates, the simulated value is closer to the observed value.

The calibrated HEC-RAS 5.0 based model has been also used to validate the flow for the year 2004 and the value of R^2 was found to be 0.8306.

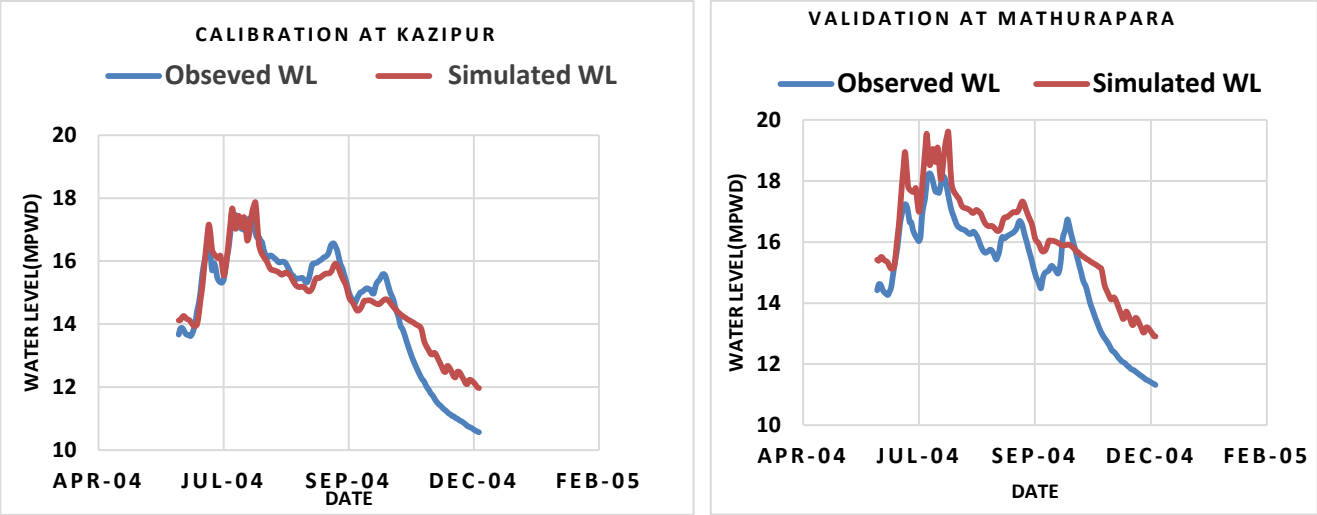

Fig. 4: Plotting of Calibration at Kazipur and Validation at Mathurapara

The calibrated and validated model has been used to generate water surface profiles for different flow conditions. At first, 2004 flood discharge water profile has been generated. Water surface profiles of one-day-interval from June to December have been generated for five years from 2004 to 2008. The generated water surface profile data have been exported in GIS format data to develop flow inundation map. Besides, floodplain delineation is done by HEC RAS 5.0 software itself and shown in RAS Mapper. No GIS help is needed here. Shape file of different flood extend can be produced for different time. Then we exported the shape file into GIS and calculated the area of inundation. Our model simulation map and MODIS data map also shows the approximate result. In fact, flood in 2005, 2006,2007 also shows a significant similarity with both model and MODIS map (Figure 5).

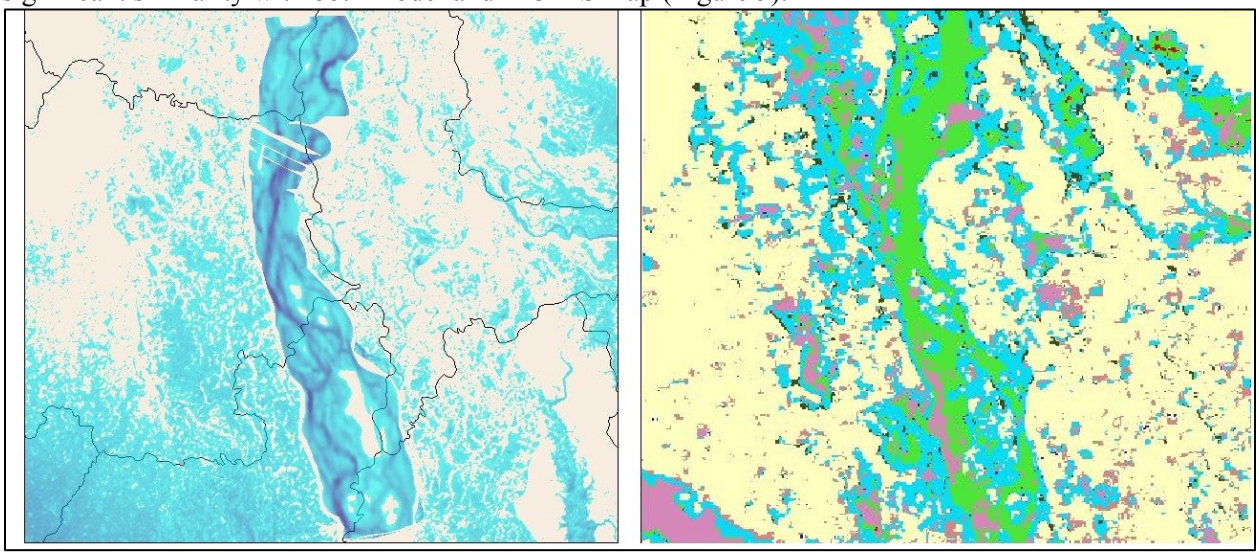

MODEL FLOOD MAP MODIS FLOOD MAP

Fig. 5: Qualitative comparison between simulated and observed flood map of 02 October, 2004

RESULT AND DISCUSSION

After the model calibration and validation, flood extent and inundation maps have been prepared for different time series. Unsteady simulation has been performed for analysis of the changing flood pattern with time. Finally, we estimated the levee impact on the flood inundation area. We completed unsteady simulations for the year of 2004 to 2008. Summary of the observed result is shown in table1.

Table1: Inundation area, maximum discharge and percent inundation in different years

Year	Maximum discharge (cumec)	Inundated area (sq.km)	Percent inundation
2004	83945	3593	52.29
2005	55340	1848	26.9
2006	46791	707	10.3
2007	94236	5001	72.79
2008	64354	2234	32.53

Then we have made analysis upon the flood pattern for the year of 2004, 2007 and 2008. The flood of 2004 shows a massive inundation. The analysis is briefly represented in the figure 6. As per our model result, it is seen that flood starts from third quarter of June and peak occurs at late July. Sirajgonj, Tangail and Bogra were mostly affected by that flood. 2007 flood seems to be more extensive than the flood of 2004. Here the peak occurs lately nearly at mid-August. The flood sustained for a long period compared to the other ones. According to the flood map generated from model simulation it is seen that peak occurs at the end of September and its duration was much short compared to 2004 and 2007. Now, the levee elevation plays important role in controlling the floodplain area. For analysis of its effect, we set up two levees at left and right side of the river which are about 14 km long. The levees were meant to resist the flooding of Tangail district on the right side and Sirajgonj on the left of the river. Analysis on simulation

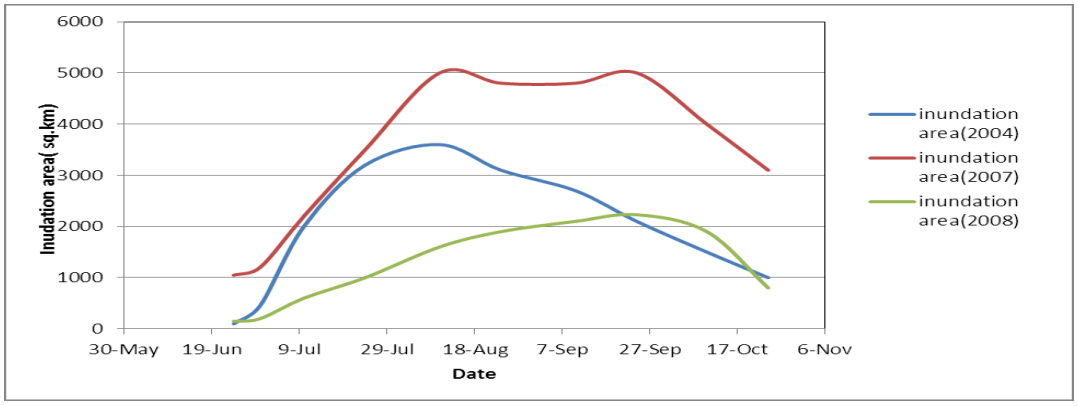

Fig. 6: Analysis of the flood patterns for different years

shows that flood extent decreases significantly due to the levee set up (70-80% in our case). We tried with a levee on an average of 16.25mPWD elevation all through the span.

CONCLUSION

This study presents a systematic approach in the preparation of flood inundation and flood hazard maps with the application of combined hydrodynamic 1D and 2D model, HEC-RAS and GIS. The change of flooding with time is also shown in this study by performing unsteady flow analysis and flood mapping. The major tools used in this method are a combination of 1D/2D numerical model HEC-RAS 5.0 and ArcGIS for spatial data processing and HEC-GeoRAS for interfacing between HEC-RAS and ArcGIS.

Here, establishment of Hydrodynamic model through coupling of 1D river and 2D floodplain was made for the Jamuna River. Calibration and validation of the model show good correlation between the observed and simulated data. The value of correlation coefficient, R is 0.93 and 0.83 for calibration and validation respectively. Comparison between observed flood from MODIS image and model result were satisfactory. Application of levee can be computed by the model. Establishment of a levee of about 2m height reduces flood extent about 85%.

REFERENCES

Abera, Z. (2011). *Flood Mapping and Modeling on Fogera Flood Plain: A case study ofRibb*
ArcGIS, (2007). *ArcView Geographical Information System User's Manual*.Environmental Systems
Bhuiyan, M. A. H., Rakib M. A., Takashi K., Rahman M. J. J. and S. Suzuki (2010). Regulation of Brahmaputra-Jamuna river around Jamuna bridge site, Bangladesh: Geoenvironmental impacts. *Journal of Water Resource and Protection*.
HEC-GeoRAS, (2009). *An extension for support of HEC-RAS using Arcview User's Manual*. U.S. Army Corps of Engineers Hydrologic Engineering Center, Davis, California.
Research Institute (ESRI), University of Pennsylvania, USA.
River. M.Sc Thesis, Depatment of civil engineering, Addis Ababa University, Ethiopia.
Rahman, M. M., Hossain M. A. and M. A. Bhattacharya (2007).Flood management in the flood plain of Bangladesh. *International Conference on Civil Engineering in the New Millennium: Opportunities and Challenges (CENM).*

CHANGES OF HYDRO-MORPHOLOGY OF SHITALAKHYA RIVER AND EFFECT OF PROPOSED BRIDGE USING HEC-RAS 1D MODEL

S. A. Saki* & M. M. Miah

Department of Water Resources Engineering, Bangladesh University of Engineering and Technology, Dhaka, Bangladesh
**Corresponding Author: saki.afzal@gmail.com*

ABSTRACT
Knowledge on hydro-morphologic behaviour of a river is for essential design of bridges and hydraulic structures; flood control; planning, maintaining and controlling reservoir, training and stabilization of rivers. The purpose of the study is to analyse hydrological and morphological characteristics of the river and predict the scour and afflux caused by a proposed bridge using HEC-RAS 1D model. For this purpose several morphological and hydrological parameters were analysed from the collected satellite images, cross sectional data, water level data and discharge data. For proposed bridge, a model was set up in HEC-RAS 1D, calibrated and validated**.** Scour and afflux were computed using the collected bridge data. Negligible amount of erosion and deposition occurred in the study reach and some shifting in thalweg were observed. No significant shifting in river banks occurred during the study period (1981 to 2011). A decreasing trend was observed in maximum water level and maximum annual discharge. So navigability of the river is being threatened greatly. The scour and afflux were found within limit indicating the viability of bridge construction.

Keywords: Hydro-morphology; afflux, scour; thalweg movement, HEC-RAS 1D

INTRODUCTION
Shitalakhya, one of the main circulating rivers of Dhaka city, has ample importance in navigation, industrial purpose and economy of Bangladesh. The parent river of Shitalakhya is Old Brahmaputra. The river getting its flow through Banar River and then flows down via Ghorashal, Narayanganj and Madanganj. Finally it discharges into the river Dhalweswari, opposite to Munshiganj town. The River is used for navigational purpose, fishing, farming, industrial use and water supply. The lowering of water level and decrease of discharge has hampered the navigability of the river. The river is used for transboundary carrying goods along with navigational purposes. The river is one of the sources of municipal water of Dhaka city. Several parameters govern the hydrologic and morphologic characteristics of the river. Previous studies reported reduction of flow depth and degradation of water quality (IWM 2006; Hossain et al.; 2014; Rouf et al., 2013; Shaikh, 2006). There are two bridges on this river. There is a plan of constructing 3rd Shitalakhya Bridge on the river and the present study focuses on the changes in hydro-morphology of the river throughout the study period and the effect of bridge in terms of afflux and scour.

CURRENT HYDRO-MORPHOLOGICAL CONDITION OF SHITALAKHYA
The Shitalakhya River is running in a soil bed with a high resistance to erosion. Firstly, the river velocity seldom reaches the value sufficiently high enough to erode this bank. Secondly, the structures along the banks, function more or less as fixation points for the river current. The original river banks are resistant to scouring, as they consist of ferruginous laterite clay. However; recent deposits are

subjected to continuous erosion and deposition. This is because runoff as well as tidal influences have sufficient high velocity to erode and deposit the river bed materials.

METHODOLOGY

Data Collection

For hydrological and morphological analysis cross section data of different years for stations L-1 to L-19, discharge data for several years (1990-2010) at Demra station (BWDB station No. 179) and water level data at Lakhpur (BWDB station No. 177) and Demra (BWDB station No. 178) for 1981 to 2010 were collected from Bangladesh Water Development Board (BWDB). Data pertaining to the proposed bridge were collected from Roads and Highways Department (RHD). The satellite (LANDSAT) images were collected and analyzed for determining the shift of bank line. The satellite images of 1975, 2000 and 2015 were collected for this purpose.

ANALYSIS OF DATA

Morphological Data Analysis

The morphological analysis was carried out using the obtained cross sectional data, satellite images, and historical maps. Cross-section at different stations (L1 to L19) were plotted and superimposed in Microsoft Office Excel for years 1981, 1992, 2001 and 2009. The variation in cross section was determined in terms of cross sectional area, top width and maximum depth at different stations. The analyses were done for the year 1981, 1992, 2001 and 2009. Satellite images collected from CEGIS, were superimposed in ArcGIS to analyse bank line shift.

Hydrological Data Analysis

Analysis of water level and discharge data was carried out to ascertain the hydrological condition of the Shitalakhya River. The maximum water level and the maximum discharge for different years were plotted in Microsoft Office Excel to show the variation with time. The maximum and minimum discharge and water level of a river are important for the design of a structure. So Design High Water (DHW) and Design Low Water (DLW) were determined using Gumbel's distribution method.

Model Setup

The river bank and centre line was generated by HEC-GeoRAS. Collected cross section data and geometric data were assigned in HEC-RAS. The model was initially run for unsteady flow. For this, flow hydrograph was used as upstream boundary condition and stage hydrograph was used as downstream boundary condition**.** The model was calibrated [Fig. 1] using daily water level of year 2009 at Lakhpur station.

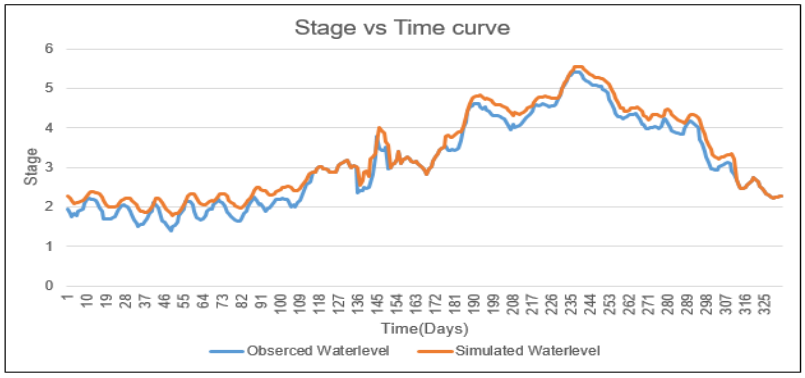

Fig. 1: Calibration Curve of Unsteady Model for the Shitalakhya River

Calibrated 'n' value was found to be 0.018. The model was validated [Fig. 2] for year 2014 for same station and Manning's 'n' value of 0.018. The ratio of the root mean square error to the standard deviation of measured data (RSR) and Nash-Sutcliffe efficiency (NSE) value showed in table 1.

Table 1: Model Performance Analysis

	RSR	NSE
Calibration	0.258	0.716
Validation	0.506	0.835

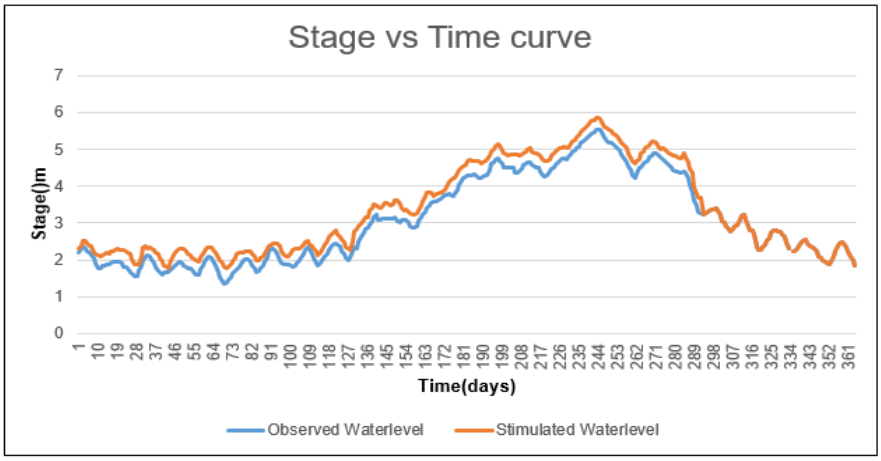

Fig. 2: Validation Curve of Unsteady Model for the Shitalakhya River

Calibration and validation indicated good performance of model. The collected bridge data such as geometric data, pier and abutment details were used as input. The model was run under steady condition for this purpose. Pier scour, contraction scour and abutment scour were obtained as output.

RESULTS AND DISCUSSIONS

Results of the analysis reveal that both the banks were stable and did not change much during the study period [Fig. 3].

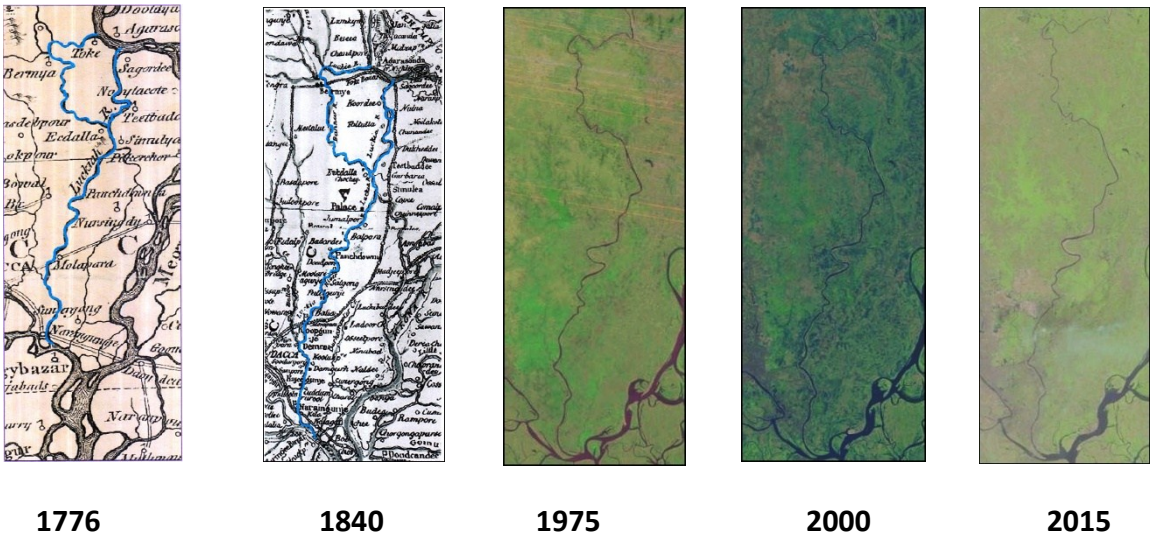

Fig. 3: Maps of Different Years Showing the Changes in Plan Form of the Shitalakhya River

The variation of top width, cross sectional area and maximum depth for these stations are given in table 2.

Table 2: Changes in area, top width and maximum depth of the river

Year	Area (m^2)	Top Width (m)	Maximum Depth(m)
Station L-1			
Year 1981	1333.63	121.23	13.15
Year 1992	1482.18	105.31	13.69
Year 2001	1128.41	152.35	14.23
Year 2009	1607.41	155.74	14.83
Station L-7			
Year 1981	1958.1	150.47	16.64
Year 1992	2195.23	159.86	13.49
Year 2001	1811.46	177.04	13.22
Year 2009	2401.09	177.87	13.44

The cross sectional area reduced marginally during 1981 to 2001 at the upper reach stations (L-1 to L-10) but increased [Fig. 4] in the downstream stations (L-11 to L-19). Almost all the stations showed an increasing trend of cross-sectional area from 2001 to 2009.Similar trend was observed for top width and maximum depth.

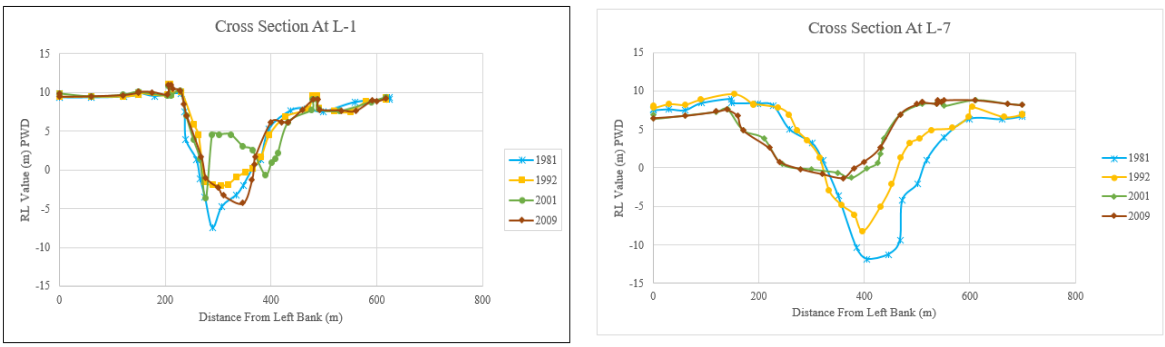

Fig. 4: Changes in Cross-Section for different years at L-1 and L-7

The thalweg movement was very insignificant during 1981 to 1992. But during the period of 1992 to 2009 the thalweg movement occurred significantly due to erosion and deposition which is shown in [Fig. 5(a)] and [Fig. 5(b)]

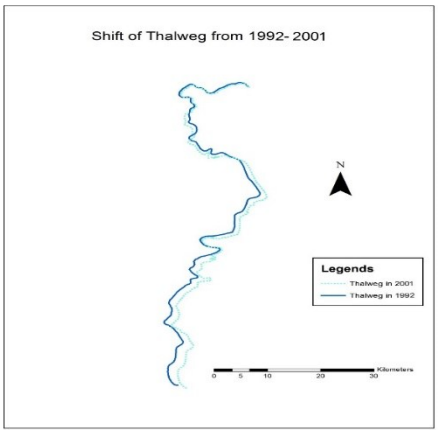

Fig. 5(a): Plan View of Shitalakhya River showing Thalweg Movement from 1992 to 2001

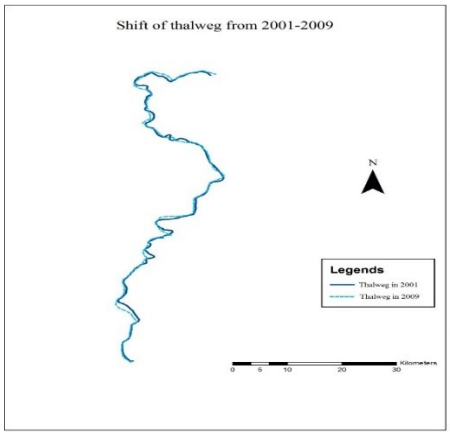

Fig. 5(b): Plan View of Shitalakhya River showing Thalweg Movement from 2001 to 2009

The hydrological data as showed in [Fig. 6(a)] reveal that water level remained almost same from 1981 to 2012. The average value of water level was found to be 4.8m PWD. There was some variation due to natural calamities like floods, surges, etc. But the water level showed a decreasing trend after 2004 may be due to low prevailing discharge. The design high water was found to be 10.24m PWD for station 177 and 7.5m PWD for station 179 for 100 years return period. On the other hand the low water of 0.96m PWD for station 177 and 0.82m PWD for station 179 for 100 year return period. There was a declining trend in the maximum annual discharge of the river [Fig. 6(b)]. The annual peak discharge reduced from 1850 m^3/s to 1550 m^3/s during the last decade. The design discharge for Demra station was found to be 3288 m^3/s for 100 years return period and the dominant discharge was found to be 1436.67 m^3/s. The decrease in discharge might occur due to siltation in the river. Proper dredging work should be done in the river bed for the survival of Shitalakhya River.

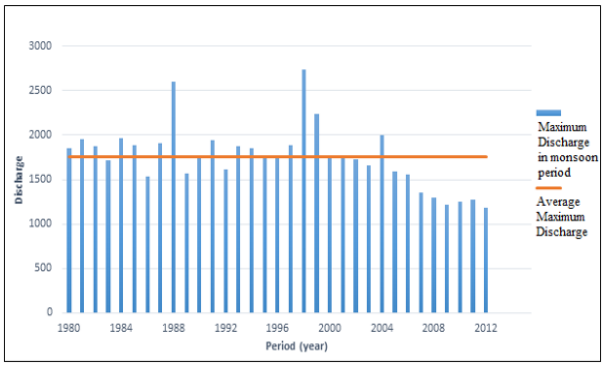

Fig. 6(a): Changes in Maximum water level in Different Years

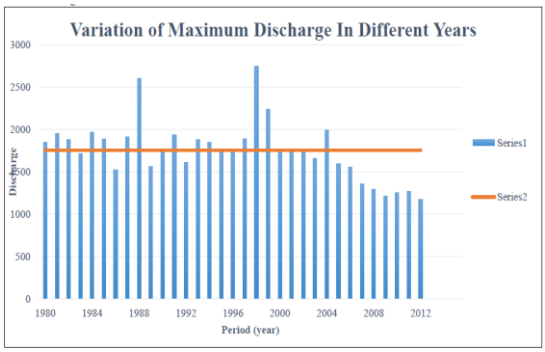

Fig. 6(b): Changes in Maximum Discharge in Different Years for monsoon period

The effect of proposed bridge was predicted in terms of afflux and scour. The afflux was determined and the value was found to be 0.3m which remained within the allowable limit. The pier scour is found to be 3.6m, the abutment scour is 0.3m for left channel and 0.3m for the right channel. The contraction scour depth is 0.7m for left bank, 1.3m for main channel and 0.6m for right channel. Scour due to contraction, pier and abutment is shown in the [Fig. 7].

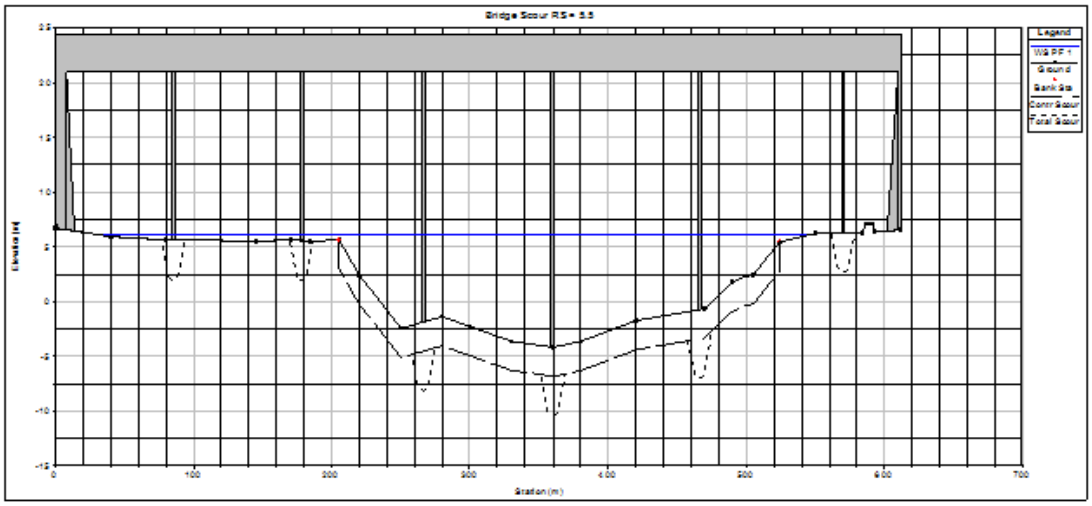

Fig. 7: Combined Effect of Contraction, Pier and Abutment Scour

REFERENCES

Hossain, S; Rahman, M; Nusrat, F; Rahman, R and Anisha, N.F. 2014. *Effects of Climate Change on River Morphology of Bangladesh and A Morphological Assessment of Shitalakhya River*. Journal of River Research Institute (RRI), pp 1-13.

Institute of Water Modeling (IWM). 2006. *Feasibility and Mathematical Model Study of Approaching and Investigating Strategy for Rehabilitating The Buriganga-Turag- Shitalakhya River System and Augmentation of Dry Season Flow in the Buriganga River*. Final Report.

Rouf, T and Miah, MM. 2013. *A Comprehensive Study on Hydro-Morphology and Water Quality of Shitalakhya River* proceeding of the International Conference on Climate Change Impact and Adaptation (I3CIA-2013), pp 985- 993.

Shaikh, MKI. 2006. *A Study on Some Geometric Parameters of Shitalakhya RIver*. B.Sc. Engineering Thesis, Department of Water Resources Engineering, Bangladesh University of Engineering and Technology, Dhaka.

SCALE-DEPENDENT RELIABILITY OF THE PRECIS MODEL IN RAINFALL PROJECTION FOR COASTAL AREAS IN BANGLADESH

M. S. Mondal & M. N. Sakib*

Institute of Water and Flood Management, Bangladesh University of Engineering and Technology, Dhaka, Bangladesh
**Corresponding Author: sakib.sajon@gmail.com*

ABSTRACT
The regional climate model, PRECIS, has been widely used throughout the world to generate climate change projection for impact studies and adaptation. In spite of its wide application, a stringent validation of the model is yet to be reported. In this study, we assessed the performance of the model in simulating annual, monthly and extreme rainfalls over southwest coastal regions of Bangladesh by using a number of statistical techniques. The results indicated that the PRECIS model could capture the overall spatial pattern of mean annual and monthly rainfalls very well. However, the inter-year variability was poorly simulated by the model. In addition, the model could not capture the rainfall extremes. Even spatial aggregation of rainfall data did not improve the reliability of the model. Therefore, further improvements of the model and/or its driving GCM are warranted for its practical use in generation of rainfall scenario.

Keywords: Rainfall variability and extremes; PRECIS; reliability; and spatial and temporal scales

INTRODUCTION
Bangladesh is one of the most climate change vulnerable countries in the world. Along with a small geographical area and a huge population, the country is located at the confluence of the three mighty rivers – the Ganges, the Brahmaputra and the Meghna. To assess the potential impacts of climate change on different socioeconomic sectors, climate change scenarios are developed. Global Climate Models (GCMs) and Regional Climate Models (RCMs) are used to derive future scenarios of different hydro-climatic variables. RCMs are used to dynamically downscale coarser resolution climatic variables into finer resolution ones and to better represent meso-scale climatic phenomena. These models involve complex interactions between atmospheric, oceanic and land processes and as such exhibit a lot of uncertainties in projected climates. The regional models can add value to GCM projections, but only for certain variables and locations (Feser et al., 2011) as RCMs develop their own climatology which is not consistent with the driving global datasets precipitation (Syed et al., 2013). The downscaling strategy also involves the introduction of uncertainties associated with model physics (Stainforth et al., 2005). Providing Regional Climates for Impacts Studies (PRECIS) is a RCM developed by the Hadley Center of the United Kingdom. It is a hydro-static, primitive equation grid point model containing 19 levels described by a hybrid vertical coordinate. Since its release, the model has been extensively used in different parts of the world to generate climate change scenarios. (Islam et al., 2008; Islam, 2009) generated rainfall and temperature scenarios of Bangladesh by running the model at a horizontal resolution of 50 km. It was reported that the model overestimated the pre-monsoon season rainfall and underestimated the monsoon season rainfall and the model generated rainfall is not directly useful in application purposes. A regression-based approach was also proposed to adjust the model generated rainfall. (Nowreen et al., 2015) studied the changes in rainfall extremes in the northeastern part of Bangladesh using the PRECIS generated rainfalls. Though they mention that the model 'nicely capture the long-term rainfall' of the northeastern part, a visual comparison of the monthly average observed and model rainfalls reported in their Figure 2 did not provide such indication. The PRECIS model was used to develop high resolution climate change scenarios over India (Kumar et al., 2006). The model was found to be overestimating the all-India summer monsoon rainfall and underestimating the variability. There was significant positive bias in the rainfall during the onset phase of the monsoon (May and June). (Revadekar et al., 2011) studied

precipitation extremes over India based on a comparison of baseline and future simulations of PRECIS. The authors, however, did not report the performance of the model in simulating baseline extremes which could be done by a comparison of observed and simulated rainfall extremes during the base period. (Zacharias et al., 2015) reported that the PRECIS generated rainfalls across India had a bias of +34% to -89% in annual scale, indicating 'poor performance of the model in simulating the baseline rainfall patterns'. The model also simulated more rainy days in the baseline period than observed. The PRECIS simulation was found to capture the shape of the annual rainfall cycle over the western and central Himalayas (Kulkarni et al., 2013). However, for the eastern Himalayas where Bangladesh is located, the peak of the rainfall hydrograph was simulated two months earlier in May or June. In this study, the performance of the model in simulating the rainfall over coastal areas in Bangladesh is evaluated. The selection of the coastal region is guided by the fact that the region is the most vulnerable within the country to climate change, and a number of vulnerability studies are currently being conducted for the region using the PRECIS projection (for example, the Ecosystem Services for Poverty Alleviation (ESPA) project funded by the Department for International Development [DfID], and the DEltas, vulnerability and Climate Change: Migration and Adaptation (DECCMA) project funded jointly by DfID and International Development Research Center [IDRC] are using the PRECIS projection).

METHODOLOGY

The reliability of the PRECIS model in simulating rainfall over coastal areas of Bangladesh was assessed by employing a number of statistical techniques. Among the techniques, a pattern similarity statistic suggested by (Santer et al., 1995) is widely used to compare observed time-evolving change patterns of a climatic variable with the model-predicted signal patterns. Such pattern/map correlation between the model-simulated and observed rainfalls was computed for a base period of 1986-2005. The same period was used in the fifth assessment report of IPCC (2013) as the base period. The pattern correlation was computed for annual, seasonal, monthly, annual maximum, 99^{th} percentile and 95^{th} percentile rainfalls. The pattern correlation method was used by IPCC in its second and third assessment reports. In addition to the spatial-pattern correlation, temporal correlation, root mean square difference (RMSD) and mean absolute difference (MAD) between the model and observed rainfalls were computed to check the adequacy of the model projections. For each grid, yearly rainfall time series was generated first for each rainfall variable. Then the presence of temporal trend in each variable was investigated and, where present, it was removed by detrending. The correlation between the detrended model and observed rainfalls was then computed. The detrending was done to avoid spurious correlation solely due to the presence of trends in the series. The statistical significance of the correlation was determined by applying the standard Student's *t*-test. From the 20 yearly values of a variable corresponding to a grid point, a grid point average value of the variable was obtained. The pattern correlation was obtained from the different grid point average values between the model and observed series. The simulated daily rainfall was available from the Met Office, UK for a period of 1971-2099 at an approximate horizontal resolution of 0.22°×0.22° (25 km×25 km). The data was generated from the PRECIS regional climate model driven by atmosphere-ocean coupled HadCM3 boundary conditions. Measured daily rainfall data were collected from the Bangladesh Meteorological Department (BMD), Dhaka. There are 13 observational stations of BMD within and around the study area. The BMD rainfall data is considered reliable and is widely used in scientific studies (Mondal et al., 2008; Mondal et al., 2012) and government documents. We used data from 7 stations within the study area for the purpose of generation of baseline map.

RESULTS AND DISCUSSIONS

The average annual rainfall over the study area for the base period (1986-2005) was found to be 1857 mm from the model simulation. The same rainfall was found to be 2171 mm from the observed data. Thus, the average rainfall from the model simulation was about 15% less than the observed rainfall. The spatial distribution of both the model and observed mean annual rainfalls are given in [Fig. 1]. Both low and high rainfall areas are overestimated in the model. However, if we find the pattern correlation in mean annual rainfalls between the observed and simulated rainfalls, a high correlation coefficient of 82% appears. This high correlation may be spurious and is probably due to the similar

spatial variation pattern in the two data sets. The MAD and RMSD were found to be 17% and 19%, respectively.

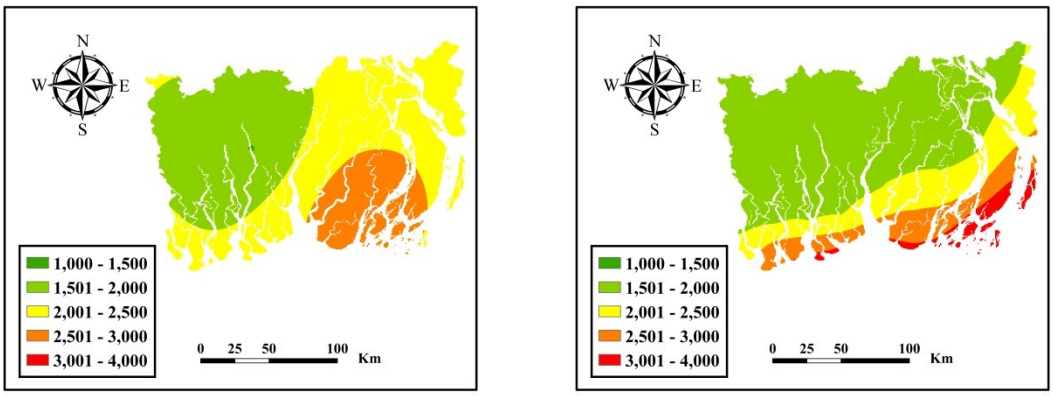

Fig. 1: Comparison of spatial distribution of observed (left) and simulated (right) mean annual rainfalls over the base period (1986-2005)

The point-to-point correlation between the observed and corresponding simulated annual rainfalls is given in Table 1. It is seen from the table that the correlation coefficient varies widely – from -8% at Satkhira to +61% at Patuakhali. The MAD and RMSD of the simulated rainfalls vary from 16-30% and 20-31%, respectively. Thus, there is a large error in simulated annual rainfall over the study area.

Table 1: Performance of the PRECIS model in simulation of annual rainfall in coastal areas of Bangladesh

Station	Correlation coefficient	MAD (%)	RMSD (%)
Satkhira	-0.08	21	28
Khulna	0.16	20	24
Barisal	0.19	21	27
Bhola	-0.08	24	30
Mongla	0.21	24	26
Patuakhali	0.61	30	31
Khepupara	0.22	16	20

Comparisons of probability density functions (pdfs) between observed and simulated rainfalls over the base period at different locations of the study area were made. Such comparisons for two locations (Khulna and Barisal) are shown in [Fig. 2]. It is seen from the figure that neither the location parameter nor the shape parameter of the observed rainfall is captured by the simulated rainfall. The location parameter is underestimated in model simulation and the shape parameter always has a higher peak and smaller base in simulated rainfall. Also, the pdfs from the observed rainfalls appear to be about symmetric, whereas that from the simulated rainfalls appear to be either negatively (Khulna) or positively (Barisal) skewed.

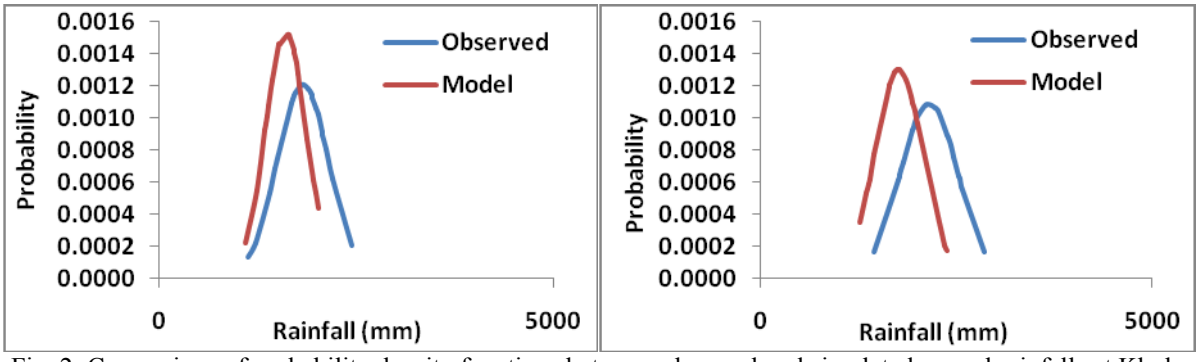

Fig. 2: Comparison of probability density functions between observed and simulated annual rainfalls at Khulna (left) and Barisal (right) during the base period (1986-2005)

The performance of the model in simulating monthly rainfalls was assessed. The assessment was made only for those months which have monthly rainfalls greater than zero in all the years. Presence of zero rainfalls makes the computed statistics, such as correlation coefficient, unreliable. The model fails to capture the monthly rainfall characteristics at individual stations as the correlation coefficients are often low or negative, and MADs and RMSDs are high. As an example, the correlation coefficients are negative for the month of September at all the seven stations of the study area. This indicates that the model is not able to capture the inter-year rainfall variability of September, the last month of the monsoon season. This could be due to the failure of the model in capturing the monsoon recession from the coastal region adequately. The MAD varies from 44-51% and RMSD from 55-82% for September. The inter-year variability of rainfall is poorly captured for the months of July and August of the monsoon season. However, it is interesting to note that the pattern correlations are quite high for these months. For example, the pattern correlations for the months of June, July, August and September were found to be 86, 87, 87, 76% respectively, which are very high. Thus, it appears that the pattern correlation may not be a good indicator to judge the performance of a climate model. Comparisons of pdfs between observed and simulated rainfalls for different months at different locations were also done. The results were more or less similar for different months. As an example, the comparison for the month of June indicated that there were a negative bias in scale parameter and a positive bias in shape parameter. A further comparison was made between observed and simulated annual maximum rainfalls with their pdfs. The shape parameter of the pdf for Mongla and the scale parameter of the pdf for Barisal are poorly simulated by the model. The underestimation of the scale parameter and shape parameter was found to be almost universal throughout the study area. This indicates that the annual maximum rainfall was underestimated by the model. The correlation coefficients were negative in 5 out of 7 locations for which observed data were available. It thus appears that the uncertainty in simulated annual maximum rainfall is higher than that of annual average rainfall.

Consistency, and hence reliability, of the model results are also assessed by comparing the simulation results among different future time periods. The results for mean annual rainfall are shown in [Fig. 3]. It is seen from the figure that the rainfall is projected to be mainly increased during the period of 2021-2040. The major increase is expected to be over the Barisal-Bhola-Jhalakathi region. The pattern of increased rainfall is also evident for the period of 2041-2060. However, there is a shift in the zone of maximum change. For 2021-2040, the zone of maximum change is near the north-east side, whereas for 2041-2060, it is near the north-west. The reason for this east to west shift of the zone is not understood. Moving to the period of 2061-2080 in the figure, we see that a decrease in rainfall manifests over the entire region. The same is also true for the period of 2081-2100. Thus, one can deduce that the rainfall would decrease in the long term. Again, it is not clear whether there is any physical basis of this decrease or it is simply the result of the incapability of the model to simulate the rainfall.

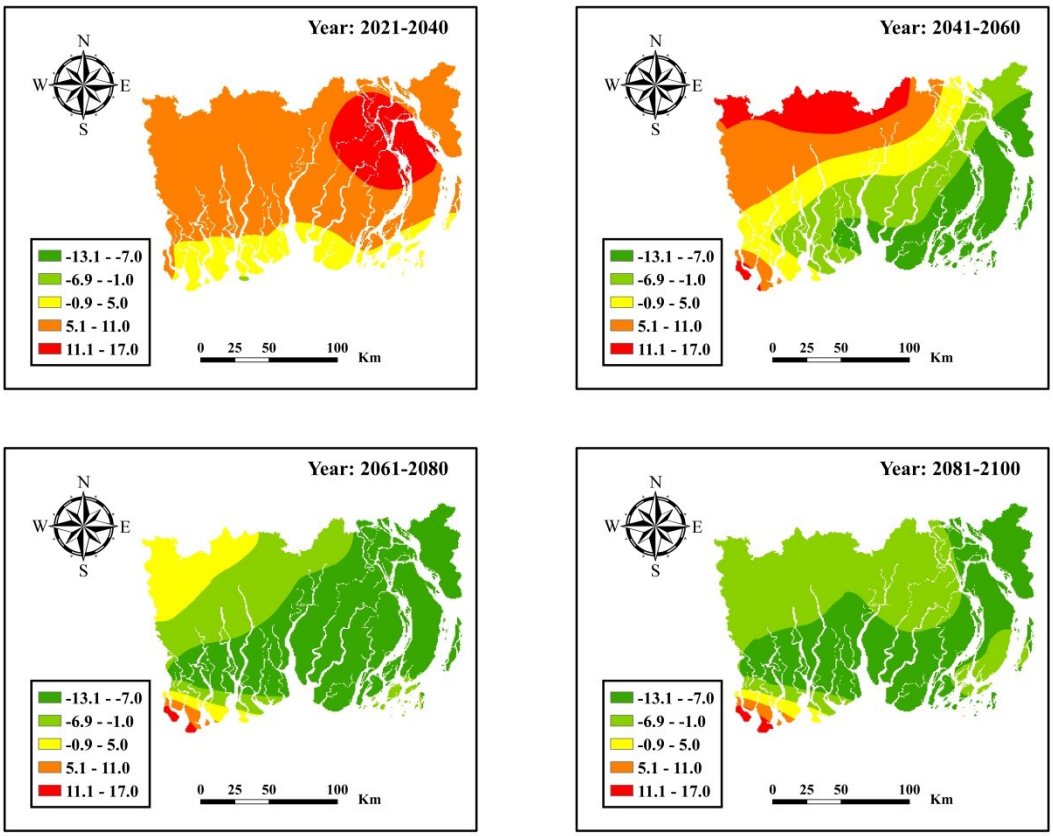

Fig. 3: Changes in mean annual rainfall (%) in different future periods over base period (1986-2005) from the PRECIS model simulation.

Spatial distribution of the linear trends and their statistical significance is calculated. It is seen that majority of the study areas have negative or no trends in annual rainfalls. The trends are positive only towards the northern margin. The p (significance level) values are also large (>0.05) which indicates that the trends are not statistically significant at the confidence level of 95%.The spatial distribution of the change in the 95th percentile (not shown) rainfall indicates that the change is entirely positive for the period of 2021-2040, mainly positive for 2041-2060, largely negative for 2061-2080 and mainly positive for 2081-2100. This temporal change in sign is difficult to understand physically and may simply be due to the inadequacy of the model in capturing the important rainfall processes and features. Overall, the trend is found to be small and statistically insignificant (not shown). Same analyses for the annual maximum rainfall, 99th percentile, 90th percentile and 80th percentile were carried out and the results were more or less similar to the above results in relation to the 95th percentile.As discussed earlier, there is a high pattern correlation between the observed and simulated rainfalls of the base period, but the correlation coefficient is small and sometimes negative at individual locations. This indicates that the model captures the overall spatial pattern of temporal mean rainfall, but fails to capture the inter-year variability of rainfall. To see if this failure is due to the spatial resolution of the model, the pdfs of annual rainfalls were estimated for each cell, for averaged rainfalls of five cells and for averaged rainfalls of nine cells. A visual comparison of the one-, five- and nine-cell pdfs (not shown) indicated that there was no significant difference among the three types of pdfs. This indicated that even after aggregation, the inter-year variability could not be captured. The problem could be due to the poor boundary condition of the PRECIS model obtained from the driving GCM, or due to the internal structure of the PRECIS which fails to capture the dynamic characteristics of the rainfall over the southern coastal Bangladesh. So, it is highly unlikely that it had captured the rainfall extremes.

CONCLUSIONS

The PRECIS climate model simulates the annual and monthly spatial rainfall patterns of the southwest coastal Bangladesh very well. The value of the spatial pattern correlation coefficient was

found to be +0.82 for the average annual rainfall and the values were between +0.76 and +0.87 for the average monthly rainfalls. However, the model fails to capture the inter-year variability in both annual and monthly rainfalls. For annual rainfall, the temporal correlation coefficients were from -0.08 to +0.61 depending on locations. Such coefficients for monthly rainfalls were between -0.67 and +0.47 depending on locations and months. In case of annual maximum rainfall, the correlation coefficients were negative in most of the cases. Thus, the finer is the temporal scale of rainfall, the less reliable is the model simulated rainfall. The reliability also does not improve with spatial aggregation of the rainfall data. Thus, any projection of rainfall variability and extremes based on the PRECIS model is likely to be highly uncertain.

ACKNOWLEDGMENTS

The PRECIS data received from the IWFM partner of the collaborative research on 'Assessing health, livelihoods, ecosystem services and poverty alleviation in populous deltas' is gratefully acknowledged.

REFERENCES

Feser, F; Rockel, B; Storch H; Winterfeldt, J and Zahn, M. 2011. Regional climate models add value to global model data: a review and selected examples, *Bull Am Meteorol Soc*., 92: 1181-1192.

IPCC .2013. Climate change 2013: the physical science basis, Contribution of Working Group I to the Fifth Assessment Report of the Intergovernmental Panel on Climate Change, Cambridge University Press.

Islam, MN. 2009. Rainfall and temperature scenario for Bangladesh, *The Open Atmospheric Science Journal*., 3: 93-103.

Islam, MN; Rafiuddin, M; Ahmed, AU and Kolli, RP. 2008. Calibration of PRECIS in employing future scenarios in Bangladesh, *Int. J. Climatol*., 28: 617-628.

Kulkarni, A; Patwardhan, S; Kumar, KK; Ashok, K and Krishnan, R. 2013. Projected climate change in the Hindu Kush-Himalayan region by using the high-resolution regional climate model PRECIS, *Mountain Research and Development.,* 33(2): 142-151.

Kumar, KR; Sahai, AK; Kumar, KK; Patwardhan, Revadekar, JV; Kamla, K and Pant, GB. 2006. High-resolution climate change scenarios for India for the 21st century, *Current Science.*, 90(3): 334-345.

Mondal, M.S., Islam, A.K.M.S. and Madhu, M.K. (2012). Spatial and temporal distribution of temperature, rainfall, sunshine and humidity in context of crop agriculture, Comprehensive Disaster Management Program, Ministry of Food and Disaster Management, Dhaka.

Mondal, MS and Hossain, MMA. 2008. Characterizing long-term changes of Bangladesh climate in context of agriculture and irrigation, Climate Change Cell, Department of Environment, Dhaka.

Nowreen, S; Murshed, SB; Islam, AKMS; Bhaskran, B and Hasan, MA. 2015. Changes of rainfall extremes around the haor basin areas of Bangladesh using multi-member ensemble RCM, *TheorApplClimatol*., 119: 363-377.

Revadekar, JV; Patwardhan, SK and Kumar, KR. 2011. Characteristic features of precipitation extremes over India in the warming scenarios, *Advances in Meteorology*., 2011: 1-11.

Santer, BD; Taylor, KE; Wigley, TML; Penner, JE and Jones, PD. 1995. Towards the detection and attribution of an anthropogenic effect on climate, *Climate Dynamics*., 12: 77-100.

Stainforth, DA; Aina, T; Christensen, C; Collins, M; Faull, N; Frame, DJ; Kettleborough, JA; Knight, S;Martin, A; Murphy, JM; Piani, C; Sexton, D; Smith, LA; Spicer, RA; Thorpe, AJ and Allen, MR. 2005. Uncertainty in predictions of the climate response to rising of greenhouse gases, *Nature.*, 433: 403-406.

Syed, FS; Iqbal, W; Syed, AAB and Rasul, G. 2013. Uncertainties in the regional climate models simulations of South-Asian summer monsoon and climate change, *ClimDyn*., 42(7): 2079-2097.

Zacharias, M; Kumar, SN; Singh, SD; Rani, DNS and Aggarwal, PK. 2015. Evaluation of a regional climatic model for impact assessment of climate change on crop productivity in the tropics, *Current Science*., 108(6): 1119-1126.

ASSESSMENT OF COASTAL SCOUR OF SANDWIP CHANNEL FOR DESIGN OF A JETTY

M. A. Matin[1*], M. Z. Abedin[2] & A. N. Mowrin[3]

[1]*Department Water Resources Engineering, Bangladesh University of Engineering and Technology, Dhaka, Bangladesh*
[2]*Department Civil Engineering, Bangladesh University of Engineering and Technology, Dhaka, Bangladesh*
[3]*Department of Civil engineering, Stamford University, Bangladesh*
[*]*Corresponding Author: matinmabuet81@gmail.com*

ABSTRACT
Hydrographic survey chart supplied by BIWTA has been utilized to assess the available navigable draft in the vicinity of a proposed jetty location. It has been seen that the jetty end at distance 360 m from the vicinity of existing shore line. According to the BIWTA hydrographic survey chart, the depth range at the shore line is about 3.4 m to 3.7 m. However at the Jetty end the available low water depth ranges from 4.7m to 5.25 m. The depths have been added to tidal range that found to vary between 3.0 m to 5.0 m. Assessment of scour has been done using Herbich et al. method. Local scour and total scour for various wave length and wave period have been computed. Variation of dimensionless scour depth (D_s/H) for various dimensionless wave heights (H_s/H) has been generated. It is seen that total scour depth (D_s) is much higher as compared to local scour for a given pile diameter and bottom velocity. For BIWTA Jetty at Sandwip local the scour at pile of diameter 1.5 m was found to be approximately5.22 m. Using the same method, the estimated total scour depth has been calculated as 12 m.

Keywords: Coastal scour; hydrographic chart; Sandwip channel; total scour; jetty pile

INTRODUCTION
The characteristics of the coastal morphology of the study area might be better understood if the morphological processes that govern the long-term natural and/or human induced changes at the coastal part are known. Due to scarcity of historical geological and morphological data at the vicinity of the project location, historical morphological changes have not always been analysed.
The subject of scour (and siltation) at coastal structures continues to receive much interest in the consulting and research fields. Coastal structures can be categorized as having four functions, either (1) to provide permanent protection against flooding (e.g. dykes and seawalls), (2) water level control during storm surges (e.g. barriers) or (3) benefits in coastal management such as preventing shoreline erosion (e.g. seawalls, breakwaters, groynes), or (4) for other industrial or economic functions such as harbour breakwaters and jetties, outfalls/intakes, and wind farms. As such, the topic of scour at coastal structures can be said to cover structures built on the shoreline as well as structures built in tens of metres of water, and waves and currents operate in varying combinations and relative magnitudes (Jiang, et al. 2004). In engineering projects scour needs to be considered in two phases, the installation/construction phase and the operational phase. The limiting case for design may require consideration of the erosion of seabed soils adjacent to the completed foundation. However, it is also important to evaluate what kind of scour might develop during installation as it might have a direct bearing on the stability of the structure that is being built, or on the construction methodology that is adopted. In most of the cases, the main issue for design relates to the target scour development that can be expected under design conditions, i.e. location, depth and extent, but knowing the time development is also important in some cases. A general approach for assessing the mobility of the sea bed soil at a structure was presented by Whitehouse (1998). This requires input data on waves, currents and water depth (chart depth plus water level variation). These inputs may be determined from modeling or analysis of field measurements made over a sufficiently long time, with analysis for

relevant return period conditions. The input data are combined at a point A to produce a set of robust inputs and once combined with information on the soil characteristics obtained from the site investigation they are analysed to provide information on the bed shear stress and the critical value of bed shear stress for erosion of the soil. An experimental study on scour around a pile subject to combined wave and current is given by Sumer and Fredsøe, (2001). Irregular waves were used in the experiments carried out both for codirectional waves and for waves propagating perpendicular to the current. The measured scour depth is plotted as a function of $U_{cw} = U_c/(U_c + U_m)$ in which U_c is the undisturbed current velocity and U_m is the maximum value of the undisturbed orbital velocity at the sea bottom.

STUDY AREA AND ITS CHARACTERISTICS

Sandwip Island is surrounded by the tide-dominated East Hatiya Channel, the Sandwip Channel, and the channel linking Urirchar. Available data for the last 75 years (1913-1988) show that Sandwip was reduced to about 50% of its original size, with considerable erosion northwest and accretion southeast. Map comparisons show that erosion on the northwest coast of Sandwip accelerated after 1963. It was about 200m per year between 1913 and 1963 and about 350m per year between 1963 and 1984. Urirchar grew from 3 sq km in 1963 to 46 sq km by 1981.

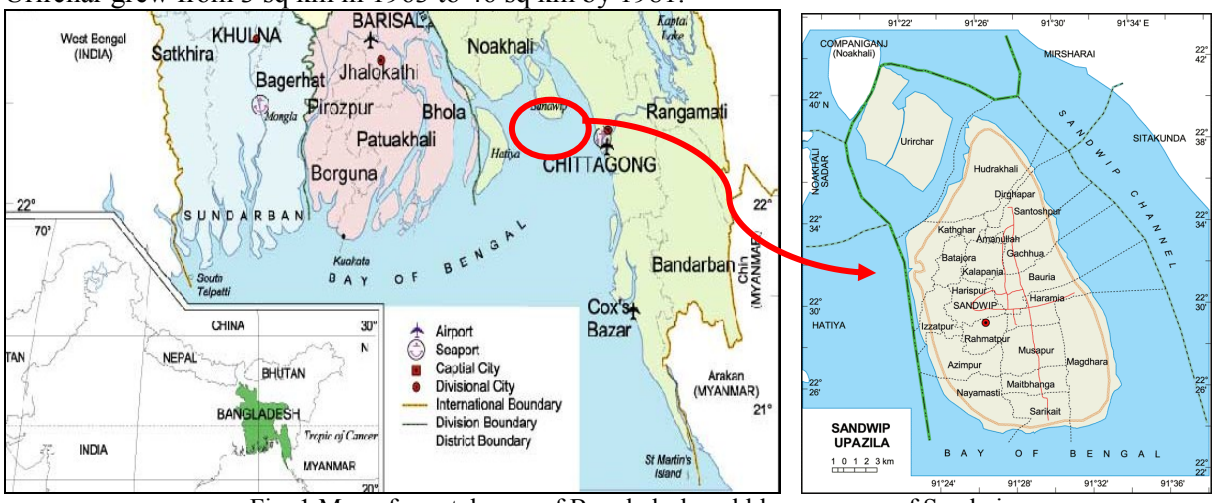

Fig. 1 Map of coastal zone of Bangladesh and blow-up map of Sandwip

*Tidal Range and Depth Averaged Velocity at Sandwip Channel***:** Sandwip Tide Chart shows the largest known tidal range at Sandwip as 2.87m (August 2, 2015). Tide Times are BDT (UTC +6.0hrs). Last Spring High Tide at Sandwip was on Sun 02 Aug, 2015 (height: 2.60m). Next high Spring Tide at Sandwip will be on Sat 15 Aug (height:2.40m). However, Sandwip Tidal range Max.4.83 mMin. 0.79 was observed in 2008. Tide datum was Mean Lower Low Water (Satellite). Table 1 shows the depth average velocity of Sandwip channel.

*Morphology of Sandwip Channel:*Chittagong coastline remained relatively stable over the years. In the north, considerable accretion took place due to a closure damon the Feni river. The reason for its relative stability is perhaps the near-isolation of Sandwip Channel from the distributary network in recent times. Coastal plains are inundated every day by tides coming from sea. Sediments are generally consisting of clay with silty materials. It is worthwhile to mention that the present morphological features of the stream/creeks may alter due to any man-made activities as well as naturally induced hazards. At present, Sandwip Channel is tide-dominated, allowing a net import of fine sediments. Review of previous studies shows that the no significant changes in channel morphology have been observed. Reza (2010) analysed cross-sectional data of various years as shown in Figure 2. It is seen that maximum bed level changes to about 9 m at the thalweg.

Table 1 : Depth averaged velocity of Sandwip channel (Alam, et.al 2014)

Location	Measured depth Average Velocity, (m/s)	Maximum velocity for T=100year, (m/s)	Maximum velocity for 2011 flood, (m/s)
North Sandwip	1.13	1.3	1.08
North East Sandwip	1.79	1.8	1.59
South-east Sandwip	1.82	1.9	1.71

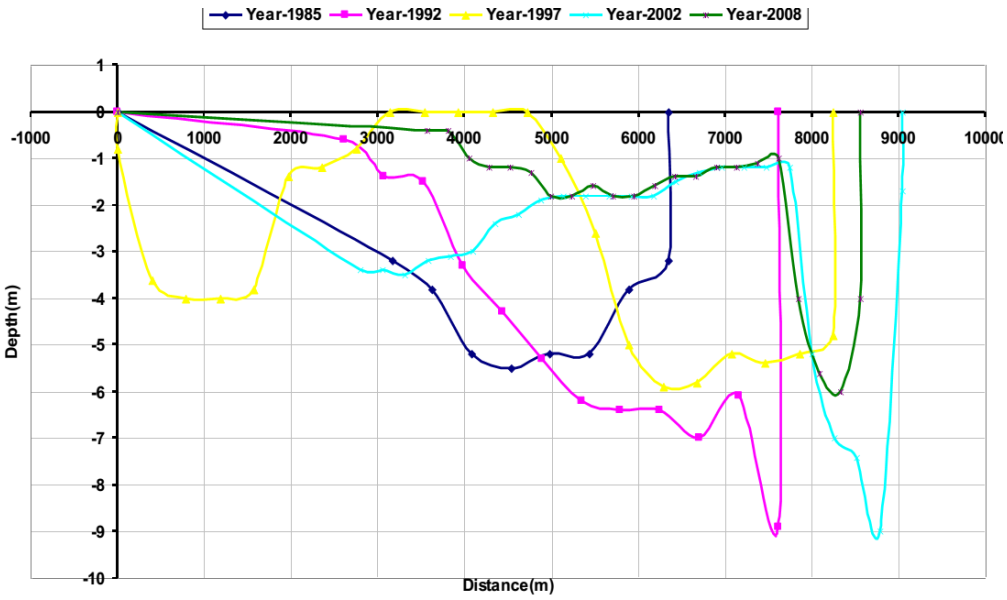

Fig. 2: Superimposed cross-sections of various years of Sandwip Channel (source: Reza, 2010)

METHODOLOGY

Available formula for the computation of coastal scour has been analysed. As a thumb rule, local scour around a pile has been estimated as 2 to 3 times of pile diameter. However, some formula calculates the local scour due to current action and wave. Nearshore coastal piles are always vulnerable to both wave and current action. For a more complete description of scour prediction methods for scour at vertical piles can be found in Einstein and Weigel, (1970) and Herbich et al. (1984). Based on test results from a laboratory study, they made tests run to examine effects of waves, currents, and the combination of the two. Herbich et al. concluded that scour at the base of vertical piles caused by wave action alone is insignificant when the piles are in relatively deeper locations. They proposed a procedure consists of number of empirical (laboratory based) equationsto estimateboth local and total scours. The procedure has been adopted for present scour calculation. Hydraulic data used in this analysis were collected from secondary sources (Hydrographical data collected from BIWTA). Field visit has also been made in September 2014to observe the tidal and morphological characteristics at Sandip channel at the vicinity of proposed site whereBIWTA jetty would be constructed. BIWTA constructed a landing Jetty at Swandip channel in early year 2000 to facilitate inland passengers and cargoes and they cross the channel to Sandip headquarters from Kumira (Shitakunda). Unfortunately this jetty has not been operational in last 15 years due to considerable damage immediately after its construction. Reasons of such damage of jetty have not been explored, but it can be anticipated that proper design and constructional procedure might not been maintained. Some recent photographs (Photo:1 to Photo: 4) are shown to observe the condition of the old jetty at Sandwip side.

Photo:1 Damaged BIWTA Jetty at Sandwip side at high tide (September, 2014)

Photo: 2Ferry vessel of BIWTA has beenanchored away from jetty at Sandwip (Sept. 2014)

Photo:3 Damaged BIWTA jetty at Sandwip side low tide (September, 2014)

Photo:4 Damaged BIWTA jetty near shoreline at Sandwip (September, 2014)

RESULT AND DISCUSSIONS

Local scour and total scour for various wave length and wave period have been computed. As for typical results, Fig.3 to Fig.6 show the variation dimensionless scour depth (D_s/H) for various dimensionless wave heights (H_s/H) for various combinations of wave heights and periods. It is seen that total scour depth(D_s) is much higher compared to local scour for a given pile diameter and bottom velocity. The computed scour depths are very much sensitive to wave height (H_s) especially at shallower water depth (H).

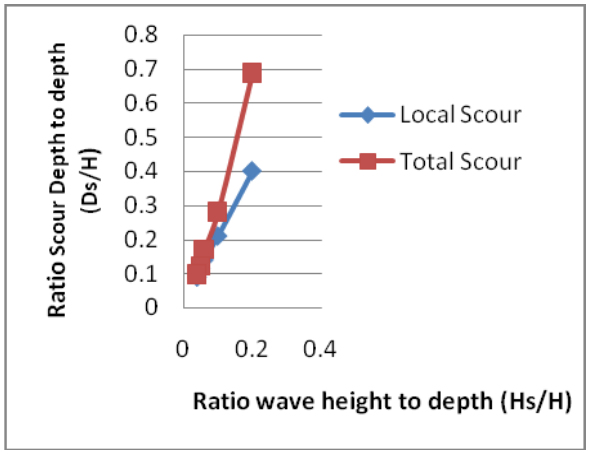

Fig. 3: Scour depths ratios (D_s/H) Vs. (H_s/H) for H_s=1m, T=1s

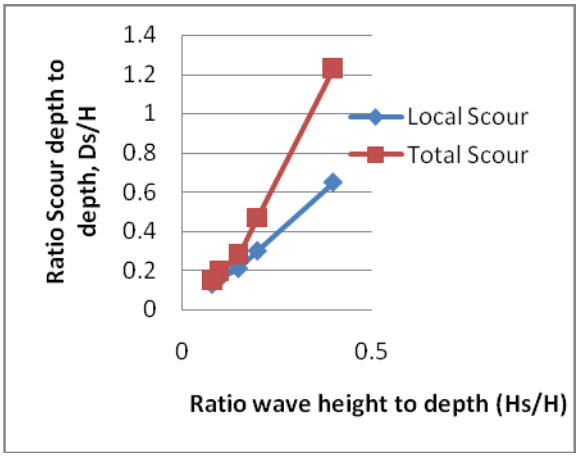

Fig. 4: Scour Depths ratios (D_s/H) Vs. (H_s/H for H_s=2m, T=2 s

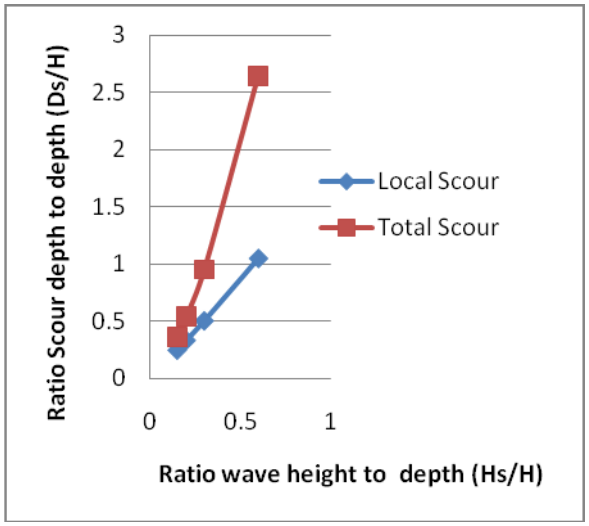

Fig. 5: Scour depths ratios (D_s/H) Vs. (H_s/H) for H_s=3 m, T=3s

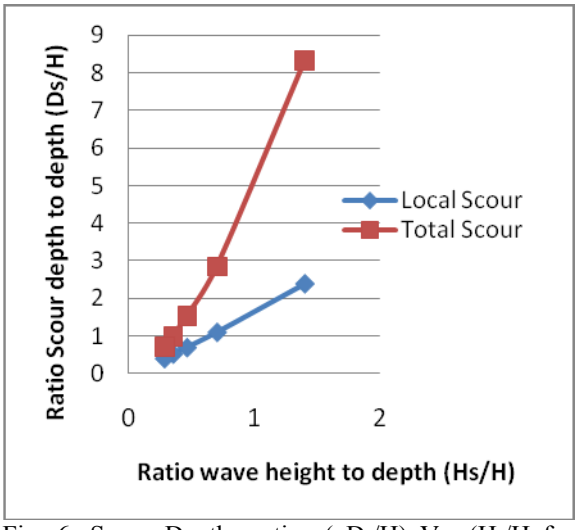

Fig. 6: Scour Depths ratios (D_s/H) Vs. (H_s/H for H_s=7m, T=3 s,

The hydraulic and bed material parameters provided in Table 2 have been used to estimate the bed scour. The local scour at pile of diameter D= 1.5 m was found to be about D_{sl}=5.22 m. Using the same method the estimated total scour depth has been calculated as D_{st}=12 m (BIWTA, 2016).

Table 2: Data used for scour calculation and scour values

Pile diameter (m)	D= 1.5
Wave height (m)	H_s= 2.0
Wave Period (s)	T= 4.5
Depth (m)	H= 8.0
Grain size (mm)	D_g= 0.15
Rel. Density	Δ = 1.65
K. Viscosity(m^2/s)	ν = 0.0000011
Bottom vel.(m/s)	v_b= 0.67

Design scour depth curves for various input values such as, velocity, depth, pile size and bed material size have also been generated for the users. In order to avoid any adverse effect in the vicinity of jetty piles, regular monitoring of river bank and bed condition in the vicinity of the bridge site and around the piers is recommended. A water level gauge should be installed with the jetty piles for regular monitoring of water level at the jetty site. Regular monitoring of scour at the vicinity of piles and at

the piles is recommended so that any adverse scour can be monitored for emergency protective measures.

CONCLUSIONS

Proper understanding of the coastal morphology and thus assessment of local scour for any intervention of coastal line is vital importance. Design of coast line Jetty structures requires scour depth for adequate pile length and size. In such cases, morpho-dynamics of the site need to be assessed. It has been estimated that local scour in Sandwip channel for a near shore pile of 1.5 m diameter is about 5.22 m. Using the same method the estimated total scour depth has been estimated as12 m for the given pile size. Number of curves showing the scour depth for various input values can also be generated for design purposes. Post-construction suggestions have to be made so that countermeasure can be taken for any adverse impact on bed morphology.

ACKNOWLEDGMENTS

The authors are grateful to the BIWTA officials for providing the opportunity of the work, and for supplying hydrographical data of Sandip channel at the vicinity of proposed Jetty area.

REFERENCES

Alam, R;Islam, MS; Hasib, MR and Khan. MZH. 2014. Characteristics of Hydrodynamic Processes in the Meghna Estuary due to Dynamic Whirl Action, *International organization of Scientific Research,* 4(6) 39-50

BIWTA. 2016. Design of proposed BIWTA Jetty at Sandip, Final design Report, April. BUET, 2016

Einstein, H. A., and Wiegel, R. L. 1970 (Feb). "A Literature Review on Erosion and Deposition of Sediment Near Structures in the Ocean (U)," *Final Report HEL-21-6, US Naval Civil Engineering Laboratory*, Port Hueneme, CA.

Herbich, John B;Schiller, Robert E; Jr., Dunlap;Wayne A and Watanabe, Ronald K.1984. Seafloor Scour; *Design Guidelines for Ocean-Founded Structures*," Marine Technology Society.

Reza, I. 2010. *An Assessment of water level and bed level change of Lower Meghna*, M. Engg. Thesis, Dept. of WRE, BUET, September. 2010, p. 178,

Sumer, B. and Fredsøe, J. 2001. Scour around Pile in Combined Waves and Current. *J. Hydraul. Eng.*, 10.1061/(ASCE)0733-9429(2001)127:5(403), 403-411.

Jiang, J, Ganju, NK and Mehta, AJ. 2004. Estimation of contraction scour in riverbed using SERF. *Journal of Waterway, Port, Coastal, and Ocean Engineering*, 130, 215-218.

Whitehouse, RJS. 1998. Scour at Marine Structures. Thomas Telford. 216 pp.

IDENTIFYING PARAMETERS OF RAINFALL INTENSITY-DURATION-FREQUENCY RELATIONSHIP: A CASE STUDY FOR NORTH-EASTERN REGION IN BANGLADESH

M. M. Rasel[1*] & S. A. Esha[2]

[1]*Department of Civil Engineering, Ahsanullah University of Science and Technology, Dhaka, Bangladesh*
[2]*Department of Water Resources Engineering, Bangladesh University of Engineering and Technology, Dhaka, Bangladesh*
[*]*Corresponding Author: munshimdrasel@gmail.com*

ABSTRACT
The objective of this research is to identify the parameters of Rainfall IDF relationship at North-Eastern region of Bangladesh. Two common frequency analysis techniques Gumbel and Log Pearson Type III (LPTIII) distribution were used to develop the IDF relationship from rainfall data of this region. Yearly maximum rainfall data for last 41 years (1974-2014) from Bangladesh Meteorological Department (BMD) was used in this study. The results obtained using Gumbel method are slightly higher than LPT III distribution method. The chi-square goodness of fit test was used to determine the best fit probability distribution. The parameters of the IDF equations and coefficient of correlation for different return periods (2, 5, 10, 25, 50 and 100 years) were calculated by using nonlinear multiple regression method. It was found that intensity of rainfall decreases with increase in rainfall duration. Further, a rainfall of any given duration will have a larger intensity if its return period is large. In other words, for a rainfall of given duration, rainfalls of higher intensity in that duration are rarer than rainfalls of smaller intensity.

Keywords: Rainfall intensity; rainfall duration; rainfall frequency; Gumbel's extreme value distribution method; Log Pearson Type III

INTRODUCTION
Rainfall intensity-duration-frequency (IDF) curves are graphical exemplifications of the amount of water that falls within a given period of time in catchment areas (Dupont et al., 2000). IDF curves are used to aid the engineers while designing urban drainage works. The establishment of such relationships was done as early as 1932 (Chow ,1988 ; Dupont et al.,2006). Since then, many sets of relationships have been constructed for several parts of the globe. However, such relationships have not been accurately constructed in many developing countries. Koutsoyiannis et al.(1998); Koutsoyiannis et al. (2003) cited that the IDF-curves allow for the estimation of the return period of an observed rainfall event or conversely of the rainfall amount corresponding to a given return period for different aggregation times. In Bangladesh water logging and flood is a common problem during Monsoon period because of inadequate drainage system. In order to solve this problem new drainage design is needed where rainfall data of different duration is needed. But due to instrumental limitation these data were not available. In the present study, annual maximum rainfall series is considered for Rainfall Frequency Analysis (RFA). Rainfall in a region can be characterized if the intensity, duration and frequency of the diverse storms occurring at that place are known. The frequency-data for rainfalls of various durations, so obtained, can be represented by IDF curves, which give a plot of rainfall intensity versus rainfall duration and recurrence interval. In recent studies, various authors attempted to relate IDF relationship to the synoptic meteorological conditions in the area of hydrometric stations (Dupont et al. 2006; Mohymontl et al. 2004). Matin et al.(1984), in their study developed the IDF curve for North-East region Bangladesh and also observed that the rainfall data in this region follow Gumbel's Extreme Value Distribution. developed The short duration rainfall IDF curve was developed for Sylhet with return period of 2, 5, 10, 20, 50, and 100 years (Chowdhury et al. 2007). Kim et al. (2008) improved the accuracy of IDF curves by using long and short duration

separation technique. They derived IDF curves by using cumulative distribution function (CDF) for the site under consideration using multi-objective genetic algorithm. Khaled et al. (2011) applied L-moments and generalized least squares regression methods for estimation of design rainfall depths and development of IDF relationships. Rashid et al. (2012) applied Pearson Type-III distribution for modelling of short duration rainfall and development of IDF relationships for Sylhet city in Bangladesh. In this context, an attempt has been made to estimate the rainfall for different return periods for different durations of 'n' such as 10-min, 20-min, 30-min, 60-min, 120-min, 180-min, 360-min, 720-min, 1440-min adopting Gumbel distributions for development of IDF relationships for North-Eastern regions of Bangladesh using updated data. Model performance indicators (MPIs) such as correlation coefficient (R) was used to analyse the performance of the developed IDF relationships by Gumbel distributions & LPTIII method for estimation of rainfall intensity of the stations under study.

METHODOLOGY

For this study 24 hour daily rainfall data from year 1974 to 2014 was collected from Bangladesh Meteorological Department (BMD) for North-Eastern region. From the daily data maximum yearly rainfall data was used in the analysis. For accurate hydrologic analyses, reliable rainfall intensity estimates are necessary. The IDF relationship includes the estimate of rainfall intensities of different durations and recurrence intervals. Two common frequency analysis techniques were used to develop the relationship between rainfall intensity, storm duration, and return periods from rainfall data for the regions under study. These techniques are: Gumbel distribution and LPT III distribution.

Estimation of Short Duration Rainfall

Chowdhury et al. (2007), used Indian Meteorological Department (IMD) empirical reduction formula to estimate the short duration rainfall from daily rainfall data in Sylhet city and found that this formula give the best estimation of short duration rainfall. In this study this empirical formula "EQ. (1)" was used to estimate short duration rainfall of six stations of Central region of Bangladesh.

$$P_t = P_{24} \sqrt[3]{\frac{t}{24}} \quad (1)$$

Where, P_t is the required rainfall depth in mm at t-hr duration, P_{24} is the daily rainfall in mm and t is the duration of rainfall for which the rainfall depth is required in hr.

Gumbel Theory of Distribution

Gumbel distribution methodology was selected to perform the flood probability analysis. The Gumbel method calculates the 2, 5, 10, 25, 50 and 100 year return intervals for each duration period and requires several calculations. Frequency precipitation PT (in mm) for each duration with a specified return period T (in year) is given by the following equation:

$$PT = Pave + KS \quad (2)$$

Where K is Gumbel frequency factor given by:

$$K = -\frac{\sqrt{6}}{\pi}\left[0.5772 + \ln\left[\ln\left[\frac{T}{T-1}\right]\right]\right] \quad (3)$$

Where Pave is the average of the maximum precipitation corresponding to a specific duration.
In utilizing Gumbel's distribution, the arithmetic average in Eq. (2) is used:

$$P_{ave} = \frac{1}{n}\sum_{i=1}^{n} Pi \quad (4)$$

Where Pi is the individual extreme value of rainfall and n is the number of events or years of record. The standard deviation is calculated by EQ. (5) computed using the following relation:

$$S = \left[\frac{1}{n-1}\sum_{i=1}^{n}(Pi - Pave)^2\right]^{1/2} \quad (5)$$

Where S is the standard deviation of P data. The frequency factor (K), which is a function of the return period and sample size, when multiplied by the standard deviation gives the departure of a desired return period rainfall from the average. Then the rainfall intensity, I_T (in mm/h) for return period T is obtained from:

$$I_T = \frac{Pt}{Td} \quad (6)$$

Where T_d is duration in hours.

Log Pearson type III

The LPT III probability model is used to calculate the rainfall intensity at different rainfall durations and return periods to form the historical IDF curves for each station. In the same manner as with Gumbel method, the frequency precipitation is obtained using LPT III method. The simplified expression for this latter distribution is given as follows:

$$P^* = \log(\mathrm{Pi}) \quad (7)$$

$$P_T^* = Pave^* + K_n S^* \quad (8)$$

$$Pave^* = \frac{1}{n}\sum_{i=1}^{n} P^* \quad (9)$$

$$S^* = \left[\frac{1}{n-1}\sum_{i=1}^{n}(P^* - Pave^*)^2\right]^{1/2} \quad (10)$$

Where P_T*, Pave*, S* are as defined previously in previous but based on the logarithmically transformed Pi values; i.e. P* of Eq. (7). KT is the Pearson frequency factor which depends on return period (T) and skewness coefficient (Cs). The skewness coefficient, Cs, is required to compute the frequency factor for this distribution. The skewness coefficient is computed by "Eq. 11"

$$C_S = \frac{n\sum_{i=1}^{n}(Pi^* - Pave^*)^3}{(n-1)(\mathrm{n}-2)(\mathrm{S}^*)^3} \quad (11)$$

By knowing the skewness coefficient and the recurrence interval, the frequency factor, KT for the LPT III distribution can be extracted. The antilog of the solution in Eq. (7) will provide the estimated extreme value for the given return period.

Derivation of IDF equation

The IDF formula are the empirical equations representing a relationship between maximum rainfall intensity as a dependent variable and other parameters of interest; for example the rainfall duration and frequency as independent variables. Two approaches were tried to estimate the equation parameters.

A. By applying the logarithmic conversion, where it is possible to convert the equation into a linear equation, thus to calculate all the parameters related to the equation.

B. Estimation of the equation parameters by using nonlinear regression analysis: Using the Solver function of the ubiquitious spreadsheet programme Microsoft Excel, which employs an iterative least squares fitting routine to produce the optimal goodness of fit between data and function. The R^2 value calculated is designed to give the user an estimate of goodness of fit of the function to the data.

Goodness of fit test

The aim of the test is to decide how good is a fit between the observed frequency of occurrence in a sample and the expected frequencies obtained from the hypothesized distributions. A goodness of fit

test between observed and expected frequencies is based on the chi-square quantity, which is expressed as "Eq. 12"

$$\chi^2 = \sum_{i=1}^{k} (O_i - E_i)^2 / E_i \qquad (12)$$

Where χ^2 is a random variable whose sampling distribution is approximated very closely by the chi-square distribution. The symbols Oi and Ei represent the observed and expected frequencies, respectively, for the i-th class interval in the histogram. The symbol k represents the number of class intervals. If the observed frequencies are close to the corresponding expected frequencies, the χ^2 value will be small, indicating a good fit; otherwise, it is a poor fit. A good fit leads to the acceptance of null hypothesis, whereas a poor fit leads to its rejection. The critical region will, therefore, fall in the right tail of the chi-square distribution. For a level of significance equal to a, the critical value is found from readily available chi-square tables and χ^2 > constitutes the critical region.

RESULTS AND DISCUSSIONS

According to the IDF curves, rainfall estimates are increasing with increase in the return period and the rainfall intensities decrease with rainfall duration in all return periods. Rainfall intensities rise in parallel with the rainfall return periods. The results obtained from the two methods have good consistency.

Table 1: The parameters values used in deriving formula

Region	Parameter	Gumbel Method	Log Pearson III Method
North-Eastern	c	759	664
	m	0.268	0.255
	e	0.667	0.666

Table 1. shows the parameters values obtained by analyzing the IDF data using the two methods and those are used in deriving formulae for the two regions. Fig.1 and Fig.2 show results of the IDF curves obtained by Gumbel and LPT III methods for North-Eastern region. It was shown that there were small differences between the results obtained from the two methods, where Gumbel method gives slightly higher results than the results obtained by Log Pearson III. This is shown also from parameters of the derived equation for calculating the rainfall intensity using the two methods.

Parameters of the selected IDF formula were adjusted by the method of minimum squares, where the goodness of fit is judged by the correlation coefficient. The results obtained showed that in all the cases the correlation coefficient is very high, and ranges between 0.998 and 0.987, except few cases where it ranges between 0.986 and 0.978 when using LPT III at 50 and 100 years. This indicates the goodness of fit of the formulae to estimate IDF curves in the region of interest. For each region the results are given as the mean value of the points results.

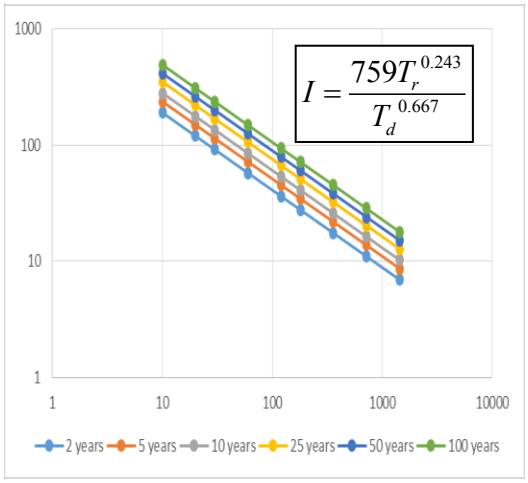

Fig.1: IDF curve by Gumbel method

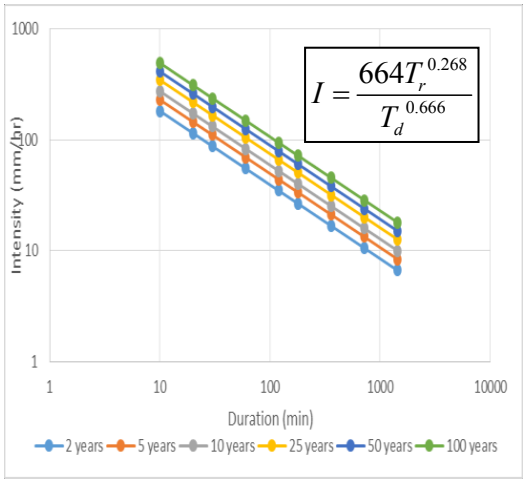

Fig.2 : IDF curve by LPTIII method

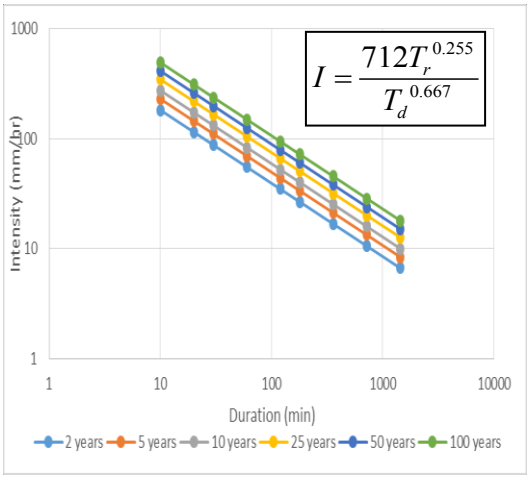

Fig.3 : IDF curve by average

Also,goodness-of-fit tests were used to choose the best statistical distribution among those techniques. Results of the chi- square goodness of fit test on annual series of rainfall are shown in Table 2. As it is seen most of the data fit the distributions at the level of significance of =0.05, which yields <3.84. Only the data for 10 min do not give good fit using Gumbel method distribution. Also the data for 10, 20, 30 min using LPTIII method do not give good fit.

Table 2: Results of chi-square goodness of fit test on annual maximum rainfall

Region	Distribution	Duration (min)								
		10	20	30	60	120	180	360	720	1440
North-Eastern	Gumbel	5.54	3.49	2.66	1.67	1.0	0.80	0.50	0.319	0.201
	LPTIII	8.24	5.19	3.95	2.49	1.5	1.1	0.7	0.47	0.298

CONCLUSIONS

Since Bangladesh has different climatic conditions from region to region, a relation for each region has to be obtained to estimate rainfall intensities for different durations and return periods ranging between 2 and 100 years. It was found that Gumbel method gave some larger rainfall intensity compared to LPT III distribution. In general, the results obtained using the two approaches are very close at most of the return periods and have the same trend. The parameters of the design storm

intensity for a given period of recurrence were estimated for each region. The results obtained showed a good match between the rainfall intensity computed by the methods used and the values estimated by the calibrated formulae. The results showed that in all the cases data fitted the formula with a correlation coefficient greater than 0.97. This indicates the goodness of fit of the formulae to estimate IDF curves in the region of interest for durations varying from 10 to 1440 min and return periods from 2 to 100 years. The chi-square test was used on one hand to examine the combinations or contingency of the observed and theoretical frequencies, and on the other hand, to decide about the type of distribution which the available data set follows. The results of the chi-square test of goodness of fit showed that in all the durations the null hypothesis that the extreme rainfall series have the Gumbel distribution is acceptable at the 5% level of significance. Only few cases in which the fitting was not good obtained by using the LPT III distribution. Although the chi-square values are appreciably below the critical region using Gumbel distribution and few values are higher than the critical region using LPT III distribution, it is difficult to say that one distribution is superior to the other. Further studies are recommended whenever there will be more data to verify the results obtained or update the IDF curves.

ACKNOWLEDGMENTS

Authors are indebted to the Bangladesh Meteorological Department (BMD) for providing the necessary meteorological data.

REFERENCES

Chow, VT. 1988. Handbook of Applied Hydrology. McGraw-Hill Book.

Dupont, BS.; Allen, DL. 2006. Establishment of Intensity–Duration–Frequency Curves for Precipitation in the Monsoon Area of Vietnam. Kentucky Transportation Center, College of Engineer, University of Kentucky in corporation with US Department of Transportation.

Haddad, K.2011.Design rainfall estimation for short storm durations using L-moments and generalised least squares regression-application to Australian data. *Int J Water Res Arid Environ* 1 (2011): 210-218.

Kim ,T; Shin, J.; Kim , K. and Heo, J. 2008. Improving accuracy of IDF curves using long- and short duration separation and multi-objective genetic algorithm. World Environmental and Water Resources Congress. 2008, 1-12.

Koutsoyiannis, D ; Demosthenes K and Alexandros M. 1998. A mathematical framework for studying rainfall intensity-duration-frequency relationships. Journal of Hydrology 206.1 (1998): 118-135.

Koutsoyiannis, D. 2003. On the appropriateness of the Gumbel distribution for modelling extreme rainfall. Proceedings of the ESF LESC Exploratory Workshop held at Bologna. 2003.

Matin , MA and Ahmed SMU.1984. Rainfall Intensity Duration Frequency Relationship for the N-E Region of Bangladesh. *Journal of Water Resource Research.* 5(1).

Mohymont1,B .; Demaree1,GR. and Faka2,DN. 2004. Establishment of IDF-curves for precipitation in the tropical area of Central Africa-comparison of techniques and results. Department of Meteorological Research and Development, Royal Meteorological Institute of Belgium, Ringlaan 3, B-1180 Brussels, Belgium.

Rashid, M M.; Faruque, SB and Alam, JB. 2012. Modeling of short duration rainfall intensity duration frequency (SDRIDF) equation for Sylhet City in Bangladesh. *ARPN Journal of Science and Technology* 2.2 (2012): 92-95.

HYDRO-METEOROLOGICAL INVESTIGATION OF 2015 FLASH FLOOD IN EASTERN HILL BASIN BANGLADESH

M.S. Hossain[1*], G. M. T. Islam[2], S. U. Raihan[1], S. M. Q. Hassan[3] & R. H. Khan[4]

[1]*Flood Forecasting and Warning Center, Bangladesh Water Development Board, Dhaka, Bangladesh*
[2]*Institute of Water and Flood Management, Bangladesh University of Engineering and Technology, Dhaka, Bangladesh*
[3]*Bangladesh Meteorological Department*, Dhaka, Bangladesh
[4]*Regional Integrated Multi-Hazard Early Warning System, Thailand*
[*]*Corresponding Author: sazz176@yahoo.com*

ABSTRACT
The present study examines hydro-meteorological aspects of flash flood event during the last week of June 2015 in Eastern Hill Basin that caused severe damage to human lives as well as physical infrastructures. The consecutive extreme rainy days was responsible for the flash flood event. The one day maximum rainfall was recorded at Cox's Bazar 467 mm, Teknaf 218 mm, Chittagong 172 mm, Bandarban 153 mm and Lama 276 mm and a comparative analysis of monthly normal and actual rainfall showed that the basin received 92% more rainfall in the month of June, 2015. Frequency analysis of daily maximum rainfall has been carried out for Cox's Bazar gauge station, and the result shows that rainfall at Cox's Bazar exceeded 100 years return period. The water level all the rivers in the basin flowed above Danger Levels and caused inundation in vast area. The extreme rainfall caused flash flood, and it resulted debris/mud flow from the hilly areas, disrupting road communication and washed away several lives. The study showed that result of Numerical Weather Prediction (NWP) model and European Centre for Medium-Range Weather Forecasts (ECMWF) ensemble forecast predicted very well in ahead of the flash flood event.

Keywords: Flash flood; rainfall; water level; flood damage; frequency analysis

INTRODUCTION
Flash floods are flood events where the water levels rise rapidly after a rainfall event, typically within a few hours. According to WMO, flash flood can be defined as a rapid onset flood of short duration with a relatively high peak discharge (WMO, 2007).The rainfall intensity and the hydrology of the catchment are both important factors in the flash flood dynamics, i.e. a given amount of rainfall in a given time may or may not result in a flash flood, owing to such factors as antecedent precipitation, soil permeability, terrain gradients, and so on (CSFFWS, 2006).
Eastern Hill Basin covers the greater Chittagong and Chittagong Hill Tract districts of Bangladesh. The Eastern Hill Basin of Bangladesh predominantly consists of hilly terrain and long strip of lowland coastal plains along the Bay of Bengal. This physical feature makes it vulnerable to flash flood as well as land slide. Heavy rainfall causes flash flood in different parts of the basin during monsoon period. The river systems and topography show that the rivers of this basin are composed of five hydraulically independent systems. These are- Muhuri-Feni, Karnafuli-Halda-Ichamati, Sangu, Matamuhuri and Bakkhali river system. The five river systems drain into the Bay of Bengal independently. Fig. 1 shows the study area.

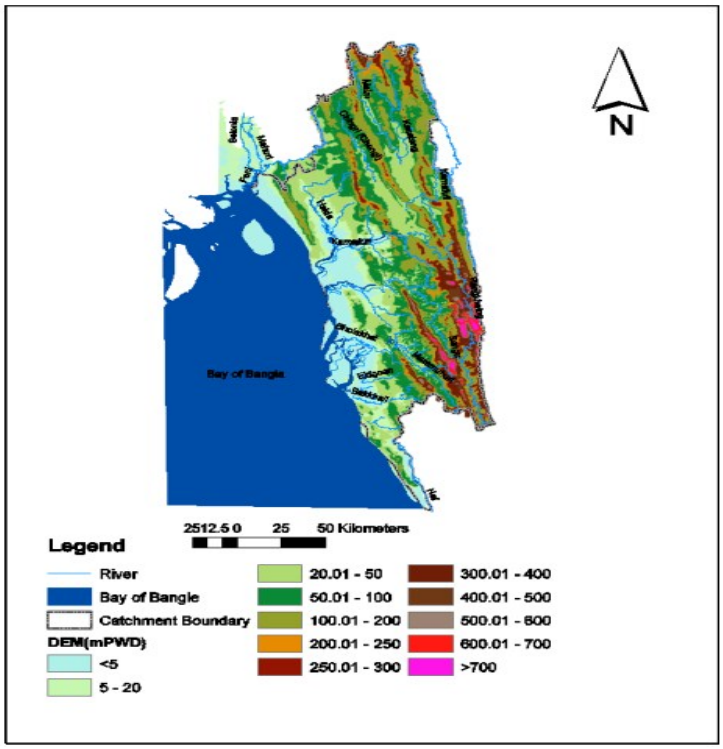

Fig.1: Eastern Hill Basin in Bangladesh

In June 2015, this basin received exceptionally higher rainfall than any other previous events (FFWC, 2015). The flash flood event of 2015 which occurred in last week of June is quite different from the historical events in terms of meteorological and hydrological phenomenon. This caused huge damage to physical infrastructures and washed away many lives. Some places for affected by flood which was never affected flood in recent history. The present study looks into the hydro-meteorological analysis of the 2015 flash flood event of this basin. It allows understanding of the characteristics of the meteorological behaviour of the event like intensity and amount of precipitation that caused severe damage. The hydrological conditions of the rivers like water level or flow played significant role in creating flooding situation. The present study finds out the number of days above Danger Level of flood water of the major rivers in the basin.

METHODOLOGY

The study is based on the analysis of related hydrological and meteorological data collected from the secondary sources like Bangladesh Water Development Board (BWDB) and Bangladesh Meteorological Department (BMD).Table 1 and Table 2 show the list of Meteorological and Hydrological gauge stations respectively and fig. 2 shows the locations of the gauges which have been used for the present study. Analysis includes calculation of normal rainfall for the month of June and compared with the actual rainfall. Two and five days total rainfall has also calculated that created flash flood event. The impact of the intensity of rainfall (3 hourly rainfall data) has been analysed to find the hydrological response. Frequency analysis of daily maximum rainfall data has been carried out to estimate rainfall for different return period.

Table1: List of rainfall gauge stations

Station Name	**Latitude**	**Longitude**
Cox's Bazar	21.450	91.967
Teknaf	20.867	92.300
Chittagong	22.350	91.817
Bandarban	22.194	92.219
Lama	21.793	92.212

Table2: List of water level gauge stations

Station	River	**Longitude**	**Latitude**
Lama	Mathamuhuri	92.2124	21.7926
Bandarban	Sangu	92.2192	22.1941
Dohazari	Sangu	92.0665	22.1571
Chiringa	Matamuhuri	92.0827	21.7727
Ramu	Bakkhali	92.1100	21.4260

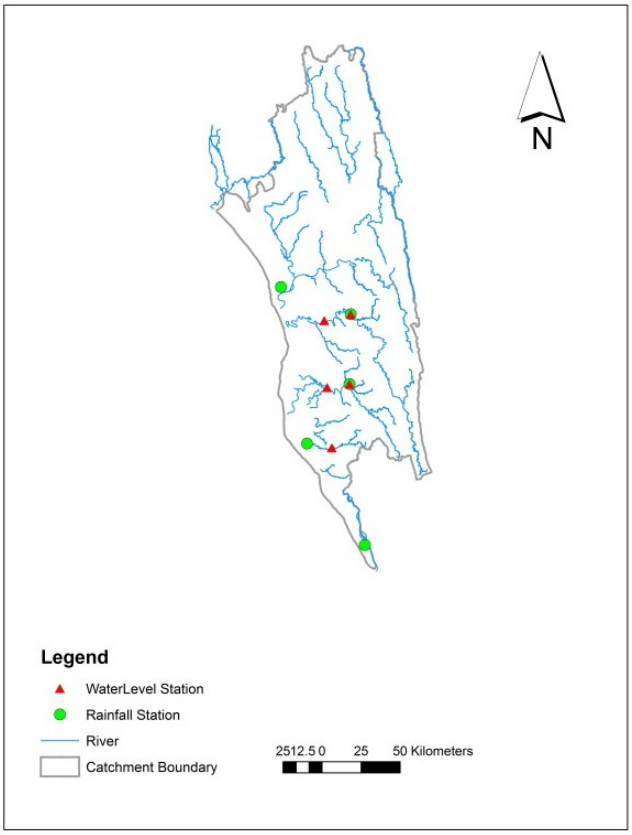

Fig. 2: Map of Gauge location in the study area

Results and Discussions

Rainfall Situation

Usually Eastern basin receives heavy rainfall during monsoon period. During June of 2015 all the rainfall measuring stations in this basin received above normal rainfall. Table 3 shows normal and actual rainfall. The Cox's Bazar and Teknaf had received more rainfall than monthly normal rainfall. Overall the basin received 92 % more rainfall than its monthly normal rainfall in June,2015.

Table 3: Normal and Actual Rainfall (mm) in South Eastern Hill Basin in June 2015

Station	Normal (mm)	Actual (mm)	Deviation (mm)
Bandarban	542.70	872.00	329.30
Lama	712.60	1330.00	617.40
Chittagong	628.40	763.00	134.60
Cox's Bazar	881.20	1551.00	669.80
Teknaf	262.00	1290.10	1028.10
Total	3027.00	5806.00	92 % more rainfall

The Synoptic situation shows that a low pressure had prevailed over Bangladesh along with active monsoon. The combination of these two weather phenomenon has created a favourable condition for heavy rainfall and the whole Eastern Hill Basin received very heavy to extreme rainfall. Table 4 presents the high amount of rainfall during the flash flood event in June, 2015.

Table 4: Recorded Rainfall during the flash flood Event

Date	Cox's Bazar	Teknaf	Chittagong	Bandarban	Lama
23/06/2015	75	0	111	157	274
24/06/2015	99	0	172	126	107
25/06/2015	467	213	154	140	276
26/06/2015	210	218	111	149	250
27/06/2015	263	215	81	46	71
28/06/2015	81	62	23	10	39

Table 5: 1-day maximum, 2-day and 5-day rainfall (in mm) at different gauge stations

Stations	**1-day Maximum**	**2-day total**	**5-day total**
Cox's Bazar	467	566	1120
Teknaf	218	432	710
Chittagong	172	326	541
Bandarban	157	283	618
Lama	276	381	987

To investigate the cumulative effect of rainy days, 1-day maximum, 2-days and 5-days total rainfall amount was calculated (Table 5). The result shows consecutive very heavy to extreme rainfall had triggered the flash flood event. Frequency analysis of daily maximum rainfall was carried out for the same stations and result is presented in Table 6. According to frequency analysis Cox's Bazar received rainfall which has 100 year return period.

Table 6: Frequency analysis of rainfall data at Cox's Bazar

		Station: Cox's Bazar							
PDF	**Return Period**							**PPCC**	**Rank**
	2	**5**	**10**	**20**	**25**	**50**	**100**		
Normal	212.70	267.74	296.51	320.27	327.19	347.01	365.07	0.9009	5
Log Normal	204.84	256.13	287.87	314.02	326.06	353.38	380.27	0.9016	4
Pearson	193.97	252.73	296.98	341.81	356.37	401.86	447.56	0.9809	2
Log Pearson Type-III	196.36	250.29	292.29	351.67	351.67	400.89	454.63	0.9847	1
Extreme Value	201.96	259.75	298.01	334.71	346.35	382.22	417.82	0.9616	3

Rainfall forecast

ECMWF medium range weather forecast and WRF Predictions captured the event almost one week in advance. WRF Weather Forecast Model output which was simulated every day and ECMWF forecast for the whole week showed extremely heavy rainfall event in the Eastern Hill Basin. The heavy rainfall forecast for 72, 96 and 144 matched with the observed rainfall trend. For instance, 84 hour forecast of WRF Model and 144 hour forecast of ECMWF based on 20 June, 2015 showed extremely heavy rainfall event (Fig.3)

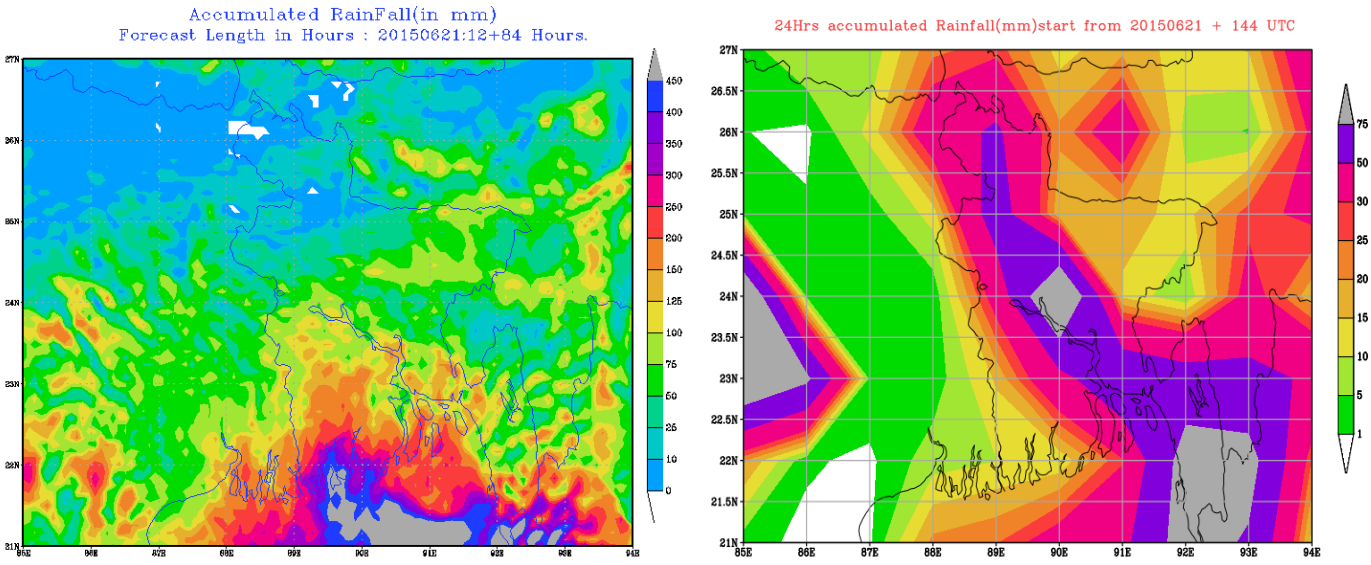

(a) (b)

Fig. 3: (a) WRF model forecast for June 21-24 and (b) ECMWF forecast for June 26 of extremely heavy rainfall, 2016 (Bangladesh Flash Flood Guidance System, FFWC)

Hydrological condition of major rivers

Muhuri, Karnaphuli, Halda, Sangu, Matamuhuri,Feni, Bakhkhali are the major rivers in this basin and all the rivers are flashy in nature. Water levels of the river Sangu, Matamuhuri and Bakhkhali crossed their respective danger levels during the flash flood event. However, the water level of these rivers did not cross the historical recorded highest (Table 7).

Table 7: Comparative WL of Few Stations in the South Eastern Hill Basin for June 2015

River	Station	Recorded Maximum (m)	Danger Level (m)	Peak Water Level 2015	Days above Danger Level
Sangu	Bandarban	20.70	15.25	16.1	1
Sangu	Dohazari	9.05	7.00	8.00	3
Matamuhuri	Lama	15.46	12.25	14.03	2
Matamuhuri	Chiringa	7.03	5.75	7.40	4
Bakhkhali	Ramu		5.79	7.13	3

The hydrological response is very quick for all these rivers due to high hydraulic gradients. The rivers got bank full flow immediately after the rainfall. The fig. 4 shows the hydrological response of Bakhakhali river during the flash flood event.

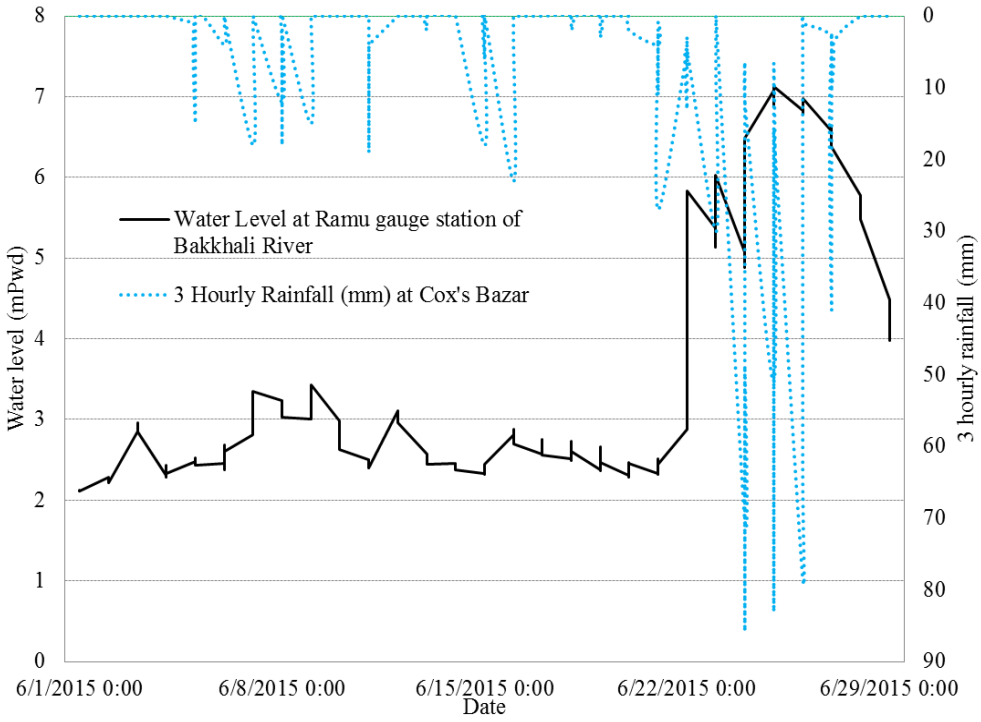

Fig. 4: Hydrological response of Bakhakhali River

CONCLUSIONS

The Flash flood event of 2015 was an exclusive one for Eastern Hill Basin as the whole basin received extreme rainfall for about a week; water level crossed danger levels, causing severe damages in some places. Hydrological analysis shows Rivers are extremely flashy in nature. At the same time initial soil moisture was favourable for flash floods due to rainfall at the beginning of June. However, this study did not investigate the soil moisture condition. The study shows single day heavy rainfall did not cause the flash flood, but continuous heavy rainfall during the week from 21 to 28, contributed to the event. NWP forecast is very useful for forecasting such flash flood events. Local Disaster managers may follow the NWP products from BMD's website and the flash flood guidance provided by FFWC. This will help them to take precautionary measures for reducing loss of invaluable human life and assets. As flash flood in this area comes with subsequent landslides, so, proper measure should be taken for the people who live at the foot hill.

REFERENCES

CSFFWS .2005. *Consolidation and Strengthening of Flood Forecasting and Warning Services*, Dhaka: Ministry of Water Resources. Bangladesh Water Development Board. Flood Forecasting and Warning Centre Final Report Volume I- Main Report**,** DHI Water and Environment In association with IWM, NCG, Mott Macdonald, Aqua, BDPC, GKSS, Prip Trust.

FFWC. 2015. *Annual Flood Report*. Dhaka: Bangladesh Water Development Board

WMO. 2007. Global approach to address flash floods. *MeteoWorld* (June, 2007).World Meteorological Organization.[online] Available at: www.hrc-lab.org/publicbenefit/downloads/wmo-flashflood.pdf [Accessed 4 May 2016].

A STUDY ON RIVER SYSTEM, HYDROLOGY AND SURFACE WATER SALINITY OF SUNDARBANS RIVERS

M. A. Rahman* & S. J. Dipa

Department of Water Resources Engineering, Bangladesh University of Engineering and Technology, Dhaka, Bangladesh
**Corresponding Author: mataur@wre.buet.ac.bd*

ABSTRACT
Sundarbans, consists of 10,200 sq. km of Mangrove forest, spread over Bangladesh (6000 sq. km) and India (4200 sq. km). Kobadak, Kholpetua, Rupsa, Shibsa, Pashur, Baleshwar, Raimangal, Arpangasia, Sakbaria are the main rivers passing through Sundarbans. The river system is important for ecosystem of Sundarbans which depends on the availability of adequate fresh water. The surface water salinity increases rapidly after construction of Farakka Barrage on the Ganges river at India and withdrawal the Ganges fresh water. Also water level largely affects the surface water salinity. The recent increase in water and soil salinity has upset the natural equilibrium of the delicate ecological balance. So salinity will be a major issue in future. The study aims to assess the present condition of the surface water salinity, water level fluctuation and the spatial and temporal variation of salinity of all rivers through Sundarbans.

Keywords: Surface water salinity; water level; river system; Sundarbans

INRODUCTION

The Sundarbans is the largest mangrove forest in the world and is intersected by a complex network of tidal waterways, mudflats and small islands of salt-tolerant mangrove forests. It lies at the mouth of the Ganges and is in South West part of Bangladesh, in the district of greater Khulna. The Sundarbans is a part of the world's largest delta formed by the rivers Ganges, Brahmaputra and Meghna (Islam, 2011). The study area encompasses the entire Sundarbans with all river, their tributaries and land. The rivers which almost surrounded Sundarbans are Kobadak, Kholpetua, Rupsa, Shibsa, Pashur, Baleshwar, Raimangal, Arpangasia and Sakbaria. These rivers play an important role to Sundarbans and its ecosystem. The Sundarbans ecosystem depends on the availability of adequate fresh water. With the commissioning of Farakka Barrage, the downstream discharge at Ganges was drastically reduced. The salinity trends in the Sundarbans are not fixed from both soil and water perspective. The recent increase in water and soil salinity has upset the natural equilibrium of the delicate ecological balance required for the healthy growth and existence of the rich flora and fauna (Khan et al., 1994). Consequently, scarcity of water during the dry season (Feb-June) and widespread flowing of excess water in the wet season damages the crops and the ecosystems (Haque and Alam, 1995). The Ganges fresh water withdrawal in the upstream area in India resulted in three types of negative impacts in the downstream catchment. The problems are fresh water reduction, increase of salinity and disturbance of growth and habitat have been identified. The increase of salinity in the Ganges distributaries has also lead to ecological impacts on the world's largest mangrove forest, the Sundarbans (Siddiqi, 2001). Salinity in the river system of southwest coastal region increases steadily from December through February, reaching maximum in the late March and early April (EGIS, 2000). Figure 1 shows the area of Sundarbans and its river systems. This study aims to assess the hydrology and surface water salinity of Sundarbans rivers.

Fig.1: The Sundarbans and its river system

METHODOLOGY

Bathymetry, water level and surface water salinity data of the Sundarbans rivers during 2003 to 2014 were collected from Bangladesh Water Development Board. The inventory of the measuring locations is presented in Table 1, Figure 2 and Figure 3.

Cross-section was plotted in Excel to see variation of rivers cross-section. Water level was analyzed during high tide and low tide and then tidal range was determined. Surface water salinity was analyzed during dry/pre-monsoon period and post-monsoon period for high tide and low tide. Finally variation of surface water salinity with river water level was seen.

ANALYSIS, RESULTS AND DISCUSSIONS

Cross-Sectional variation from 2001 to 2013 of Kobadak River at station RMKBD16 and RMKBD17 are shown in Fig. 4 and Fig. 5. Fig. 4 shows aggrading character of river due to sedimentation. In the year 2001, 2005 and 2008 there was a slow sedimentation process, but in 2013 there developed dune at middle of the channel. Fig. 5 shows degrading character of river due to erosion. In 2001, 2005 and 2008 there was a very slow sedimentation process, but in 2013 there is a depression at middle of the channel.

Table 1: Inventory of measurement station

Nature of Data	River Name	Station Name	StationID
Water Level	Kobadak	Kobadak Forest Office	SW165
	Rupsa-Pasur	Mongla	SW244
	Bhadra	Sutarkhali_Forest Office	SW29
	Gorai-Madhumati	Rayenda	SW107.2
	Betna-Kholpetua	Protapnagaa	SW26
	Sibsa	Nalianala_Hadda	SW259
Salinity	Kobadak	Tahipur	SW161
	Rupsa-Pasur	Mongla	SW244
	Bhadra	Dumuria	SW28
	Gorai-Madhumati	Rayenda	SW107.2
	Rupsa-Pasur	Khulna	SW241
	Sibsa	Nalianala-Hadda	SW259
Cross-Section	Rupsa-Passur		PR16- PR17
	Kobadak		KBD12-KBD14

Fig.2: Location of Water Level Stations

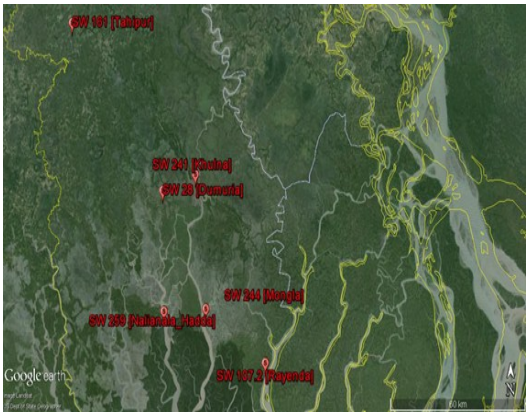

Fig.3: Location of Surface Water Salinity Stations

Water level is analyzed for the period of 2005 to 2014 at Kobadak Forest Office and Mongla, Sutarkhali_Forest Office, Rayenda, Protapnagar and Nalianala-Hadda stations of Sundarbans rivers. Generally, water level is relatively high during monsoon period (July-Oct) and relatively low during pre-monsoon or dry period (March-May). Figure 6 shows the maximum and minimum water level from 2005 to 2014 for Betna-Kholpetua River at Station-SW26. Tidal ranges at the different stations of some rivers passing through Sundarbans are given in Table 2.

In this study surface water salinity of Sundarbans area is assessed by using salinity data as Electrical Conductivity (EC) and as Chloride Ion Concentration (Cl-). Salinity data are analyzed to visualize the changing pattern of surface water salinity over year and also for the period 2003 to 2013. Fig. 7 and Fig. 8 show the variation of surface water salinity as Electrical Conductivity (EC) and concentration of chloride (Cl-) during high tide and low tide for time period 2003 to 2013. These two figures show that salinity is almost same during high tide and low tide. Fig. 9 and Fig. 11 show that surface water salinity as Electrical Conductivity (EC) and as Chloride Ion Concentration (Cl-) during high tide becomes maximum in April-May. The increasing rate of EC is 29.6% in 2002 to 2011 and Cl- is 5.42% in 2008 to 2011 during the month of April-May (pre-monsoon period) which is seen in Fig. 10 and Fig. 12.

Water level largely affects the surface water salinity (Table 3 and Table 4). When water level increases the water salinity decreased or vice versa. Water level is highest during monsoon period at high tide and lowest during dry-period at low tide. Table 5 shows the maximum and minimum water level and their corresponding surface water salinity at various stations during high tide and low tide. Water level and salinity relation of station SW 241 (Fig. 13 and Fig. 14) shows that at high tide maximum water level is 3.41 mPWD while corresponding electrical conductivity is 401 ppm and concentration of chloride is 201ppm and at minimum water level of 0.36 mPWD the corresponding electrical conductivity is 6500 ppm and concentration of chloride is 1774ppm. From the above analysis it can be noticed that at downstream river named Kobadak at station SW165, the tidal range or water level is maximum (1.15-6.68mPWD) than the upstream river named Rupsa-Passur at station SW244 and Bhadra at station SW29 (Table 2). Also for last decade during high tide and low tide, at downstream station (SW165) water level is maximum (4 mPWD) and minimum (-2.58 mPWD) than at upstream station (Table 5). Surface water salinity is maximum at downstream rivers situated at south-west and minimum at upstream rivers situated south-east during low tide. At station SW241 Surface water salinity is maximum (19100 ppm) than station SW161 (601) during low tide and pre monsoon period (Table 5).

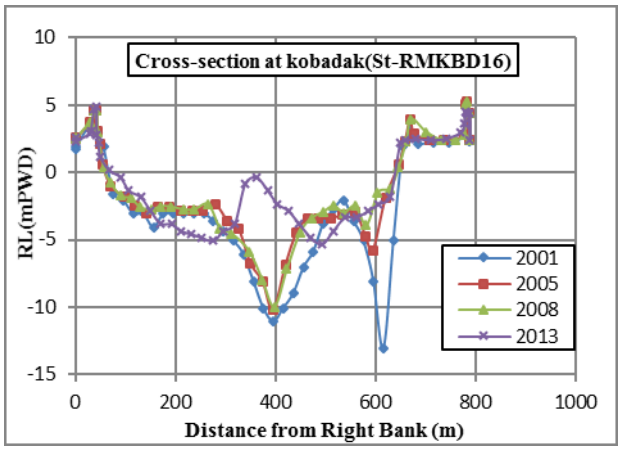

Fig. 4: Cross-Sectional variation of Kobadak River at Station-RMKBD16

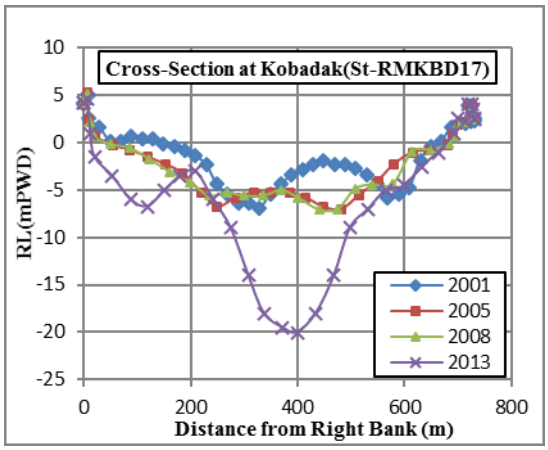

Fig. 5: Cross-Sectional variation of Kobadak River at Station-RMKBD17

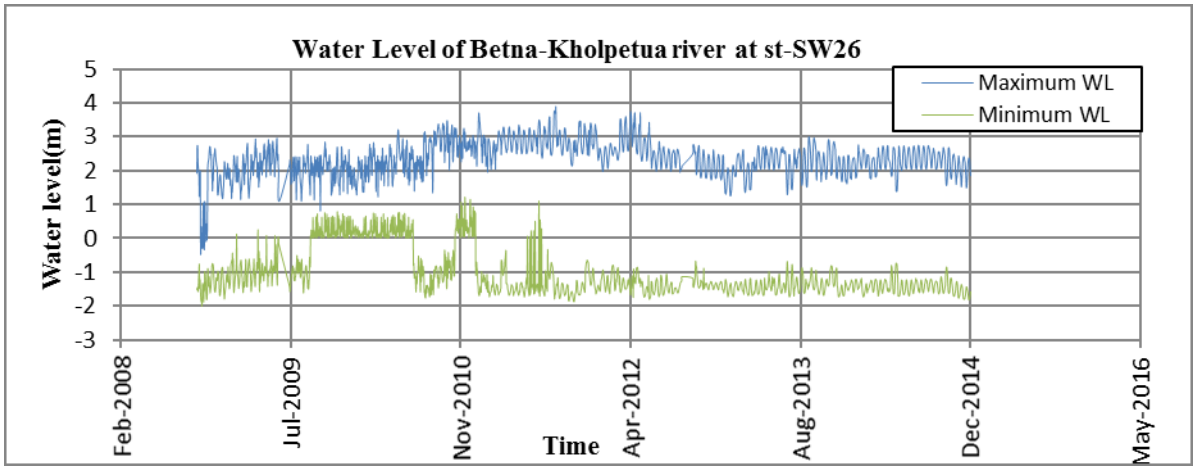

Fig.6: Water Level variation of Betna-Kholpetua River at Station-SW26.

Table 2: Tidal Ranges at different station of different rivers

Station No	Station Name	River name	Tidal Range(m)
SW165	Kobadak Forest Office	Kobadak	1.15-6.38
SW244	Mongla	Rupsa-Pasur	0.54-4.34
SW29	Sutarkhali_Forest Office	Bhadra	1-4.28
SW107.2	Rayenda	Gorai-Madhumati	0.16-3.60
SW26	Protapnagar	Betna-Kholpetua	0.67-5.57
SW259	Nalianala_Hadda	Sibsa	0.45-4.56

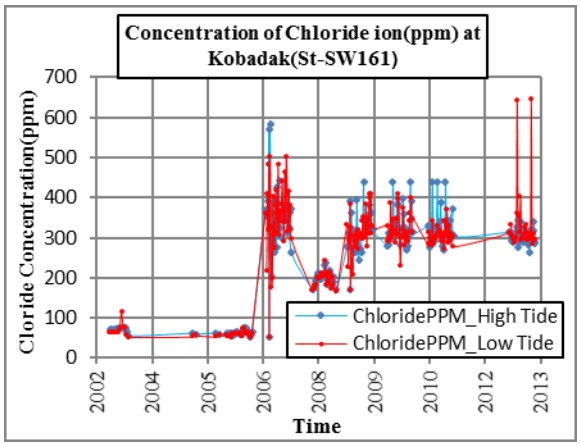

Fig. 7: Surface Water Salinity (Concentration of Cl^-) variation of Kobadak River at Tahipur Station (SW161).

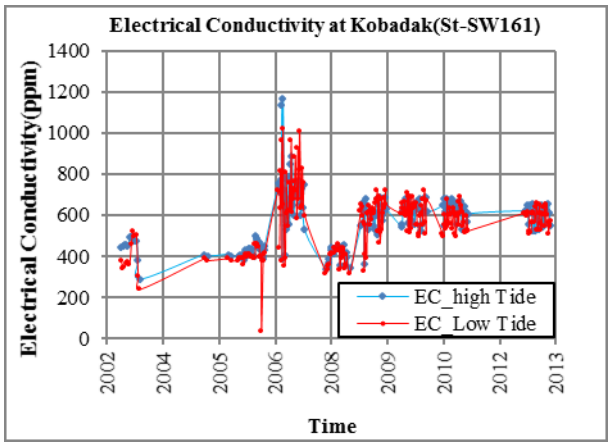

Fig. 8: Surface Water Salinity (EC) variation of Kobadak River at Tahipur Station (SW161).

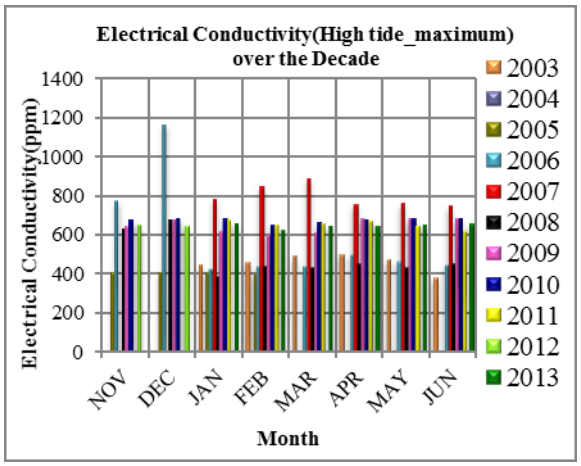

Fig. 9: Variation of Maximum Salinity (EC) during High Tide of Kobadak River at Station-SW161.

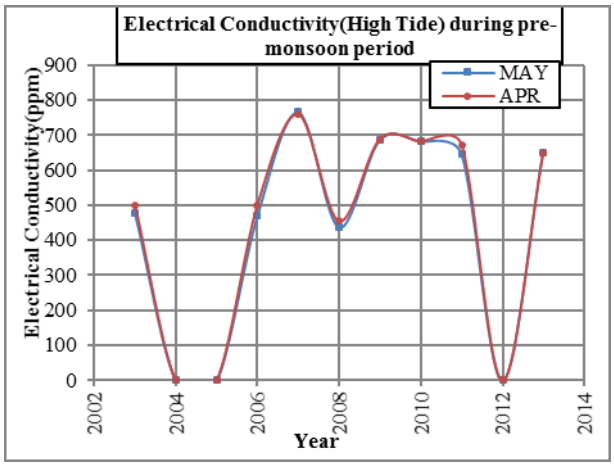

Fig. 10: Maximum Salinity (EC) during High Tide of Kobadak River at Station-SW161 in April-May

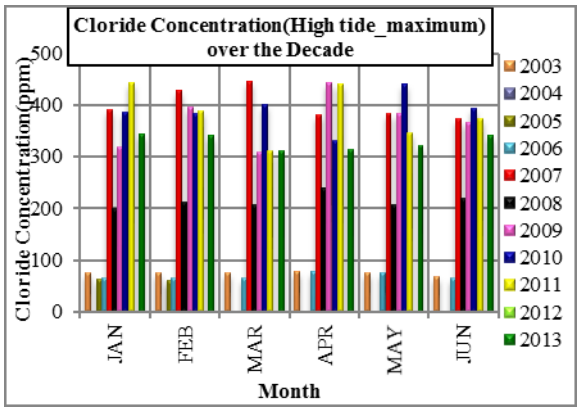

Fig. 11: Variation of Maximum Salinity (Concentration of Cl-) during High Tide of Kobadak River at Station-SW161

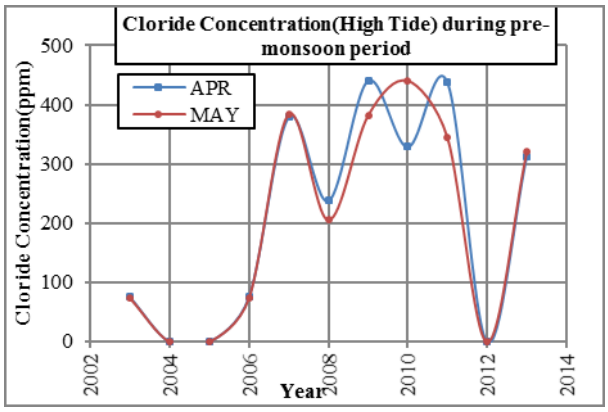

Fig. 12: Maximum Salinity (Concentration of Cl-) during High Tide of Kobadak River at Station-SW161 in April-May

Table 3: Increasing rate of surface water salinity (EC)

Station	Result	Pre-Monsoon High Tide	Post-Monsoon High Tide	Pre-Monsoon Low Tide	Post-Monsoon Low Tide
SW 241	Change	20.44 %	2.90 %	207.10 %	20.83 %
	Years	2004~2007	2004~2006	2005~2007	2004~2006
SW 244	Change	28.34 %	67.50 %	60.69 %	49.40 %
	Years	2003~2013	2004~2013	2003~2013	2005~2012
SW 28	Change	23.98 %	11.11 %	11.50 %	53.49 %
	Years	2003~2006	2004~2005	2008~2013	2004~2012
SW 259	Change	2.94 %	15.18 %	9.09 %	20.67 %
	Years	2007~2009	2006~2010	2007~2010	2004~2009
SW107.2	Change	14.87 %	5.91 %	17.64 %	17.93 %
	Years	2008~2011	2008~2010	2007~2009	2006~2010
SW 161	Change	29.60 %	46.05 %	36.24 %	41.67 %
	Years	2003~2010	2003~2012	2005~2011	2005~2012

Table 4: Increasing rate of surface water salinity (Cl-)

Station	Result	Pre-Monsoon High Tide	Post-Monsoon High Tide	Pre-Monsoon Low Tide	Post-Monsoon Low Tide
SW 241	Change	50.00 %	6.67 %	55.86 %	29.41
	Years	2005~2008	2004~2006	2005~2007	2004~2008
SW 244	Change	60.92 %	20.00 %	10.58 %	41.05 %
	Years	2003~2013	2004~2005	2005~2013	2005~2012
SW 28	Change	16.34 %	58.33 %	16.34 %	37.93 %
	Years	2010~2012	2004~2012	2010~2012	2005~2012
SW 259	Change	3.51 %	9.09 %	3.70 %	9.09 %
	Years	2007~2010	2006~2009	2007~2010	2006~2009
SW107.2	Change	20.24 %	6.29 %	20.00 %	6.28 %
	Years	2008~2011	2008~2010	2008~2011	2008~2010
SW 161	Change	67.80 %	5.42 %	30.00 %	44.74 %
	Years	2008~2011	2008~2012	2003~2013	2005~2012

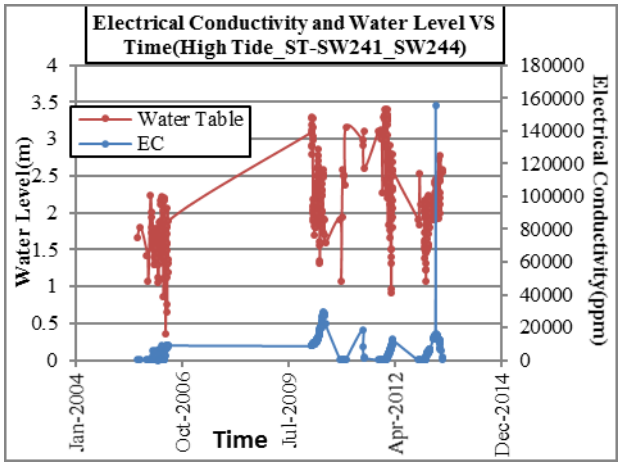

Fig. 13: Variation of Surface water salinity (EC) with water Level from 2005-2013 at station SW241 for High Tide

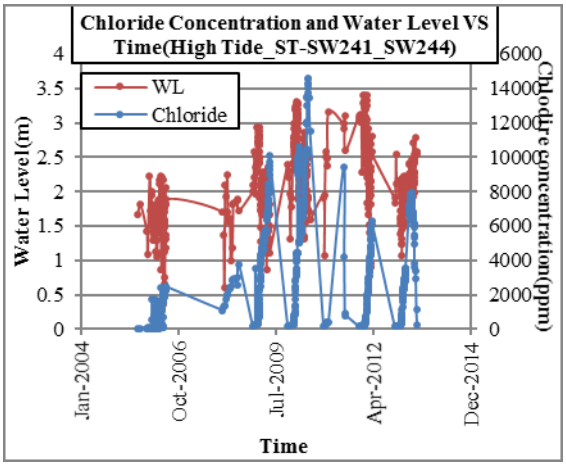

Fig. 14: Variation of Surface water salinity (Cl-) with water Level from 2005-2013 at station SW241 for High Tide

Table 5: Maximum and minimum Water level and their corresponding surface water salinity at various station during high tide and low tide.

		High Tide		Low Tide	
Station No	**Type**	**WLmax(m)**	**WLmin(m)**	**WLmax(m)**	**WLmin(m)**
SW241	WL(mPWD)	3.41	0.36	1.13	-1.49
	EC(ppm)	401	6500	6020	19100
	Cl^-(ppm)	201	1774	3010	9550
SW244	WL(mPWD)	3.41	0.36	0.68	-1.49
	EC(ppm)	1890	18000	1670	18000
	Cl^-(ppm)	930	6300	820	9000
SW259	WL(mPWD)	3.2	0.83	0.42	-1.69
	EC(ppm)	34000	4200	11000	5710
	Cl^-(ppm)	17000	4100	5500	2860
SW107.2	WL(mPWD)	3.8	0.55	1.65	0.05
	EC(ppm)	6000	3710	1210	6000
	Cl^-(ppm)	3000	1850	610	3000
SW161	WL(mPWD)	4	-0.5	-0.6	-2.58
	EC(ppm)	557	614	620	601
	Cl^-(ppm)	310	309	331	328
SW28	WL(mPWD)	2.95	1.38	0.85	-1
	EC(ppm)	10000	7470	1850	11000
	Cl^-(ppm)	5000	3730	940	5500

CONCLUSIONS

There are a number of rivers pass through Sundarbans and discharges into Bay of Bengal. Surface water salinity of Sundarbans rivers plays an important role for the existence of Sundarbans ecosystem. Hydrology and surface water salinity of Sundarbans rivers are investigated in this study. Freshwater discharge from the upstream rivers plays vital role in reducing the salinity inside the Sundarbans area during flood tide. Fresh water supplies through Gorai-Madhumati-Nabaganga-Rupsha-Passur river

system and Kobadak-Betna-Kholpetua-Shibsha river system mainly influence the salinity inside Sundarbans area, which is very much critical during dry period.

REFERENCES

EGIS.2000. Environmental Baseline of Gorai River Restoration Project – Environment and GIS Support Project for Water Sector Planning, Ministry of Water Resources, Government of Bangladesh and Government of The Netherlands, p.150.

Haque, MA and Alam, SMK.1995. Post Farakka dry Season Surface and Ground Water Conditions in the Ganges and Vicinity, Women for Water Sharing, Academic Publishers, Dhaka, pp 48-64.

Islam, SN and Gnauck, N. 2011. Water salinity investigation in the Sundarbans rivers in Bangladesh, *International Journal of Water*. 6(6):74-91.

Karim, A.1994. Vegetation in Mangrove of the Sundarbans, Volume Two: Bangladesh, IUCN – The World Conservation Union, Bangkok, Thailand.

Khan, MS; Haq, E; Huq, S; Rahman, A A; Rashid, SMA. and Ahmed, H. 1994. Wetlands of Bangladesh. BCAS, Dhaka. Bangladesh.

Siddiqi, NA. 2001. Mangrove of Bangladesh Sundarbans and accretion areas, Mangrove Ecosystems Functions and Management, Springer-Verlag, Berlin, Germany, pp.142–258.

ANALYSIS OF RAINFALL DATA FOR GENERATION OF INTENSITY-DURATION-FREQUENCY RELATIONSHIPS FOR SELECTED URBAN CITIES OF BANGLADESH

S. S. Rimi* & M. A. Matin

Department of Water Resources Engineering, Bangladesh University of Engineering & Technology, Dhaka, Bangladesh
**Corresponding Author: rimi.buet10@gmail.com*

ABSTRACT
This study aims to develop rainfall IDF relationships for five major cities of Bangladesh. The selected cities are Dhaka, Khulna, Chittagong, Barisal and Rajshahi. Two well-known frequency analysis techniques such as Gumbel and Log Pearson Type III (LPTIII) distribution have been used to analyse the rainfall data. Annual maximum rainfall data series for last 60 years (1954-2014) have been collected from Bangladesh Meteorological Department (BMD). Two different procedures have been applied for estimating the short duration rainfall intensities. These are Hershfield method and an empirical formula deduced by Indian Meteorological Department (IMD). Analyses have been done for two annual maximum data series. One series consists of rainfall data of 30 years from year 1954-1982, referred as older series and another as newer series of data range from year 1983-2014. This division of historical data is made to assess the influence of climatic changes on the IDF curves if any. Chi-square test has been used to assess the goodness of fit. It is found that the Gumbel method provides better compliance than that of LPTIII method. Comparison has also been made between two methods of short duration data generation. Rainfall intensity using IMD yields larger value than the Hershfield method. In terms of percentages, IMD gives 10.49% larger for Dhaka, 2.8% for Khulna, 14.16% Chittagong, 5.9% for Barisal, and 8.46% larger for Rajshahi than that of Hershfield method. The coefficients and exponents of expression of IDF relationships for different return periods were calculated by using nonlinear multiple regression method using both the data series. Minor change of IDF curves is observed when compared the results using older and newer data series. It is anticipated that IDF curves presented for urban cities will be useful to estimate the intense runoff for the design of small hydraulic structures.

Keywords: Rainfall data; frequency analysis; short duration rainfall; IDF curves; urban cities

INTRODUCTION
Rainfall Intensity-Duration-Frequency (IDF) curves are graphical exemplifications of the amount of water that falls within a given period of time in catchment areas. One of the first step in many hydrologic design projects, such as in urban drainage design, is the determination of rainfall event or events to be used. Rainfall depth for different return period is important in case of small hydraulic structures such as culverts, small bridges, polder scheme etc. For determining short duration rainfall, Hershfield method seems indispensable in areas where the only useful data are of long duration and in such cases they probably provide the best available estimates of short duration rainfalls with return periods less than 10 years (Siddiqui, 1993). In recent studies, various authors (Dupont and Allen, 2006, Kim et al. 2008) attempted to relate IDF relationship to the synoptic meteorological conditions in the area of hydrometric stations. The short duration rainfall IDF curve was developed for North-Eastern region with return period of 2, 5,10,20,50, and 100 years (Matin, 1984) using Hershfield Method (Hershfield, 1962, Bell, 1964). Daily rainfall data analysed by (Munshi, 2014) to obtain IDF curve for North-Western region of Bangladesh was developed. However, using a long series of historical data (about 60 years) an attempt has been made to assess IDF curves for major cities of Bangladesh.

METHODOLOGY

Two well known frequency analysis techniques e.g. Gumbel and Log Pearson Type III (LPTIII) distribution were used. Chi-square goodness of fit test was used and found that the Gumbel Distribution is better fitted for study region (Rasel,M. 2014). The short duration rainfall such as 5min, 10 min , 15min, 30 min 1 hour and 2 hour data have been calculated on the basis of an empirical formula deduced by Indian Meteorological Department (IMD) (method-1) and Hershfield-Wilson diagram which is referred as method-2 (Matin, 1984, Hershfield, 1962, Bell, 1964). The coefficient of exponents of expression of IDF relationship for different return periods (2, 5, 10, 20, 50 and 100 years) were calculated by using nonlinear multiple regression method (Rimi, 2016).

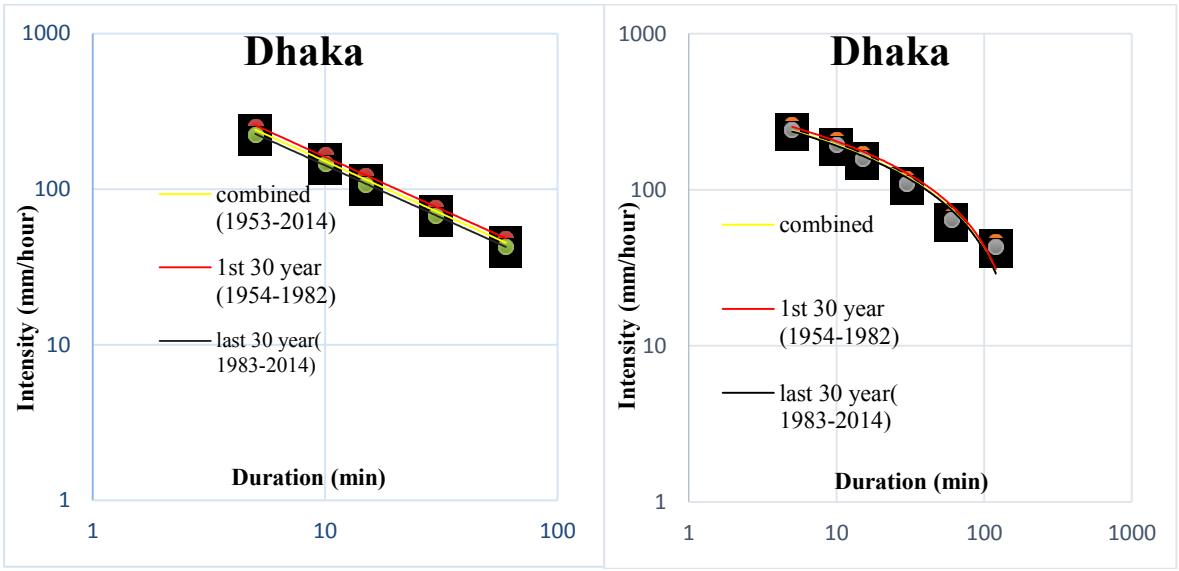

(a) (b)

Fig.1. Comparison of IDF Curve obtained from (a) Indian Method (b) Hershfield Method for Dhaka

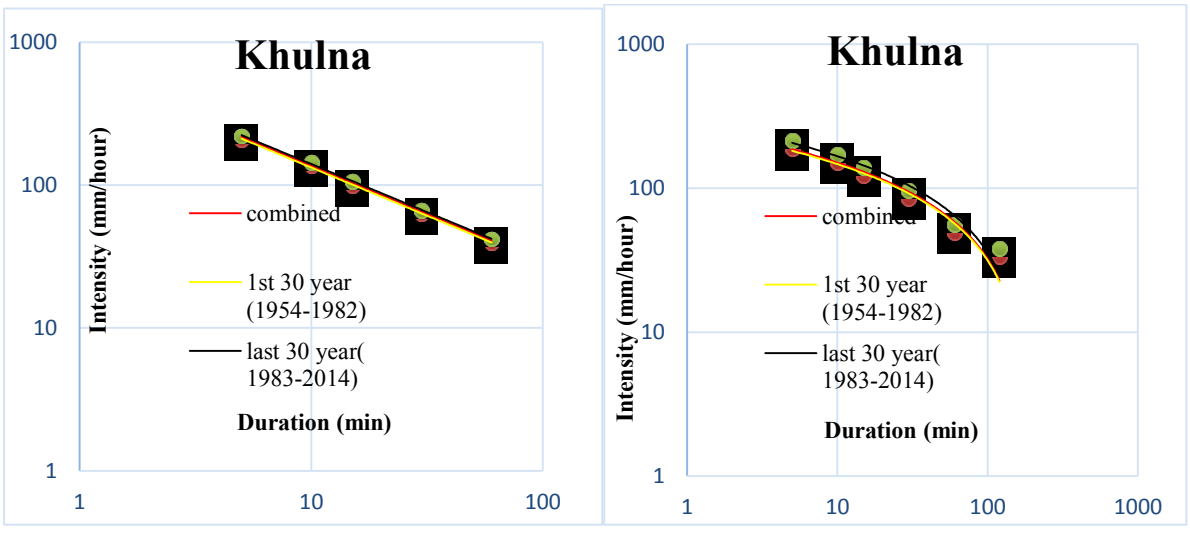

(c) (d)

Fig.2. Comparison of IDF Curve obtained from (c) Indian Method (d) Hershfield Method for Khulna

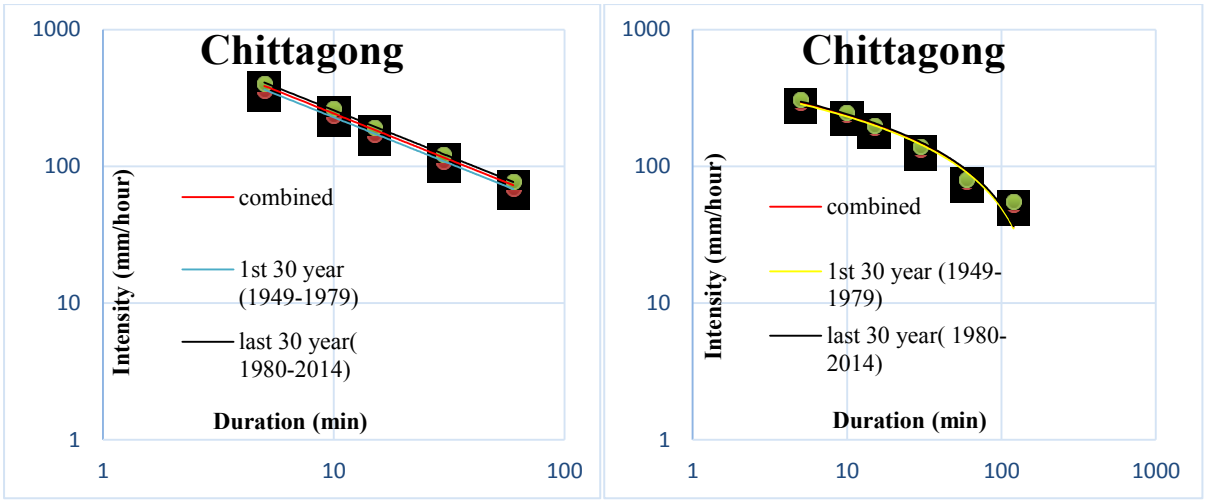

(e) (f)

Fig.3. Comparison of IDF Curve obtained from (e) Indian Method (f) Hershfield Method for Chittagong

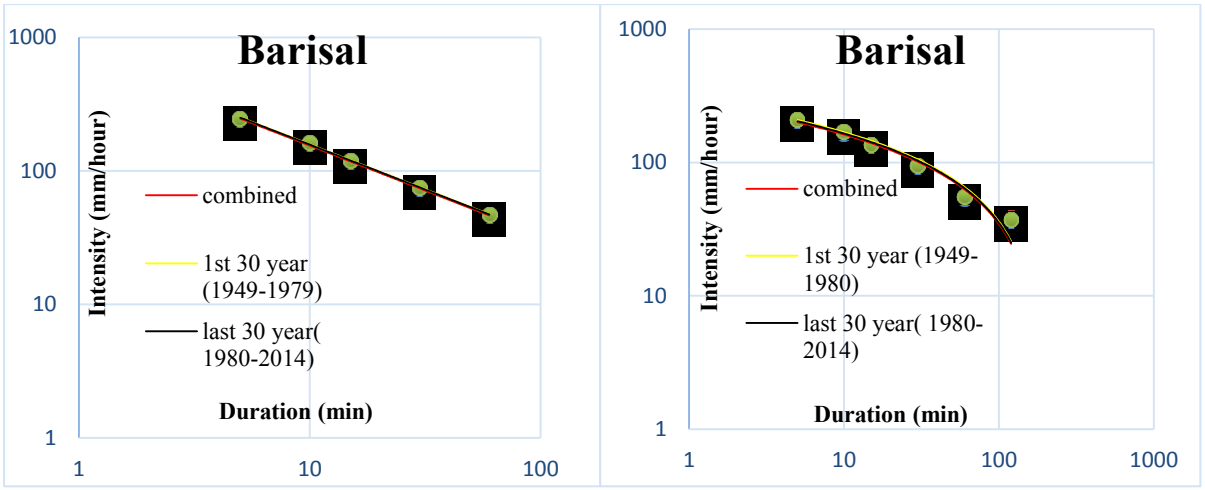

(g) (h)

Fig.4. Comparison of IDF Curve obtained from (g) Indian Method (h) Hershfield Method for Barisal

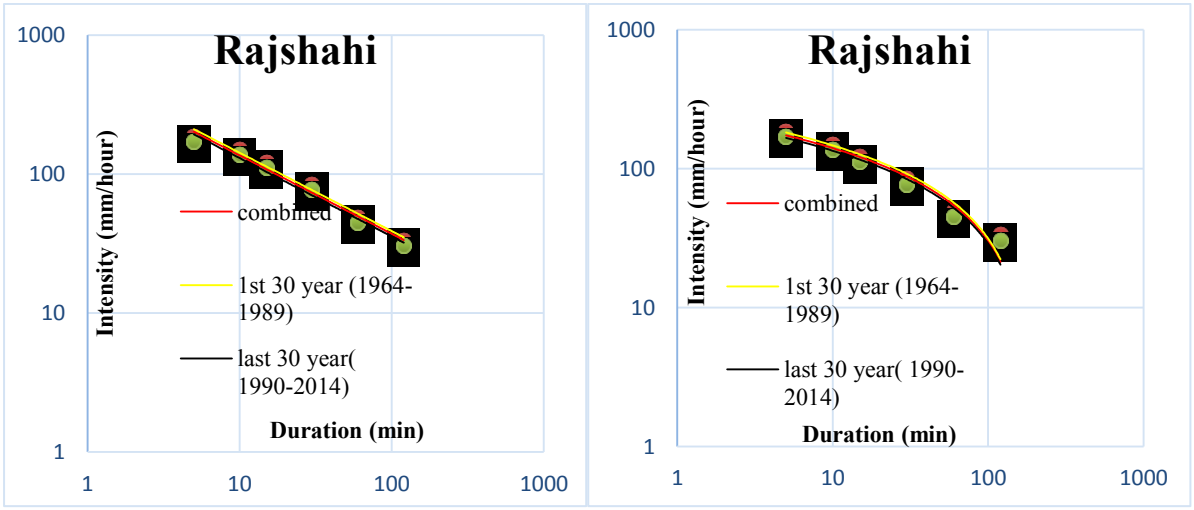

(i) (j)

Fig.5. Comparison of IDF Curve obtained from (i) Indian Method (j) Hershfield Method for Rajshahi

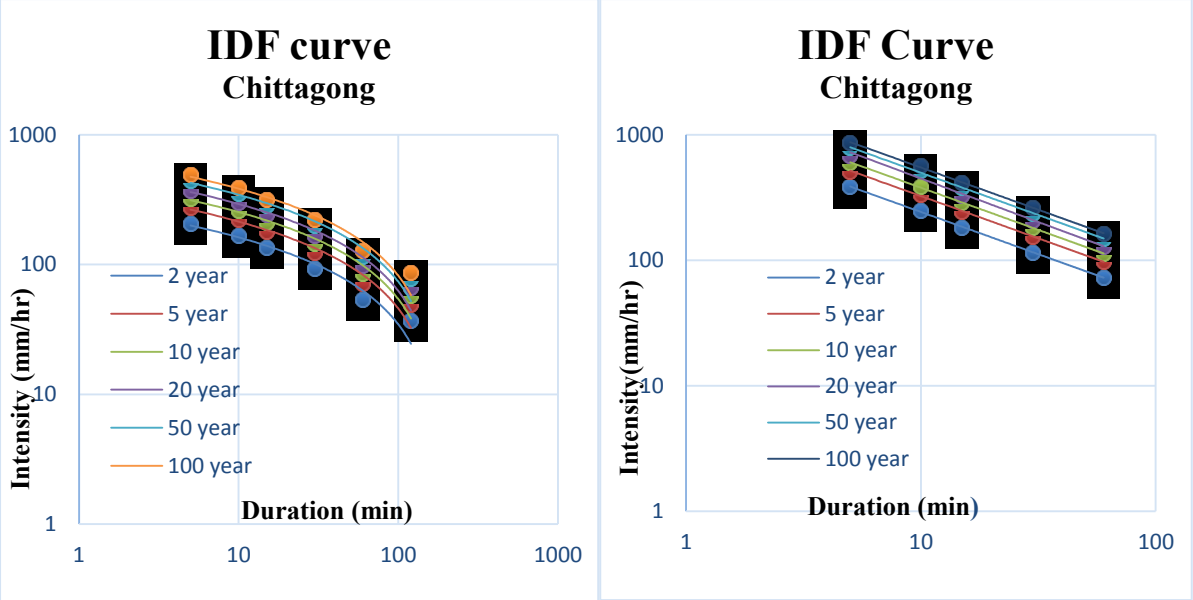

(i) (ii)

Fig.6. Generated IDF curve by using (i) Indian Method; (ii) Hershfield Method

Table-1: IDF relationships obtained using the Indian method

Urban Stations	IDF Relationship $I = \frac{CT_r^m}{T_d^e}$		% of change between older and newer series	Remarks
	From 1954-1982	From 1983-2014		
Dhaka	$I = \frac{716T_r^{0.215}}{T_d^{0.673}}$	$I = \frac{629.36T_r^{0.239}}{T_d^{0.673}}$	10.62%	Intensity decrease in last 30 year.
Khulna	$I = \frac{602.55T_r^{0.2359}}{T_d^{0.673}}$	$I = \frac{625.9T_r^{0.2614}}{T_d^{0.672}}$	5.57%	Intensity increases in last 30 years
Chittagong	$I = \frac{1012T_r^{0.1913}}{T_d^{0.676}}$	$I = \frac{1122T_r^{0.213}}{T_d^{0.673}}$	11.3%	Intensity increases in last 30 years.
Barisal	$I = \frac{700.32T_r^{0.212}}{T_d^{0.676}}$	$I = \frac{688.3T_r^{0.19}}{T_d^{0.6745}}$	3.16%	Intensity decreases in last 30 years.
Rajshahi	$I = \frac{547.7T_r^{0.2336}}{T_d^{0.673}}$	$I = \frac{544.37T_r^{0.229}}{T_d^{0.673}}$	0.96%	Intensity decreases in last 30 years.

Table-2: IDF relationships obtained using the Hershfield method:

Urban Stations	IDF Relationship $I = \frac{CT_r^m}{T_d^e}$		% of change between older and newer series	Remarks
	From 1954-1982	From 1983-2014		
Dhaka	$I = \frac{660.69T_r^{0.207}}{T_d^{0.595}}$	$I = \frac{619.15T_r^{0.202}}{T_d^{0.595}}$	7.76%	Intensity decrease in last 30 year
Khulna	$I = \frac{501.76T_r^{0..216}}{T_d^{0.563}}$	$I = \frac{512.86T_r^{0.24}}{T_d^{0.562}}$	4.09%	Intensity increases in last 30 years
Chittagong	$I = \frac{749.72T_r^{0.217}}{T_d^{0.564}}$	$I = \frac{776.24T_r^{0.217}}{T_d^{0.563}}$	3.56%	Intensity increases in last 30 years
Barisal	$I = \frac{545.52T_r^{0.217}}{T_d^{0.564}}$	$I = \frac{534.19T_r^{0.219}}{T_d^{0.5645}}$	2.016%	Intensity decreases in last 30 years
Rajshahi	$I = \frac{536.5T_r^{0.2173}}{T_d^{0.563}}$	$I = \frac{476.65T_r^{0.217}}{T_d^{0.564}}$	10.9%	Intensity decreases in last 30 years

Methods Used for Generation of Short Duration Data

***Indian Meteorological Department (IMD*) Method**: The empirical formula provided by IMD is given by,

$$P_t = P_{24}\sqrt[3]{(\frac{t}{24})} \quad (1)$$

***Hershfield Method*:** One hour data for frequencies 5, 10, 20, 50 and 100 year return periods have been calculated by using the equation presented by Bell (1969) as follows

$$P_T^{60min} = (0.35ln(T) + 0.76)P_2^{60min} \quad (2)$$

24- hour rainfall data for different return periods were then determined by equation,

$$P_T^{24hour} = (0.3602ln(T) + 0.754)P_2^{24hour} \quad (3)$$

RESULTS AND DISCUSSIONS

From the analysis it can be said that the Gumbel method of distribution provides comparatively good fit than LPT-III method. Goodness-of-fit tests were used to choose the best statistical distribution among these techniques.

In this study, the ratio of 2-year, 1-hour to 2-year, 24-hour rainfall was found to vary between 0.394 to 0.546. The mean ratio of 0.463 and a standard deviation of 0.0569 has been considered in Hershfield method for short duration data generation. Murry (1970) reported that this value lies between a range of 0.35 to 0.45 for India, in the continental United States and in South Africa the mean ratio was 0.435 and 0.50 respectively.

The comparison between IDF results obtained using older and newer annual data series and between Indian and Hershfield Method are shown in Fig-1, Fig-2, Fig-3, Fig-4, Fig-5 for five selected urban stations of Bangladesh. Comparison between the two methods are shown in Fig-2 for different return period for Chittagong city containing 60 years data series. The IDF equations of IMD method (method-1) are listed in Table 1 for the five urban stations. The percentage of change between older and newer data series for Dhaka, Khulna, Chittagong, Barisal and Rajshahi which are 10.62% , 5.57%, 11.3%, 3.16%, 0.96%. Table 2 shows the IDF relationship derived by using the Hershfield method (method-2) and the percentage change between the same period of analysis and urban station such as Dhaka, Khulna, Chittagong, Barisal and Rajshahi shows the rate of 7.76%, 4.09%, 3.56%, 2.016%, 10.9%.

Data shows that recent rainfall pattern of Bangladesh is erratic nature. No definite trends are obtained from trend analysis (Rimi, 2016). It is also suggested that short duration recording gauge data should be collected and preserved by BMD in regular basis so that the generated values to develop IDF can be better compared with real data.

CONCLUSIONS

Gumbel method estimates relatively higher rainfall intensity compared to those obtained by LPT III distribution. The results of the chi-square test of goodness of fit show that the Gumbel distribution is acceptable at the average significance level of 2.8%. Two different procedures have been adopted to generate short duration data required for IDF curves of five major cities of Bangladesh. Two annual extreme value series of rainfall data for years 1943-1982 and 1983-2014 have been used for the analyses. No significant change in IDF curves has been found, which reflects a minor influence of changing climate on IDF. Rainfall intensity using IMD yields larger value than those obtained by Hershfield method. IDF curves and relationships presented in this paper will be useful for estimation of storm runoff of urban areas of major cities of Bangladesh.

REFERENCES

Bell F. C.1969. Generalized Rainfall Intensity-Duration Frequency Relationships. Journal of Hydraulic Div. ASCE Vol. 95, HY 1

Dupont, B.S., Allen, D.L. 2006.Establishment of Intensity–Duration–Frequency Curves for Precipitation in the Monsoon Area of Vietnam. Kentucky Transportation Center, College of Engineer, University of Kentucky in corporation with US Department of Transportation, 2006

Hershfield D. M. 1962. Extreme Rainfall Relationships, Journal of the of the Hyd. Division, ASCE. Vol. 88, No. HY6. Proc. Paper 3319.

Kim T, Shin J, Kim K and Heo J. I. 2008. Improving accuracy of IDF curves using long- and short duration separation and multi-objective genetic algorithm. World Environmental and Water Resources Congress. 2008, 1-12.

Murry , J.A 1970 , Hydrological Determination of flood peaks from small catchments for design of bridge. Pub no. 140. Central Board of Irrigation and Power. New Delhi.

Matin M A.1984.Analysis of Rainfall Data for Estimating the Intensity Duration Frequency Relationship for the North-Eastern Region of Bangladesh, M ScEngg Thesis, WRE Dept, BUET.

Rasel, Munshi. 2014. Generation of Rainfall Intensity-Duration-Frequency Relationship for North-Western Region in Bangladesh, IOSR Journal of Environmental Science, vol-9.

Rimi, S.S. 2016, Analysis of rainfall data for generation of Intensity Duration frequency Relationship of selected five cities of Bangladesh, B.Sc. Engg. Thesis, WRE Dept., BUET.

Siddiqui, S.1993. Intensity Duration Frequency Relationship for Short Duration Rainfall of Selected Urban stations of Bangladesh, M. Engg Thesis, WRE Dept, BUET

GENERATION OF INFLOW HYDROGRAPHS FOR A SELECTED SMALL URBAN CATCHMENT OF DHAKA CITY

R. T. Khan&M. A. Matin*

Department of Water Resources Engineering,Bangladesh University of Engineering and Technology, Dhaka, Bangladesh
**Corresponding Author: mamatin@wre.buet.ac.bd*

ABSTRACT
This study deals with a systematic approach for the estimation of urban runoff from a small catchment. An urban catchment in Uttara area, near the Abdullahpur-Mirpur embankment, has been selected. Intense rainfall hydrographs have been generated based on the application of HEC-HMS model using the NRCS unit hydrograph method. Intensity-Duration-Frequency relationship curves are used to generate short duration design rainfall event. Three rainfall events such as 1h 2 year, 2h 5 year and 2h 10 year return period has been used for hydrograph generation. Curve number values obtained from GIS shapefiles of proposed and existing landuse maps are used in the model. The rational method has also been included to estimate the peak discharge and compare with the results obtained from the model. In this study it is found that with increased urban development, peak runoff values are significantly higher than undeveloped conditions. For sub-catchments A, B, C and D, the values of peak runoff varied by 40.2% (10.7 m^3/s-15.0 m^3/s), 2.2% (4.5 m^3/s- 4.6 m^3/s), 23.9% (17.6 m^3/s – 21.8 m^3/s) and 264% (5.0 m^3/s – 18.2 m^3/s) respectively compared to present condition under 2h 5 year return period rainfall. In addition, the time to rise to peak discharge was found to be shorter by 16.7%, 0%, 14.3% and 33.3% respectively, which means that the basin would respond more rapidly to a given rainfall condition. Losses and abstractions from rainfall was found to be lower with increased urbanization, implying that greater part of the rainfall would be converted into rainfall excess. The values of peak discharge from rational method varied from model result by 1.43% in case of sub-catchment B under 1h 2 year return period rainfall in proposed land use condition upto 80.8% in sub-catchment D under 2h 5 year return period rainfall in existing land use condition.The results of this study would be helpful for proper design of drainage structures like culverts, sluice gates, or pumping stations. Identification of local drainage pattern in terms of sub-catchment needs to be addressed for proper planning and management of urban drainage system.

Keywords: Urban catchment, IDF curves, NRCS method, hydrograph, rational Method.

INTRODUCTION
Urban drainage congestion during monsoon due to heavy rainfall causes much inconvenience and economic losses for the Dhaka city residents. The reasons behind this urban flooding can be attributed to heavy rainfall, inadequate drainage system, high water level in the peripheral rivers, unplanned urban development, encroachment and congestion of canals and urban development of local water retention bodies. The various canals passing throughout the city play an important role in carrying out the runoff to the peripheral rivers.

A master plan for flood mitigation and stormwater drainage improvement in Dhaka city was prepared in 1991 for flood protection of approximately 262 km^2 of the city. Partial implementation of this plan has protected the western half of the city from river flood by embankments and raised roads. Although internal stormwater flooding in the western part was expected to be mitigated after rehabilitating the drainage system and installing permanent pump stations, the flooding condition has been deteriorating. This declining situation calls for investigation into the causes of stormwater flooding. The urgent need to resolve urban flooding problem has been felt after a disastrous stormwater flooding caused by unprecedented rainfall in September 2004 and the preceding countrywide flood in July of the same year. At the same time, it appears to be imperative to set forth a realistic plan for flood mitigation and

stormwater drainage for the eastern part of the city. The original master plan needs revision because of the unplanned land use changes that took place since the plan was prepared.

METHODOLOGY

Both primary and secondary data were needed to fulfill the study. Primary data includes photographs of salient features to determine the flow paths, and public opinion regarding the current drainage condition of the study area. Secondary data includes GIS shape files of contour maps and existing and proposed land use data obtained from RAJUK Detailed Area Plan. The design rainfall data was generated from IDF curves of Dhaka City for the interval 1984-2013.

The first step was to delineate the boundaries of the sub-catchments. It was done based on observation of existing drainage system, sluice gates and contour map. In case of Catchment C, no outlet was found So, a sluice gate (sluice no. 3) was proposed as shown in fig.2

The lag times for the sub-catchments were determined using the NRCS lag equation, which involves Curve Number, Average Basin Slope, and Hydraulic Length of the principal drainage channel.

In the rainfall-runoff model of HEC-HMS, area, initial abstraction, curve number, imperviousness (%), lag time were given as inputs of catchment parameter. In time-series data manager, rainfall values were input as hyetographs.

For the rational method, the value of the constant, C was obtained from the land use maps, the design rainfall intensity was arbitrarily chosen as 2h 5 year, 2h 10 year and 1h 2 year return period rainfall.

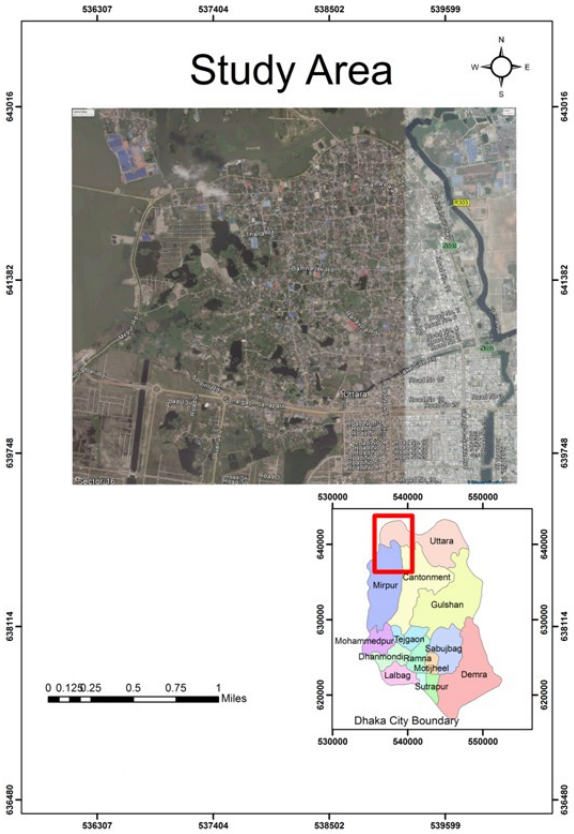

Fig. 1: Location of Study Area

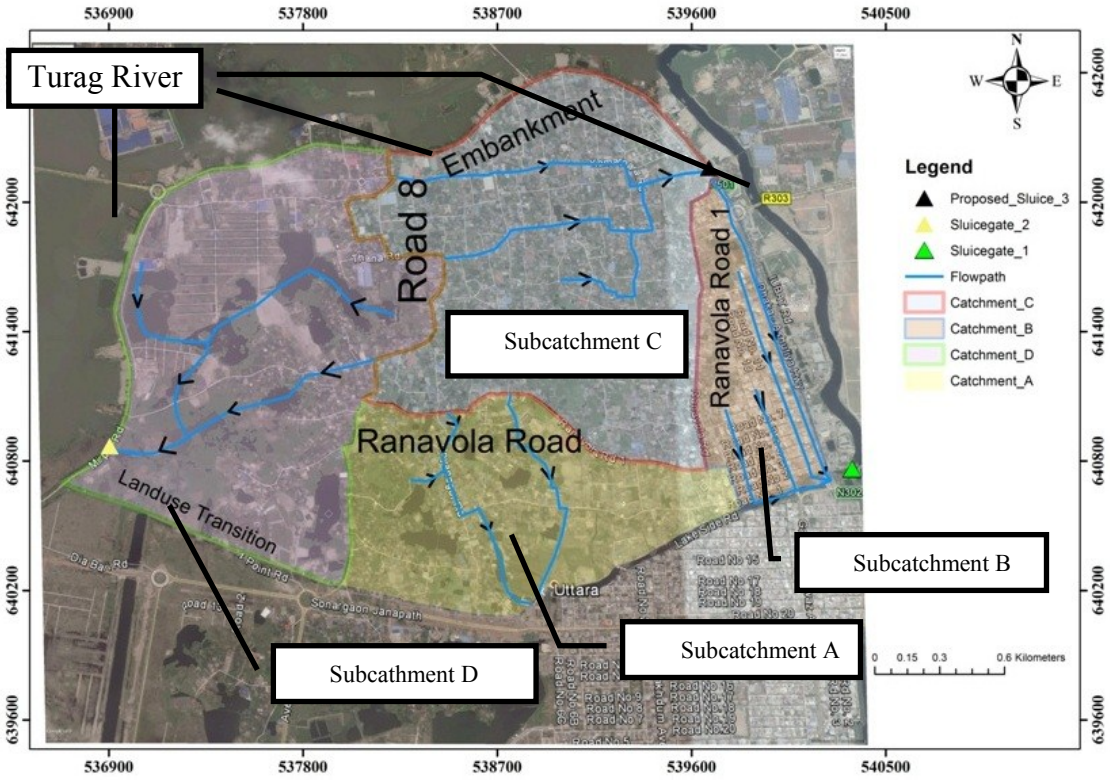

Fig 2: Subcatchments and Drainage Paths

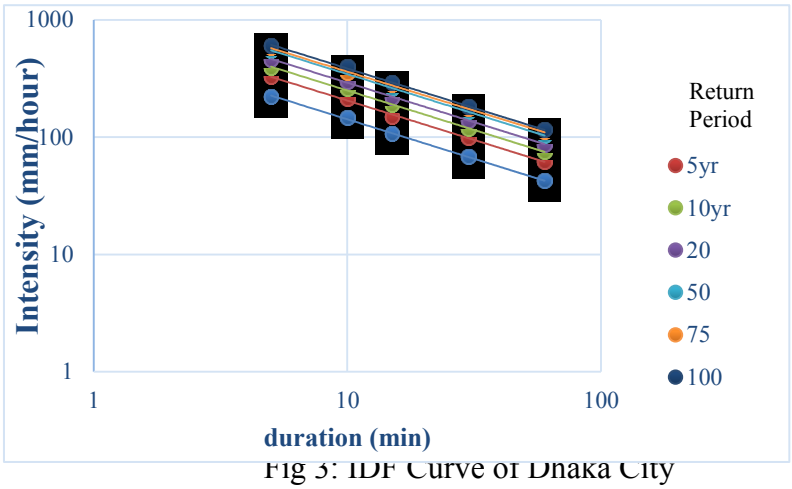

Fig 3: IDF Curve for Dhaka City

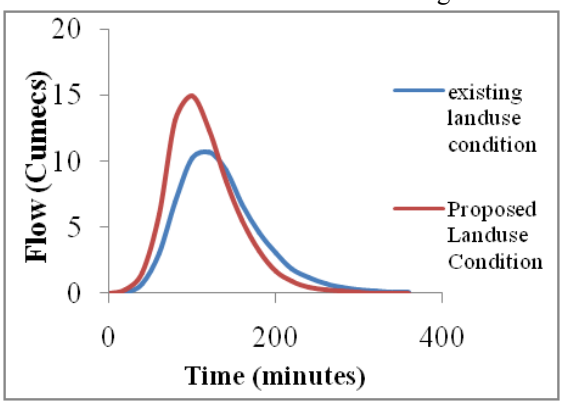

Fig 4: Hydrograph for Subcatchment A

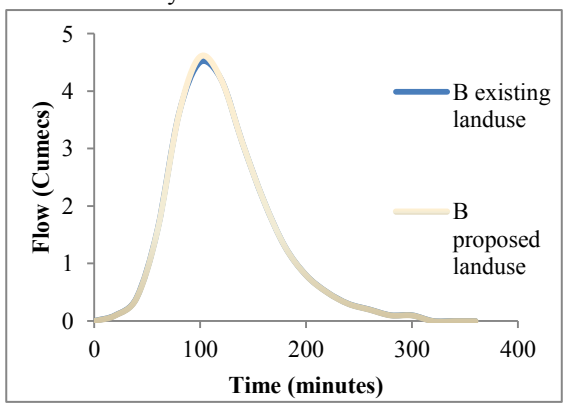

Fig 5: Hydrograph for Subcatchment B

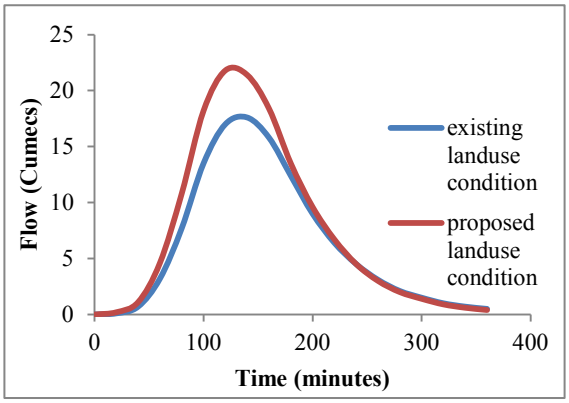

Fig 6: Hydrograph for Subcatchment C

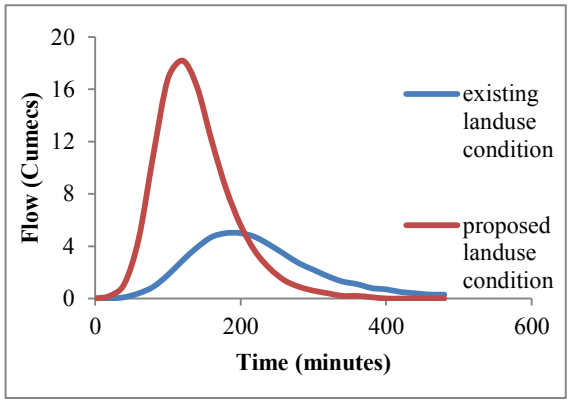

Fig 7: Hydrograph for Subcatchment D

Hydrographs for each subcatchment under different rainfall events in propsed landuse pattern:

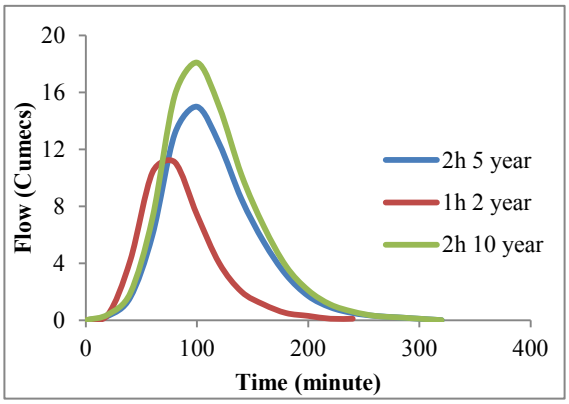

Fig 8: Hydrograph for Subcatchment A

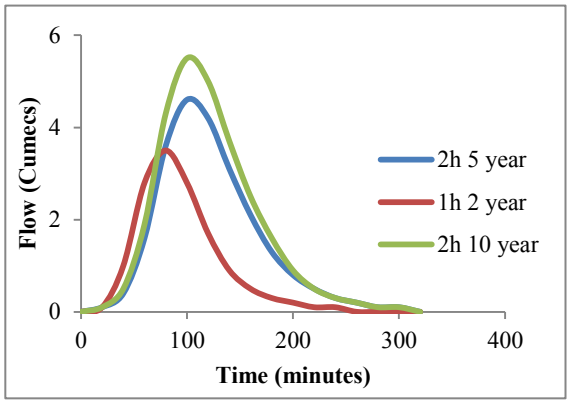

Fig 9: Hydrograph for Subcatchment B

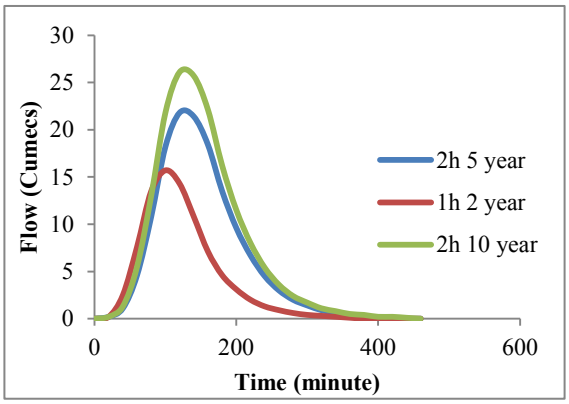

Fig 10: Hydrograph for Subcatchment C

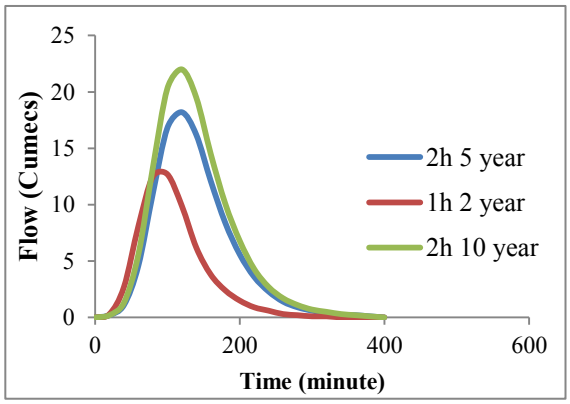

Fig 11: Hydrograph for Subcatchment D

Table 1: Subcatchment Properties

Subcatchment	Area (km^2)	Landuse Condition	Lag time, t_L (min)	Rational Method, C
A	1.33	Existing	59.4	0.66
		Proposed	44.2	0.72
B	0.41	Existing	50.7	0.76
		Proposed	50.7	0.77
C	2.24	Existing	78.8	0.74
		Proposed	73.3	0.76
D	2.03	Existing	129.7	0.44
		Proposed	62.6	0.72

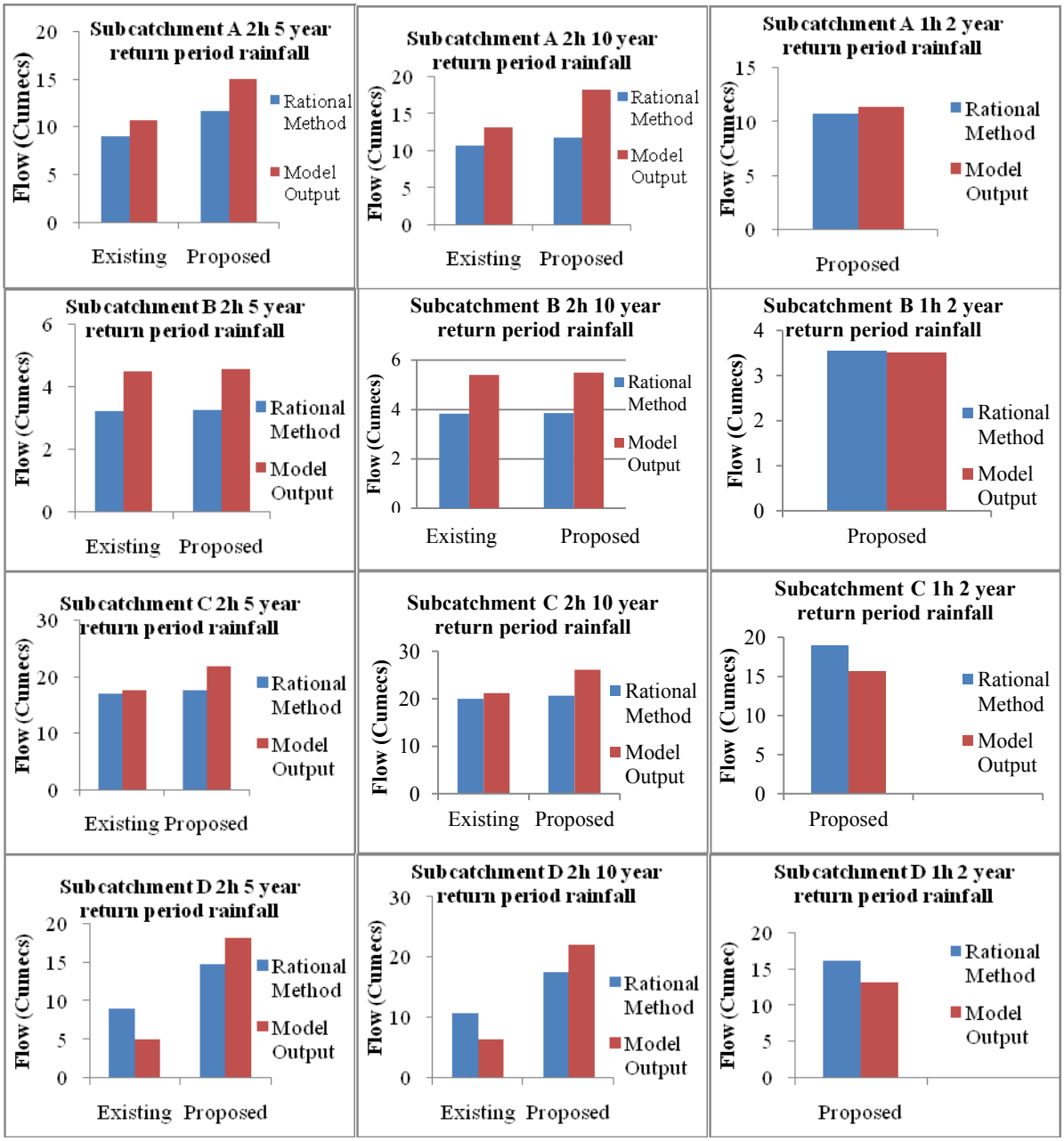

Fig. 12: Comparison between peak discharges from HEC-HMS model and Rational Method under existing and proposed landuse conditions

NRCS Lag equation:

$$t_L = \frac{l^{0.8}(2540 - 22.86CN)^{0.7}}{1410CN^{0.7}Y^{0.5}} \quad (1)$$

Average basin slope,

$Y = 100(CI)/A$ (2)

Y= average land slope, %

C= summation of the length of the contour lines that pass through the watershed drainage area on the quad sheet, ft

I= contour interval used, ft

A= drainage area, ft^2

IDF equation for Dhaka city,

$$I = \frac{629.36 T_r^{0.239}}{T_d^{0.673}} \quad (3)$$

I= intensity in mm/hr; T_r = Return Period, in Years; T_d= Duration, in minutes

RESULTS AND DISCUSSIONS

1. The variations of runoff with changing landuse pattern for the four subcatchments are shown in figures 4-7. Increased urban development produces hydrographs with greater peak discharge, less precipitation losses, and more percentage of the rainfall is converted to rainfall excess due to increased surface imperviousness. Also, the base length of the hydrographs were shorter in case of urbanized catchments, indicating that peak discharge will be reached at shorter interval from beginning of rainfall.
2. The peak design discharge was obtained from arbitrarily chosen 1h 2 year, 2h 5 year and 2h 10 year return period of rainfall. The resulting hydrographs for each subcatchment (for proposed landuse condition) for each return period of rainfall are shown in figures 8-11. It is observed from these results that for design of drainage structures, higher discharging capacities need to be selected for 2h 10 year return period rainfall. A proper return period must be selected based on economic considerations.
3. Peak discharge values obtained from rational method were almost identical in case of 1h 2 year return period rainfall. For other rainfall conditions, the results varied significantly. In urbanized subcatchments, the HEC-HMS model output yields slightly higher values of peak discharge, and in undeveloped subcatchments, the rational method produces higher values of peak discharge. The values of peak discharge from rational method varied from model result by 1.43% in case of subcatchment B under 1h 2 year return period rainfall in proposed landuse condition upto 80.8% in subcatchment D under 2h 5 year return period rainfall in existing landuse condition.

CONCLUSIONS

1. In some subcatchments of the selected area, especially in subcatchment C (2.26 km^2 area) and subcatchment A (1.33 km^2 area), local water retention bodies play an important role in storage of runoff water. Some surface drains also drain into these water bodies. But for long-term urban planning, the runoff water needs to be conveyed across the embankment into the Turag river.
2. Two sluice gates are already installed in the study area. This study reveals that the capacity of these sluice gates seems to be inadequate to drain the generated runoff water. Therefore, more drainage structure is required for this catchment.
3. During high flood levels in the peripheral Turag River, pumping facilities in addition to sluice gates may be necessary for effective drainage system.

ACKNOWLEDGMENTS

We gratefully acknowledge the contributions of Water Resources Engineering Department of BUET for providing the library facilities to support this study.

REFERENCES

HEC-HMS User's Manual. 2015. Version 4.1.[online] Chapter 1. pp 1-8. Available at: http://www.hec.usace.army.mil/software/hec-hms/documentation/HEC-HMS_Users_Manual_4.1.pdf
Subramanya, K. 2014-2015. *Engineering Hydrology.* Fourth Edition: McGraw Hill Education Private Limited. p. 189
Sultana,S.2016. *Analysis of Rainfall Data for Generation of Intensity-Duration-Frequency Relationships for Selected Urban Areas of Bangladesh.* B.Sc Engg Thesis, WRE Dept, BUET.
Wurbs, RA and James, WP. 2002. *Water Resources Engineering.* Prentice Hall. pp 462-488

ESTIMATION OF SUSPENDED SEDIMENT CONCENTRATION OF WATER BODIES USING LOW COST PORTABLE DIGITAL CAMERA

A. Haque[1*] & K. K. Adhikary[2]

[1]*Department of Civil Engineering, Military Institute of Science and Technology, Dhaka, Bangladesh*
[2]*Department of Water Resources, Bangladesh University of Engineering and Technology, Dhaka, Bangladesh*
[*]*Corresponding Author: haquearefin87@yahoo.com*

ABSTRACT
Quantitative application on remote sensing of suspended sediment is an important aspect of the engineering application of remote sensing study. In this study, image processing technique is used as a method to estimate the amount of sediment concentration to facilitate and increase the speed of measurement. Estimation of fine sediment concentration is important for using water for different domestic, drinking and other purposes, from various sources like rivers, ponds or lakes. Traditional methods for this estimation are time consuming, costly and not easily accessible, especially for rural people in Bangladesh. In this study, it is shown that digital or DSLR camera could be used to estimate the amount of concentration. To accomplish this, a number of experiments had been conducted in two types of water tanks (circular and square) with different background color (white & grey) and with variation of camera height and angle. Sediment samples of brown & grey color were collected from bottom of different water bodies (such as river bed) and had been kept in open space for air drying but instead of it, oven drying cannot be allowed as the internal molecular structural arrangement of soil grain would be damaged. After that special sieve no-63 micron (<63 μm) ASTM no-230 passing very fine sediment samples were separated for the purpose of the experiment to avoid any settlement of sediment particles. Then, a standard correlation between image data (RGB value) & concentration was determined. Using the developed correlation one can easily understand sediment concentration of water bodies, which can be an alternative efficient tool rather than the conventional one.

Keywords: RGB; Fine suspended sediment; Digital image; Concentration

INTRODUCTION
Estimation of suspended sediment concentration is important for using water for different domestic and drinking purposes, from various sources like rivers, ponds, or lakes. High suspended sediment concentrations can affect water resources by damaging turbines of hydroelectric plants, and increasing requirements for water treatment procedures; reducing reservoir and diversion dam storage capacity. However, excessive sedimentation in streams and rivers is considered to be the major cause of surface water pollution.

The traditional method to measure suspended load by direct measuring of sediment samples seems more costly, time consuming and not easily accessible especially for people living in rural areas. Remote Sensing of Suspended Sediment Concentrations in Mekong River and the Red River conducted by Wang *et al*. [2012] aimed to investigate whether suspended sediment concentration (SSC) values could be estimated directly using this technique. The drawback of the study is that the measured reflectance is affected by illumination conditions significantly. Besides, Liew *et al.* [2002] conducted a study in a highly turbid inland river (lower Jinsha River in Yunnan, China) to develop relations between in-situ water reflectance measurement and TSS concentration. It was found that the empirical method established in this study by using a band ratio can only estimate total suspended sediment at lower concentration levels up to 400 g/m^3. This study also lacks in furnishing the impact of sediment properties on the

backscattering coefficient. Lodhi *et al.* [1998] used integrated surface reflectance and found that: spectroradiometer data, integrated into the band width of Landsat-TM 4, allowed accurate estimation of suspended sediment concentration. But they failed to compare the findings to actual TM spectral data acquired over lakes and reservoirs.

Furthermore, digital camera is another new technique which can bring many advantages, as it can easily capture data at any time. Pictures are taken very close to the subject and can eliminate any side effect. The most important and difficult part of digital camera technique, is the processing of the captured images. Lim *et al.* [2003] first reported the application of digital camera in the estimation of total suspended sediment. Bejestan and Nouroozpour [2007] also used image processing technique to estimate the amount of sediment concentration which facilitated and increased the speed of measurement. This study was conducted only for the type of sediment available in Karoon banks. The equation established in this study would be varied with the type of sediment changes.

So, after analyzing and taking into account of all these limitations of the previous studies, different tanks, sediment samples and camera were used in this present study. Major purpose of this study is to define the sediment concentration as a function of digital image data in which red (r), green (g) and blue (b) components of color images as well as gray component with different sediment loads were tried to correlate. On the other hand to know the acceptable level of turbidity in streams is the second most important criteria for conducting this study.

The method for the measurement of suspended sediment concentration using digital camera is very cost effective, so only by applying this technique anyone especially rural and general people can get rid of many waterborne diseases, aware of the adverse effects of highly turbid water and be able to know the amount of level of suspended sediment concentration present in any water body.

METHODOLOGY

A number of experiments were conducted to develop a correlation between suspended sediment concentration and digital image with variation of water tank and sediment sample. The experiment was conducted during the day time when sunlight was available. Photos were taken vertically, at an angle of 45^{o}as well. Two types of tank were used- one circular (2' dia) and the other square (2' X 2 'X 2') in shape. The circular one (Fig-1) was of plastic material and the square one (Fig-2) was of perspex material. Bottom and side walls of the square tank was kept gray and that of circular one was kept white which was later changed to gray. Brown colour and gray colour clayey soils were used as suspended sediment. The soil samples were collected (Fig-6) from the bottom of two lakes in Mirpur Cantonment. The soil samples were air dried (Fig-7), pulverized and sieved through non-standard (special) sieve of 63 micron (Fig-5). The sieved material (Fig-8) was weighted and mixed with a known volume of water in different concentration. Suspended sediment concentration was produced by consecutive addition of 5mg/l, 10mg/l, 20mg/l, 30mg/l, 40mg/l, 50mg/l, 75mg/l, 100mg/l, 150mg/l, 200mg/l, 250mg/l, 300mg/l, 400mg/l and finally 500mg/l of the soil sample. During the experiment, sediments were kept in suspension by manual stirring. During higher concentration quick settlement of the sediment was observed. Photos (Fig-9, 10, 11...) were taken after each addition from a height of one foot by using NIKON D3000 DSLR camera with 10.2 megapixels as well as with Canon S110 with 10 megapixels normal digital camera (Fig-3) to check if different camera, pixel capacity and resolution have any effect on the image quality. In order to establish a relationship between turbidity and suspended sediment HANNA turbidity meter HI93703 (Fig-4) was used for the experiment which can measure turbidity within (0-1000) FTU range. Average of R (red), G (green), B (blue), their mean value and gray value were calculated from 9 pixel values (3 X 3) by using Adobe Photoshop version 8.0. Separate graphs (Fig-12) were generated for R, G, B, gray and average of RGB against concentration. Graphs for turbidity against concentration were also developed.

Fig-1: Circular tank

Fig-2: Square tank

Fig-3: Digital Camera

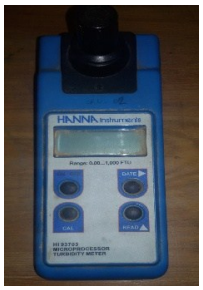

Fig-4: Turbidity

Fig-5: 63 μm sieve

Fig-6: Wet sediment

Fig-7: Dry sediment

Fig-8: Sieved brown

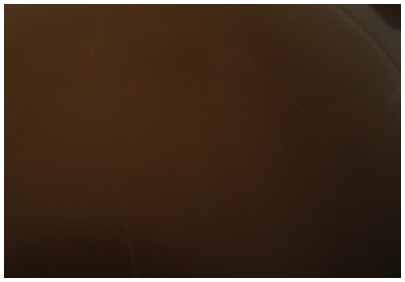

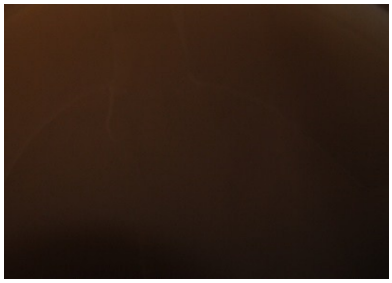

Fig-9, 10 and 11: Water with concentration (a) 5mg/l; (b) 100mg/l; (c) 500mg/l (images taken during experiment conducted in white circular tank using brown sediment)

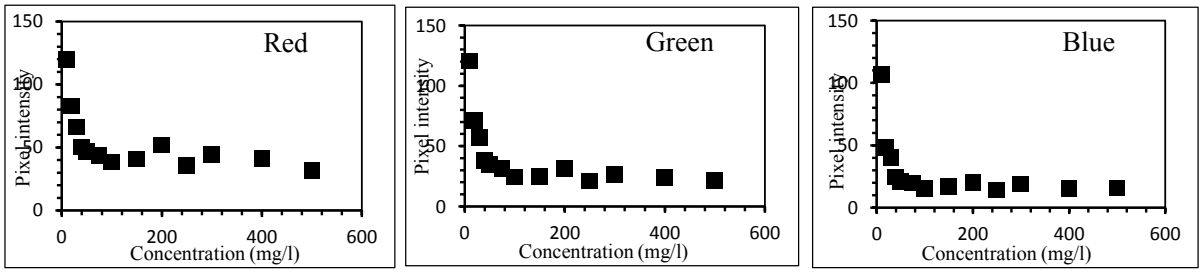

Fig- 12: Correlation between pixel intensity and sediment concentration for experiment conducted in circular white tank using brown sediment (concentration up to 500mg/l).

RESULTS AND DISCUSSIONS

It is seen that the values of pixel intensity decreases for increasing amount of concentration. But for higher concentration the values of pixel intensity remains almost constant. So values for higher concentration were discarded later.

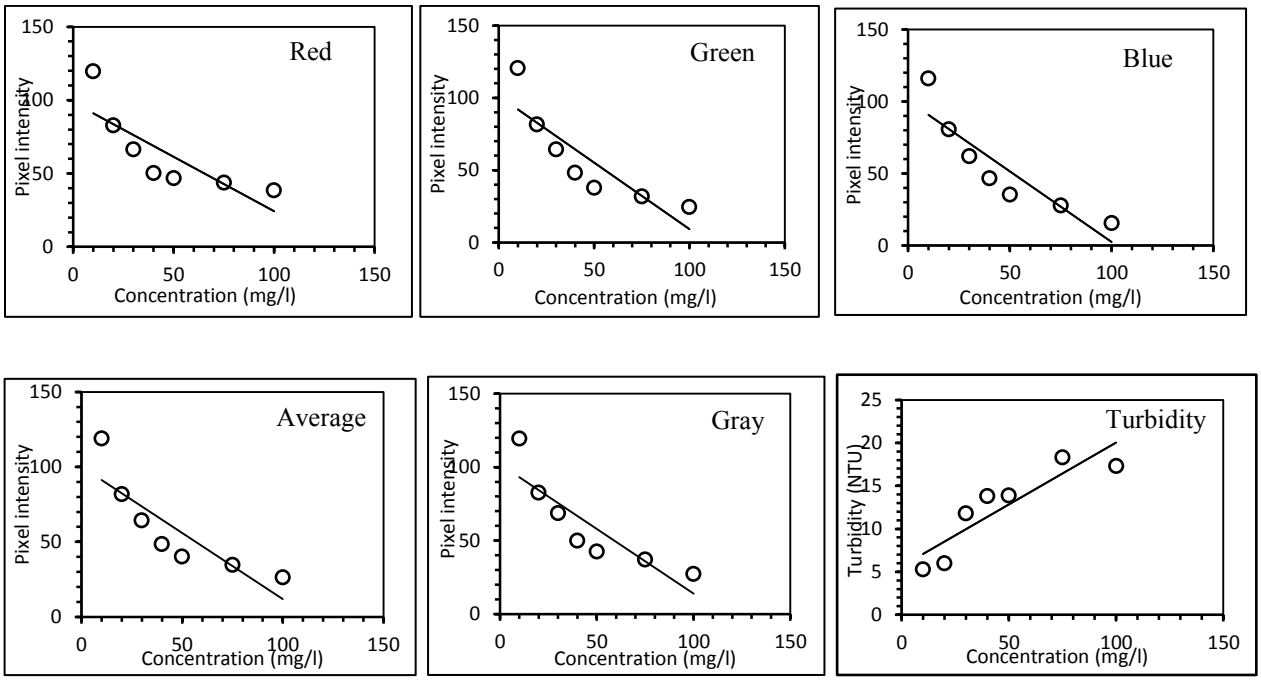

Fig-13: Correlation between pixel intensity and sediment concentration for experiment conducted in circular white tank using brown sediment (concentration up to 100mg/l)

Validation

For the validity purpose or comparison of the experimental results with the actual field data, two samples of water were collected from the Gulshan Lake (one from the bank and the other one from the middle of the lake) in two different containers and the average turbidity of these two samples were found as 22 NTU with the help of turbidity meter. Then the laboratory measurement of concentration by the process of filtration was conducted using 45 micron filter papers and the actual concentration values had been found as 59.9mg/l and 44.67mg/l, where 51.84 mg/l is the mean of these two values.

Fig -14: Pictures captured at Gulshan Lake for the purpose of Validation

Verification of Experimental Result

After observing all the graphs which was developed through the evaluation of the value of three bands of Red, Green, Blue; their mean and gray for each image with their respective concentration, it has been found that the Blue value always follows a decreasing linear trend line and gives a better result in comparison with actual field concentration which have been developed by analysing data by Excel. Though the red values shows a fairly good result of concentrations in comparison with the actual field result but dual nature of the linear trend line (y= mx+c); increasing (m=+ve) for white or decreasing (m= -ve) for grey background color of the tank makes the red value unfit or inappropriate for the measurement of SSC. The equations obtained from the green vs. concentration graphs do not produce results fair enough to compare it with the actual field results. As green and red band values are discarded, for this the equations obtained from graphs of average values of the RGB band against the concentrations are not taken into account. Grey values of the image data which was found from the grayscale by using the Adobe Photoshop software shows an almost or nearly equal values & graphs in accordance with the average values of the RGB band and that is the reason for which gray values are not also being accepted.

Final Result

From the observation of the experimental results, it is clearly visible that the experimental value for the circular shaped white background colour of the tank with brown sediment provides better result of 49.69 mg/l in comparison with the actual field result of 51.84mg/l for the determination of suspended sediment concentration. So, the standard equation of the graph (Blue value of the RGB band against concentration) for the measurement of SSC after the final analysis is, $y = -0.9812 x + 100.46$; [Here, $m = -0.9812$ and $c = 100.46$]. A general equation as well as for the turbidity has been developed for the determination of the suspended sediment concentration after averaging m and c values found from different experimental results and after finishing final analysis the standard equation stands as, $y = 0.340x + 4.499$; [Here, $m = 0.340$ and $c = 4.499$].

The user of this equation should realize that because different technologies and different models of the same technology of turbidity meters can produce significantly different outputs for the same environmental sample, only one manufacturer and model of the turbidity meter can be used to develop the relationship between the SSC and turbidity readings at a site. If a different manufacturer or a different model type of turbidity meter is used, a new relationship will need to be developed for the site. The relationship of SSC and transparency to turbidity across many streams and lakes indicates that 22 NTU is approximately equal to 51.5 mg/L for SSC. However, the relationship between turbidity and SSC can vary greatly in individual streams or even locations within a stream.

MODIFICATIONS

- Only static condition of water was considered.
- All the images were taken from a height of 1 foot. Variations were there only for angular position.
- More correctness would be acquired if light intensity could be maintained constant.
- Settlement occurs as sediments were mixed manually but settlement of sediment can be avoided by the application of mechanical stirrer.

CONCLUDING REMARKS

The conducted study showed that there exists a strong correlation between suspended sediment concentrations with pixel intensity variation of different color components. The developed camera based method of sediment concentration determination produces fairly good comparison with actual concentration measured by mass balance method. The developed technique is very efficient and cost effective compared to the traditional method, hence can be used as a first approximation for suspended sediment concentration.

Table 1: Summary table for experimental result: Equations developed from graphs with variation of camera, tank shape and background color as well as sediment type and color

Tank Shape	Back-ground color	Sediment color	Camera used	Equation for 'Red' Vs. conc.	Equation for 'Green' Vs. conc.	Equation for 'Blue' Vs. conc.	Equation for Gray Vs. conc.	Equation for Avg. Vs. conc.
Circular	White	Brown	DSLR	Y=-0.742x + 98.55	Y=-0.920x + 101.1	Y= -0.981x + 100.4	Y=-0.879x + 101.9	Y=-0.881x + 100.0
Circular	Gray	Gray	DSLR	Y= 1.048x + 83.25	Y=0.507x + 141.8	Y= -0.505x + 130.4	Y= 0.415x + 129.4	Y= 0.350x + 118.5
Circular	Gray	Brown	DSLR	Y=0.479x + 124.5	Y= -0.304x + 146.2	Y= -0.678x + 128.1	Y=-0.139x + 132.7	Y= -0.166x + 132.9
Circular	White	Gray	DSLR	Y=-0.617x + 175.1	Y= -0.686x + 188.5	Y= -0.632x + 168.1	Y=-1.140x + 188.6	Y= -0.678x + 177.8
Square	Gray	Gray	DSLR	Y=1.048x + 83.25	Y=0.507x + 141.8	Y= -0.505x + 130.4	Y= 0.415x + 129.4	Y= 0.350x + 118.5
Square	Gray	Brown	DSLR	Y= 0.471x + 125.3	Y= -0.154x + 152.5	Y= -0.940x + 113.4	Y= 0.061x + 155.3	Y= -0.229x + 131.3
Circular	Gray	Gray	Digital camera	Y= 0.286x + 143.2	Y= -0.068x + 156.2	Y= -0.519x + 132.1	Y=-0.090x + 147.2	Y=-0.101x + 143.9

REFERENCES

Bajestan M. S. and Nouroozpour S. [2007],"Use of image processing technique to estimate sediment concentration," *Journal of Applied Sciences* 7 (20); 3096-3100.

Liew S. C., Lu X. X., Chen P. and Zhou Y. [2002], "Remote Sensing Estimation of Suspended Sediment Concentrations in Highly Turbid Inland River Waters: An Example from the Lower Jinsha Tributary, Yunnan, China".

Lim, H.S., Matjafri M.Z. and Abdullah K. [2003], "Establishing a global algorithm for water quality mapping from multi-dates images," *Proceeding of the Map Asia 2003,Environmental Planning*.

Lodhi M. A., Rundquist D. C., Luoheng Han and Mark S. Kuzila [1998], " Estimation of suspended sediment concentration in water using Integrated surface reflectance," *Geocarto International,* Vol 13, No.2, Hong Kong.

Kean J. W. and Smith J. D. [2006],"Calculation of suspended sediment at gaging stations," *Proceedings of the Eighth Federal Interagency Sedimentation Conference* (8thFISC).

Wang J. J., LU X. X., Zhou Y., Liew S. C. [2012], "Remote Sensing of Suspended Sediment Concentrations in Turbid Rivers: A Field Survey," *Proceedings of Global Geospatial Conference.*

ASSESSMENT OF SALINITY INTRUSION IN THE CENTRAL COASTAL ZONE OF BANGLADESH

M. A. Rahman*, S. A. Saki, F. M. Alvee & A. T. M. H. Zobeyer

Department of Water Resources Engineering, Bangladesh University of Engineering and Technology, Dhaka, Bangladesh
**Corresponding Author: ataur91@gmail.com*

ABSTRACT

The coastal zone of Bangladesh covers about one-third of country's total land area. The coast can be broadly divided into three regions: the deltaic eastern region, the deltaic central region, and the stable deltaic western region. This study aims to assess the salinity intrusion along the central part of the coastal zone – covering Baleshwar River at the west and Karnafuli River at east. One of the most acute problems of our coastal zone is the salinity intrusion and its rapid increasing extent. Extent of saline intruded area is dependent on the sea level and discharge of fresh water through major river systems. Due to the construction of water controlling structures (like dams, barrages etc.) the supply of fresh water is decreasing day by day. Rising of sea level is aggravating the problem. In this study the vulnerability assessment due to saline intrusion in the surface water, groundwater and soil of central coastal zone of Bangladesh during the year 2000 to 2012 has been done. Based on the trend analysis of historical data, salinities have been simulated for the year 2030 and 2050. Moreover, salinity vulnerability maps for the year 2030 and 2050 using 2000 as base year have been prepared using CVI analysis.

INTRODUCTION

The coastal Zone of Bangladesh consists of 147 Upazilas under 19 districts. It covers an area of 47,201 sq. km (Islam, 2004). This area provides shelter, sustenance and livelihood for approximately 46 million people, with 2.85 million hectares of cultivable land supporting 20% of the rice production of Bangladesh (BBS, 2011).In addition to the resources provided by the coastal zone of Bangladesh, the region is also critical because it contains the world's largest mangrove forest, the Sundarbans, which have been set aside for conservation.

One of the major challenges of our coastal zone is the salinity intrusion. Water circulation in the coastal zone in Bangladesh is largely dependent on the factors like fresh water flow from the river, penetration of tide from the Bay of Bengal and the meteorological conditions like low pressure systems, cyclones, and storms surge and wind (MoWR, 2003). Both climatic and anthropogenic factors are responsible for causing salinity in the river water. However, climate induced factors such as sea level rise is the most pressing cause of salinity in coastal areas. The impact of withdrawal of freshwater water from river at any upstream site especially in dry season may cause salinity intrusion in the interior coast. For example after the commissioning of Farakka Barrage on Ganges river and its unilateral diversion of water during dry period has lead to the inward sifting of salinity lines (like1ppt, 5ppt line etc) in the southwestern region of the Bangladesh (Rahman and Alvee, 2015). This change has a significant impact on the ecosystem, social life and economy of the coastal zone. For example, many precious species of Sundarbans can survive within a very narrow range of salinity. Same goes for many water born creatures and crops. Apart from this, some of the coastal regions are already suffering from acute

drinking water problem due to salinity. If the salinity level or the extent of salinity increases further this may lead to serious social impact in those regions.

The objective of the study is to i) assess the historical salinity level of surface water, ground water and soil of the study area, ii) develop scenarios of salinity level of surface water, ground water and soil for the year 2030 and 2050, iii) develop the salinity vulnerability maps for the year 2000, 2030 and 2050. This study is important because if the extent and condition of salinity intrusion is predicted, then it can help the policy makers to plan for countermeasures to address the situation.

STUDY AREA

The area under this study covers the central coastal zone of Bangladesh [Fig. 1]. It consists of 78 Upazilas under 12 districts. The zone is between Baleshwar River at the west to Karnafuli River at the east. The study area covers the districts of Barisal, Bhola, Barguna, Chandpur, Chittagong, Feni, Jhalokati, Lakshmipur, Noakhali, Patuakhali, Pirojpur, Shariatpur totaling an area of about 21475 sq.km (about 46% of total coastal area). There are about 40 major river and channel passes through the area. In addition there are a number of khals. Combined with the rivers and channels they make up a total length of 6378 km. This rivers and channels are very important feature of the area. They plays a vital role of transporting sediment, reduce salinity, navigation and local economy.

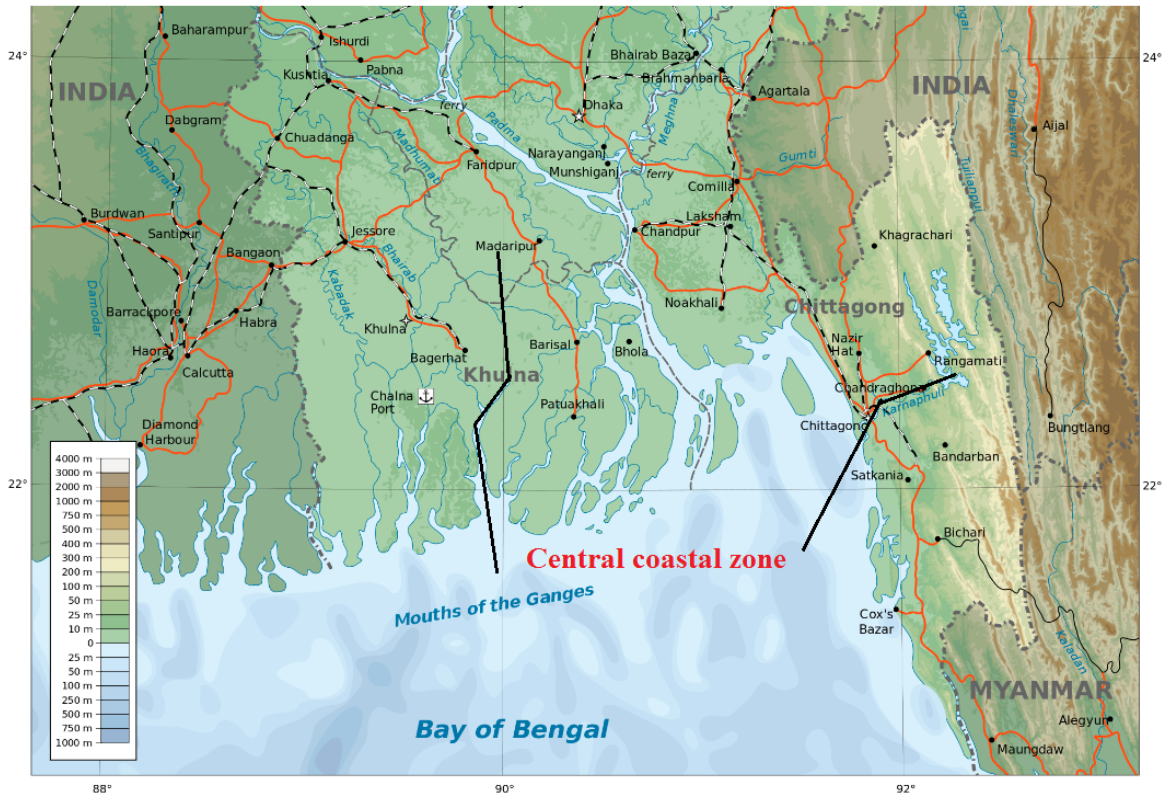

Fig. 1: Study Area: central coastal zone of Bangladesh

METHODOLOGY & DATA COLLECTION

Coastal Vulnerability Assessment towards Sustainable Management of Peninsular Malaysia Coastline has been calculated using coastal vulnerability index (CVI) (Mohamad et al., 2014). The study incorporated six variables to assess the CVI for the study area, which includes geomorphology, shoreline change rate, maximum current speed, maximum tidal range, significant wave height and sea level rise. The ranking is on a linear scale from 1 to 5 in order of increasing vulnerability; value 1 represents the lowest risk ranking assigned to the coastline whereas value 5 ranks the coastline with the highest risk. A total of 1963 km of coastline was evaluated. Vulnerability values of the variables are multiplied and square root of its average value calculates the magnitude of CVI. Similar kind of study

was also conducted on Apodi Mossoro estuary, Northeast Brazil (Boori, 2010). In that study the parameters were geomorphology, shoreline change rate, coastal slope, mean tidal range, mean significant wave height and sea level rise.

Methodology

In this study mainly two softwares were used for the data analysis purpose namely ArcGIS-10.2.2 and Microsoft Excel. At first the study area was extracted from upazila shape file prepared by CEGIS using ArcGIS-10.2.2. Surface water, groundwater and soil salinity were analyzed from the year 2000 to 2012. Using Microsoft excel, general trend of change of those parameter were analyzed. Linear interpolation method was done for assessing the values of 2030 and 2050. All the analyzed data were stored in tabular format under the created shape file. Depending on the intensity of salinity each variable was rated from 1 (least vulnerable) to 5 (most vulnerable). Table 1 shows the detail rating of the salinity parameters.

Table 1: Ratings of the variables for CVI Analysis

Variable No.	Variable name	Ranking of Coastal Vulnerabilities				
		Very low	Low	Moderate	High	Very High
		1	2	3	4	5
a	Surface water salinity (ppt)	0- 1	1-2	2-6	6-10	>10
b	Ground water salinity (ppt)	0- 1	1-2	2-6	6-10	>10
c	Soil salinity (ppt)	0- 1	1-2	2-6	6-10	>10

Then using Eq. (1), coastal vulnerability index (CVI) due to surface water salinity, ground water salinity and soil salinity of year 2000, 2030 and 2050 were calculated.

$$CVI=\sqrt{\{(a\times b\times c)/3\}} \quad \text{----------} \quad (1)$$

Here a= index for surface water salinity, b= index for ground water salinity, c= index for soil salinity. Using the CVI values the vulnerability maps were produced for the year 2000, 2030 and 2050 using ArcGIS-10.2.2.

Data collection

Majority of soil salinity data were collected from Soil Resource Development Institute (SRDI). Rest of the data was taken from PDO-ICZMP report 2005.For surface water and ground water salinity we used data from Bangladesh water Development Board (BWDB) publication and PDO-ICZMP report 2005.

DATA ANALYSIS, RESULTS AND DISCUSSIONS

For soil salinity analysis, data were received from SRDI report of year 2000 and 2009. For the year 2000 both surface water and ground water salinity data were collected from PDO-ICZMP report 2005. Data from Bangladesh water Development Board (BWDB) publication was used for the year 2012. For both cases salinity data for dry season were used. In the case of ground water salinity, salinity values at 30m depth were used.Then using Microsoft excel, trend line was developed [Fig. 2] for each type salinity of each upazila based on the historical data during the period of 2000 to 2012. Then using the CVI equation described earlier, coastal vulnerability index (CVI) for the year 2000, 2030 and 2050 were calculated [Fig. 3].

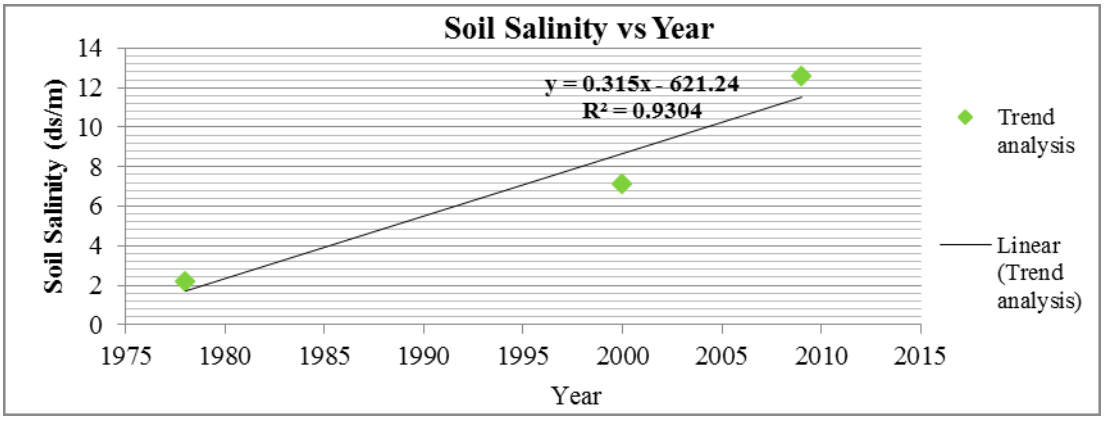

Fig.2: Trend analysis of soil salinity at Patuakhali

O	P	Q	R	S	T	U	V	W	X	Y	Z
GW 00 Index Number	GW 30 Index Number	GW 50 Index Number	SW 00 Index Number	SW 30 Index Number	SW 50 Index Number	Soil 00 Index Number	Soil 30 Index Number	Soil 50 Index Number	CVI 00	CVI 30	CVI 50
1	1	1	1	1	1	2	2	1	0.82	0.82	0.58
1	1	1	1	1	1	1	1	1	0.58	0.58	0.58
2	2	3	2	2	1	1	2	2	1.15	1.63	1.41
1	1	1	1	1	1	2	2	2	0.82	0.82	0.82
2	2	2	1	1	1	1	1	1	0.82	0.82	0.82
1	2	3	1	1	1	2	2	1	0.82	1.15	1.00
1	2	3	1	1	1	1	1	1	0.58	0.82	1.00
2	2	2	1	1	1	1	1	1	0.82	0.82	0.82
1	2	2	1	1	1	1	1	1	0.58	0.82	0.82
1	1	1	1	1	1	2	2	2	0.82	0.82	0.82
1	2	2	1	1	1	2	2	2	0.82	1.15	1.15
2	2	2	2	2	1	2	2	2	1.63	1.63	1.15
1	2	2	1	1	1	1	1	1	0.58	0.82	0.82
1	1	1	1	1	1	1	2	2	0.58	0.82	0.82
2	1	1	4	3	2	2	3	4	2.31	1.73	1.63
2	1	1	1	1	2	1	2	2	0.82	0.82	1.15

Fig.3: CVI Analysis for Salinity (sample calculation)

Salinity maps for surface water, ground water and soil salinity during the year 2000 to 2012 were created using the collected data, which are presented in Fig. 4 and Fig. 5.The predicted salinity values for the year 2030 and 2050, obtained by the trend analysis, are shown in Fig. 6 and Fig. 7 respectively. Using Arc-GIS 10.2.2 CVI index maps for the year 2000, 2030 and 2050 were created based on the CVI values [Fig. 8]. The changes of different vulnerable conditions with respect to the CVI value in different affected areas in central coastal zone in the year 2000, 2030 and 2050 are shown in [Fig.9]. The land areas of central coastal zone under low, medium and high vulnerabilities are found as 62%, 36%, 2% respectively for the year 2000, 61%, 22%, 17% respectively for the year 2030,51%, 24%, 25% respectively for the year 2050. It is very much alarming that highly vulnerable area (based on soil, surface water and ground water salinities) increases by significant amount, which is from 2% to 17% during the period 2000 to 2030 and from 17% to 25% during the period 2030 to 2050.

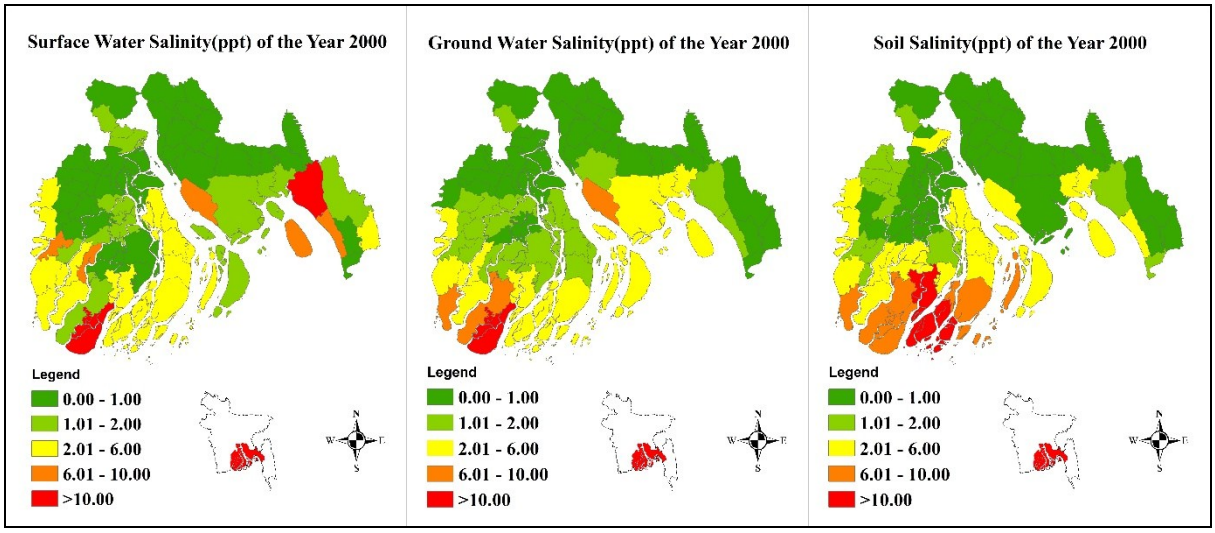

Fig.4: Surface water salinity, ground water salinity and soil salinity for the year 2000

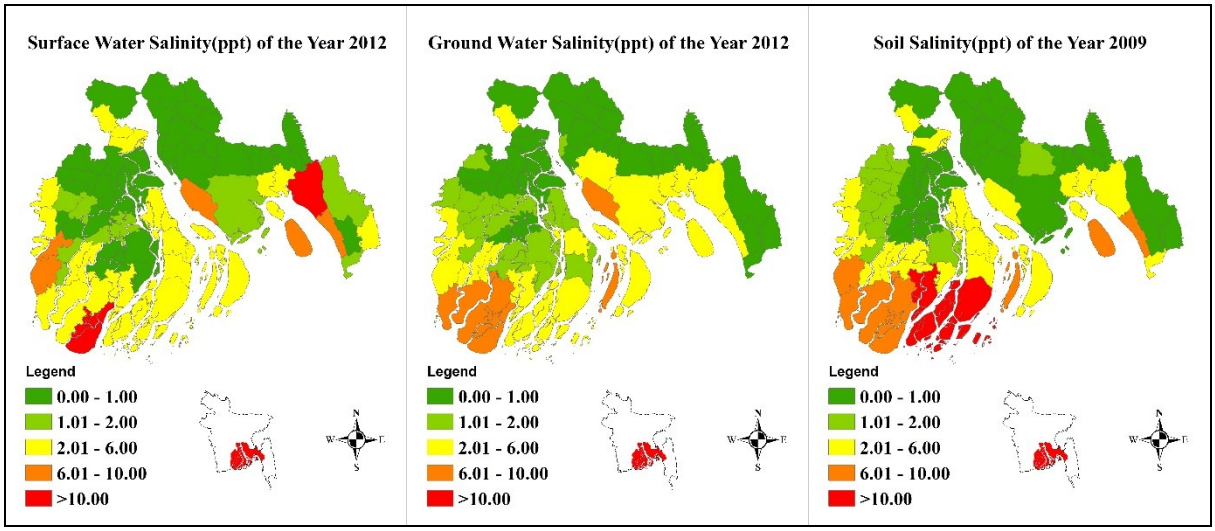

Fig.5: Surface water salinity, ground water salinity 2012 and soil salinity for 2009

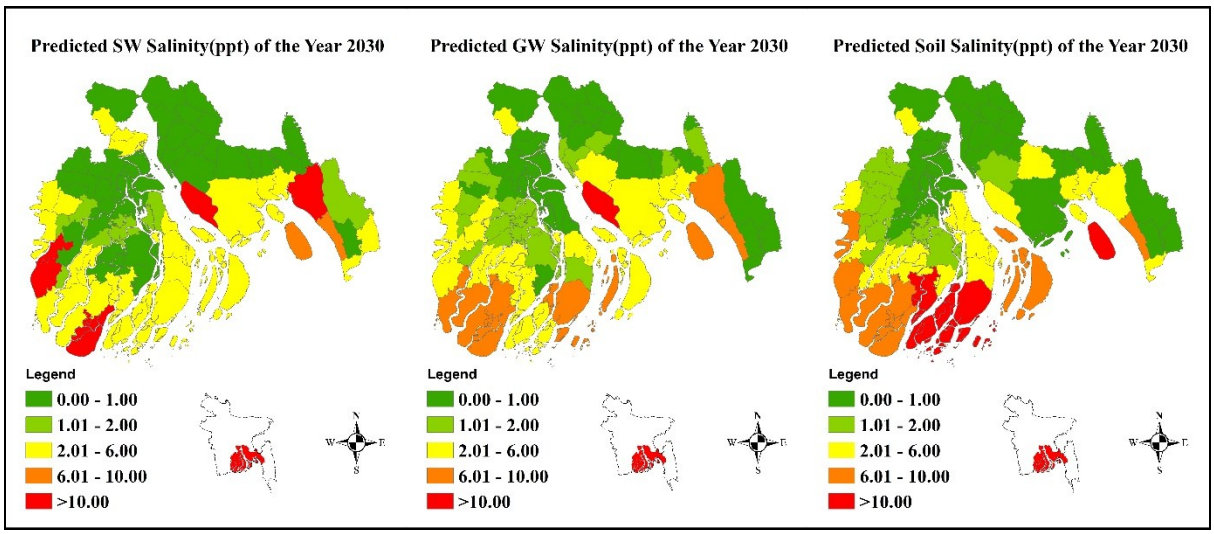

Fig.6: Predicted surface water salinity, ground water salinity and soil salinity for 2030

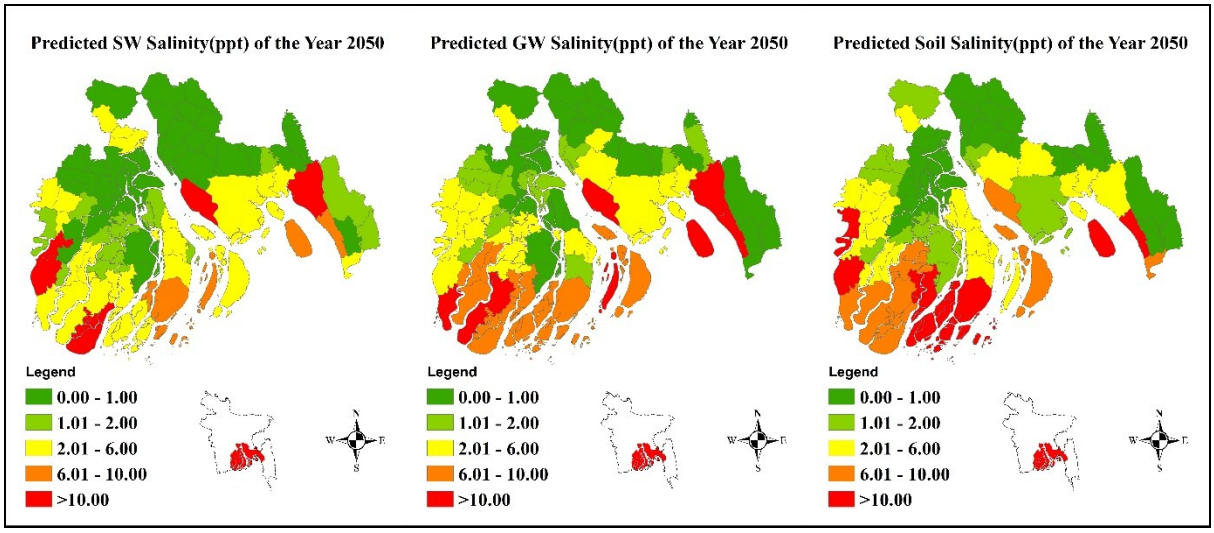

Fig.7: Predicted surface water salinity, ground water salinity and soil salinity for 2050

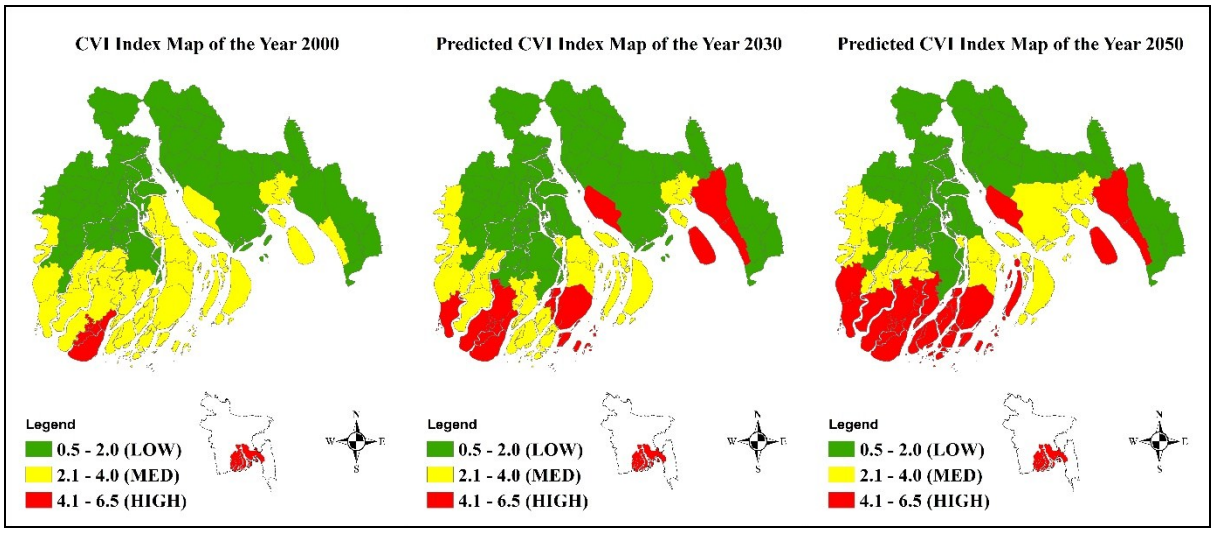

Fig.8: CVI index map for the year 2000, 2030 and 2050

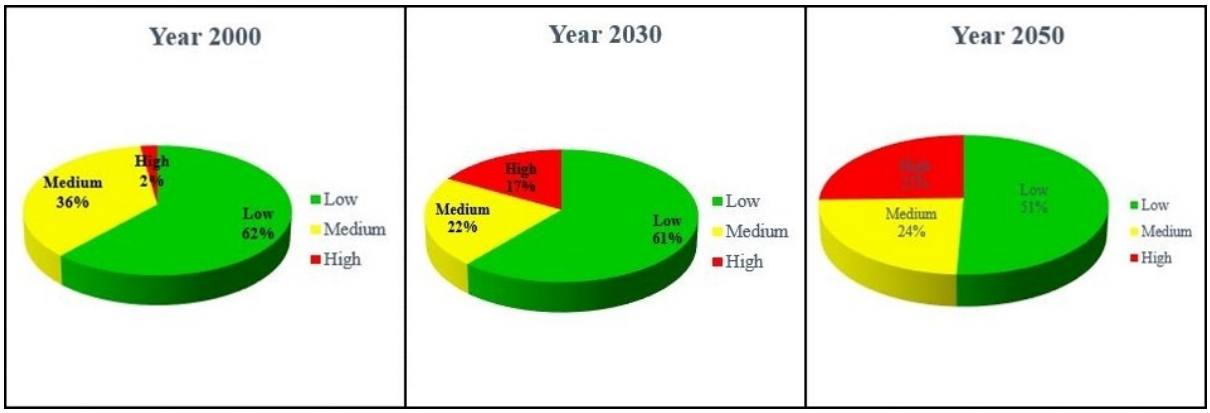

Fig.9: Low, medium and high vulnerable area of central coastal zone based on the CVI values for the year 2000, 2030 and 2050

CONCLUSIONS

Salinities of surface water, ground water and soil in the coastal area are one of the major threats for coastal environment and ecosystem. South-west coastal zone of Bangladesh has been suffering for the salinity intrusion for last few decades. Salinities in the coastal zone of Bangladesh are also increasing. This study investigates the salinity of surface water, groundwater and soil of the central coastal zone of Bangladesh. Historical salinity analysis has been done based on the observed data during the year 2000 to 2012. Trends of the historical changes of salinities are calculated and salinities for the year 2030 and 2050 are simulated following that trends. Observed historical data analysis shows an increasing trend of salinities in the study area. Future scenarios for the year 2030 and 2050 show that around one-fourth of the study area will be under highly vulnerable of salinity. Coastal zone management authorities of Bangladesh should take appropriate measures to overcome the threats of ongoing salinity intrusion and its future alarming incremental effects.

ACKNOWLEDGEMENTS

This research has been funded by the Nuffic-NICHE BGD 155 Project "Scenario development in Integrated Water Resources Management" of Department of Water Resources Engineering (DWRE), BUET. Data has been collected from Soil Resource Development Institute (SRDI) and Bangladesh Water Development Board (BWDB). The authors are grateful to Nuffic, BUET, SRDI and BWDB.

REFERENCES

Bangladesh Bureau of Statistics (BBS)-2011.

Boori, M.S. 2010. Coastal vulnerability, adaptation and risk assessment due to environmental change in Apodi Mossoro estuary, Northeast Brazil.*International Journal of Geomatics and Geosciences*. 1, (3): 620-638.

Islam, M.R. 2004. Living in the coast: Problems, opportunities and challenges. Working Paper WP011, Dhaka, Program Development Office (PDO) and Integrated Coastal Zone Management Plan (ICZMP). pp: 13-15.

Ministry of Water Resources, GoB. 2003. Knowledge Portal on Estuary Development. WP 017 Integrated Coastal Zone Management Plan Project, Dhaka: WARPO and CEGIS.

Mohamad, MF; Lee, LH. and Samion, MKH. 2014. Coastal Vulnerability Assessment towards Sustainable Management of Peninsular Malaysia Coastline.*International Journal of Environmental Science and Development*. 5(6): 533-538.

Program Development Office for Integrated Coastal Zone Management Plan (PDO_ICZMP, 2005), WARPO, Dhaka.

Rahman, MA and Alvee, FM. 2015.Vulnerability Analysis of Central Coastal Zone of Bangladesh. Proceedings of the International Conference on Climate Change and Water Security (ICCWS 2015),held at MIST, Dhaka.

CHALLENGES, VULNERABILITIES AND MANAGEMENT OF COASTAL ZONE AROUND THE WORLD

M. A. Rahman*& P. Das

[1] *Department of Water Resources Engineering, Bangladesh University of Engineering and Technology, Dhaka, Bangladesh*
Corresponding Author: mataur@wre.buet.ac.bd

ABSTRACT
The coastal zone is the interface where the land meets the ocean, encompassing shoreline environments as well as adjacent coastal waters. The high concentration of people in coastal regions has produced many economic benefits. In view of the coastal areas, vulnerability to natural hazards particularly tsunami, storm surge, erosion, salinity intrusion, sea level rise are increasing now a days. Various protection and management measures are carried out against those natural hazards. It is important to explore all the various coastal threats so that coastal managers can take proper mitigation measures. This study is focused on the major challenges and vulnerabilities at some coasts of the world, such as Japan, Netherlands, Vietnam, Sri Lanka and Bangladesh which are greatly affected by the tsunami, storm surge, erosion, cyclone, salinity etc. Management activities to mitigate the challenges by the coastal authorities of those countries have also been investigated. Details of challenges and management of Bangladesh coastal zone have been assessed. Finally some recommendations have been made of the management of the Bangladesh coastal zone.

Keywords: Coastal zone; challenges; vulnerabilities; management

INTRODUCTION
The world coastline extends over 350,000- 1,000,000 km. Within its extent, the coastal ocean and the immediately landward region of the coastal zone displays a wide diversity of geomorphologic types and ecosystems. Overall 38% of the world's population lives within 100 km of the coast or estuaries, and 44% live within 150 km of the coast. The Japanese archipelago consists of almost 4000 islands with a combined coastline of more than 34,000 kilometers (Organization for Economic Cooperation and Development ((OECD) 2002: 136). With a coastline of 3,260 kilometers, excluding islands, Vietnam claims 12 nautical miles (22.2 km; 13.8 mi) as the limit of its territorial waters .Coastline of Sri Lanka is 1,340 km long. Bangladesh has a coastline of approximately 710 km. The objective of the study is to (i) to assess the physical characteristics, resources, challenges and management of coastal zone of Japan, Sri Lanka, Vietnam and Netherlands and Bangladesh, (ii) to recommend the management activities to be improved for Bangladesh coast in light of the study done under objective no.(i).

METHODOLOGY
This study is mainly based on secondary data and published papers the coastal management issues of Japan, Netherland, Sri Lanka, Vietnam and Bangladesh regarding. The threats, challenges and management activities of the coasts of above mentioned countries are thoroughly studied and analysis was done. Secondary data of storm surge, tsunami, sea level rise, erosion on various coasts are used for analysis. This study can help to compare and relate the threats for various coast and their mitigation measures.

Analysis and Results
Japan Coast
Japan is prone to seaborne natural disasters such as typhoon-induced flooding, high waves, tsunamis etc. In addition, Japan's coastline is prone to erosion**.** The map of Japan is presented in Figure 1. Most of Japan is threatened by flooding and high waves during the typhoon season around September. In addition, the country's side facing the Sea of Japan is buffeted by strong winds and rough season the

winter. Storm conditions combined with high tides can cause especially severe damage. High tides in the three major bays of Tokyo, Ise, and Osaka, as well as in the Ariake Straits, can be amplified by storm winds. The worst recorded typhoon-induced damaged was experienced in the Ise Bay Typhoon of 1959 which caused a high tide deflection of 3.4 meters and resulted in more than 5000 deaths and damage to almost one million buildings. Damage caused by flooding has diminished in recent years, but it is unclear whether this is a result of efforts to protect the coastline, or the lack of severe typhoons in recent years. The number of storm surges and its associated death are presented in Figure 6 and Figure 7. Tsunamis are also a source of severe damage and loss of life in Japan. They can hit anywhere in Japan, but they are most common on the Pacific coast. In particular, high energy tsunamis are frequently experienced in the Sanriku region in the northeast part of the main island of Honshu. A 9.0 magnitude earthquake took place on 11th March 2011at the Pacific coast of Tohoku, 231 miles northeast of Tokyo, and caused a tsunami with 30-foot waves that damage several nuclear reactors in the area. The total of confirmed deaths and missing is nearly 22,000, which includes nearly 20,000 deaths from the initial earthquake and tsunami and about 2,000 from post-disaster health conditions.

While typhoon-induced floods and tsunamis cause enormous damage in a short period of time, the most serious damage to coastal areas has been wrought by slow coastal erosion over a long period of time. A wide variety of structures have been built in Japan with the express purpose of preserving coastal areas against the above-discussed problems of typhoon-flooding, tsunamis, and slow coastal erosion. The total length of the coastline in Japan is 34,536 km. Approximately one-half of this total (15,932 km) requires protection again coastal erosion. Structures have been built along about two-thirds (9382) km of this portion. In the 30-year period from 1962 to 1992 protective structures were built on about 4,248 km of coast. While it can be said that the coastline has been protected, it can also be said that the coastline is no longer natural. It is an artificial coastline. Of the protective structures, banks and seawalls were built primarily in the first 10 years of this 30-year period. In the next 10 years, construction of seawalls together with off-shore barriers dominated. In the last 10 years, the focus was primarily on off-shore barriers. This shift in emphasis was due to the fact that banks and seawalls were limited in their ability to stop the effects of rough seas. Off-shore barriers were found to be more effective in controlling rough sea sand coastal beach currents. Japan's first formal coastal zone management scheme was embodied in the Coastal Act of 1953. Its objective was the prevention of disasters. Japan has a nationwide tsunami warning system. The system usually issues the warning minutes after an Earthquake Early Warning (EEW) is issued, should there be expected waves.[5][6] The tsunami warning was issued within 3 minutes with the most serious rating on its warning scale during the 2011 Tohoku earthquake and tsunami. There is a good number of Tsunami shelter along the coastal zone of all over Japan.

Netherlands Coast

55% of the Netherland's area is situated below mean sea level with the deepest points at almost 7 m (Fig 2). Nevertheless, the country is considered safe from flooding by storm surges, coastal erosion and sea level rise. The number of storm surge is presented in Figure 8. In the northern part of the Holland coast (the Province of Noord -Holland) the erosion in the near shore zone is around $0.7x10^6$ m^3/yr and in deep water $0.3x10^6$ m^3/yr. At northern coastal sections sedimentation occurs around $0.9x10^6$ m^3 /yr. In deep water of the southern part of the Holland coast (the Province of Zuid-Holland) erosion occurs $0.6x10^6$ m^3/yr, while the near shore zone is gaining sediment $0.2x10^6$ m^3/yr. Coastal erosion was estimated to occur over 134 km, spread along half of the Dutch coast. In the past, the sea level in the Netherlands rose about 20 centimeters within 100 years, also caused by the subduction of the delta systems. The rising sea level caused and causes local coastal erosion and sediment deposits in mudflats of the North Sea. Recent studies expect the sea level to rise by 20-110 centimeters by 2100, on average by 60 centimeters. The coastline of The Netherlands is 350 km long of which 290 km consists of dunes and

Fig. 1: Map of Japan

Fig. 2: Map of Netherlands

Fig. 3: Map of Sri Lanka

beach flats, while the remaining 60 km is protected by dikes, dams and storm surge barriers. The beaches and shore-face, in fact the foundation of the Dutch coastal zone, almost completely consist of sand. More than half of the coastline is subject to coastal erosion. The remaining part is stable or advancing .The Dutch coast can be divided into three sections, which can be called Delta coast, Holland coast and Wadden coast (Ruig and Hillen 1997). In the Delta area in the Southwest, the coastal zone is dominated by dams, storm surge barriers and drainage sluices, closing off the tidal inlets (technical constructions resulting from the 'Delta plan'). Behind the central part of the coastline, comprising the uninterrupted coastline of the provinces South Netherlands .The sea defense measures guarantee that a storm surge level can be withstood which has a probability of only 1/10000 a year (Ruig and Joost, 1998). Until 1990 coastal defense was directed towards maintaining the defensive structure of the coastline against the sea, and solving only the most acute erosion problems. Dunes and dikes protect parts of the Netherlands which are situated below sea-level.

Sri Lanka coast

Main coastal problem in Sri Lanka (Fig 3) are soil erosion, storm surge and tsunami. The number of storm surges and its associated death are presented in Figure 9 and Figure 10.The impacts of coastal erosion are most severe along the west and southwest coasts. It has been estimated that along the western coastal segment, extending about 685 kilometers from Kalpitiya to the Yale National Park Bay, about 175000 to 285000 square meters of coastal land are lost each year (CCD 11990). Erosion rates vary greatly between different locations, and maximum local retreat rates of around 12 meters/year have been observed in some areas between Mahaoya and Lansigama. The master plan of coastal erosion management is prepared. Structural measures such as beach nourishment, offshore break water and groins are used to minimize erosion and storm surge. Shorelines have had to be protected by the construction of revetments and in some places by groins. Tsunami shelters are built. Numerical modeling is used for warning system.

Vietnam coast

The development of industrial activities, tourism as well as urban expansion in Vietnam (Fig 4) has generally been concentrated in the coastal zone. Urbanization is likely to increase in the coastal zone in the future due to unchecked population growth and human activities (Nagothu, 2005). Main coastal problem in Vietnam are soil erosion, storm surge, tsunami and tropical cyclone. In last fifty years more than 800 storm surges hit in Vietnam. The number of storm surges and its associated death are presented in Figure 11 and Figure 12. Vietnam coast consists of approximately 5,000 km of river dykes and approximately 3,000 km of sea dykes which protect the coast from strong storm surge. The recently built dikes with a reinforced surface provide protection against most waves. These dikes are built with higher crest elevation and are less erosion prone than dikes covered with grass.

Bangladesh coast

Bangladesh has a 710 km coastline connected to Bay of Bengal (Fig 5). Coastal zone is delineated based on the tidal fluctuation, salinity and storm surge risk. Around one-third of country's total

Fig. 4: Map of Vietnam

Fig. 5 Map of Bangladesh

land area belongs to the coastal zone. Major coastal problems in Bangladesh are salinity intrusion, storm surge, erosion, drainage congestion etc. In the last fifty years more than 50 coastal cyclones hit in Bangladesh and more than 800000 people are died. Of the 508 cyclones that have originated in the Bay of Bengal in the last 100 years, 17 percent have hit Bangladesh, amounting to a severe cyclone almost once every three years (Ahamed et al, 2012). Of these, nearly 53 percent have claimed more than five thousand lives. The number of storm surges and its associated death are presented in Figure 13 and Figure 14. Bangladesh would be one of the most victim countries in the world due to global climate change induced sea level rise. A total of 123 flood control polders involving 5,107 km of embankment have been constructed covering approximating 1.5 million ha of the coastal area under the Coastal Embankment Project (CEP). The objective of the polders is to prevent inundation of floodplain agricultural land by saline water during high tide. Cyclone shelters are constructed to provide refuge to the exposed population during storm floods and also intended for multi-purpose use as school and community center. The National Water Management Plan (NWMP) proposes 775 multi-purpose shelters for 1.72 million people and 1,369 killas (raised earth mounds) for livestock over the next 15 years. The Cyclone Preparedness Programme (CPP) is a collaborative effort of the Ministry of Food and Disaster Management and the Bangladesh Red Crescent Society. It is one of the most successful initiatives in early warning in the South-East Asian region, internationally recognized as a "standard of excellence" with a dedicated team of community volunteers living in coastal and offshore island villages. The CPP covers 11 districts in the coastal areas. Volunteers have been trained to play a crucial role in the dissemination of cyclone warnings, evacuation, rescue, first aid, emergency relief and in the usage of radio communication equipment. CPP's 27,600 male and 5,520 female volunteers are the first line of an early warning system to the members of their communities. As an operational wing of the government's disaster management bureau, the CPP provides scheduled daily weather reports via an extensive high frequency (HF) radio transmitting system operated by volunteers throughout the coastal region of Bangladesh. In addition, government has constructed about 2,400 cyclone and flood shelters along its coastal belt. There is still a requirement to construct a further 1,500 shelters to serve 3.56 million people residing in the high risk coasts. Government has also initiated a complimentary disaster preparedness programme to promote community participation in the construction and maintenance of cyclone shelters. Presently, Bangladesh is working on developing a Tsunami Preparedness Programme as an extension to the Cyclone Preparedness Programme.

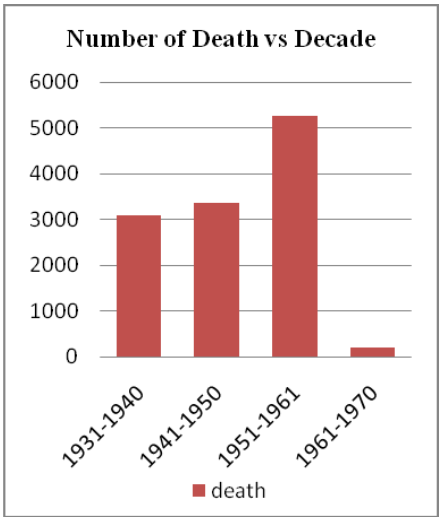

Fig. 6: No. of death due to Strom in Japan

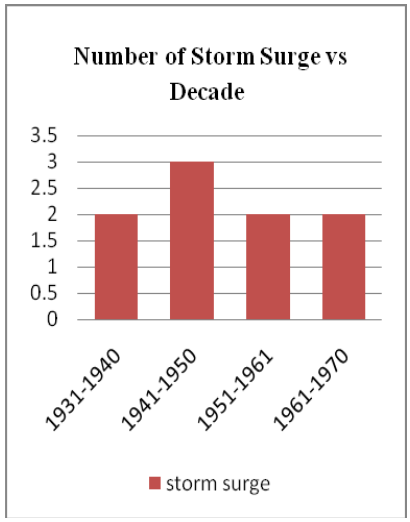

Fig. 7: No. of storm surges in Japan

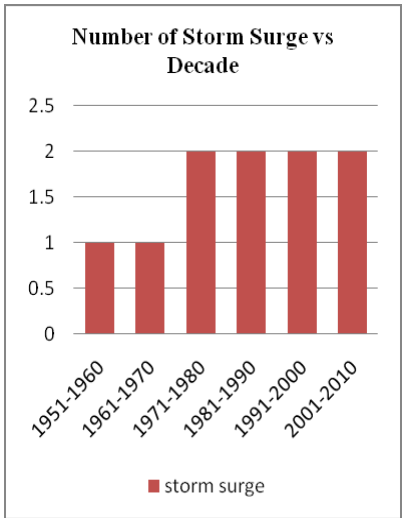

Fig. 8: No. of storm surges in Netherlands

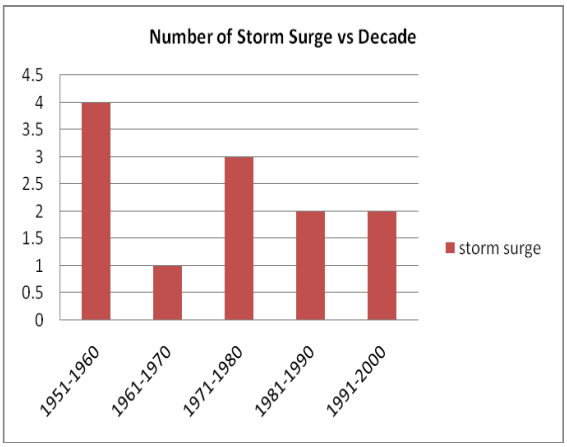

Fig. 9: Number of Storm Surges in Srilanka

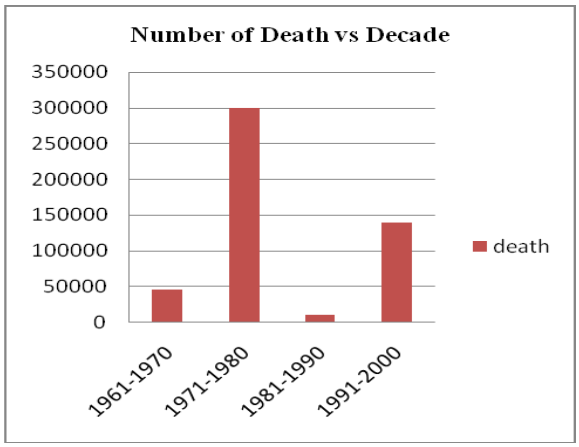

Fig. 10: Number of death due to Storm Surges

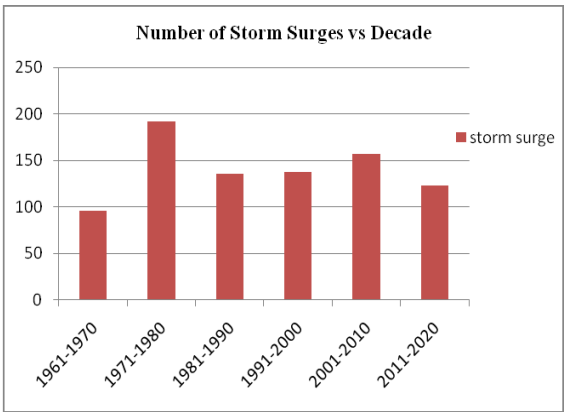

Fig. 11: Number of storm surge in Vietnam

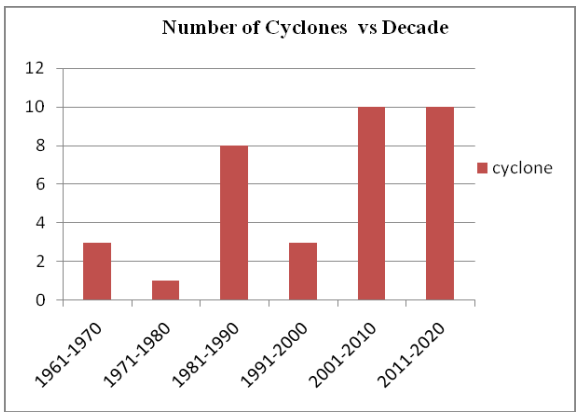

Fig. 12: Number of cyclones in Vietnam

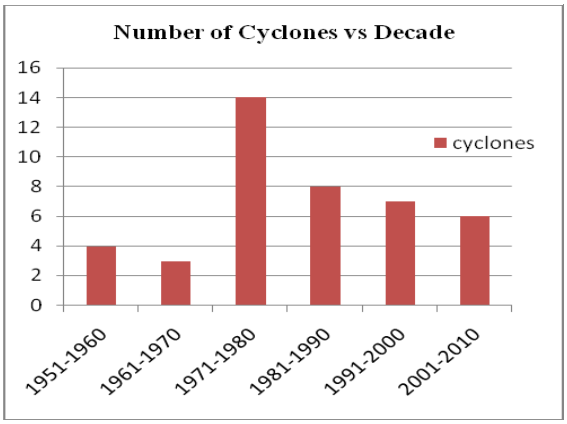

Fig. 13: Number of cyclones in Bangladesh

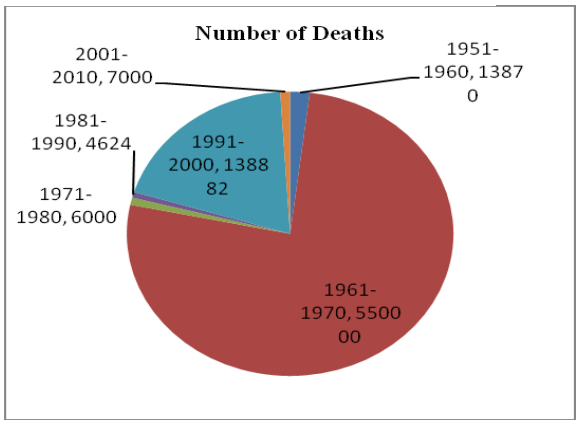

Fig. 14: No. of death due to cyclones in Bangladesh

CONCLUSIONS

Cyclone induced storm surge, tsunami, erosion, sea level rise and salinity intrusion are the major threats along the coastal zone all over the world. Countries like Japan, Netherlands, Vietnam and Sri Lanka are managing the coastal problems through both structural and non-structural measures. Structural measures include hard protection like coastal revetment, sea wall, tsunami wall, breakwater, beach nourishment etc. While non-structural measures include storm surge/tsunami warning system, storm surge/tsunami shelters, evacuation of the people at risk during disaster etc. Integrated Coastal Zone Management (ICZM) plan is being implemented in managing the coastal challenges. The coastal zone of Bangladesh is vulnerable to coastal flooding, salinity intrusion, storm surge, coastal erosion and sea level rise. Over one hundred polders consists of more than five thousand km long embankment have been constructed to obstruct the saline water intrusion during high tides. It also saves the poldered area during the low height storm surges. Storm surge warning system has been developed and cyclone shelters have been constructed along the coastal belt of Bangladesh. A project is now being conducted to study the strengthening the embankment and increasing their height named CEIP (Coastal Embankment Improvement Project). ICZMP has been prepared and some of implementation has been started. However, salinity intrusion and drainage congestion and erosion are major challenges for the managing authorities.

ACKNOWLEDGMENTS

The authors acknowledge the support from the Department of Water Resources Engineering, BUET during this study.

REFERENCES

Ahamed, S; Rahman, MM and Faisal, M.A., 2012. Reducing Cyclone Impacts in the Coastal Areas of Bangladesh: A Case Study of Kalapara Upazila . *Journal of Bangladesh Institute of Planners,* Vol. 5, pp. 185-197.

Coastal Conservation Plan, Srilanka, 1990. Coastal Zone Management Plan

Nagothu, U.S., 2005. Integrated coastal zone management in Vietnam: present potentials and future challenges, *Ocean and Coastal Management* 48 (9-10), 813-827.

Ruig, D., Joost, H.M., 1998.Coastline management in The Netherlands: human use versus natural dynamics. *Journal of Coastal Conservation 4, 127-134.*

Sikder, M.T., 2010. The Impacts of Climate Change on the Coastal Belt of Bangladesh: An Investigation of Risks & Adaptations on Agricultural Sector. *Proc. of International Conference on Environmental Aspects of Bangladesh (ICEAB10).pp. 26-28.*

DRAINAGE VULNERABILITY ANALYSIS FOR A COMBINED SEWERAGE SYSTEM USING SWMM

A. H. Tanim[1] & A. Akter [1, 2*]

[1]*Center for River, Harbor & Landslide Research, Chittagong University of Engineering and Technology, Chittagong, Bangladesh*
[2]*Department of Civil Engineering, Chittagong University of Engineering & Technology, Chittagong, Bangladesh*
[*]*Corresponding Author: aysha_akter@yahoo.com*

ABSTRACT
Proper assessment of heavy rainfall impact on urban water logging has becoming important in growing urban areas in Bangladesh. Chittagong, the second largest city often experiences inundation due to excess runoff results from heavy rainfall and thus affected the adjacent lands of combined sewerage system. Apart from storm induced excess runoff, inadequacy of drainage system and backwater effect pose severe inundation throughout the city. Unfortunately except few scattered study, there is no such database which identify the vulnerable locations both in land surface and in drainage system. The aim of this study is to identify the vulnerable nodes in a selected drainage network and thus to assess capability of existing drainage system. The USEPA Storm Water Management Model (SWMMv5) is a dynamic rainfall-runoff simulation model engaged to simulate this feature. To incorporate relevant information in SWMM environment, Arc-GIS v9.3 was used to provide topographical and land use details. As the SWMM allows for continuous simulations using historical rainfall series, this was applied in the long-term rainfall event to convert the runoff to overland flow. Finally, the model outcomes were able to delineate the inundated node of conduit network, the duration of flood and surcharges and identified the vulnerable location .Thus, it is expected that SWMM model can provide valuable decision to locate drainage vulnerable location for proper drainage management.

Keywords: Heavy rainfall; drainage; SWMM; vulnerable; water logging

INTRODUCTION
The combined sewerage systems in the unplanned urban areas usually get inundated while carrying excess runoff and wastewater. Without proper identification of the vulnerable drain/channel it is difficult to maintain such sewerage system. Moreover this drainage system always faces problem due to solid waste accumulation, forming gullies from adjacent land, excess runoff generated from changing land use pattern of urban areas as well as tidal effect from the adjacent stream(Shoukat et al, 2014). Thus projects for maintenance of the drainage system often prioritized the field survey, subjective judgements and experience; that always results misleading and temporary solution (Rashid et al, 2011). For proper management of drainage system it is always preferable to aviod the preliminary field study cost envolvements, conducting a reasonable numerical modelling study to locate the vulnerable location in the sewerage system. For several decades a number of models developed those can simulate these issues in the drainage system. Rashid et al. (2011) suggested a dynamic programming prioritize sewerage projects under limited funding conditions on the basis of potential environmental, public health, and other benefits relative to the project costs. Wu (2008) worked with stochastic integer programming for liquid waste treatment process design.With the advancement of modeling-based evaluation of satellite precipitation data. Li et al. (2004) has used remote sensing technologies to develop a distributed multi scale model including annual water balance simulation, streamflow modeling, and near real-time flood monitoring. In addition to these a number of urban hydrological models engaged to assess the impact of urbanization on its runoff carrying system. Also, O'Loughlin et al. (1996) attempted to simulate the complete water system at the catchment scale. Hsu et al. (2000) suggested SWMM model for detailed physically based description of conduit for stormwater discharges as this model specially developed for urban hydolgy. Beside the SWMM model, others

generally accepted software for stormwater drainage (and sewers) flow simulations viz. MUSIC (Dotto et al., 2011), InfoWORKS CS (Hurford et al., 2010), MOUSE (Thorndahl and Willems, 2008), and CANOE (Lhomme et al., 2004). In this paper, SWMM model has been used coupling with GIS to identify drain that are overflow during peak discharge of a selected rainfall time series i.e.June 2014 as this duration contained highest rainfall amount in the last 15 years. From the observation of runoff carried volume by drainage network, this can be decided the nodes and links are inundated.

METHODOLOGY

The Study Area

The study area (Figure 1) is located in the north-western part of Chittagong city comprise of a drainage area of 23.14 km^2. Based on the previous study by Shoukat et al. (2014) and also from the preliminary questionnaire survey, this area was selected covering several water logging prone wards i.e., Chadgaon, Panchlaish, West Halishohar and some parts of Bakalia. Based on subcatchment delineation that obtained from HEC-GeoHMS (Spatial tool of Arc-GIS) the boundary of Chittagong City Corporation area was divided into 77 subcatchments and for this study 11 subcatchments were intensively studied. Details on the physical properties of those subcatchments are tabulated on Table 1. It has 4 primary drains which collects runoff from secondary and tertiary drain finally 4 outfalls discharge the runoff to adjacent Karnafuli River (Table 1). The soil formation mainly sandy types however there are silty and clayey soil are also available.

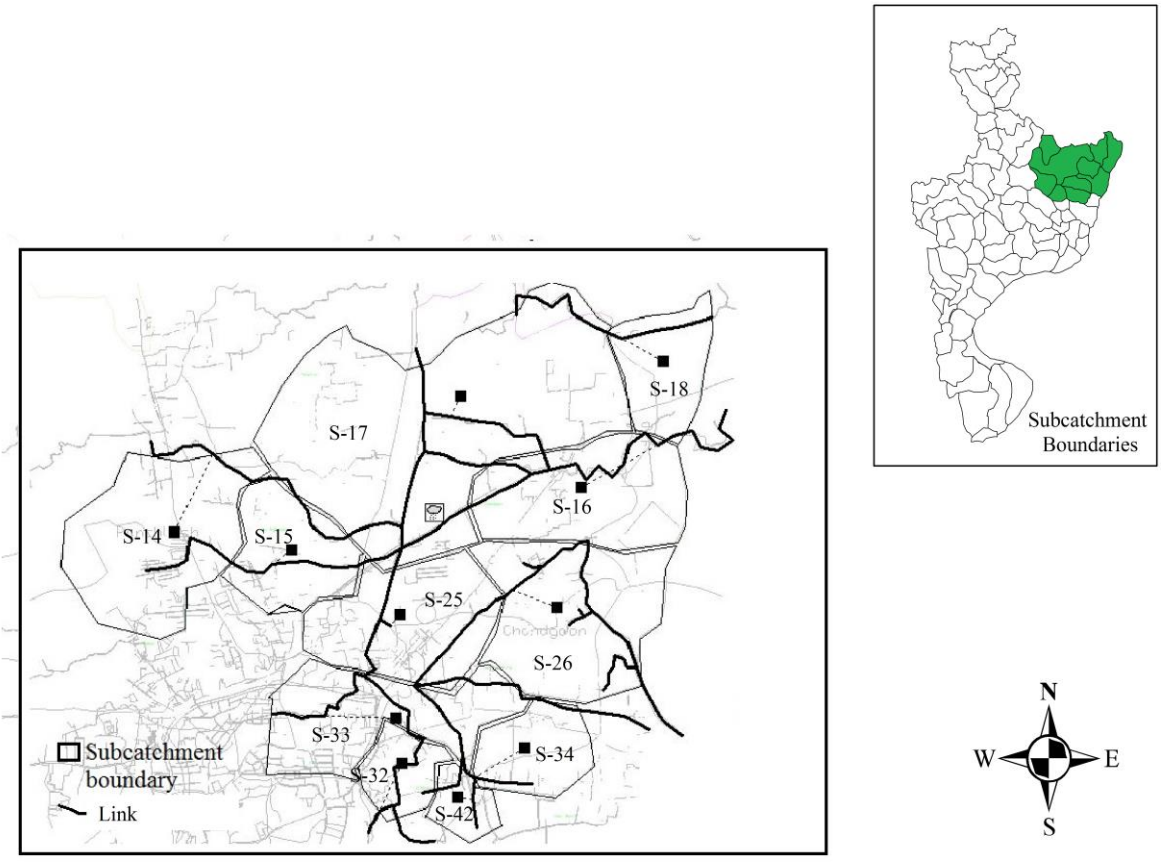

Fig. 1 Study Area

Table 1: Subcatchments Properties

Sub catchment ID	Area(hectare)	Width(m)	% imperviousness	% slope	SCS Curve Number
S-14	285.17	2485	6.84	3.17	46
S-17	667.67	3766	36.67	4.04	77
S-18	114.61	933	28.16	4.41	77
S-15	113.93	1253	16.98	2.98	65
S-16	224.24	1248	54	4.45	65
S-25	210.17	1340	39.64	3.17	66
S-26	273.95	1742	37.32	4.78	77
S-33	207.07	2637	27.44	2.44	65
S-32	62.9	1026	69.78	4.78	65
S-42	41.27	605	57.13	2.92	82
S-34	99.75	950	26.25	3.26	65

Data Collection and Preparation

The topography information was collected from SRTM 30m (http://gdex.cr.usgs.gov/gdex/) DEM data. In addition to these drainage and topography is created from CDA (2006) vector data. As most of channels are not maintained, weeds and brush uncut Manning's roughness coefficient n value ranges from 0.04 to 0.06 (Chow, 1958). Precipitation time series of year 2014 was obtained from Bangladesh Meteorological Department (BMD). Evapotranspiration was calculated using Penman-Monteith Method and Infiltration data was obtained using SCS Curve Number method.

Model Setup

Initially raw SRTM 30m data was used for terrain processing with HEC-GeoHMS terrain pre-processing tool which was used for subcatchment delineation following several steps viz. flow direction grid initialization, flow accumulation grid processing and stream link grid generation. With input stream link and flow direction catchment grid was obtained that converts to catchment vector. The catchment polygon was used further with channel topography to prepare a runoff model environment using Arc-GIS. HEC-GeoRAS channel topography was used for extraction of stream centreline, bank

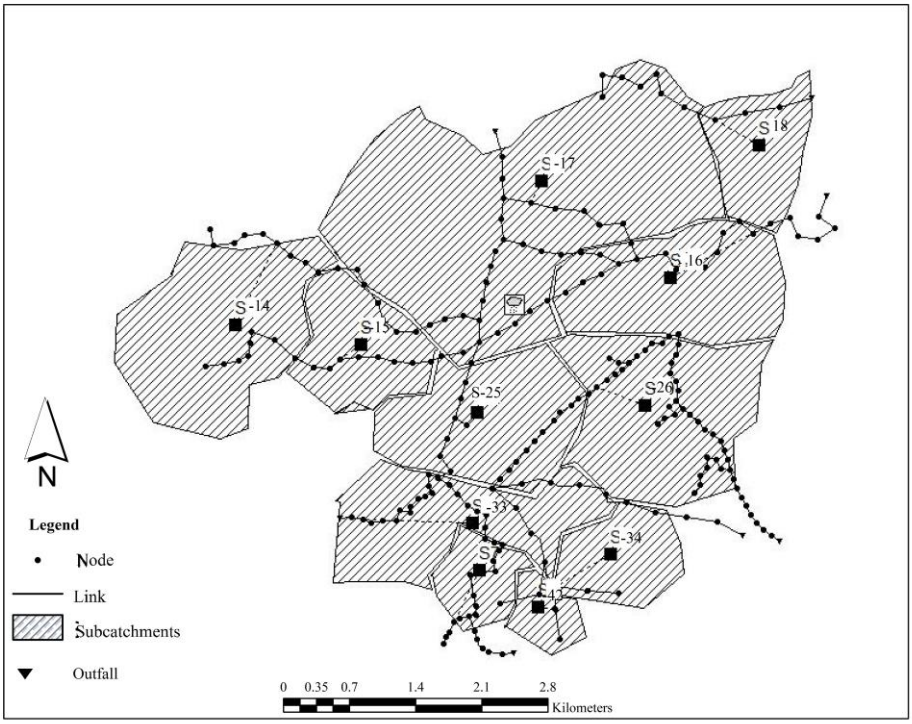

Fig. 2: Model set up

lines and channel cross section. Finally, model geometry was exported to SWMM as metadata which further regenerate in SWMM model environment. The % slope of subcatchments was obtained using spatial analysis of Arc-GIS. Cross sections containing elevation data were positioned and assigned as transects and nodes were placed on each cross sections. SWMM model simulated the runoff response of the catchment area to the given amount and distribution of precipitation over a defined period of time i.e. from 1st May, 2014 to 30th September 2014. The dynamic wave routing method with a time steps of 30s is used for flow routing. A small time step of less than 1 minute is recommended for this method (Rossman 2008). Potenga rain gauge station was used for derivation of rainfall and evaporation time series.

MODEL OUTCOMES

The simulation conducted from 1st May up to 30th September 2014. Considering heavy rainfall amount water logging for 5 days from 19th June to 24th June was simulated in SWMM. Table 2 shows variation of different hydrologic parameter during Month June 2014. Figure 3 shows due to flow direction in runoff discharge was accumulating more in the red zone marked as red (Fig. 3), indicating most vulnerable zone of water logging if links have not enough capacity to drain out the runoff within the capacity of drainage. From simulation results the peak discharge of subcatchment runoff hydrograph observed at 22nd June 2014. The runoff volume exceeding the link capacity (Figure 4 link capacity more than 1 or full) can be marked as inundated. Those drains are identified as most vulnerable majority of those located in Bahadderhat, Muradpur, Sholashahar and Bakalia.

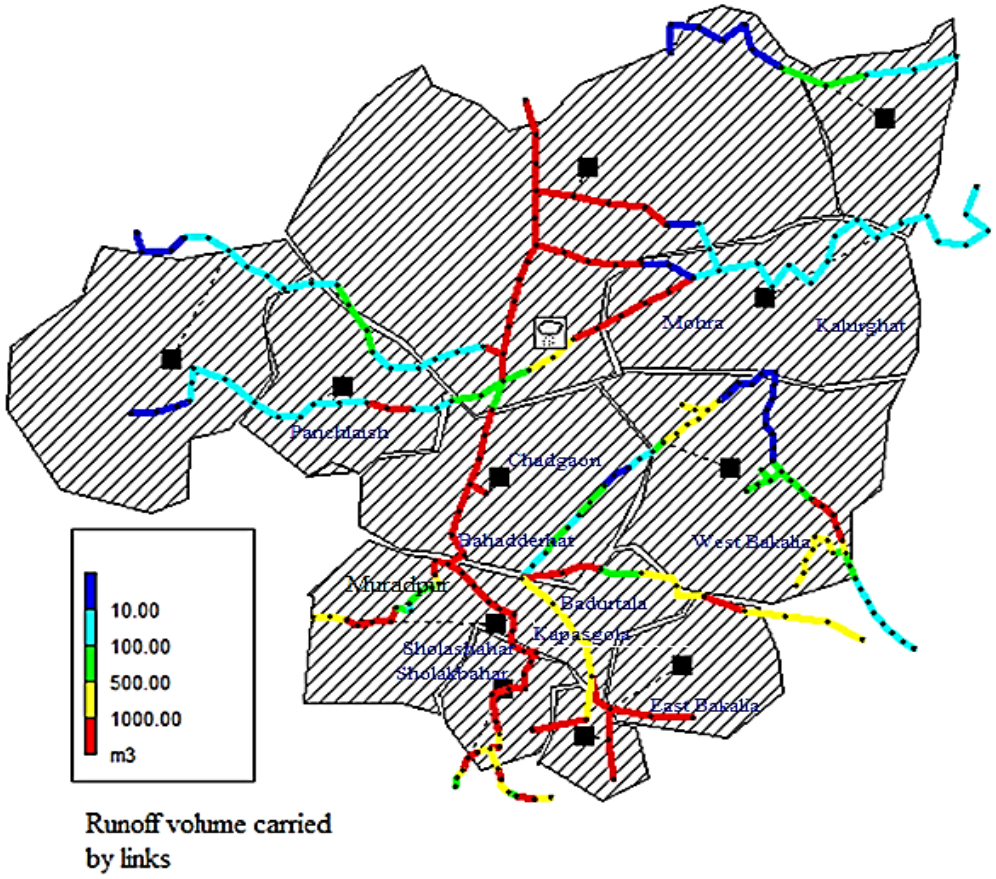

Fig. 3: Runoff volume carried by link network during month June 2014

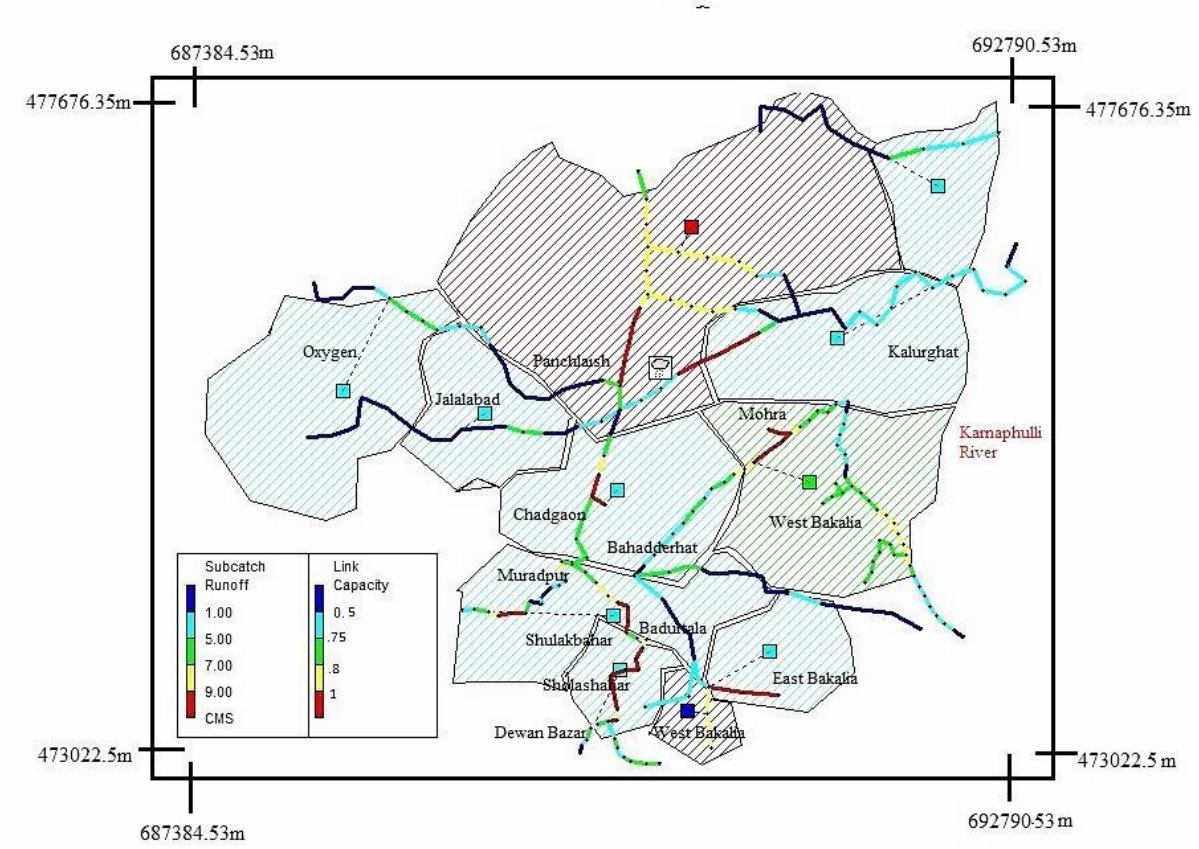

Fig. 4: Vulnerable drain and their location analyzed for water logging 22nd June,2014 (Coordinate system UTM)

Table 2: Sub catchments runoff

Subcatchment ID	Total precipitation (mm)	Total Evaporation (mm)	Infiltration (mm)	Total Runoff (mm)	Total Runoff Volume (Million liter)
S-14	1469.12	101.04	330.91	1035.88	2959.93
S-17	1469.12	104.69	80.09	1284.61	8577.00
S-18	1469.12	102.14	93.31	1275.01	1461.30
S-15	1469.12	102.07	167.96	1198.62	1605.32
S-16	1469.12	102.62	92.94	1274.83	2858.69
S-25	1469.12	103.52	122.12	1243.83	2614.18
S-26	1469.12	103.42	81.41	1285.74	3522.30
S-33	1469.12	99.70	150.04	1221.03	2528.41
S-32	1469.12	93.43	62.43	1315.13	827.22
S-42	1469.12	98.28	43.23	1329.51	548.69
S-34	1469.12	101.01	149.00	1219.24	1216.20

CONCLUSIONS

The continuity error (%) found from model analysis was -0.252%. It is recommended that less than 1% continuity error with a time steps less than one minute has a good acceptance in a terrain. The model consistently indicates that there is little to no direct runoff from pervious areas in the watershed. This was as expected due to the rapid infiltration rates encountered throughout the watershed. These findings demonstrate the importance of the correct handling of storm water runoff from developed areas. New impervious or paved areas cause almost complete runoff of precipitation if uncontrolled and conveyed directly to adjacent streams or water bodies. This results more increased amount may indicate urbanization impact on water logging problem. Special land use features of urban areas in SWMM thus can promote most reliable prediction of flood.

RECOMMENDATIONS

This Paper has outlined a model to predict runoff and base flow for the watershed. In order to fully assess the condition of the watershed regular monitoring should be needed to assess all those parameters like flow at different nodes, depth continuous rainfall recording. Further recommendation enlisted below:

- Required numbers of gages should be placed at necessary places to conduct elaborate study on water logging.
- If USGS High resolution customary 3m DEM is available, this model would provide more accurate outcomes.
- Due to tidal effect at downstream the backwater effect is remarkable, this can be simulated using tidal curves.
- The vulnerable drainage network shown in Figure 4 can be regarded for improvement of drainage facility in Chittagong city areas.

6. ACKNOWLEDGEMENTS

The authors wish to express their sincere gratitude to the Center for River, Harbor and Landslide Research, CUET for providing relevant technical and logistic supports. The authors also owe their profound gratitude to NGO Forum for accelerating the questionnaire survey during 'World Water Day' celebration program.

REFERENCES

Ahmed, S; Mohit, SA and Akter, A. 2014. A Study on water logging reduction in Chittagong City, *Proceedings of the 2nd International Conference on Civil Engineering for Sustainable Development(ICCESD-2014*),107-108.

Chow, VT. 1958. *Open Channel Hydraulics*, McGRAW-HILL Book Company, INC., pp. 108-123.

Dotto, CBS; Kleidorfer, L, Deletic, A; Rauch, W; McCarthy, DT; Fletcher, TD. 2011. Performance and sensitivity of stormwater models using a Bayesian approach and long-term high resolution data. *Environ. Modell. Software*, 26(10), 1225-1239.

Hsu, MH; Chen, SH; Chang, TJ. 2000. Inundation simulation for urban drainage basin with storm sewer system. *J. Hydrol*., 234(1-2), 21-37.

Mitchell, VG; Duncan, H; Inman, M; Rahilly, M; Stewart, J; Vieritz, A; Holt, P; et al. 2007. *State of the art review of integrated urban water models*. Lyon, Frances, 507-514

Hurford, AP; Maksimovic, C; Leitao, JP. 2010. Urban pluvial flooding in Jakarta: applying state-of-the art technology in a data scarce environment. *Water Sci. Technol.*, 62(10), 2246-2255.

Lhomme, J; Bouvier, C; Perrin, JL. 2004. Applying a GIS-based geomorphological routing model in urban catchments. *J. Hydrol*., 299(3-4), 203-216

Li, ZD; Yang, B; Gao, Y; Jiao, Y; Hong, and T. Xu, 2014: Multi-scale Hydrologic Applications of the Latest Satellite Precipitation Products in the Yangtze River Basin using a Distributed Hydrologic Model. *J. Hydrometeor*. doi:10.1175/JHM-D-14-0105.1, in press.

Rashid, MM; PE and Donald F. Hayes, 2011. Dynamic Programming Methodology for Prioritizing Sewerage Projects, *J. Water Resour. Plann. Management*,137(2): 193-204

O'Loughlin, G., Huber, W., Chocat, B., 1996. Rainfall-runoff processes and modelling. *J. Hydraul. Res.*1250, 34(6), 733-751.

Wu, EM. 2002.*Stochastic integer programming analysis for waste water treatment plant design.Management information systems 2002: Incorporating GIS and remote* sensing C. A. Brebbia, ed.,WIT, Southampton, UK, 25-34

Rossman, LA. 2008. SWMM5 Manual Storm Water Management Model. 80

Thorndahl, S and Willems, P. 2008. Probabilistic modelling of overflow, surcharge and flooding in urbandrainage using the first-order reliability method and parameterization of local rain series. *Water Res*.,42(1-2), 455-466.

EFFECTIVE WATER DISTRIBUTION NETWORK FOR CUET CAMPUS

M. H. Kabir*, M. T. Hossain, A. Khair, M. Hassan & M. H. Ali

Department of Civil Engineering, Chittagong University of Engineering and Technology, Chittagong, Bangladesh
**Corresponding Author: humayun_ce@yahoo.com*

ABSTRACT
Chittagong University of Engineering and Technology campus is fully dependent on ground water. The existing water distribution network is unable to fulfil the increasing water demand as per VISION-2020, adding new stuffs, students, teachers, departments, halls, buildings etc. This study aimed at determining future water demand and providing a new effective water distribution system. The present (2016) water demand is 395480 gpd, whereas water demand of CUET campus after 2020 will be 583700 gpd.

Keywords: Ground water; vision 2020; future demand; effective water distribution system

INTRODUCTION
Water is not only the essential element for existence of life but also the symbol of advanced civilization whereas all old civilizations were founded centring water source. But with the increasing of world population useable water demand for life also increasing wherein useable water sources are limited. So now, only any well planned and designed water distribution system can meet the current and future demand with our limited water resources. CUET is a small area with a population of more than 4000. In near future it would be increased to several times and then to meet the water demand with limited resources will be the challenge for civil engineers. Here we proposed a modified water distribution network for future CUET campus of year 2020.

METHODOLOGY
1. Design flow calculation by $Q = \frac{fqPf}{1-0.01w}$ formula.
2. Diameter adjustment by Hazen-Williams formula and other minor losses.
3. Flow adjustment by Hardy Cross method**.**

Table 1: Consumption of water

Nature of consumption	Quantity (gpcd)	Nature of consumption	Quantity (gpcd)
Office building	10-15	Single family houses	35-50
Educational institutions	10-25	Multifamily houses	50-9
Hostels and halls of residence	30-40	Restaurants	0.5-5
Hospitals	130-350	(per person per meal)	
Factories	10-20	Laundries	3-6
		Domestic animals	3-15

(M.A. Aziz, 1975)

Besides, peak factors of water consumption for rural areas, upazilla town, and district headquarter and city corporations are 3,2,2,1.5 respectively.

Zone Wise Water Distribution Network
We divided CUET campus into 12 zones. Each zone consists of a certain number of populations that's why a main outlet required for each zone. To meet every zonal demand we covered all zones under a loop distribution system which contains 15 different loops

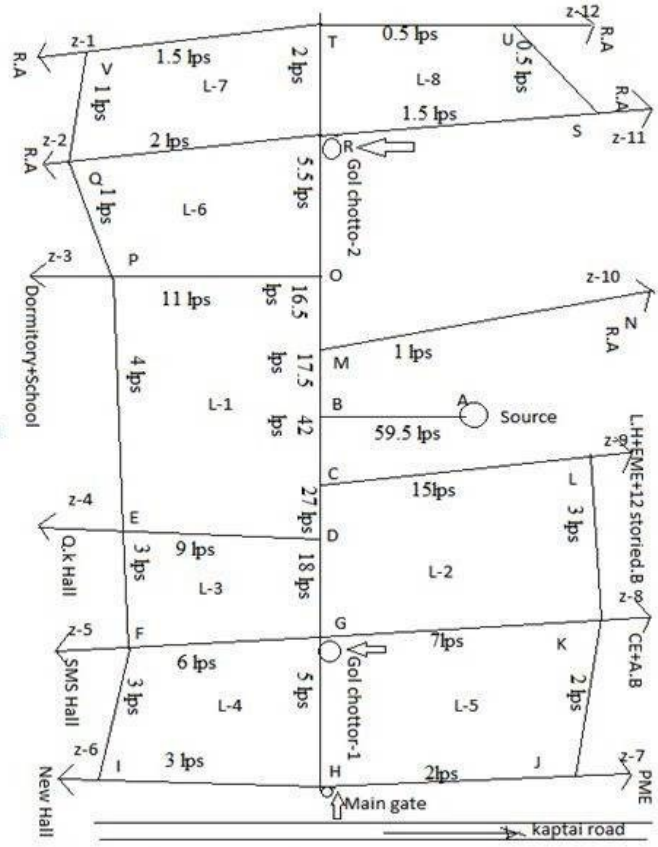

Fig 1: Proposed pipe network of CUET campus (with assumed flow)

Design Flow

$$Q=\frac{fqPf}{1-0.01w}$$ (Feroze, 2000)

Q=peak design flow the water supply distribution system is designed for peak water demand of future population. The Design flow can be computed by using the equation per day,

f=peak factor, q=average water consumption, Pf =design population, w= loss and wastage.

Now this equation can be simplified to calculate design flow in lps (litter per second) from gpd (gallon per day).

$$Q = \frac{2\times A\times 3.785}{(1-0.01\times 10)\times 24\times 3600}$$, A=q Pf

$$= 9.735\times 10^{-5}\times A$$

1 gallon= 3.785 litre, W=Loss=10%, f = 2

Table 2: Sample of design flow calculation for zone-1

Zone	Building	Population	Water requirement	Total demand (gpd)	Design flow (lps)	Design flow(round figure)
Z-1	8 different buildings	450	450×50	22500	2.2	2.5

Similarly; zone-2, zone-3, zone-4, zone-5, zone-6, zone-7, zone-8, zone-9, zone-10, zone-11, zone-12 require the design flow of 2,6,10,6,6,4,8,12,1,1,1 lps respectively.

Adjustment of Diameter by Calculation of Head Loss

Available pressure head at source= 35m.

Allowable head loss in any root=17 m.

Available pressure head at end (for three storied building) =14 m (S.K. Garg)

Available pressure head at end (for five storied building) =20 m (S.K. Garg)

The process of adjustment of diameter is done by method of trial and error. Hazen-William has given a solution of calculating head loss per unit length of pipe. The Hazen-Williams equation can be written as-

$Q=3.7\times10^{-6}C\ D^{2.63}\ (H/L)^{0.54}$

Q=peak flow, D=diameter (mm), H=head loss (m),
L=length of pipe (m), C=roughness co-efficient, H/L= slope= S.
For definite value of C=120 the equation becomes-

$H_f/L=1.59\times10^{6}(Q^{1.85}/D^{4.87})$ (Feroze, 2000)

Major Head loss occur due to friction and can be calculated from this equation as-

$H_f=(H/L)\times L$

The process involved in the design is to make a pipe layout, assume the pipe size and then work out the terminal pressure head which could be made available at the end of each pipe section when discharging peak flow. The available pressure heads are checked to see whether they correspond to permissible residual pressure head, if not the pipe size is changed and then the system is reinvestigated until satisfactory condition are obtained.
There are several minor losses are to be taken into account such as-

Loss at entrance- $h_{en}=\frac{0.5v^2}{2g}=0.025v^2=0.041\frac{Q^2}{D^4}$, (Khurmi, 2003)

Here, v,g,Q,D are the velocity at entrance point, gravitational acceleration, discharge and Pipe diameter respectively.

Loss at exit- $h_{ex}=\frac{v^2}{2g}=0.051\ v^2=0.0823\frac{Q^2}{D^4}$, (Khurmi, 2003)

Here, v,g,Q,D are the velocity at exit point, gravitational acceleration, discharge and Pipe diameter respectively.

Loss for contraction- $h_c=k_L\frac{v^2}{2g}=0.051\ k_L\frac{Q^2}{D^4}$, k_L= 0.1-0.45, (khurmi, 2003)

Fig: pipe suddenly contracted

Consider a liquid flowing in a pipe having a sudden contraction in 2-2
Let, D1= diameter of section 1-1
D2= diameter at section 2-2

Losses of head due to sudden contraction, $h_c=\underline{k_L}\frac{v^2}{2g}$

The constant $\underline{K_L}$ depends upon the ratio D1/D2.

D1/D2	1	1.1	1.25	1.5	2	2.5	3	3.5	4
kL	0	0.1	0.19	0.28	0.375	0.4	0.42	0.43	0.45

Loss due to sudden enlargement- (Borda-Carnot equation)

$h_{el}=\frac{(v_1-v_2)^2}{2g}=0.051\ (v_1-v_2)^2=0.082\ (\frac{Q_1}{Q_1^2}-\frac{Q_2}{Q_2^2})^2$, (Khurmi, 2003)

Where v_1, v_2 are the velocities and Q_1, Q_2 are the discharges on the two sides of the section in where sudden enlargement occurs.

Loss due to bending (only for T-junction)

$h_b = 0.2 \frac{v^2}{2g} = 0.016 \frac{Q^2}{D^4}$, (Munson, Young, SI version)

Table 3: Sample of Trial for Loop-1(BCDEPOMB) to Adjust Pipe Diameter

Loop	Pipe	Q	D	L	H_f/L	H_f	h_{en}	h_{ex}	h_c	h_{el}	h_b	H_t	Δ
	BC(+)	42	160	128	0.029	3.78	0.11	0.22	0	0	0.04	4.15	0.13
	CD(+)	27	160	134	0.013	1.75	0.046	0.09	0	0	0	1.88	
L-1	DE(+)	9	110	110	0.0106	1.17	0.023	0.05	0.013	0	0.009	1.25	
	BM(-)	17.5	160	76	0.0058	0.44	0.019	0.04		0	0.007	0.51	
	MO(-)	16.5	160	30	0.0052	0.16	0.017	0.03		0	0	0.21	
	OP(-)	11	110	140	0.0154	2.15	0.034	0.07	0.019		0.013	2.29	
	PE(-)	4	80	368	0.0111	4.1	0.016	0.03	0.009	0.001	0.006	4.17	

Terminal Pressure at Various Points

At point A, assumed pressure where the source located is 35 m. Same as pressure at other points from B to I we can get by deducting head loss from pressure available at previous point. For an example at point A, the available pressure is 35 m and when water travel through AB path then it get total head loss 4.97.So the available pressure at point B is 35-4.97=30.03. Same as R=29.31-1.55=27.76, S=27.76-0.549=27.21,C=30.03-4.155=25.87, D=25.87-1.88=23.9, T=27.76-0.601=27.16, U=27.16-0.264=26.9, E=23.9-1.25=22.75, F=22.75-0.698=22.05, Q=27.03-0.518=26.5, V=26.5-0.77=25.74, G=23.9-0.45=23.45, H=23.45-2.043=21.40, O=29.52-0.209=29.31, P=29.31-2.28=27.03, I=21.40-0.825=20.5, J=21.4-1.66=19.74, K=23.45-3.807=19.643, L=25.87-4.346=21.52, M=30.03-0.509=29.52, N=29.52-1.213=28.3 m.

- All terminal residual pressures are between the limit of available pressure>18m. (S.K. Garg)

Flow Adjustment

The determination of probable flow in each pipe in a pipe network requires complicated and tedious trial and error solutions. In any looped pipe network two conditions must be satisfied.

- ❖ The flow entering a junction must equal the flow leaving it.
- ❖ The algebraic sum of the pressure drop (head loss) around any closed loop must be zero.

Hardy- Cross developed a method of successive approximation in which the circuits are balanced, distribution of flow is determined and the above two conditions of flow are satisfied.
According to Hardy-Cross-

$$\Delta_c = \frac{\sum H}{x \times \sum \frac{H}{Q}}$$ here, $\sum H$=sum of head loss and x=1.85

Sample of Trial for Adjustment of Flow

Table 4: LOOP-1(BCDEPOMB)

Loop	pipe	Q_1	D	L	H_f/L	H_f	h_{en}	h_{ex}	h_c	h_{el}	h_b	H_t	H_t/Q	Δc	Q_2
	BC(+)	41.96	160	128	0.0295	3.77	0.11	0.22	0	0	0.043	4.148	0.099	0	41.96
	CD(+)	27.03	160	134	0.0131	1.75	0.046	0.09	0	0	0	1.889	0.07	0	27.03
	DE(+)	8.95	110	110	0.0105	1.15	0.022	0.05	0.013	0	0.009	1.242	0.139	0	8.95
L-1														0	
	BM(-)	17.54	160	76	0.0059	0.45	0.019	0.04		0	0.008	0.512	0.029	0	-17.54
	MO(-)	16.54	160	30	0.0053	0.16	0.017	0.03		0	0	0.21	0.013	0	-16.54
	OP(-)	11.15	110	140	0.0157	2.2	0.035	0.07	0.02		0.014	2.343	0.21	0	-11.15
	PE(-)	4.04	80	368	0.0114	4.18	0.016	0.03	0.009	0.001	0.006	4.244	1.05	0	-4.04
Δ c= 0.0096(negligible)											∑	-0.03	1.61		

RESULT AND DISCUSSION

As per our calculation shown as sample templates in previous discussion, we got our required flows as well as adjusted diameters of pipes presented in the table below for different zones.

Pipe	Length (m)	Adjusted diameter (mm)	Adjusted flow (lps)		Pipe	Length (m)	Adjusted diameter (mm)	Adjusted flow (lps)
AB	75	160	59.5		HI	121	80	2.95
BC	128	160	41.96		FI	190	80	3.05
CD	134	160	27.03		KJ	198	90	1.88
DE	110	110	8.95		HJ	210	70	2.12
BM	76	160	17.54		PQ	145	60	1.11
MO	30	160	16.54		OR	222	100	5.39
OP	140	110	11.15		RQ	266	70	1.93
PE	368	80	4.04		QV	220	60	1.04
CL	349	130	14.88		RT	190	80	1.99
LK	302	80	2.88		TV	220	60	1.46
DG	64	160	18.08		RS	298	80	1.47
GK	352	100	7		SU	185	50	0.47
EF	100	100	3.02		TU	110	50	0.53
FG	105	90	6.04		MN	345	60	1
GH	210	90	5.07					

Here we like to mention that we tried to present a sample of outline for simple water distribution network in where water transmission depends on gravity flow only and whole territory is almost flat. But our CUET campus is not totally flat through its whole territory so pumping system might have been adopted in some outlet points located too high than our assumed elevation.

CONCLUSIONS

CUET is located at Raojan thana under Chittagong district which is about 25km away from city corporation area. Its water supply system is totally relied on ground water. In this campus, present water demand (2016) is 395480 gpd and as per vision 2020 future demand is 583700 gpd. Due to different losses present distribution system can't provide water in each point with required pressure and amount as well as future demand cannot be satisfied for improper pipe dimension. Only a new proper designed water distribution system oriented by all necessary data and measurement can fulfil the water demand aroused for vision 2020 project. In this circumstance our proposal of effective water distribution system if adopted with real features and required measures then it can solve all future problems engaged with water distribution system.

ACKNOWLEDGEMENT

Praise to Allah, for giving us ability, patience, knowledge for completion this work. The authors wish to express their sincere gratitude to their supervisor Dr. Md. Hazrat Ali, Professor, Department of Civil Engineering, Chittagong University of Engineering and Technology (CUET), for his academic advices direction and constant encouragement to the work. We would like to express our gratitude to all the teachers and stuffs of the department also.

BIBLIOGRAPHY

S. Khurmi, edition: 2003, A Text Book of Hydraulics, Fluid Mechanics and Hudraulic Machinesr, S. Chand & Company Ltd.

M.A. Aziz, copyright 1975, A Textbook of Water Supply Engineering, Hafiz Book Centre Dacca.

M. Feroze Ahmed, Md. Mujibur Rahman, First Edition: June, 2000, Water Supply & Sanitation, ITN-Bangladesh

Bruce R. Munson,Donald F. Young, Theodore H Okiishi, Wade W. Huebsch, Sixth Edition, Fundamentals Of Fluid Mechanics- Copyright @2010 By John Wiley & Sons, Inc, U.K

S. K. Garg. 3rd edition (1984), Water Supply Engineering- Khanna Publishers.

ANALYSIS OF SATELLITE BASED EVAPOTRANSPIRATION FOR SELECTED CLIMATE STATIONS OF BANGLADESH

M. S. Basir[1*], N. Jahan[2] & S. Halder[1]

[1]*Department of Civil and Water Resources Engineering, Chittagong University of Engineering and Technology, Chittagong, Bangladesh*
[2]*Department Water Resources Engineering, Bangladesh University of Engineering and Technology, Dhaka, Bangladesh*
[*]*Corresponding Author: samiunbasirbuet@gmail.com*

ABSTRACT
Evapotranspiration (ET) is one of the important components of hydrological cycle. An accurate estimation of ET is of vital importance in planning, designing and operation of irrigation and water resources system. However it is difficult to measure ET directly. In this study, the usefulness of evapotranspiration product from the Moderate Resolution Imaging Spectroradiometer (MODIS) was assessed. For this purpose, several meteorological data of temperature, humidity, sunshine hour, wind speed of Rajshahi, Bogra and Rangpur climate stations were collected from Bangladesh Meteorological Department (BMD) to estimate evapotranspiration. Daily reference evapotranspiration (ET_0) was calculated by using FAO Penman-Monteith (P-M) method then converted into eight days cumulative ET_0. MODIS evaptranspiration product (MOD16) was collected from the Oak Ridge National Laboratory. Then the Eight days cumulative ET from the P-M method was compared with the eight days MOD16 products over a period 10 years from 2001 to 2010. This comparison shows that the MODIS ET values match well with the actual ET values throughout the year except for Kharif-I (March to June) season. This study also demonstrates that MODIS Enhanced Vegetation Index (EVI) can be used as a useful predictor of evapotranspiration. From the results it is found that EVI values are very small (around 0.2 to 0.3) in Kharif-I (March to June) season, which indicates very little vegetation. So it is noticed that, excluding Kharif-I (March to June) season, comparison shows a significant relation between Penman ET and Satellite ET.

Keywords: Evapotranspiration; Penman-Monteith method; Enhanced Vegetation Index (EVI); Moderate Resolution Imaging Spectroradiometer (MODIS); MOD16

INTRODUCTION
Apart from precipitation, the most significant component of the hydrologic budget is evapotranspiration. Evapotranspiration varies regionally and seasonally according to ambient environmental conditions, such as climate condition, land cover, land use, soil moisture, and available radiation etc. Because of this variability, research for integrate water resources modelling, dynamic crop-weather modelling and drought monitoring, a thorough understanding of the evapotranspiration process and knowledge about the evapotranspiration is needed. As precipitation falls and soaks into the soil, a plant absorbs it and then transpires it through its leaves, stem, flowers, and/or roots. When this is combined with the evaporation of moisture that was not directly absorbed by the soil, a significant amount of water vapor is returned to the atmosphere. Through evapotranspiration and the hydrologic cycle, forests or other heavily wooded areas typically reduce a location's water yield. Knowledge of evapotranspiration is important for irrigation scheduling but it is also an important factor for other land use applications such as septic tank drain fields, water shed water budgeting, and climate and weather models. ET can be used as a historical tool but usually it is predicted or used in a forecast to help irrigators optimize irrigation.
Evapotranspiration calculations based on the remote sensing data have been developed rapidly for the last 20 years, and several methods have been adopted by different research groups and used in related study

area successfully. By far, we got no information on any undertaken research on MODIS product (MOD16) in Bangladesh yet. So in this study we tried to make comparison between this MODIS product (MODIS ET) and actual ET so as to determine the appropriateness of using this MODIS product. The great advantage of satellite based evapotranspiration is that where there is no climate stations, satellite image gives us evapotranspiration data of this place. Satellite image gives continuous data of any place and it is low cost and easily accessible.

Objectives of the Study

The main objective is to analyze the evapotranspirtaion for selected climate stations of Bangladesh through combination of remotely sensing and meteorological observations. The specific objectives are given below:

- To calculate the evapotranspiration from the climate data for selected climate stations of Bangladesh using Penman-Monteith method.
- To extract the evapotranspiration data from the MODIS satellite for the same climate stations.
- To compare the evapotranspirations from Penman-Monteith method and satellite based method.
- To assess the possibility to improve the satellite based evapotranspiration estimation.

Study Area

The study area is the divisional climate stations of Bangladesh. Rajshahi, Bogra, Rangpur are the climate stations under this study area. Latitude, Longitude and elevation above mean sea level of each station are given in the Table 1.

Table 1: Latitude, Longitude, and Elevation of the selected study area

Station Name	Latitude	Longitude	Elevation (Above mean sea level)
Rajshahi	24°22'N	88°40'E	23m
Bogra	24°51'N	89°22'E	26m
Rangpur	25°42'N	89°22'E	36m

METHODOLOGY AND DATA

Meteorological data of selected climate stations were collected from Bangladesh Meteorological Department (BMD). Daily data of the following variables are collected from BMD for the period of 2001 to 2010: i) Minimum Temperature, ii) Maximum Temperature, iii) Relative Humidity, iv) Sunshine hours, v) Incoming Solar Radiation, vi) Wind Speed, and vii) Wind Direction

MODIS satellite images acquired by TERRA instrument is used. For each climate stations evapotranspiration data has been downloaded from the Oak Ridge National Laboratory (ORNL) during the periods of 2001 to 2010. The resolution of the satellite data is 1 km. For the validation purpose Enhance Vegetation Indices (EVI) data also download from the Oak Ridge National Laboratory (ORNL) during the same periods of 2001 to 2010.

Meteorological Data Processing

The FAO Penman-Monteith method is maintained as the sole standard method for the computation of ET_o from meteorological data. Equation [1] is used for calculating ET_o from meteorological data.

$$ET_0 = \frac{0.408\Delta(R_n - G) + \gamma\frac{900}{T+273}u_2(e_s - e_a)}{\Delta + \gamma(1 + .34u_2)} \quad (1)$$

Where

$ET_{o=}$ reference evapotranspiration [mm day^{-1}], R_n =net radiation at the crop surface [MJ m^{-2} day^{-1}], G =soil heat flux density [MJ m^{-2} day^{-1}], T =mean daily air temperature at 2 m height [°C], u_2 =wind speed at 2 m height [m s^{-1}], e_s =saturation vapour pressure [kPa], $e_{a=}$ actual vapour pressure [kPa], e_s -e_a =saturation vapour pressure deficit [kPa], D =slope vapour pressure curve [kPa $°C^{-1}$] g=psychrometric constant [kPa $°C^{-1}$]

RESULTS AND DISCUSSIONS

The focus of this study is on the comparison of satellite (MODIS) and actual (Penman-Monteith) ET. For this the time series of actual and satellite ET for Rajshahi station has been plotted during periods of 2001 to 2010 [Fig. 1]. As MODIS satellite provides ET per 8 day so the daily penman ET has been converted into 8 day basis.

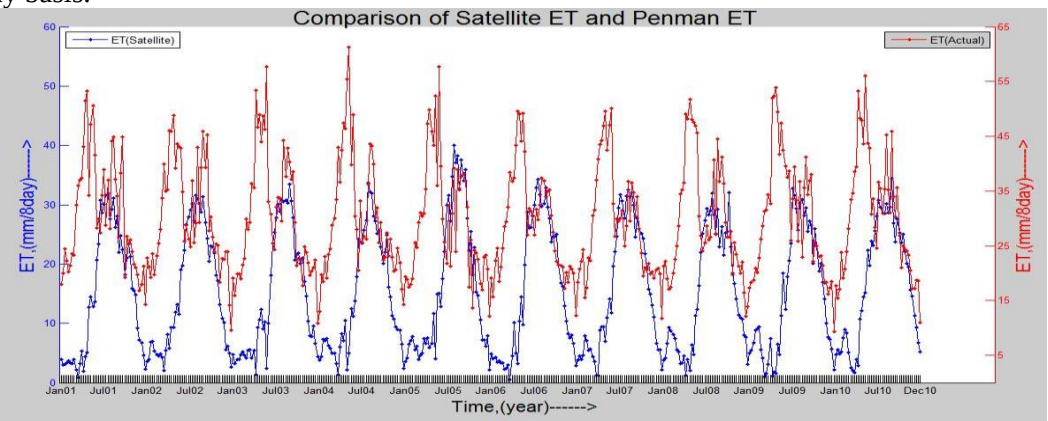

Fig. 1: Comparison of satellite and actual ET of Rajshahi station

From the time series plot it is observed that MODIS ET always lowers than the Penman (Actual) ET [Fig. 1]. At the beginning of the year MODIS gives very low ET when actual ET is high.

In this study the time series of satellite and actual ET of Bogra and Rangpur stations has been also plotted to compare with each other throughout the year of that area. It is noticed that Bogra and Rangpur stations also follows similar pattern of comparison [Fig.2].

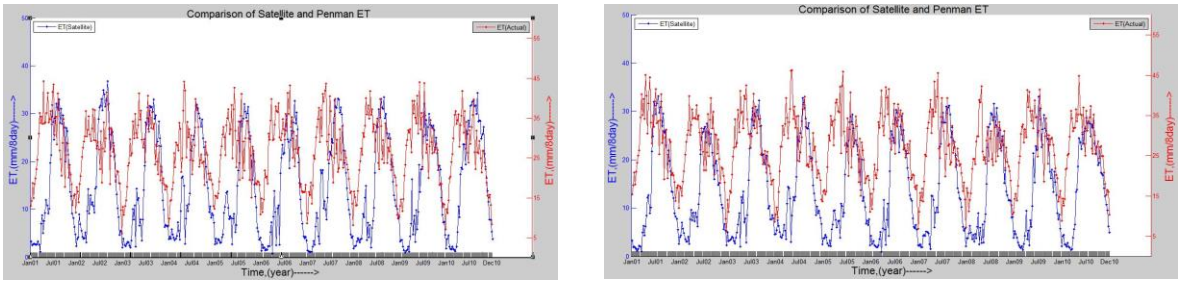

Bogra Rangpur

Fig. 2: Comparison of satellite and actual ET

Comparison of Satellite and Actual ET in Kharif-II Season

As the whole cycle does not match, it has been tried to find out the comparison season by season. As far as it is understand that the study area may be cultivated with one crop and it was Kharif-II (July to October). In the Kharif-II (July to October) season, comparison gives very good correlation. In this season actual ET gives very close value with satellite ET. When green vegetation present in the field they provide good correlation than the other period. It is observed that correlation between satellite and actual ET is 0.138 in the Kharif-II season [Fig. 3]. Also the observed root mean square error is 4.37 mm/8day. Other stations i.e Bogra, Rangpur also gives similar pattern of result.

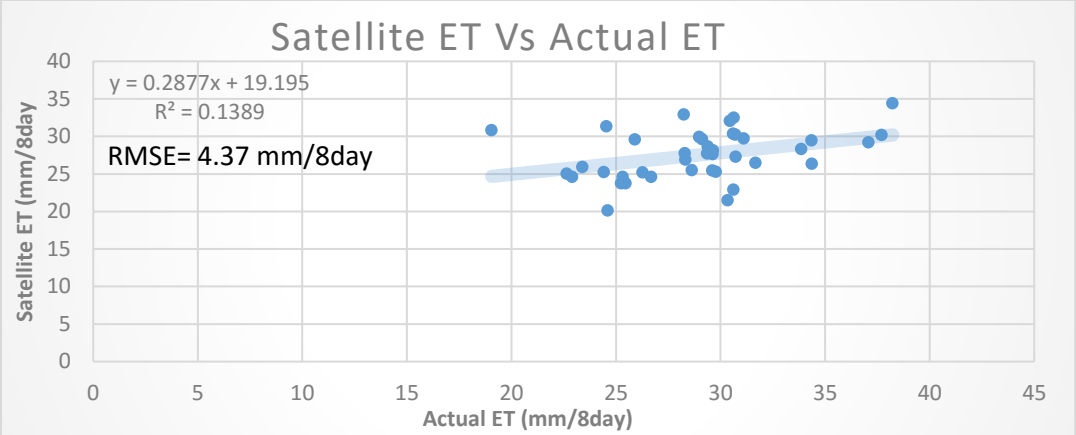

Fig. 3: Satellite ET Vs Actual ET in Kharif-II Season for Rajshahi station

Satellite and Actual (Penman-Monteith) ET Improvement

Three types of rice are grown in Bangladesh. Aus, Aman, Boro. Aus is grown in Kharif-I season (March to June) and it is grown in very small area in Bangladesh nowadays and are not irrigated. From the results it is found that EVI values are very small (around 0.2 to 0.3) in that period which indicates very little vegetation. So probably in that area no Aus crop is cultivated. So excluding Kharif-I period it is observed a notable increase in R^2 between Penman ET and Satellite ET.

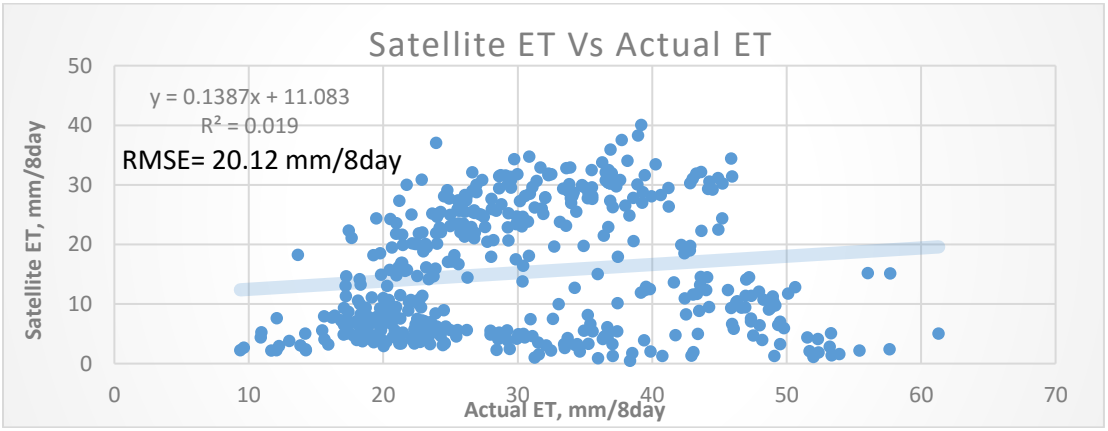

Fig. 4: Regression of Actual and satellite ET (including all season) for Rajshahi station

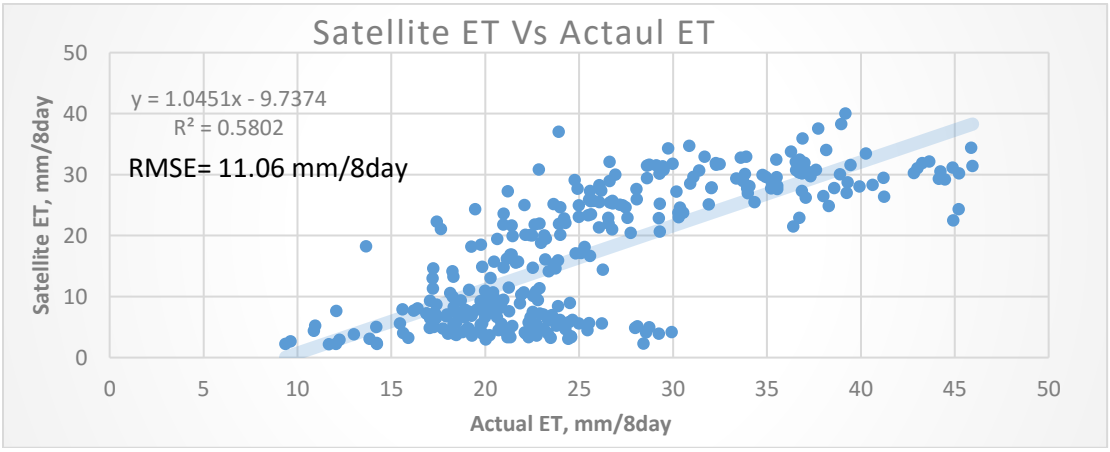

Fig. 5: Regression of Actual and satellite ET (Excluding Kharif-I season) for Rajshahi station

From the regression analysis between satellite and actual ET including Kharif-I season it has been observed very poor correlation (R^2 value is 0.019) [Fig. 4]. But excluding Kharif-I period it has been observed a notable increase in R^2 between satellite and actual ET [Fig. 5]. After excluding Kharif-I season R^2 value is 0.58. Here only Rajshahi stations result have been shown but Bogra and Rangpur stations also follows similar pattern.

Estimation of Penman ET from EVI

Kharif crops are grown in the spring or summer season and harvested in late summer or in early winter. Kharif season is divided into Kharif-I (March to June) and Kharif-II (July to October). Since the EVI values are very small (around 0.2 to 0.3) in that period which indicates very little vegetation. As the comparison does not perfect match, it has been tried another procedure, which is to estimate the penman ET by using EVI. There is a good correlation between penman ET and satellite ET (excluding Kharif-I season), which indicates that EVI value can be used to calculate penman ET [Fig. 6].

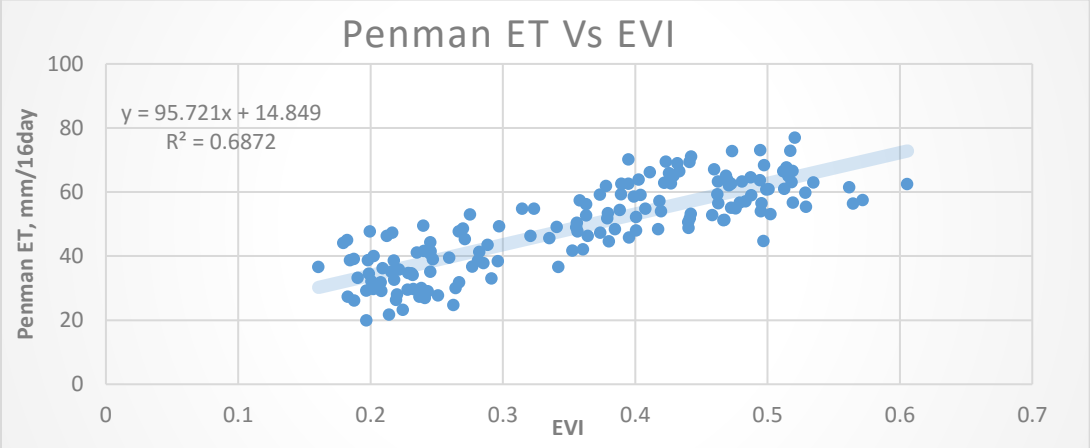

Fig. 6: Estimation of Penman ET from EVI (Excluding Kharif-I season)

CONCLUSIONS AND RECOMMENDATIONS

The main objective of this study was to assess the performance of MODIS ET product for estimating Penman ET for the agricultural areas of Bangladesh. To accomplish this objective, first actual ET was calculated by Penman-Monteith method from some selected stations and then satellite ET was obtained from the same climate stations. After comparing calculated actual ET with satellite ET, it is noticed that there are slightly shifting between the patterns of these two ET's. It is also noticed that actual ET is always higher than satellite ET, since it is not found enough information on crop pattern of the selected areas or due to the limitation of MODIS ET or Penman ET.

From the results it is found that EVI values are very small (around 0.2 to 0.3) in that period which indicates very little vegetation. So probably in that area no Aus crop is cultivated. It is noticed that excluding Kharif-I period there is a notable increase in R^2 between Penman ET and Satellite ET. As the comparison does not show perfect match, it has been tried another alternative procedure, which is to estimate the penman ET by using EVI.

The results showed that satellite ET does not perfectly match with the Penman ET. This can be due to the limitation of MODIS ET algorithm. Moreover Penman method also has some limitation. This method does not incorporate other stresses such as moisture stress, so slight mismatch is expected. Therefore further study is necessary to estimate actual ET by field experiment. In this study the performance of MODIS ET was evaluated for three stations. Future study is necessary to evaluate the applicability of MODIS ET for other areas and for other land use type of Bangladesh. This study shows that EVI can be used to estimate Penman ET. However further validation is necessary to determine whether Penman ET can be computed from EVI for other areas of Bangladesh

ACKNOWLEDGEMENTS
Praise to Allah, for giving us ability, patience, knowledge for completion of this work. The author is grateful to Bangladesh Meteorological Department (BMD) for giving their valuable climatic data. The author also thankful to Water Resources Engineering Department, BUET; for giving facilities to make this research.

REFERENCES
Amin, M.G.M., Ali, M.H. and Islam, A.K.M.R. 2004. Agro-climatic analysis for crop planning in Bangladesh. *Journal of Agricultural Engineering*, 15(1&2): 31-40.
Allen, R.G., Pereira, L.S., Raes, D., Smith, M. 1998. Crop evapotranspiration — guidelines for computing crop water requirements. *FAO Irrigation and Drainage Paper 56*. Food and Agriculture Organization of United Nations, Rome, Italy.
Bala, S.K and Islam, A.K.M.S. 2012. Assessment of Crop Water Deficit and Estimation of Yield of Wheat in Greater Dinajpur Region Using MODIS Data. Final Report, IWFM, BUET, Dhaka-1000.
Bastiaanssen, W.G.M., Menenti, M., Feddes, R.A. and Holtslag, A.M. 1998. A remote sensing surface energy balance algorithm for land (SEBAL)-Formulation. *Journal of Hydrology*, 212-213, 198-212.
Hargreaves, Z.A. Samani, et al. (1985). "Reference crop evapotranspiration from temperature." Transaction of ASAE 1(2):96-99.
Islam, M. S. and Morision, J. I. L. 1992. Influence of solar radiation and temperature on irrigated rice grainnyield in Bangladesh. *Field Crops Research*, 30: 13-28.
Karim, Z., Ahmed, M., Hussain, S.G. and Rashid, K.B. 1994. Impact of climate change on the production of modern rice in Bangladesh. *Crop modeling study, US Environmental Protection Agency, EPA* 230-B-94-003, Washington DC.
Madhu, M.K. 2011. *Trends in climatic variables and their combined effects on irrigation water requirement and yield of wheat*. M. Sc. Thesis (WRD), Institute of Water and Flood Management, BUET.
Masud, M.B. and Ferdous, J. et al. (2011). "Water Deficit Period for Irrigated Agriculture Based On Evapotranspiration and Dependable Rainfall." *Bangladesh Res. Pub. J*. 5(4): 321-328.
Mondal, M.S. and Islam, A.K.M.S. 2012. Spatial and Temporal Distribution of Temperature, Rainfall, Sunshine and Humidity in Context of Crop Agriculture. Institute of Water and Flood Management (IWFM), BUET, Dhaka-1000.
Rahman, M.R., Salehin, M. and Matsumoto, J. 1997. Trend of monsoon rainfall pattern in Bangladesh. *Bangladesh J. Water Resource*, 14-18, 121-138.
Rahman, M.M. 2009. *Effects of climate change on T. aman cultivation in Bangladesh*. M.Sc. Thesis (Environmental Engineering), Department of Civil Engineering, BUET.
Shopan, A.A., Islam, A.K.M.S. and Dey, N.C. 2013. Estimation of evapotranspiration of boro rice in the northwest region in Bangladesh. Institute of Water and Flood Management (IWFM), BUET, Dhaka-1000, Bangladesh.
Zaman, S. and Mondal, M.S. 2011. Dimming in sunshine duration of Bangladesh and its impact on rice evapotranspiration and production. *Third International Conference on Water and Flood Management*, Organized by Institute of Water and Flood Management, held during 8-10 January, Dhaka, pp. 857-864.